THE UNIVERSITY OF NEWCASTLE UPON TYNE

DEPARTMENT OF CIVIL ENGINEERING

A STUDY OF DISSOLVED AIR FLOTATION TANK DESIGN VARIABLES AND SEPARATION ZONE PERFORMANCE

BY

MOHD NORDIN BIN ADLAN

B.Sc., M.Sc., M.I.E.(Malaysia), P.Eng.(Malaysia)

FEBRUARY 1998

Thesis submitted to the University of Newcastle Upon Tyne
for the Degree of Doctor of Philosophy
in Environmental Engineering

ACKNOWLEDGEMENTS

I would like to express my appreciation to my supervisor Mr D. J. Elliott for his assistance and guidance throughout the course of this study. Without his guidance and critical review during the preparation of this thesis I would never have completed my work.

I would also like to express my gratitude to Dr G. Noone of Severn Trent Water for his assistance and co-operation to enable me to conduct this study at the Severn Trent Water. I am also indebted to Severn Trent Water which has provided me with the financial assistance to conduct this study. Thanks are also due to all the staff of the Severn Trent Water who has directly or indirectly involved with this study.

I am grateful to Dr A. V. Metcalfe and Dr E. B. Martin from the Department of Engineering Mathematics who have made helpful comments and suggestions in the application of statistical techniques for site investigation and data analyses.

My special thanks also goes to the laboratory staff of the Department of Civil Engineering, particularly Mr. J. Hamilton, Mr. D. Innes and Mrs. P. Johnston for the co-operation and assistance throughout the course of the study.

I wish to thank you my wife Norsiah, for her support, encouragement and patience throughout the course of this research work. This gratitude is extended to my children Nor Aini, Nor Faridah, Najib, Farid and Nabil for being well behaved during the course of my work.

ABSTRACT

A study of velocity and turbidity distributions in the separation zone of dissolved air flotation (DAF) tanks was carried out at Frankley and Trimpley Water Treatment Works of Severn Trent Water. Sampling of velocity was made using an Acoustic Doppler Velocimeter (ADV). The instrument is capable of measuring velocities as low as 1 mm/sec and producing three dimensional velocity data. Sixty-four points set at equal intervals within the tank were monitored and the flow rate corresponding to the velocity for each point was recorded. The same points were used for the sampling of turbidity within the tank and the corresponding flow rate for each sampling point was also recorded. The aim of the study was to establish the relative importance of tank design parameters within the separation zone.

The ADV probe was found suitable to be used in the investigation based on the data quality obtained. The study indicated that there are some differences in the flow patterns compared to Computational Fluid Dynamics (CFD) models found in the literature. The plan view contour plots indicated that velocities in the x, y and z directions at a quarter depth from the surface of the tank were unstable with irregular velocity patterns. However the CFD models indicated that the flow at this depth was uniform. Also at this depth the vertical velocity was predominantly downward which suggested that the solid liquid separation process is inefficient.

Tank physical parameters were found to have a highly significant effect on the velocity distribution using analysis of variance (ANOVA) and analysis of covariance (ANCOVA). These analyses involved higher order interactions and independent predictor variables. The results from the higher order models are difficult to interpret. Thus simple second-order empirical models were used. Empirical models were developed using regression analyses to describe the observed velocity within the tank. These models are appropriate for design purposes. Although the models are not precise, the standard statistical techniques used for data analyses are found to be

useful to compare, analyse and develop the appropriate model from the velocity data obtained during the investigation.

In terms of turbidity removal, there was no significant difference in the average turbidity readings between different depths of the tank. Comparison of turbidity at different lengths of the tank indicated that the average turbidity readings were identical between three quarter length of the tank from the baffle and at the extreme end of the tank. The results confirm that there were not enough air bubbles within the separation zone for turbidity removal. The size of tank at Frankley can also be reduced by 15% so that the difference between the average flow rate and the surface area between the tank at Frankley and Trimpley is the same. It is expected that the reduction in size will not affect the turbidity within the separation zone due to non significant turbidity removal within this zone.

TABLES OF CONTENTS

LIST OF FIGURES AND PLATES

LIST OF TABLES

LIST OF SYMBOLS AND ABBREVIATIONS

$\overline{X}$	mean for X
$\overline{Y}$	mean for Y
$\hat{Y}$	predicted value
$\bar{x}$	sample mean
$\bar{x}_i$	sample mean and sample size for level i or the overall mean in the i treatment
x_i	sample size
$\hat{x}_{ij}$	estimate of the corresponding observation y_{ij}
ρ_g	density of gas
ρ	density of liquid
σ	density of sphere or surface tension in dyne/cm or the value from a t-table
μ	dynamic viscosity or population mean or overall mean
ν	kinematic viscosity
η	single collector efficiency
ε_{ijkl}	random error component
$\Delta\rho$	the difference of density between liquid and gas
$(\tau\beta\gamma)_{ijk}$	interaction terms at ith, jth and kth levels
$(\tau\beta)_{ij}$	interaction terms at ith and jth levels
$(\tau\gamma)_{ik}$	interaction terms at ith and kth levels
$(\beta\gamma)_{jk}$	interaction terms at jth and kth levels
η_1	collision efficiency
η_2	attachment efficiency
σ^2	population variance
ϕ_b	bubble volume concentration
η_D	single collector efficiency due to diffusion
ρ_f	density of floc
ρ_f	fluid density
μ_f	fluid viscosity
η_G	single collector efficiency due to gravity

τ_i	ith treatment effect or the effect of ith level of a factor
η_I	single collector efficiency due to interception
ε_i	the difference between the observed and fitted value for each point in the regression analysis
ε_{ij}	random error component or the usual NID (0, σ^2) random error term
β_j	effect in the jth tank or effect of the jth level of a factor
γ_k	effect of the kth level of a factor
μm	micron
ρ_n	particle density
ρ_p	particle density(gm/ml)
α_{pb}	attachment efficiency
ρ_{sat}	saturated density of air
ρ_w	density of water in gm/cm^3
a	levels of factor A or radius of bubble/sphere
A_b	projected area of bubble
AC	alternating current
A_C	cross-sectional area of flotation chamber, m^2
ADV	Acoustic Doppler Velocimeter
Ah	the horizontal area of the unit
ANOVA	analysis of variance
a_P	mass of air precipitated
A_S	surface area of flotation chamber
b	levels of factor B
b_1	the slope of the fitted straight line
c	levels of factor C, run or treatment
C_a	concentration of air remains in solution at atmospheric pressure
CAL	calibration model
CCTV	camcorder television camera
C_d	dimensional drag coefficient for the particle
CFD	computational fluid dynamics
CI	confidence interval
C_i	the influent suspended solids

cm	centimetre
cm/sec	centimetre per second
c_o	suspended particle concentration upstream from the collector
C_o	the effluent suspended solids
C_r	concentration of air released in the tank
c_s	concentration of air in the saturated fluid
C_s	concentration of air in the saturated liquid
d	diameter of collector or bubble/sphere
D	drag force
D	effective depth of flotation chamber
d	grain diameter
d1	depth at 10cm from the floor of the tank
d2	at one-quarter depth of the tank
d3	at half depth of the tank
d4	at three-quarter depth of the tank
d_a	diameter of bubble
DAF	dissolved air flotation
d_{av}	volumetric mean diameter of bubble in cm
d_b	diameter of bubble
DC	direct current
d_e	equivalent diameter of bubble
DF	degrees of freedom
df	degrees of freedom
d_f	diameter of floc
d_h	the diameter projected on the horizontal plane
d_p	diameter of suspended particle
f	efficiency factor for the saturator
F	the F-test based on F-distribution i.e. between-group variance divided by within-group variance
FTU	Formazin turbidity unit
g	acceleration due to gravity

G	dimensionless settling velocity of particle or volumetric flow rate of air generated under decrease in pressure(cubic cm/sec)
G_j	the body force acting on the particle
gm	gram
gpm	gallon per minute
h	depth from the liquid surface to bubble in cm
H_E	Henry`s Law constant in dyne/cm^2
hr	hour
Hz	Hertz
i	ith observation
j	jth observation
k	Boltzmann`s constant or Henry's law constant
K	influent saturation factor or particle inertia parameter
k_b	Boltzmann`s constant for bubble
K_B	Henry's law constant
KN	kilonewton
Kpa	kilopascal
L	effective length of flotation chamber
LDV	Laser Doppler Velocimeter
m	metre
m/hr	metre per hour
Max.	maximum
mg/l	milligram per litre
Min.	minimum
min.	minute
ml	millilitre
mld	million litres per day
mm	millimetre
m_p	mass of particle
MS	mean squares
mV	millivolts
M_w	molecular weight of water in g/g.mole

N	number observation points in the tank
n	sample population or sample size or number of replicate
n_a	bubble concentration
N_b	numbers of bubbles generated per cubic cm of water
n_i	sample mean and sample size for level i
nm	nanometre
N_p	particle number concentration
p	level of significance
p	absolute pressure or significance level
P	saturator pressure in atmospheres
P_A	dissolved pressure in dyne/cm^2
PAC	polyaluminium chloride
p_B	vapour pressure
Pe	peclet number = $2a_cU / D$ where a_c is the radius of the spherical media grain, U is the approach velocity to the filter and D is the Brownian diffusion coefficient of the suspended particle
P_o	atmospheric pressure in dyne cm^2
Pos.	position
ppm	part per million
psi	pound per square inch
Q	influent flow rate(m^3 sec) or volumetric flow rate of liquid (cubic cm/sec)
R	gas constant in erg/K.mole
R	ratio of total removal of solid after flotation
r	recycle ratio or correlation coefficient
R^2	coefficient of determination
R_b	bubble radius(cm)
Re	Reynolds number
r_n	particle radius
r_p	particle radius(cm)
R_r	recycle ratio
RT	retention time
RUN	replication of the experiment

S	area of bubble
s	standard deviation
s^2	estimate of population varianve within treatment
s_B^2	estimate of sample variance between treatment
sec	second
s_p	pooled standard deviation
SS	sum of square
STDEV	standard deviation
T	absolute temperature in Kelvin or detention time, sec
t	dimensionless time or t-ratio
T	temperature
u	component of velocity field due to bubble
u	dimensionless component of bubble velocity field
U	terminal velocity
U_b	bubble rise velocity
u_j	velocity of fluid
u_o	water velocity
v	component of particle velocity or dimensionless component of particle velocity or velocity
V	voltage output or volume of bubble
V_A	generated air volume
VACM	Propeller Vector Averaging Current Meter
V_b	volume of air occupied by a single spherical bubble
V_H	horizontal velocity
v_j	particle velocity
$Vmax$	maximum voltage
V_{mes}	measured velocity
$Vmin$	minimum voltage
V_{neg}	negative velocity
v_o	approach velocity of fluid
Vol.	volume
V_{pos}	positive velocity

V_r	the rising velocity of a single particle/air bubble
Vrange	velocity range
V_T	vertical rise rate of suspended solids, m/sec
Vx	velocity in x direction
Vy	velocity in y direction
Vz	velocity in z direction
V_{zero}	zero velocity
W	width of flotation chamber(m)
WinADV	software to analyse velocity from the ADV probe
WTW	water treatment works
x	axis
x, y	Cartesian position co-ordinates
x_B	mole fraction of the solute
X_i	ith observation
x_{ij}	(ij)th observation or the jth observation in the sample from population i, $x_{i.}$
x_{ijkl}	the observed response variable
X_n, Y_n	nth observation for X and Y
y	axis
Y_i	ith observation
z	axis

CHAPTER 1

INTRODUCTION

Dissolved air flotation (DAF) is one of the methods used in water treatment to separate solids from a body of liquid. The DAF process was initially used for the recovery of fibres and white water in the paper industry (Gregory, 1997). Its suitability for potable water clarification was realised in the mid-1960's in Finland and Sweden. One of the first people to initiate the use of the DAF process for potable water treatment in the United Kingdom was Dr. Packham. The programme of investigation was then intensified by the Water Research Centre. DAF technology was brought into the United Kingdom from Sweden during the 1975-76 drought. In the early days the development of the process appeared to be more of an art rather than science due to too many design and operation variables (Gregory, 1997).

Interest in the process arises due to its higher surface loading rate than conventional gravity sedimentation which results from a shorter retention time. Further advantages include rapid start-up, effective removal of algae, its suitability to treat soft, low alkalinity upland waters, stored lowland waters and low turbid water. Experience in South Africa indicated that the DAF process was capable of treating raw water turbidity of 500 NTU with the treated water turbidity not exceeding 1 NTU (Kolbe, 1997).

Longhurst and Graham (1987) reported that there is a great variation of DAF tank sizes and shapes found in the United Kingdom. They indicated that the surface overflow rate (rise rate or surface loading or sometimes hydraulic loading) is the fundamental design criterion for the tank. There are two different methods of calculating the surface loading. In the first, the calculation is calculated based on the surface area of the separation zone and in the second, on the total surface area of the flotation cell. Longhurst and Graham (1987) indicated that the latter was normally used in practice. They also indicated that there was no clear evidence to suggest that a certain aspect ratio (i.e. length:width ratio) is superior to the others. However

Franklin *et al.* (1997) suggested that higher aspect ratios work better. It is therefore rather difficult to make any judgement based on two contradictory reports.

Although DAF technology has been widely used for potable water treatment, discussions with Severn Trent Water (Noone, 1995) indicated that there was a lack of information on the suitable design procedures for the DAF tanks. In fact at Severn Trent Water various tank configurations have been used. There is no standard procedure to design the tank. Noone (1995) also indicated that the roles of flocculation and flotation are extremely important to maximise the removal of particles before filtration. The water industry felt that a fundamental understanding of different tank configurations is important in order to develop a standard tank design procedure.

In early 1995 a meeting was held with the technical staff of Severn Trent Water to identify the problems faced by the treatment plant managers and process advisors on the existing flotation plants. The results from this meeting indicated that there was a lack of understanding on flow encountered within the flotation tanks. A number of other questions were also raised, an extremely important one was regarding the effectiveness of particle removal. This indicated that there was a lack of information on the characteristic of turbidity distribution within the tank.

It is therefore considered necessary to investigate the actual flow and turbidity characteristics within the separation zone of a DAF tank with the possibility of developing appropriate models to describe the velocity distribution within the tank for design purposes. To achieve this, it is considered necessary to investigate a full scale treatment works rather than using a laboratory model so that the uncertainty factor can be addressed appropriately. Discussions with Severn Trent Water also indicated that a full plant study must be carried out under normal operational conditions so that the outcome of the results are based on the actual day to day operation and relevant to the industry. A collaboration programme was established between the University of Newcastle and Severn Trent Water. Five treatment works with different sizes and

shapes were identified and two were considered feasible with respect to cost and safety.

The present study was carried out on a full scale dissolved air flotation plant of Severn Trent Water with the main objective being to develop the design procedures within the separation zone of the DAF tank.

This thesis was structured with different chapters in accordance with the sequence of activities carried out during the study period. In Chapter 2, a literature review was written to provide a general background of the present technology. Chapter 3 includes a summary of the literature review and an outline of the research objective. This is followed by a description of the methods and equipment used in the investigation (Chapter 4). It was also felt necessary to describe the statistical techniques used during data analyses so that its application can be properly understood (Chapter 5). Velocity data were analysed in Chapter 6. Chapter 7 is concerned with an analyses of the relationship between tank dimensions, flow and velocity distributions. It describes and proposes appropriate statistical models for the design of flotation tanks. In Chapter 8, turbidity distributions in the DAF tanks were analysed and the appropriateness of the statistical models (i.e. models developed in Chapter 7) in relation to turbidity removal were discussed. Finally in Chapter 9 the conclusions of the study were made and further research work proposed.

CHAPTER 2

LITERATURE REVIEW ON DISSOLVED AIR FLOTATION (DAF)

2.1 INTRODUCTION

There are many types of flotation process available for different applications. The technology has been applied in industries such as in mineral processing (Gaudin, 1939; Merrill and Pennington, 1962), wastewater clarification (Travers and Lovett, 1985; Krofta *et al.*, 1987, 1988; Wang *et al.*, 1989), artificial recharge (Puffelen *et al.*,1995) and potable water treatment (Childs *et al.*, 1977; Nickols *et al.*, 1995). Basically the flotation process is used to separate solids from a body of liquid.

This chapter discusses the historical development of flotation processes and the kinetics of bubble-floc attachments for potable water treatment. Theoretical aspects of bubble-floc attachments are initially reviewed followed by the design and operation parameters currently used in the water treatment process. At the end of the chapter a summary on the current knowledge is given which identifies the gaps in knowledge in flotation tank design.

2.2 HISTORY

In the field of water treatment, flotation processes involve separation of solids from liquid using gas bubbles. They have been used in the mining and chemical processing industries for over 100 years (Edzwald and Walsh, 1992). However the history of flotation goes back even earlier. The ancient Greeks used this process to separate minerals from the gangue over 2000 years ago (Gregory and Zabel, 1990). The development of the process to modern practices took many years. According to Kitchener (1984), Haynes was able to separate minerals using oil in 1860. His method was patented. In 1905 Salman, Picard and Ballot developed a process to separate sulphide grains from water by adding air bubbles and a small amount of oil to enhance the process. This was called 'froth flotation'. In 1910 T. Hoover developed the first flotation machine which was not much different from today's equipment. A few years later, in 1914 Callow introduced a new process called 'foam

flotation'. This process involved the introduction of air bubbles through submerged porous media. In fact froth and foam flotation processes are generally known as dispersed-air flotation and are used widely in the mineral industry at the moment.

The development of the electrolytic flotation process can be traced back to 1904. The process was suggested by Elmore who showed that electrolysis could produce bubbles for flotation. It was not used commercially at that time.

Dissolved-air flotation was patented in 1924 to Niels Peterson and Carl Sveen in Scandinavia (Lundgren, 1976). It was initially used to recover fibres and white water in the paper industry. The use of DAF in the treatment of waste water and potable water began in the late 1960's. Edzwald and Walsh (1992) reported that dissolved air flotation has been used for water clarification in Europe especially in the Scandinavian countries for more than 20 years. Heinanen, (1988) in his survey on the use of flotation in Finland indicated that the first dissolved air flotation plant for potable water clarification was constructed in 1965 and by 1988 there were 34 plants in operation. However the first application of flotation for a water reclamation plant was introduced in the early 1960s in South Africa (Longhurst and Graham, 1987). In the United Kingdom, the first full-scale water treatment plant using this process was commissioned in 1976 at the Glendye Treatment Works of the Grampian Regional Council, Scotland (Zabel, 1978). Experiments carried out by researchers at the Water Research Centre showed that flotation is a more rapid method of solid-liquid separation than sedimentation (Packham and Richards, 1975).

2.3 TYPES OF FLOTATION

Flotation may be defined as the transfer of a solid from the body of a liquid to the surface by means of bubble attachment (Zabel and Hyde, 1977; Zabel, 1978). Different methods of bubble generation give rise to different types of flotation processes (Zabel and Melbourne, 1980). There are three types of flotation process and these are as follows:-

1. Electro- or electrolytic flotation.

2. Dispersed air flotation.

3. Dissolved air flotation.

2.3.1 Electro-flotation

Under this process, bubbles (oxygen and hydrogen) are generated by passing an electric current between two electrodes in a dilute aqueous solution (Ward, 1992). The material used for the electrode is normally made of aluminium or steel (Zabel and Melbourne, 1980). The anodes are prone to corrosion while the cathodes are subject to scaling by carbonate deposition (Degremont, 1991). As a result, frequent problems were encountered with sacrificial electrodes leading to high maintenance and replacement costs together with delay in the operation of the system.

The bubbles produced by the electro-flotation process are normally small and do not create a turbulent environment to the flocs (Barrett, 1975; Coulson *et al.*, 1991). Thus the removal of low density particles is expected to be efficient under appropriate conditions (Zabel and Melbourne, 1980). This process is suitable for effluent treatment (Ho and Chan, 1986), sludge thickening and water treatment installations of 10 to 20 m^3/hour. Figure 2.1, shows a typical arrangement of an electro-flotation tank.

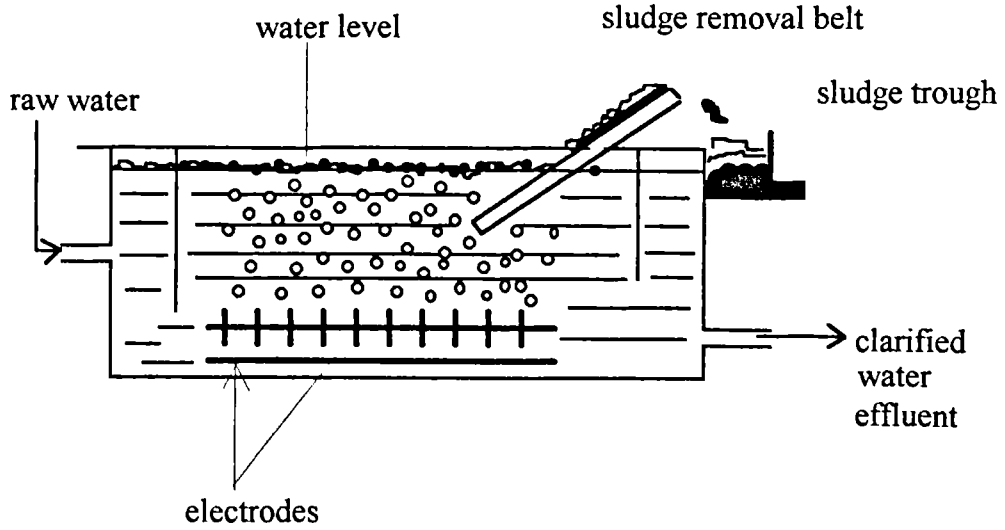

Figure 2.1 - Electro-flotation tank (Source: Zabel, 1978)

2.3.2 Dispersed Air Flotation

This process has two different systems to generate bubbles namely, foam flotation and froth flotation. In the foam flotation system, bubbles are generated by forcing the air through a porous media made out of ceramic, plastic or sintered metal (Zabel and Melbourne, 1980). Figure 2.2 shows a typical arrangement for bubble generation through a media or diffuser.

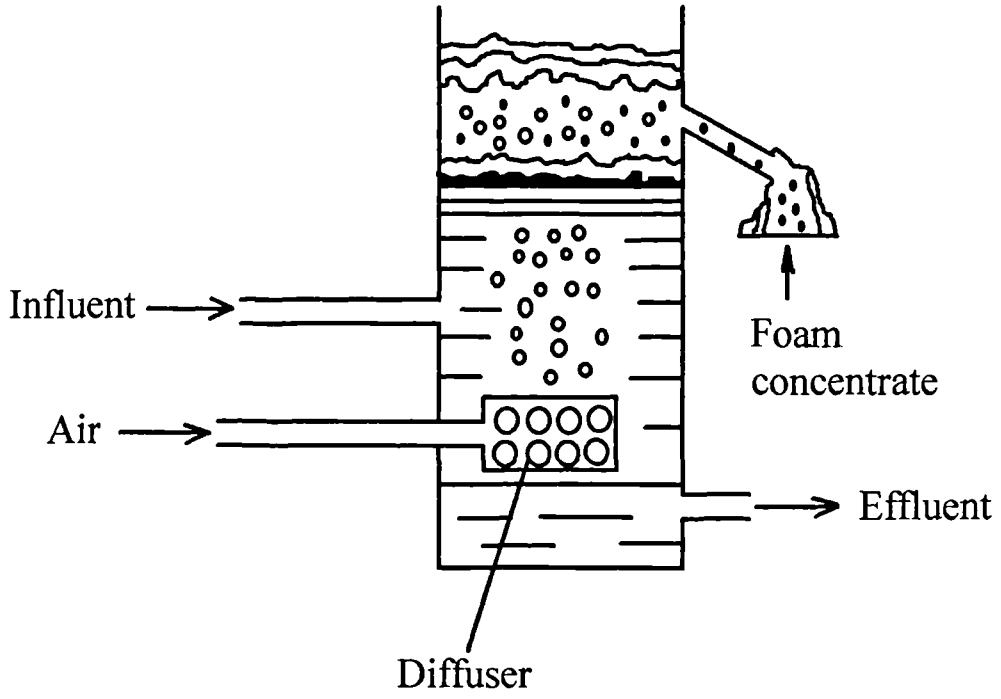

Figure 2.2 - Foam flotation (Source: Zabel, 1978)

In the froth flotation system (as shown in Figure 2.3) a high speed impeller or turbine blade rotating in the solution is used to produce air bubbles.

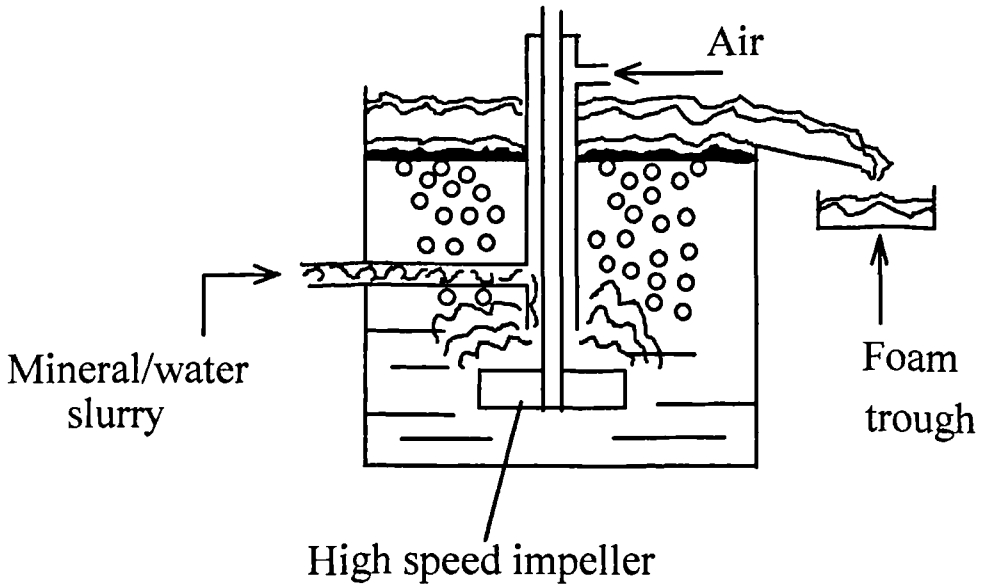

Figure 2.3 - Froth flotation (Source: Zabel, 1978)

Dispersed air flotation normally produces large air bubbles of more than 1mm in diameter (Barnes *et al.*, 1981). Its application is mainly for the separation of minerals and removal of hydrophobic materials such as fat emulsions in selected waste water treatment. This process has been assessed for potable water treatment but was not suitable (Zabel and Hyde, 1977).

2.3.3 Dissolved Air Flotation (DAF)

There are three main types of dissolved air flotation processes available. These are as follows:

1. Vacuum flotation
2. Micro-flotation
3. Pressure flotation

2.3.3.1 Vacuum Flotation

Kalinske (1958) indicated that vacuum flotation was the original form of dissolved air flotation. It is used for the recovery of fibres in the pulp and paper industry. In this process, water is saturated with air under atmospheric pressure and then a vacuum is applied to the flotation tank. Small air bubbles will be released in the tank and they

will agglomerate with the particles and move up to the surface of the liquid. There are at least three main disadvantages associated with the process. These are as follows:

1. Batch process instead of continuous
2. Sophisticated equipment required to maintain the vacuum
3. Amount of air available is limited by the capacity of the vacuum

2.3.3.2 Micro-flotation

This process was developed in Sweden and has been used widely in the Scandinavian countries for the treatment of domestic sewage and industrial effluents. Prior to micro-flotation, sewage is normally treated by screening, grit removal, primary settlement and chemical treatment. In the micro-flotation process, water is passed down and up a shaft of approximately 10 metres deep. The whole water column will be subjected to hydrostatic pressure (Hemming *et al.*, 1977; Zabel and Melbourne, 1980). Water will be aerated as it passes the down-flow section and air dissolves in the water due to an increase in hydrostatic pressure. Polyelectolytes may be added in the down-flow section to aid floc agglomeration and increasing the hydrophobility of the solids. In the up-flow section, the pressure is decreased and some fine air bubbles will be released. The quantity of air is dependent on the depth of the shaft. Figure 2.4 shows a typical arrangement of a micro-flotation system. This process is restricted to small sewage and effluent treatment. It is an effective process for the separation of humic acid, organic colloids, silica and bacteria from water (Rubin and Lackey, 1968; Cassell *et al.*, 1971, 1975; Mangravite *et al.*, 1975; Edzwald and Walsh, 1992). This process is not practical in water treatment due to the high cost incurred in chemical collectors (e.g. lauric acid) and frothers (e.g. ethanol). Besides that an unacceptable limit of organic and surfactant content will be left in the drinking water (Malley, 1988).

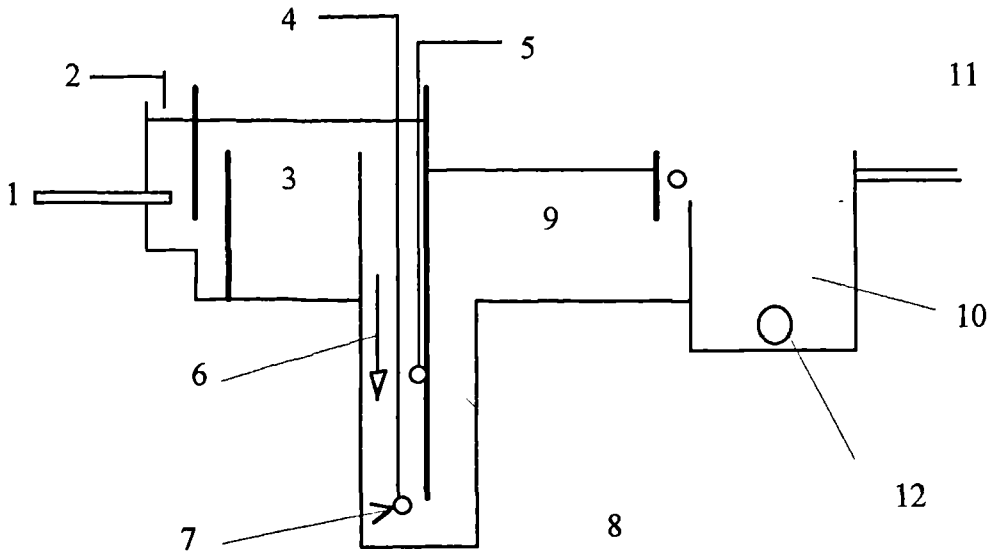

1. Waste water intake 2. Precipitation chemical 3. Flocculation tank
4. Compressed air 5. Polymer dosage 6. Shaft for aeration 7. Aeration
8. Riser 9. Flotation tank 10. Sludge tank 11. Effluent 12. Sludge outflow

Figure 2.4 - Micro-flotation system (Source: Hemming *et al.*, 1977)

2.3.3.3 Pressure Flotation

Pressure flotation is the most common process used in dissolved air flotation. Initially air is dissolved in water under pressure. Then a reduction of pressure to atmospheric is made. This enables air bubbles to be produced. There are three basic types of pressure dissolved air flotation processes. These are as follows:

1. Full-flow pressure flotation
2. Split-flow pressure flotation
3. Recycle-flow pressure flotation

If the entire influent is pressurised and aerated, it is called full-flow pressure flotation. If part of the influent is pressurised while the rest flow directly to the flocculation/flotation tank, it is called split-flow pressure flotation. Full-flow and split-flow processes are not suitable for surface water treatment due to high shear at the saturation stage which would break up the preformed flocs (Rees *et al.*, 1980; Krofta and Wang, 1982; Wang and Wang, 1989). In the recycle-flow flotation, the influent is not pressurised but part of the effluent is pressurised and saturated with air.

The disadvantage of this system is the need to resize the flotation tank if an additional recycle-flow is made (Rees *et al.*, 1980). Figures 2.5, 2.6 and 2.7 show general arrangements for different types of pressure dissolved air flotation processes.

Tibke and Beaumont (1993) indicated that the most widely accepted flotation process to treat potable water is by coagulation and flocculation followed by recycled dissolved air flotation. Malley and Edzwald (1991b) reported that researchers at the Water Research Centre (WRc) in England found that recycle dissolved air flotation was the most practicable process to treat potable waters.

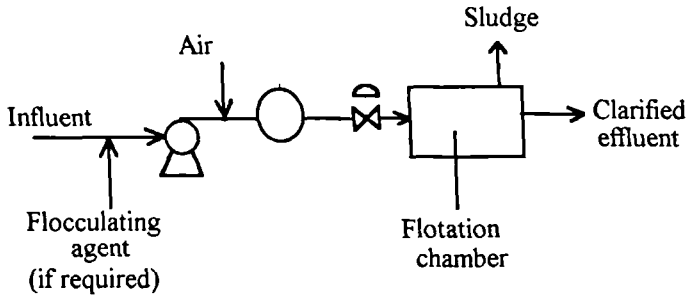

Figure 2.5 - Full-flow pressure flotation (Source: Zabel, 1980)

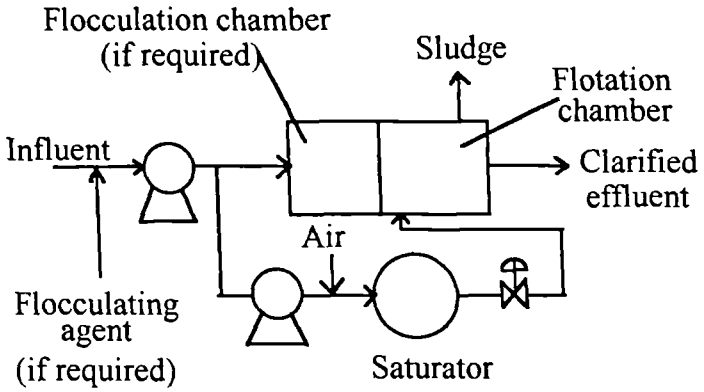

Figure 2.6 - Split-flow pressure flotation (Source: Zabel, 1980)

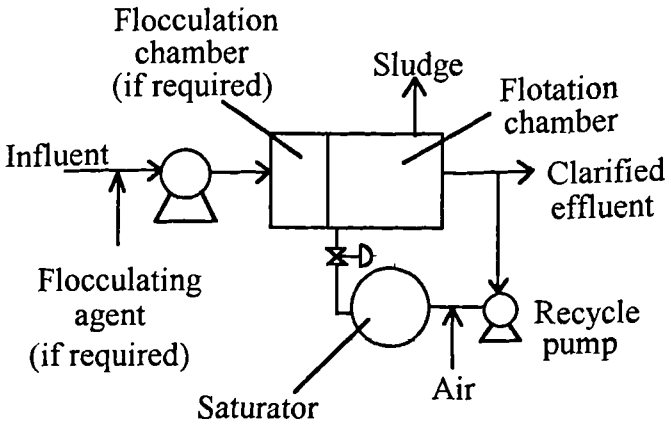

Figure 2.7 - Recycle-flow pressure flotation (Source: Zabel, 1980)

2.4 RESEARCH WORK ON DAF FOR POTABLE WATER CLARIFICATION

A number of research works to assess the effectiveness of DAF for the clarification of potable water were carried out by different organisations and researchers, particularly in the United Kingdom, South Africa and United States. These include research done by Water Research Centre (Packham and Richards, 1972a, 1972b, 1975; Hyde, 1975; Hyde *et al.*, 1977; Rees *et al.*, 1979), universities and research institutes in the United Kingdom (Urban, 1978; Swailes, 1979; Lister, 1982; Repanas, 1992), South Africa (Vuuren *et al.*, 1965; Bratby and Marais, 1974, 1977; Offringa, 1995) and in the United States (Vrablik, 1959; Ettelt, 1964; Cassell *et al.*, 1975; Krofta and Wang, 1985; Malley and Edzwald, 1991a)

2.4.1 Bench-scale and Plant Studies

2.4.1.1 Research Works in United Kingdom and Europe

The first bench-scale flotation apparatus by Packham and Richards (1972b) was constructed from perspex, with a capacity of 1.2 litres, 75mm in diameter and with a stainless steel paddle driven at variable speed by an electric motor. The capacity of the pressurised air saturation vessel was 1 litre, filled with 700ml of distilled water and maintained at a pressure of 340 KN m^2. The air was released into the vessel through a needle valve. The results of this study showed that surface active agents

could be discarded for water treatment using dissolved air flotation. Efficient flotation could be achieved by the addition of 5% by volume or less, of water saturated with air at 340KN/m^2. The process retention time for water clarification was found to be shorter than sedimentation. Packham and Richards (1975) concluded that the dissolved air flotation process could be considered for water clarification due to possible advantages over sedimentation in terms of algal removal, lower capital cost and the ability to produce sludge with higher solids content. Algal removal is important because its presence may cause some problems such as taste, odour and blocking of filters (Eades and Brignal, 1995).

Packham and Richards (1975), later tried to determine the effects of chemical treatment of the flocculation process using aluminium sulphate and ferric sulphate based on the design parameters of a pilot plant in South Africa (van Vuuren *et al*, 1967). They also investigated the air requirement for DAF, characteristics of sludge, the effects of skimming on treated water quality, algal removal as compared to sedimentation and the ability of DAF to treat turbid waters. The flotation unit which had been used in South Africa consisted of a conical tank with a feed flow of 15 gallons per minute (gpm), total retention time of 20 minutes, upward flow of 15 feet/hour (i.e. 4.57m/hr), horizontal flow 15 feet/hour and downward flow of 15 feet/hour (van Vuuren *et al.*, 1967). Air was introduced prior to the impeller of the centrifugal pump so that micro-bubble aeration could be achieved. The tank was used to purify sewage works effluents. Prior to this investigation, van Vuuren *et al.* (1965) had made an assessment on the removal of algae in water reclamation by flotation. Two types of flotation tanks were investigated i.e. vertical and radial flow tanks. The vertical tank was 4 feet deep and 3 feet internal diameter. The depth from the surface to the distributor arms was 12 inches. The retention period was 8 minutes at a flow rate of 22gpm with a vertical flow velocity of approximately 28 feet/hour. The radial flow tank was 8 feet in diameter, 23 inches deep with an energy dissipator-cum-air escape tank situated in the centre having a diameter of 23 inches, 16 inches deep with its brim 4 inches above the water level of the main tank. For an influent flow of 90 gpm, the retention time was less than 7 minutes and the flow over the brim of the inner tank amounted to 15 gpm/ft run of its circumference. A comparison of the

performance of both tanks was made and the results showed that the radial flow tank had the advantage of consistently better removal of faecal *E.Coli.* There were no significant differences in the physical and chemical performance of the two tanks.

The flotation tank used by Packham and Richards (1975) was designed with a flow rate of 1.8 m^3/hour and retention times of 7 minutes and 20 minutes in the flocculation and flotation tanks respectively. Coagulants were added in the flash mixer with a capacity of 0.055m^3 prior to four-stage flocculation followed by flotation. The capacities of the four-stage flocculator and flotation tank were 0.22 and 0.6 cubic metres respectively. These tanks were connected in series by 80mm PVC pipes. The flotation tank was 0.9m in diameter of cylindrical shape with a conical bottom section. The overall depth was 1.45m. The tank had a conical bottomed inner tank at the centre with a 0.65m diameter and 0.95m depth. Flexibility in the flow rate for raw water was allowed between 1.2 and 2.4 m^3/hour. Water from the River Thames was used for the study. There was a considerable variation in raw water quality during the study period. The turbidity varied between 1.8 and 78 FTU (i.e. Formazin turbidity unit), the colour between 0.22 and 0.128 (expressed as an optical density measurement at 400nm), pH 7.7 to 8.4 and the water temperature was between 2.5 and 18^{0}C. Maximum algal count of 72,000 cells/ml was recorded during peak turbidity and colour due to occasional flood.

The outcome of the studies showed that performance at the flotation stage was very dependent on the efficiency of flocculation. There was no significant difference between using ferric sulphate and aluminium sulphate in the flocculation process. The clarification process could be improved if aluminium sulphate was combined with polyelectrolyte. The efficiency of DAF with respect to colour, turbidity and residual coagulation concentrations was equivalent to sedimentation. In terms of algal removal, DAF performed better than sedimentation. On the air requirement using Thames water, the addition of 4 to 6% by volume of water saturated with air at 340 KPa could produce a good flotation process. Other advantages learned from this study include a low rate of head loss at the filter bed, good filtered water quality and sludge with a higher solid content of 2 to 10%.

Hyde (1975) used a similar design to Packham and Richards (1975) but altered the shape of the flotation tank in the form of a flat bottomed rectangular basin with a capacity of 8.2 m^3/hour. His pilot plant consisted of a flash mixer tank, a four stage flocculation tank, a 2.4m x 0.3m x 1.2m deep flotation tank and a 0.3m diameter rapid-gravity filter. The objectives of the study were to investigate the effects of flocculation, dissolved air addition, coagulant dose, plant throughput and raw water quality on treated water quality. The results of the study showed that the retention times in the flash mixer, flocculator and flotation tank were $1\frac{1}{2}$, 9 and $5\frac{1}{2}$ minutes respectively. This would produce a desirable treated water quality. However when the raw water turbidity rose to 100 FTU and colour to 45° Hazen, the retention time in the flotation tank had to be increased to $6\frac{1}{2}$ minutes to get a similar result on treated water quality. The increased retention time in the flotation tank may not be necessary due to the fact that residual turbidity is a function of the length of the rapid-mix period as reported by Letterman *et al.* (1973). This observation is based on their investigation of the influence of rapid-mix parameters on flocculation where the measurements of residual turbidity were carried out after a fixed sedimentation process of 30 minutes. On algal removal, after adding 5 mg/litre of chlorine prior to coagulation, algae concentration would normally be less than 1500 cells ml in the flotation treated water. This result was based on raw water having algal counts of 30,000 to 150,000 cells ml and predominantly the *'Stephanodiscus Hantzschii'* species. The air requirement for the flotation process to produce an optimum treated water turbidity was 6 to 8% recycle at 345 KPa. The optimum quantity of air required was 5 to 7gm air m^3 of raw water. This result confirmed the earlier work done by Packham and Richards (1975). A comparison between packed and unpacked saturators at water temperature of 11 ° C, showed that the efficiency of the unpacked saturator was 60 to 65% of the efficiency of the packed saturator. Finally Hyde (1975) suggested that further investigations need to be carried out in the following areas:

1. Optimisation of the flocculation process to give efficient flotation
2. Sludge removal methods for large-scale plants and
3. Operating experience with different types of water.

In the Netherlands, Stork (1977) reported that a pilot plant study was carried out on river and well water using a flotation process for the treatment of potable water. The length, width and depth of the flotation tank were 3.60m, 1.0m and 1.8m respectively. The recycle ratio was 2.5 to 10% and the applied saturator pressure was 7 atmospheres. Prior to flotation, the raw water was coagulated with chlorinated ferrous sulphate and rapidly mixed using a mechanical mixer. This was followed by two-stage flocculation in an equal tank volume of $5.04m^3$. The outside diameter of the paddle used for flocculation was 1.22m. The dimensions of the paddle blade were 1.5m high, 0.115m wide and 0.04m thick. Tapered flocculation was employed. In the first compartment, the mixing speed was 6 rpm (revolutions per minute) and in the second compartment 5 rpm. The results of the study for surface water showed that algal removal was effective without any increase in coagulant dose. There was also no clear influence of coagulant dose on turbidity and flotation treated water. Results from the treatment of deep well water showed that the residual coagulant in the flotation treated water was rather high due to the shorter length of the flotation tank. The dimensions of the tank used in this study were 1.425m length, 0.97m width and 1.8m depth. Further research work in the Netherlands indicated that there is a need to investigate the capability of DAF to remove micro-organisms in order to reduce chlorine or ozone dosage (Puffelen *et al.*, 1995).

In Sweden and Finland, case studies performed on a drinking water treatment plant showed that the flotation process was superior to sedimentation (Rosen and Morse, 1977). The advantages of flotation included shorter flocculation time, higher surface loading and filtration rate, longer backwash interval for the filter (longer filter run), drier sludge content and better algal removal. However turbidity removal was not effective during winter due to the extreme temperatures encountered in the Scandinavian countries. The reason could be explained from Equation 2.4 (Section 2.4.2.1) where at a lower temperature, the viscosity is higher, causing lower rising rate of the bubbles. Thus a longer time would be required to separate the particles from the liquid.

In England, Rees *et al.* (1979) continued with further investigations on five different types of water from different water undertakings. Five plants, each with a capacity of $95m^3$ /hour were constructed to treat the following waters:

1. Three-day stored water with algal problem (Langham Treatment Works, Essex Water Company)
2. Water from a flashy, hard stream (Buklesham Pumping Station, Anglian Water Authority)
3. Turbid river water (Strensham Treatment Works, Severn-Trent Water Authority)
4. Low turbidity, highly coloured water (Arnfield Treatment Works, North West Water Authority)
5. Nutrient-rich, long-term stored water with algal problems (Ardleigh Treatment Works, Ardleigh Reservoir Committee)

The objectives of the study were to assess the effectiveness of the process for different types of water, to develop full-scale plant design criteria and to look for proper methods of sludge removal.

The result of the investigation for stored water with algal problems showed that aluminium sulphate performed better than ferric sulphate. Algal removal could be further enhanced by pre-chlorination. When compared to sedimentation, DAF performed much better, for example *'Aphanizomenon'* algal species with 179,000 cells ml in raw water was found to have 23,000 cells/ml in water treated by sedimentation and only 2,800 cells ml when treated by flotation. Process comparison reported by Rosen and Morse (1977) showed that 95% removal of algae could be achieved using DAF compared with 65% using sedimentation. However the pilot plant experienced by Kaur *et al.* (1994) indicated that the DAF plant was not particularly effective for the removal of algae compared to a sand/anthracite filter. For high turbidity river water and low turbidity highly coloured water, the performance of DAF could be improved if a slightly higher dose of coagulant is added. At higher raw water turbidity of 140 to 155 FTU, turbidity could be reduced by reducing the flow rate at the treatment plant from 95 to 85.5 m^3/hour. However there was no attempt to find the relationship between turbidity removal and different

output capacities of the plant. In terms of colour removal, it was found that sedimentation was better than flotation. Raw water of 45^0 Hazen became 2^0 Hazen after flotation and zero after sedimentation. However the output (surface loading) of sedimentation tanks was only 0.9 m/hour compared with 12 m/hour (i.e. $m^3/m^2/hr$) using flotation. Rees and co-workers also indicated that a three-stage flocculation of 12 minutes without tapering was sufficient to produce a good flotation process. The same idea of non-tapering was suggested by Zabel and Melbourne (1980) except for those plants treating turbid river water. They indicated that the mean velocity gradient should be $70sec^{-1}$. In chemical waste water treatment, Ødegaard (1995) also indicated that tapered flocculation was not suitable and suggested the optimum velocity gradient for flocculation/flotation should be 60 to $80sec^{-1}$. However the importance of tapered mixing has long been used for flocculation design (Hudson and Wolfner, 1967) and its effectiveness has been recognised by many authors (Kawamura, 1976). Experimental works by Klute *et al.* (1995) and pilot and full-scale plants studies by Schofield (Schofield *et al.*, 1991; Schofield, 1995a; Schofield, 1995b) indicated that tapered G (velocity gradient) values between 25 to 80 sec^{-1} are favourable. However their findings may only be appropriate to the particular type of water used. The finding by Rees *et al.* (1979) may form another option in water treatment design particularly with the coagulation and flocculation processes. Further work may be needed to confirm those conflicting results. Pressures between 350 and 420 KPa (i.e. between 3.5 and 4.2 bar) and recycle of 7 and 8% were adequate for an optimum performance (Rees *et al*, 1979). The total air requirement was between 7 to 10gm of air per cubic metre of treated water. This result was in an agreement with the works of Vosloo *et al.* (1986). For sludge removal, a mechanical device was recommended so that sludge with high solid content could be removed.

2.4.1.2 Research Work in United States

In the United States a flotation process for water clarification was suggested by Hopper (1945). He investigated 34 different raw water surface supplies which were normally used in North Carolina. A wetting agent was employed for foam flotation and his results indicated that the average reductions in turbidity, suspended solids and bacteria were approximately 70%, 79% and 90% respectively. The figure on turbidity

removal reported by Wang and Mahoney (1989) was only around 45% and colour removal was at approximately 50%. Further investigations were conducted by Hopper and McCowen (1952) on the toxicity of certain surface-active agents, the chemistry of the process, the bacteriology, the parasitology, the effects of temperature as well as the use of an electron microscope assisted in the determination of how small a particle could be removed. The results of the investigation may be summarised as follows:

1. The quaternary ammonium compound could be used as a surface-active agent provided that its residual concentration after treatment is less than 1 part per million (ppm).
2. The surface-active agent used worked very well in the flotation process for the purification of water.
3. The removal of bacteria achieved could be up to 99%, computed by the plate count method.
4. 100% cyst (*E.histolytica*) removal could be achieved in treating water with a turbidity of 300ppm.
5. The process could work for both hot and cold water (34^0F).
6. 95%.of particles measuring 259 μ m could be removed.
7. The water should be chlorinated in the usual manner before leaving the treatment plant.

Recently Edzwald and Walsh (1992) made laboratory and pilot plant investigations on dissolved air flotation under the sponsorship of the American Waterworks Association Research Foundation. The primary objectives of this research work were as follows:

1. To look into the air requirement for the process (in terms of percentage recycle or bubble volume concentration) as a function of raw water quality and flocculated turbidity for clay waters, waters containing fulvic acid (FA) or natural colour and waters containing algae.

2. To make a comparison between dissolved air flotation and conventional gravity settling (plain sedimentation) processes for the above waters for different pretreatment conditions, flocculation times and overflow rates.

3. To investigate the effects of flocculation time on dissolved air flotation performance.

In order to proceed efficiently with the objectives, typical design and operation parameters for dissolved air flotation process were compiled from various sources. These parameters are listed in Table 2.1.

Table 2.1-Typical design and operation parameters for DAF
(Source: Edzwald and Walsh, 1992)

PARAMETER	DESIGN VALUES RANGE	DESIGN VALUES TYPICAL
CHEMICAL PRETREATMENT:		
Coagulation dose	Determine from jar test	
Flocculation time (minutes)	5 - 30	20
G value (per second)	10 - 150	70
FLOTATION TANK DESIGN:		
Detention time (minutes)	5 - 15	10
Depth (m)	1.0 - 3.2	2.4
Overflow rate (m/hr.)	5 - 15	8
Freeboard (m)	0.1 - 0.4	0.3
AIR SATURATION SYSTEM:		
Operating pressure (KPa)	350 - 620 (50 - 90psi)	485 (70psi)
Recycle ratio (%)	6 - 30	6 - 12
Bubble size (μm)	10 - 120	40 - 50
Saturator efficiency, packed (%)		90
Saturator efficiency, unpacked (%)		70
SLUDGE:		
Percent solid (%)	0.2 - 6	3

Three phases of studies were conducted by Edzwald and co-workers. In phase 1, it was to vary the recycle or bubble volume concentration for three synthetic waters

(clay water, aquatic fulvic acid water and water containing algae). In phase 2, an examination of air requirements at two concentrations for each synthetic water at a temperature of 6 ± 2^0C was carried out. While in phase 3, side-by-side comparisons of DAF with conventional gravity settling (plain sedimentation) were done.

Bench-scale studies were conducted using a DAF system manufactured by Aztec Environmental Control Ltd., United Kingdom. For pilot plant studies, a continuous flow DAF unit manufactured by PURAC, Inc., was used.

Results of bench-scale studies showed that for a bubble volume concentration of 4600 ppm or less it was able to treat all types of water used. This included fulvic acid with dissolved organic carbon of 2 to 15 mg/l, clay with 20 to 100 mg/l and algae of $2x10^4$ to $5x10^5$ cells/ml. However cold water of 6 ± 2^0C gave higher turbidity than warm water of 20 ± 2^0C. Comparisons of DAF to conventional gravity settling (plain sedimentation) showed that the overflow rate was in the ratio between 6:1 and 12:1. Large-size flocs were not required because it has been shown that by using pinpoint-size flocs for water spiked with 10^4 cells ml higher turbidity removal could be achieved. Further works by others (Klute *et al.*, 1995; Bunker *et al.*, 1995) showed pinpoint-size flocs were favourable. Floc size in the range of 30 to 45μm at pH 6.0 was reported to have given the best particle removal efficiency. Removal of ultraviolet absorbance, dissolved organic carbon and true colour at the same pH and coagulant dose indicated that the performance of DAF and conventional gravity settling were the same.

In the pilot plant studies flocculation times of 8 or 16 minutes gave good results for floated and filtered water quality. Long periods of flocculation are not necessary for the DAF process (Edzwald *et al.*, 1992). These results are probably appropriate to the pilot plant and have limited application. Survey works by Haarhoof and Vuuren (1995) on 12 treatment works in South Africa showed that flocculation times vary from 5 to 120 minutes whereas in Finland the range was 20 to 127 minutes for 30 treatment plants (Heinanen,1988). The flocculation period is very much dependent on water temperature and therefore shorter times could be achieved in South Africa

compared to Finland. Further results from Edzwald *et al.*, (1992) indicated that a particle size of approximately 20 μm with 8 minutes of flocculation was reported to produce an excellent performance for flotation. If the flocculation process was abandoned, then a poor performance on flotation was observed. However other workers (Ho and Tan,1989) reported that the removal of suspended solids was only increased marginally from 94.4% to 97% when flocculation was introduced prior to flotation for the treatment of palm oil mill effluent. The study (Edzwald *et al.*, 1992) also revealed that the reduction of ultraviolet absorbance and removal of dissolved organic carbon were not dependent on flocculation time but on coagulation. Further works by Plummer *et al.* (1995) on the same pilot plant showed that 10 minutes of flocculating time was good enough for DAF to produce a lower water turbidity than sedimentation. The removal of *cryptosporidium* (i.e. protozoa that causes diarrhoeal disease) was found to be more effective using DAF than plain sedimentation under a variety of treatment conditions.

Prior to the above investigation, extensive laboratory studies (Edzwald and Wingler, 1990; Malley and Edzwald, 1991b) were made to examine the fundamentals of DAF for the treatment of drinking water and to develop a rational basis for facility design and operation. These studies showed that DAF performance was dependent on raw water quality, pretreatment, bubble size and bubble volume concentration. However the actual laboratory measurement of bubble size was not conducted during the study period (Edzwald, 1996). A conceptual model was developed by Malley and Edzwald (1991a) to describe the performance of DAF for drinking water treatment. The removal of particles from water by collisions between bubbles and particles as the air bubbles rise in the tank was discussed and Stokes equation was applied. In fact the same equation had been used by other researchers and authors to describe the terminal velocity in flotation (Li and Lam, 1964; Chorlton, 1967; Packham and Richards, 1972a; Reay and Ratcliff, 1973; O'Melia, 1985; MacConnell *et al.*, 1991; Ward, 1992 etc.). The work of Yao *et al.* (1971) on a transport model in water and waste water filtration helped to form the basis of the above conceptual model together with the work by O'Melia (1980,1985), Flint and Howarth (1971), Reay and Ratcliff (1973), Spielman and Goren (1970, 1971) and Spielman and Fitzpatrick (1973).

2.4.1.3 Research Work in South Africa

In South Africa, besides the work done by van Vuuren *et al.* (1967), Bratby and Marais (1974, 1975a, 1975b) contributed considerable knowledge to the field of flotation studies. Bratby and Marais made an attempt to identify parameters influencing the flotation process and determine their inter-relationships. The objectives of their investigation were generally as follows:

1. Development of an efficient flotation system.
2 Determination of parameters which influence the bubble-particle attachment.
3 Establishing any relationship between the fundamental parameters that influence solid removal and thickening of floated solids.

The bench-scale system investigated by Bratby and Marais, (1974) consisted of a saturation and flotation unit. For the saturation unit, three methods of air dissolution were investigated i.e. using sparged air system, pump suction air injection system and packed column system. The latter was found to be superior. The flotation unit used by Bratby and co-worker consisted of two chambers namely upper and lower chambers. The upper chamber of the tank had a constant cross-sectional area and was attached to the lower chamber in which the cross-sectional area increased with depth. According to the authors, this shape gave several advantages such as an increase in opportunity for contact between rising bubbles and particles, providing a rolling effect for the agglomerates as they rise up the slope and thus helping to produce larger agglomerates, and finally the thickened agglomerates at the top could discharge freely into the trough without any mechanical assistance.

The water sample used throughout the experiment was algal-laden waste water from an oxidation pond. Tests were carried out to determine the effect of pH and anions on bubble-particle adhesion. Different pH values were tested for three different coagulants (i.e. ferric chloride, ferric sulphate and aluminium sulphate) for optimum coagulation and flotation. Comparisons of turbidities obtained from the jar test and the actual floated water turbidity (effluent turbidity) with different pH and chemical

dosages were made using a nephelometer. The results showed that the optimum coagulant dose for flotation was 50mg/l as Fe^{3+} at pH 5.65 when ferric chloride was used. This value was not much different from the result of the jar test. The effluent turbidity recorded was 6 on the nephelometer scale. When ferric sulphate was used as a coagulant with an optimum dose of 50mg/l as Fe^{3+} based on a jar test, the optimum pH value for flotation was 5.8 with an effluent turbidity of 11. The increase in turbidity reading suggested that sulphate anions may impair the bubble-particle adhesion. In order to confirm this hypothesis, Bratby and Marais (1974) used aluminium sulphate as a coagulant for the next test. It showed that the effluent turbidity was 18.5 at an optimum dosage of 25mg/l as Al^{3+} and with optimum pH of 5.5. This confirms the hypothesis.

2.4.1.4 Summary of Findings

The results of research on dissolved air flotation which were related to water quality parameters are summarised in Table 2.2 (a). Table 2.2 (b) presents a summary of findings on DAF process performance.

Table 2.2 (a) - Summary of DAF performance related to water quality characteristics

PARAMETERS	FINDINGS	AUTHORS
1.Algae Removal	(a) Better than sedimentation	Packham and Richards (1972b,1975), Hyde (1975), Edzwald and Walsh (1992), Rosen and Morse (1977), Rees *et al.* (1979), Van Vuuren *et al.* (1967)
	(b) Alum performed better than ferric sulphate	Rees *et al.* (1979)
	(c) 95% removal compared with 65% from sedimentation	Rosen and Morse (1977)
2. Colour and turbidity removal	(a) DAF performed same as sedimentation	Packham and Richards (1975)
	(b) Colour of 45° Hazen and turbidity less than 100 FTU is limiting point for DAF	Hyde (1975), Rees *et al.* (1979)
	(c) DAF removed 70% of turbidity and 79% of suspended solids	Hopper (1945)
	(d) Removal of true colour at the same pH and coagulant dose, DAF performed same as sedimentation	Edzwald and Walsh (1992)
	(e) Not much different in result using ferric sulphate or alum	Packham and Richards (1975)
	(f) Turbidity removal not effective in extreme winter conditions	Rosen and Morse (1977), Edzwald and Walsh (1992)
	(g) DAF removed 30 to 45 7% of turbidity and 40.8 to 50.5% of colour	Wang and Mahoney (1989)
3. Residual coagulant concentration	(a) DAF performed the same as sedimentation	Packham and Richards (1975)
4 Bacteria	(a) 99% could be removed	Hopper (1945)
5. Protozoa	(a) *Cryptosporidium* removal more effective using DAF compared with sedimentation	Plummer *et al.* (1995)

Table 2.2 (b) - Summary of DAF performance related to process parameters

PARAMETERS	FINDINGS	AUTHORS
1. Performance at flotation stage	(a) Dependent on the efficiency of flocculation	Packham and Richards (1975), Edzwald *et al.* (1992)
2. Velocity gradient in flocculation	(a) Non-tapering:	Rees *et al.* (1979)
	(i) 70 per sec.	Zabel & Melbourne (1980)
	(ii) 60 to 80 per sec.	Ødegaard (1995)
	(b) Tapered (25 to 80 per sec.)	Stork (1977), Klute *et al.* (1995); Schofield *et al.* (1991); Schofield (1995a, 1995b)
3. Retention times	(a) In flash mixer: 1 1/2 minutes	Hyde (1975)
	(b) In flocculation tank: 7 min ;9 min ;12 min.;8 min.;20 to 127 min ;5 to 120 min.	Packham and Richards (1975); Hyde (1975); Rees *et al.* (1979); Edzwald *et al.* (1992); Heinanen (1988); Haarhoff and Vuuren (1995)
	(c) In flotation tank 20 min ,5 1/2 min.	Packham and Richards (1975); Hyde (1975)
4 Overflow rate	(a) 2 to 4 mm/sec by flotation and 0.3 to 1 3 mm/sec by sedimentation	Packham and Richards (1972)
	(b) DAF:Sedimentation by the ratio 6 1 to 12.1	Edzwald and Walsh (1992)

2.4.2 Theory of Flotation

The principles of flotation based on bubble generation, bubble attachment and solid separation were discussed by Packham and Richards (1972a). They indicated that different techniques of aeration would give rise to different types of flotation system. In the case of bubble-particle attachment several theories were forwarded by various researchers on how the process could take place. These can be summarised as follows:

1. Bubbles grow by precipitation from a supersaturated solution on the surface of the particles (Taggart, 1945)

2. Bubble-particle attachment involves chemical and physical aspects such as surface energy, surface tension, adsorption, contact angle, polarity, surface reactivity, surface condition and adding air-adhering agents to some minerals (Gaudin, 1939)
3. An 'induction time' is required to allow the thin liquid layer between bubble and particles to drain away so that coalescence can occur (Sutherland, 1948)
4. If the surface conditions of the particles are appropriate, the bubbles will collide and coalesce with the particles (Klassen and Mokrousov, 1963)
5. The particle follows its trajectory as it approaches a bubble and this trajectory will be dependent on viscous effects and Reynolds number (Flint and Howarth, 1971)

Vrablik (1959) however indicated that the following mechanisms are important for the bubble attachment process to take place:

1. Adhesion of gas bubbles with the suspended phase as a result of collisions or by nucleation.

2. The trapping of gas bubbles in a floc structure

3. The absorption of gas bubbles into a floc structure as it is formed

In dissolved air flotation, bubble attachment could proceed by all of the above methods. This is due to small bubble size which rise slowly under a small Reynolds number. The adhesion process relies heavily on the application of colloid surface chemical phenomena (Shaw, 1991). The significant effect of electrical potential in adhesion has been discussed by some workers (Collin and Jameson, 1976, 1977, Usui and Sasaki, 1978; Usui *et al.*, 1981). For the bubble-particle attachment process to take place, Bratby and Marais (1974) indicated that it has to be proceeded with destabilisation. Mechanism 1 in principle does not require flocculation but destabilisation between bubbles and particles. Mechanisms 2 and 3 require destabilisation between particles and a certain degree of flocculation before or during flotation However, J.A.Kitchener in his review on flotation (Kitchener, 1984)

indicated that flotation should be viewed as a stochastic event where the chance of a given particle arriving at the froth level is the product of three probability terms:

Chance of flotation =	probability of particle/ bubble collision	X	probability of attachment	X	probability of retention of attachment

2.4.2.1 Kinetics of Flotation

Harper,(1972) indicated that experiments seldom agree with the prediction that a bubble rising in a Newtonian liquid can be treated as if isolated, unless great care is taken to remove impurities. A bubble with constant surface tension rising under gravity will rise steadily if:

1. Its motion is stable relative to random small disturbances

2. The time taken to approach very close to terminal velocity is very much less than the time required for the bubble to change its size significantly.

At a low Reynolds number, the retarding or drag force is parallel and opposite to the terminal velocity with a magnitude of:

$$D \quad 6\pi a\mu U \tag{2.1}$$

where D – drag force
a = radius of bubble
μ= dynamic viscosity
U = terminal velocity

Equation 2.1 was obtained by Stokes for the slow motion of a sphere in viscous fluid (Li and Lam, 1964; Gaudin, 1939). The expression is usually known as Stokes' law for the resistance to a moving sphere (Batchelor, 1988). The derivation of Stokes' law is based on the assumption that the motion of the spherical particle is extremely slow, the liquid medium boundary is at an infinite distance from the particle and also is of a large volume compared with the dimensions of the particle (Shaw, 1991). Clift

et al. (1978) indicated that bubbles are closely approximated by spheres if the interfacial tension and/or viscous forces are much more important than inertia forces and the 'spherical' term can be used if the minor axis to major axis ratio lies within 10% of unity.

When a solid sphere falls vertically in a liquid, the viscous liquid produces a terminal velocity U. By equating the weight of the sphere to the upthrust plus drag (Chorlton, 1967), the following equation is obtained:

$$\begin{aligned} \tfrac{4}{3}\pi a^3 \sigma g &= \tfrac{4}{3}\pi a^3 \rho g + 6\pi a \mu U \\ U &= \tfrac{2}{9}(\sigma-\rho)a^2 g\,\mu \end{aligned} \qquad (2.2)$$

where a = radius of sphere
σ = density of sphere
ρ = density of liquid

Packham and Richards (1972a) indicated that the alum sludge from a DAF water treatment plant rose at a rate of 20 to 35 mm/sec. The rising velocity is far greater than the settling velocity of an aluminium or iron floc encountered in a water treatment works (i.e. normally less than 0.5 mm/sec). Basing their judgement on the fact that the rising rate of the floc in flotation was far greater than the settling rate, Packham and Richards (1972a) considered the rate of separation of suspended matter in the flotation process from the viewpoint of the Stokes' equation governing the motion of a sphere through a viscous medium and thus indicated that Equation 2.2 was appropriate to describe the rise rate of the particle in the flotation process. Packham and Richards (1972a) in reviewing Equation 2.2 were of the opinion that if the size of the suspended matter is increased, a higher separation rate may be achieved. This is due to the fact shown by Equation 2.2 that the rate of separation is directly proportional to the square of the radius of the particles, the difference in the densities of liquid and the suspended particles and inversely proportional to the liquid viscosity.

Research carried out in Russia (Levich, 1962) showed that at small Reynolds numbers, gas bubbles moved like solid spheres. Theoretical values of bubble rise

velocity in water were not in agreement with much experimental data. For a gas bubble which is assumed to behave like a solid, its surface can sustain a finite shear stress, the tangential velocity of the surface is everywhere zero relative to the centre of the bubble, and the conventional Stokes solution applies. According to Jameson (1984) a force balance equation will result as follows:

$$6\pi\mu Ua \quad \tfrac{4}{3}\pi a^3(\rho-\rho_g)g \tag{2.3}$$

When the density of gas ρ_g is negligible compared with the density of liquid ρ, the terminal velocity is given by,

$$U=\frac{2\rho g a^2}{9\mu} \tag{2.4}$$

Equation 2.4 shows that the rise velocity of a bubble is controlled by the size of the bubble and the viscosity of the fluid. If the radius of the bubble is increased, the rise velocity will be increased. The kinematic viscosity is affected by the density and the temperature of the fluid. An increase in temperature will result in the decrease in viscosity and hence an increase in bubble rising velocity. Shannon and Buisson (1980) indicated that bubble rise rates at 80°C increased three times compared to those at 20°C.

Force balance is presented in terms of drag coefficient C_D by Harper, (1972) as follows:

$$C_D=\frac{force.on.bubble}{\frac{1}{2}\rho U^2\pi a^2}=\frac{\frac{4}{3}\pi\rho g a^3}{\frac{1}{2}\pi\rho U^2 a^2}=\frac{4gd}{3U^2} \tag{2.5}$$

This coefficient is the force per unit cross-sectional area, made dimensionless by the dynamic pressure $\frac{1}{2}\rho U^2$. Substituting from Equation 2.4 into Equation 2.5 yields:

$$C_D=24 \quad Re \tag{2.6}$$

where *Re* is the Reynolds number. Equation 2.6 is used for viscous resistance at low Reynolds numbers, *Re* less than 0.5 (Fair *et al.*, 1968). The same equation was used

by Vrablik (1959) to determine the maximum bubble size of 130 microns for a complete viscous flow. He indicated that the maximum value of Reynolds number for laminar or viscous flow is 1.13. The relationship governing bubble size, laminar flow, bubble rising velocity (as per Equation 2.4) and temperature has been established. This relationship is shown in Table 2.3. The optimum bubble rise velocity for the DAF system is about 300mm/minute (Krofta and Wang, 1989). The rising velocity should not be below 125 mm/minute or more than 500 mm/minute.

Table 2.3 - Relationship between bubble size, rise velocity, temperature and laminar flow (Source: Malley, 1988)

Bubble size (μm)	Rise Velocity (m/hr) Above Which Turbulent Flow Exists*		Terminal Rise Velocity (m/hr) Based on Stokes' Law	
	4°C	20°C	4°C	20°C
10	565	360	0.125	0.196
20	283	180	0.499	0.783
30	188	120	1.12	1.76
40	141	90	2.00	3.13
50	113	72	3.12	4.89
80	70.7	45	7.99	12.5
110	51.4	32.7	15.1	23.7
120	47.1	30	18.0	28.2
130	43.5	27.7	21.1	33.1•
140	40.4	25.7	24.5	38.3•
160	35.3	22.5	31.9	50.1•
170	33.2	21.2	36.1•	56.5•

* Based on a critical Reynold's Number of 1.0 for the upper limit of laminar flow.

• Indicates the terminal rise velocity will result in turbulent flow.

Experimental work by Fukushi *et al.* (1995) showed that Equation 2.4 could not be used to describe bubble rise velocity. This is due to the turbulent environment which occurs in the mixing zone (reaction zone) of the DAF tank. They suggested that the following equation is more appropriate and agreed with their experimental results:

$$U \quad \frac{\rho g a^2}{3\mu} \tag{2.7}$$

Table 2.4 - Models developed by Fukushi *et al.* (1985) and Edzwald *et al.* (1990), (Source: Fukushi *et al.*, 1995)

Models	Fukushi *et al.* (1985)	Edzwald *et al.* (1990)
Generated Air Bubbles:		
Size range d_a (μm)	10-120 (average 60)	10-100 (average 40)
Rise velocity (cm/sec)	$gd_a^2/12\nu$	$gd_a^2/18\nu$
Zeta potential (mV)	-150 at pH 7	not measured
Pressure P (kPa)	392	345-585
Recycle ratio r	0.1	0.08
Concentration n_a (cm^{-3})	10^4-10^5	10^4-10^5
Produced flocs:		
Size range d_f(μm)	10^0-10^3	10^0-10^2 (10-30μm is best)
Density ρ_f(g/cm^3)	floc density function	1.01 (assumed)
Suitable mobility (μm/secVcm)	0 - +1 (clay floc) -1 - +1 (colour floc)	0.5 or less
Bubble-floc collision and attachment		
Collision model	population balance model	single collector collision
Flow regime	turbulent flow	laminar flow
Mechanism	locally isotropic turbulence, viscous subrange diffusion	Brownian diffusion, interception, gravity settling
Attachment mechanism	electrical-charge interactions (coverage of precipitated coagulant on a floc surface)	electrical-charge interaction, water layer at floc surface
Rise velocity of agglomerate (cm/sec)	0.1 - 2.6 (observed)	about 0.3 (nearly equal to bubble rise velocity)

g=gravity d_a=diameter of bubble ν=kinematic viscosity
d_f=diameter of floc ρ_f=density of floc

A comparison on the properties of air bubbles produced in the dissolved air flotation process was made by Fukushi *et al.* (1995) to those developed by Edzwald *et al.* (1990). There are many discrepancies existing between both models. These are shown in Table 2.4. The model which was developed in 1985 by Fukushi and co-workers was based on the population balanced model of bubbles and flocs in a turbulent flow environment (PBT model). However the model developed by Edzwald

was derived from a single collision theory in a laminar flow condition (SCC model). In the SCC model collision occurs due to Brownian diffusion, interception and gravity settling. Fukushi *et al.* (1995) indicated that Brownian diffusion and gravity settling cannot be dominant for a normal floc (10-1000 μm) and bubble size range in flotation. Interception also cannot be dominant because in practice the mixing zone is apparently in a turbulent flow where a certain energy dissipation occurs.

In fact the literature survey indicated that Equation 2.7 was originally suggested by V. G. Levich in 1962. Levich (1962) indicated that Equation 2.7 is applicable for small Reynolds numbers, $Re<<1$ and when the following inequality holds:

$$\frac{ga^3}{3\upsilon^2} \angle\angle 1 \tag{2.8}$$

where $\upsilon \quad \mu/\rho$ (i.e. kinematic viscosity equals dynamic viscosity divided by density of liquid). If the medium is water, the size of moving bubbles will be $a<<2\text{x}10^{-2}$ cm. Levich also indicated that the theoretical value of the drag coefficient for a gas bubble in water is equal to $\frac{8}{\text{Re}}$ (i.e. one and one-half times smaller than for a solid sphere). This value is not in agreement with Equation 2.6. However Levich indicated that Allen's experimental results (Levich, 1962) with small Reynolds numbers completely disagree with the theory and lead to values for the drag coefficient which coincide exactly with the drag on a solid sphere.

A mathematical equation for solid/liquid separation was developed by Howe (Packham and Richards, 1972a) limited to flotation of discrete particles without the interference of surface active forming agents. It was derived from a differential equation of motion which was expanded to give solutions for the rising velocity of a particle with changes in the applied rising force, particle diameter, liquid viscosity and particle density (Howe, 1958). The equation is as follows:

$$R = 1 - e^{-\left(\frac{V_r}{Q\ Ah}\right)} \tag{2.9}$$

where R = ratio of total removal of solid concentration after flotation to the inflow solid concentration

$= 1\text{-}C_o/C_i$

C_o = the effluent suspended solids

C_i = the influent suspended solids

V_r = the rising velocity of a single particle/air bubble

Q = the flow applied to the flotation unit

Ah = the horizontal area of the unit

Equation 2.9 is limited to discrete particles without the interference of surface-active forming agents.

Karamanev (1994) in his article on the rise of bubbles in quiescent liquid indicated that equations based on the model of bubble with internal circulation often fail to describe the real systems adequately. This is because even highly purified liquids (such as triple distilled water) contain enough surface-active components to affect internal bubble recirculation. Recirculation is normally due to the presence of surface-active substances and the resulting variable surface tension leads to a change in boundary conditions of the bubble (Levich, 1962). According to Karamanev (1994) the most reliable semi-empirical equation is that of Davies and Taylor:

$$U \quad 25V^{1/6} \tag{2.10}$$

where V is the volume of the bubble. However this equation works only for large, spherical cap-shaped bubbles. The drag coefficient C_D of the gas bubble calculated on the basis of equivalent sphere diameter by most authors was found to have a large deviation of C_D as a function of Reynolds number when different liquids are used. The assumption made by most authors for free-falling heavy spheres behaving exactly like free rising solid spheres is found to be incorrect especially for particles with densities less than 0.3gm/cm^3 and Re>130 rising in water. Karamanev (1994) suggested the following equation based on the balance of forces acting on a rising bubble:

$$\tfrac{1}{2} C_D S \rho U^2 = \Delta \rho g V \tag{2.11}$$

where ρ is the liquid density, Δρ is the difference of density between liquid and gas and S is the area of bubble. In order to obtain C_D based on real bubble geometry, the area S should be determined from the diameter projected on the horizontal plane circle, d_h; $S \quad \pi d_h^2 \quad 4$. Then the volume of the bubble is calculated using the equivalent diameter; $V \quad \pi d_e^3 \quad 6$. These values are substituted into Equation 2.11 and become:

$$C_D = \frac{4g\Delta\rho d_e^3}{3\rho d_h^2 U^2} \tag{2.12}$$

Equation 2.11 can be written in terms of U:

$$U = \left(\frac{8gV}{\pi C_D d_h^2}\right)^{1/2} \tag{2.13}$$

By substituting from Equation 2.12, then:

$$U = \left(\frac{8g}{6^{2/3}\pi^{1/3}C_D}\right)^{1/2} V^{1/6}\frac{d_e}{d_h} \tag{2.14}$$

For Re less than 130, Karamanev suggested that C_D can be calculated using the following equation:

$$C_D = \frac{24\left(1+0.173Re^{0.657}\right)}{Re} + \frac{0.413}{1+16300Re^{-1.09}} \tag{2.15}$$

For spherical bubbles at Re less than 1, then $C_D \quad 24\,Re$ and $d_e/d_h - 1$ and Equation 2.12 transforms to Stokes equation.

2.4.2.2 Solubility of Air

In flotation, the quantities of air used are normally expressed in terms of volume of air supplied per volume of water treated (Edzwald and Walsh, 1992) and Henry's Law is used when treating saturated water as a dilute solution of air in water (Vrablik, 1959). It must be remembered that Henry's law was originally based on his experiment with N_2, O_2, N_2O, H_2S and CO_2 and only with water at one temperature. The concept that the law could be used for general application is unfounded (Gerrard, 1980). However experimental work on wastewater with dissolved solids up to 1000mg/l with pressures up to 500KPa showed that Henry's law constant could be

used to calculate the mass of dissolved air (Lovett and Travers, 1986). For ideal-dilute solutions where the solute obeys Henry's law but not Raoult's law and the solvent obeys Raoult's law, then the use of Henry's law is applicable (Backhurst *et al.*, 1974; Atkins, 1994).

$$p_B \quad x_B K_B \tag{2.16}$$

where p_B is the vapour pressure, x_B is the mole fraction of the solute and K_B is constant.

Based on Henry's law, Edzwald and Walsh (1992) suggested the following equation:

$$c_s = f\frac{p}{k} \tag{2.17}$$

where c_s is the concentration of air in the saturated liquid, p is the absolute pressure, k is the Henry's Law constant and f is the efficiency factor which is about 70% for unpacked saturators and up to 90% for packed systems. Values of k at 0^0C and 25^0C are 2.72 and 4.53 Kpa/mg/l respectively.

However, others (Takahashi *et al.*, 1979; Ward, 1992) indicated that Henry's Law is not strictly applicable when treating saturated water. The equation has to be modified (Ward, 1992) with an exponent m on the pressure p as follows:

$$c_s = \frac{p^m}{k} \tag{2.18}$$

Klassen and Mokrousov (1963) in their review on the solubility of gases in water were of the opinion that the solubility of gases depends on the partial pressure, temperature and concentration of other substances in the solution. If the partial pressure is increased then the solubility of gas will be increased. However if the concentration of soluble substances in water is increased, gas solubility will be decreased as a result of complexing definite quantities of water molecules in the form of hydrated ions. Edwards (1984) added that if the total pressure is less than 507 Kpa (5 atmospheres), the solubility for a particular partial pressure of solute gas is normally independent of the total pressure of the system. In its relationship to temperature, the solubility of a gas will be decreased when the temperature is

increased (Vrablik, 1959; and Eckenfelder *et al.*, 1958). This is as illustrated in Figure 2.8. In the case of distilled water, when the temperature is increased from zero to 30°C, the solubility of air is reduced by 45%. Liquid solubility of the gases varies as shown in Table 2.5.

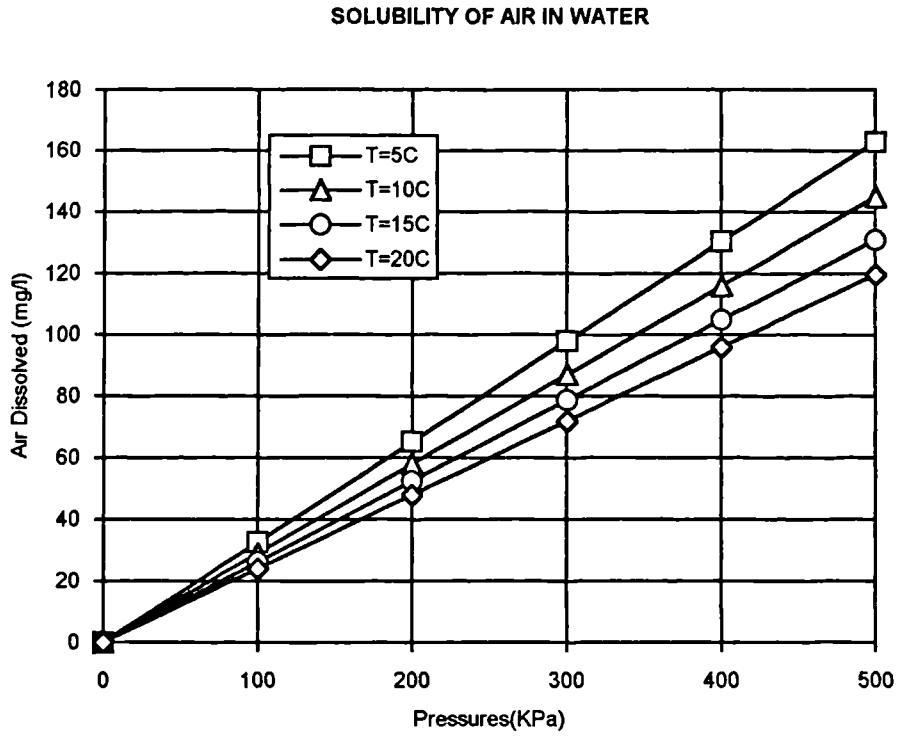

Figure 2.8 - Solubility of Air in Water (Source: Zabel and Melbourne, 1980)

Bratby and Marais (1975b) in their studies on saturator performance indicated that it would be difficult to achieve full saturation at a saturator pressure less of than 350KPa. From an economic point of view, the efficiency of the saturator system was important. They found that by using a packed system of 0.5m depth with Raschig rings of 25mm diameter, full saturation was achieved at saturator pressures beyond 250KPa for a surface loading up to 2500m/day. A similar level of saturation was found by Zabel and Hyde (1977) using a packed saturator of 0.75m depth with 25mm Berl saddles.

For design purposes Bratby and Marais (1977) suggested that at a temperature of 20°C with a pressure of 3 atmospheres, the concentration of air precipitated on reducing the pressure to atmospheric is given by the following equation:

$$a_p \quad 19.5P \ mg \ litre \tag{2.19}$$

where P is the saturator pressure in atmospheres.

Table 2.5 - Solubility of various gases at 20°C and 760mm Hg (Source: Vrablik, 1959)

Types of Gas	Cubic cm gas/Cubic cm water	Gram of gas/100 gm of water
Nitrogen	0.015	0.0019
Oxygen	0.031	0.0043
Hydrogen	0.018	0.00016
Carbon dioxide	0.88	0.17
Carbon monoxide	0.023	0.0028
Air	-	1.87
Hydrogen sulphide	2.58	0.38
Sulphur dioxide	39.4	11.28

2.4.2.3 Bubble Generation

Rykaart and Haarhoff (1995) indicated that the geometrical design and operating conditions of the injection nozzles were important determining factors for bubble size. They reported that saturation pressure does not have a consistent effect on nozzle efficiency. There were contradicting claims regarding whether a higher pressure produces smaller bubbles (Takahashi *et al.*, 1979; Gulas *et al.*, 1980) or a higher pressure produces bigger bubbles (Ramirez, 1980; Lovett and Travers, 1986). But Jone and Hall (1981) reported that there was no significant relationship between pressure variation and bubble size.

Studies by Bratby and Marais (1975b) showed that the shape and roughness of the valve, the degree of turbulence and dilution of saturator feed downstream of the valve and the concentration of particulate nuclei in the dilution water had a negligible effect on the precipitation of air from a solution (i.e. mass of air precipitated to unit volume of saturator feed). However these findings were contradicted by those reported by others (Takahashi *et al.*, 1979; Rykaart and Haarhoff, 1995) in terms of the shapes and roughness of the valves. Rykaart and Haarhoff (1995) showed that at a saturator

pressure of 500 Kpa nozzle with a bend in its channel produced a bubble size of 49.4 μm (median diameter) compared to a nozzle with a tapering outlet which produced 29.5μm. When the saturator pressure was reduced, the bubble sizes were reduced.

For a continuous flow dissolved air flotation plant, Edzwald and Walsh (1992) predicted that the concentration of air released in the tank (C_r) would be as follows:

$$C_r = \left[\left(\frac{C_s - C_a}{1 \quad R_r}\right)R_r - K\right] \tag{2.20}$$

where C_a is the concentration of air that remains in solution at atmospheric pressure, R_r is the recycle ratio which is equal to the recycle flow rate divided by the influent flow rate, and K is the influent saturation factor defined as $(C_a\text{-}C_o)$ where C_o is the concentration of air in the influent water. In most cases C_o is saturated and this means K 0. In order to find the bubble volume concentration (ϕ_b), Edzwald and Walsh (1992) suggested that C_r should be divided by the saturated density of air (ρ_{sat}) as shown in the following equation:

$$\phi_b \quad C_r / \rho_{sat} \tag{2.21}$$

In order to get the generated air volume at the same temperature under atmospheric pressure Takahashi *et al.* (1979) used the following equation by considering air as an ideal gas:

$$V_A = \left(\frac{\rho_w}{M_w}\right)\left(\frac{P_A - P_O}{P_O}\right)\frac{RT}{H_E} \tag{2.22}$$

where ρ_w is the density of water in gm/cm^3, P_A is the dissolved pressure in dyne cm^2, P_o is the atmospheric pressure in dyne cm^2, R is the gas constant in erg/K.mole, T is the absolute temperature in Kelvin, M_w is the molecular weight of water in g/g.mole, and H_E is the Henry's Law constant in dyne cm^2.

By assuming all the dissolved air in water changes into bubbles, then from Equation 2.18, the theoretical generated flow rate will be obtained. The experimental results by Takahashi *et al.* (1979) showed that the generated air flow rate increased with an increase in dissolved pressure and also with an increase in liquid flow rate. In order

to obtain the volume of air occupied by a single spherical bubble, V_b, Takahashi and co-workers suggested the following equation:

$$V_b = \left(\frac{P_O + \rho_w g h + 4\sigma \ d_{av}}{P_O} \right) \frac{\pi}{6} d_{av}^3 \tag{2.23}$$

where; h is the depth from the liquid surface to the bubble in cm, σ is the surface tension in dyne/cm and d_{av} is the volumetric mean diameter of bubble in cm. According to the authors the effect of liquid depth is negligible thus the measurement of bubble diameter was carried out at the top of flotation tank. The number of bubbles generated per cubic cm of water could be obtained from Equation 2.24:

$$N_b = \frac{G \ Q}{V_b} \tag{2.24}$$

where G is the volumetric flow rate of air generated under decrease in pressure (cubic cm/sec) and Q is the volumetric flow rate of liquid (cubic cm/sec). Their experimental results showed that by increasing the dissolved pressure and liquid flow rate, the number of bubbles will be increased. The geometry of nozzle also affects the bubble size. By using a needle valve, Takahashi and co-workers obtained the following equation:

$$N_b = 1x10^4 \left(\frac{P_A - P_O}{P_O} \right)^2 Q \tag{2.25}$$

Comparisons of the calculated and experimental values of the number of bubbles were made and the results were claimed to be remarkably in agreement with the equation used.

For an efficient solid-liquid separation process, small bubbles are needed (Cassell *et al.*, 1975; Collin and Jameson, 1976; Rovel, 1977). Bubble sizes in the range of 20 to 80 microns are capable of good attachment to floc particles. Larger bubbles will create a hydraulic disturbance along their rising path towards the surface and a decrease in the surface area. For example one 2mm bubble contains the same amount

of air as 64,000 bubbles of 50 microns in size. Cassell *et al.* (1975) reported that the optimum bubble size in the microflotation process is approximately 50 microns.

2.4.2.4 Collision

Reay and Ratcliff, (1973) in their studies of dispersed air flotation defined the collection efficiency of a bubble as the fraction of particles in the bubble's path which are actually picked up by the bubble. Particles of about 3 microns diameter or larger will not be affected by Brownian motion. They will be in contact with the bubble only if their hydrodynamically determined trajectories come within one particle radius (r_p) of the bubble. This region is called the collision regime. By considering the collision regime in which the Brownian diffusion is negligible (Gochin, 1990), the collection efficiency of a bubble can be expressed as:

$$\eta=\eta_1 x\ \eta_2 \tag{2.26}$$

where η_1 = collision efficiency,.i.e. the fraction of particles in the bubble's path which actually collided with the bubble

η_2 – attachment efficiency, i.e. the fraction of particles colliding with the bubble which actually stick to it

Equation 2.26 indicates that η_2 will depend mainly on the chemical nature of the particle surface, the bubble surface and the thin film of liquid draining from between them. Reay and Ratcliff (1973) also reported on the predicted collision efficiency together with a graph drawn and $\eta_1=1.25\left(r_p/R_b\right)^{1.9}$ for $\left(\rho_p/\rho_f\right)=1$, and $\eta_1=3.6\left(r_p/R_b\right)^{2.05}$ for $\left(\rho_p/\rho_f\right)$ 2.5 and η_1 is roughly proportional to $\left(r_p/R_b\right)^2$ over the density range used. The symbols used in the above expression are interpreted as follows:

r_p – particle radius (cm)

R_b bubble radius (cm)

ρ_p – particle density (gm/ml)

ρ_f = fluid density (gm/ml)

Since η_I is proportional to R_b^2, the average number of particles picked up by a bubble (by assuming η_I is constant) should be roughly independent of bubble size and the flotation rate should be proportional to bubble frequency (i.e. the amount of bubbles rather than bubble diameter over the entire range of particle sizes). This prediction is applicable to bubbles of diameter up to 0.1 mm (Reay and Ratcliff, 1975). However when latex particles (3 to 9 microns) having almost the same density as water and larger zeta potential (+10.6mV) were used in the experiments, they could not get so close to the bubble surface (Reay and Ratcliff, 1975). This means the bubble-particle collision model is not appropriate for latex particles.

Flint and Howarth (1971) in their review on the collision efficiency of small particles with spherical air bubbles reported that the collision of a particle with a bubble would depend on the balance of viscous, inertial, and gravitational forces acting on the bubble. Besides that the form of streamlines around the bubble also play an important role in whether or not collision takes place. Flint and Howarth (1971) formulated an equation of motion of a small spherical particle relative to a spherical bubble rising in an infinite pool of liquid in the jth direction as follows:

$$m_p \frac{av_j}{at} = G_j + C_d\left(u_j - v_j\right) \tag{2.27}$$

where G_j – the body force acting on the particle, for raindrop collision, $G_j=0$. In flotation there is clearly a component of relative acceleration due to gravity because the bubble and particle are of distinctly different densities.

C_d – dimensional drag coefficient for the particle, depending on the shape of the particle and the Reynolds number past it. For a spherical particle, the drag will be the same in all directions.

v_j – particle velocity.

u_j = the velocity the fluid would have at the position of the particle if no particle were there. For fine particles in flotation, it is assumed that the flow around the particle has an insignificant effect compared with the

flow pattern due to the bubble; u_j then depends on the shape of the bubble and the Reynolds number around it.

t time

By considering the relative two dimensional motion of a spherical bubble and particle where the bubble is held stationary at the origin of the co-ordinate system by a liquid flow equal to the bubble rise velocity in the negative direction (Figure 2.9), then Flint and Howarth, (1971) suggested the equation of motion for the particle as follows:

$$\tfrac{4}{3}\pi r_p^3 \rho_p \frac{\partial v_y}{\partial t} = 6\pi\mu_f r_p\left(u_y - v_y\right) \tag{2.28}$$

$$\tfrac{4}{3}\pi r_p^3 \rho_p \frac{\partial v_x}{\partial t} = -\tfrac{4}{3}\pi r_p^3\left(\rho_p - \rho_f\right)g - 6\pi\mu_f r_p\left(u_x - v_x\right) \tag{2.29}$$

Reducing the above equations to dimensionless form and introducing the variable v, u and t, and parameters K and G:

$v_x^* = {}^{v_x}/_{u}$ $\qquad$ $v_y^* = {}^{v_y}/_{u}$

$u_x^* = {}^{u_x}/_{u}$ $\qquad$ $u_y^* = {}^{u_y}/_{u}$

$t^* = {}^{tu}/_{r_b}$

and $K \quad 2\rho_p r_p^2 u \quad 9\mu_f r_b$,

$G = 2\left(\rho_p - \rho_f\right)r_p^2 g \quad 9\mu_f u$

i.e. $K\dfrac{\partial v_y^*}{\partial t^*} = u_y^* - v_y^*$

$K\dfrac{\partial v_x^*}{\partial t^*} = -G - u_x^* + v_x^*$

where: r_n = particle radius

ρ_n = particle density

ρ_f – fluid density

v component of particle velocity

t = time

μ_f fluid viscosity

u = component of velocity field due to bubble

x, y – cartesian position co-ordinates

u – dimensionless component of bubble velocity field

v = dimensionless component of particle velocity

t = dimensionless time

K = particle inertia parameter

G = dimensionless settling velocity of particle

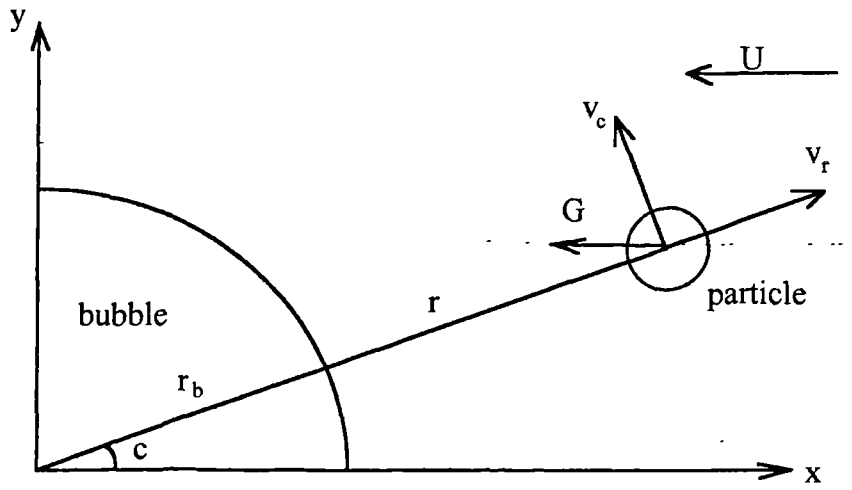

Figure 2.9 - Geometry of bubble-particle system (Source: Flint and Howarth, 1971)
Note: r_b – radius of bubble, r = radial coordinate, G = dimensionless settling velocity of particle, U = bubble rise velocity, c = spherical coordinate, v = component of particle velocity.

According to Flint and Howarth (1971) calculation for K down to 0.001 shows that the collision efficiency remains substantially constant for $0.001<K<0.1$, meaning that collision efficiency is virtually independent of K and independent of whether Stokes or potential flow is assumed. They suggested that for a fine particle characterised by K less than 0.1, inertial effects of the particle may be neglected and single bubble collision efficiency η, can be calculated from:

$$\eta = G/(1+G) \tag{2.30}$$

However Flint and Howarth (1971) indicated that in the flotation tank the collision efficiency may be several times as great as those predicted from single bubble calculations. This may be due to at least three reasons:

1. The presence of hindering effects of the neighbouring bubbles which reduced the rising velocity of the bubble. For fine bubbles this could lead to an increase in collision efficiency
2. Difference in the shape of liquid stream-lines around the bubble. The greater the number of bubbles, the closer the assemblage and the straighter the stream-lines. This result in the increase of collisions between the particles and bubbles
3. The motion of particles upstream from the target bubble is influenced by the layers of bubbles ahead and thus is no longer parallel to the direction of bubble motion.

The above opinion which was expressed by Flint and Howarth is found to be in agreement with Fukushi *et al.* (1995) as the latter showed that a single-collector collision model was not appropriate in the dissolved air flotation process. Furthermore King (1982) indicated that the calculated collision efficiency based on the works of Sutherland (1948), Flint and Howarth (1971), Woodburn *et al.* (1971) and Reay and Ratcliff (1973) were not in agreement with each other.

2.4.2.5 Interception and Diffusion

According to Yao *et al.* (1971), a single particle of filter media is a collector and if any suspended particle is in contact with the collector then a process known as interception occurs. The contact efficiency of a single media particle or collector is the ratio of the rate at which the particles strike the collector to the rate at which particles flow toward the collector, which can be expressed as follows:

$$\eta = \frac{\textit{rate at which particles strike the collector}}{u_o c_o \left(\frac{\pi d^2}{4}\right)} \tag{2.31}$$

where u_o – water velocity

c_o suspended particle concentration upstream from the collector where the flow is undisturbed by the presence of the grain

d – grain diameter

In the case of flotation the single collector efficiency (η) may be defined as follows (Malley and Edzwald, 1991a; Edzwald *et al.*, 1990):

$$\eta = \frac{particle\text{-}bubble\ collision\ rate}{particle\ bubble\ approach\ rate} \tag{2.32}$$

Reay and Ratcliff (1973) indicated that sub-micron particles will reach the bubbles mainly by Brownian diffusion. In the diffusion regime, collection efficiency will be decreased with the increasing particle radius, r_p. Flotation of these sub-micron particles could be improved if they were agglomerated into floc of suitable size in the collision regime. Theoretical calculations were made on particles with diameter less than 0.2 microns and bubbles size of 75 microns. At normal temperatures and pressures, particles smaller than 1 micron in diameter suspended in gases or water will exhibit a Brownian motion which is sufficiently intense to produce collision with a surface immersed in the fluid (Friedlander, 1967). Yao *et al.* (1971) in describing basic transport mechanisms in water filtration explained that when a particle in suspension is subjected to random bombardment by molecules of the suspending medium, then a Brownian movement of the particle known as diffusion takes place. Numerical and analytical determinations of single-collector efficiency were discussed by Yao and co-workers based on the works of previous investigators and the following equations were established:

$$\eta_D = 4.04 Pe^{-2/3} = 0.9\left(\frac{kT}{\mu d_p d v_o}\right)^{2/3} \tag{2.33}$$

$$\eta_I \quad \frac{3}{2}\left(\frac{d_p}{d}\right)^2 \tag{2.34}$$

$$\eta_G = \frac{(\rho_p - \rho)}{18\mu v_o} g d_p^2 \tag{2.35}$$

where η_D, η_I and η_G are the theoretical values for single collector efficiency when the sole transport mechanisms are diffusion, interception and gravity settling respectively. Pe is the Peclet number (i.e. $P_e = \frac{2R_b U_b}{D_f}$ where R_b is bubble radius, U_b is bubble rising velocity and D_f is particle diffusivity in cm^2/sec) , k is the Boltzmann's

constant, T is the absolute temperature, d_p is the diameter of suspended particle, d is the diameter of collector or bubble which is equal to d_b, v_o is the approach velocity of fluid and ρ is the density of fluid which is equal to ρ_f.

Then for the total single collector efficiency of a media grain, the expression can be written as follows (Yao *et al.*, 1971; O'Melia, 1985):

$$\eta_T \quad \eta_D + \eta_I + \eta_G \tag{2.36}$$

Edzwald and Walsh (1992) used the same theoretical approach used in filtration (Yao *et al.*, 1971;O'Melia, 1985) to developing a conceptual model for flotation. Thus the following equations are introduced:

$$\eta_D = 0.9\left(\frac{k_b T}{\mu d_p d_b U_b}\right)^{2/3} \tag{2.37}$$

$$\eta_I = \tfrac{3}{2}\left(\frac{d_p}{d_b}\right)^2 \tag{2.38}$$

$$\eta_G = (\rho_p - \rho_f)\frac{g d_p^2}{18\mu U_b} \tag{2.39}$$

By comparing the equations used in filtration to the above equations, the approach velocity of fluid and Boltzmann's constant have been changed to U_b (bubble rise velocity) and k_b (Boltzmann's constant for bubble) respectively. This is done to suit the mechanisms involved in flotation.

Ward (1992) in his review on capture mechanisms introduced a new form of equations for η_D and η_G by substituting the bubble rise velocity U from Equation 2.4 into Equation 2.37 and 2.39 with the following result:

$$\eta_D = 6.18\left(\frac{kT}{\rho_f g d_p}\right)^{2/3}\left(\frac{1}{d_b}\right)^2 \tag{2.40}$$

$$\eta_G = \left(\frac{d_p}{d_b}\right)^2 \frac{(\rho_p - \rho_f)}{\rho_f} \tag{2.41}$$

Results on single collector efficiency by Edzwald and Walsh (1992) show that a minimum in efficiency occurs at a particle size of around 1 micron.

For removal efficiency, Edzwald and co-worker used the same principle used in Equation 2.26, changing only the symbols of the expression as follows:

$$R=\alpha_{pb}\eta_T(100\%) \tag{2.42}$$

where α_{pb} is the attachment efficiency.

If the total number concentration of bubbles (N_b) is considered, then Edzwald and co-worker suggested the following equation for particle removal:

$$\frac{dN_p}{dt}=-\left(\alpha_{pb}\eta_T\right)A_bU_bN_bN_p \tag{2.43}$$

where A_b is the projected area of bubble and N_p is the particle number concentration. By having a bubble volume concentration of $\Phi_b = \pi d_b^3 N_b / 6$, and substituting into Equation 2.43 then;

$$\begin{aligned}\frac{dN_p}{dt}&=-\left(\alpha_{pb}\eta_T\right)\frac{\pi d_b^2}{4}U_bN_p\frac{6\Phi_b}{d_b^3}\\&=-\left(\frac{3}{2}\right)\left(\frac{\alpha_{pb}\eta_TU_b\Phi_bN_p}{d_b}\right)\end{aligned} \tag{2.44}$$

The particle number concentration removal in terms of flotation tank depth can be rewritten as:

$$\frac{dN_p}{dH}=-\frac{3}{2}\left(\frac{\alpha_{pb}\eta_T\Phi_bN_p}{d_b}\right) \tag{2.45}$$

Edzwald and co-worker also produced a summarised table of their model parameters for DAF facilities. This is as shown in Table 2.6. However this model has not been tested or verified (Edzwald and Walsh, 1992).

Table 2.6 - Model parameters for DAF facilities (Source: Edzwald and Walsh, 1992)

Parameter	Affected by	Comments
Pre treatment		
α_{pb} (particle-bubble attachment efficiency)	Particle-bubble charge interaction and hydrophilic nature of particles	Improve α_{pb} by chemical pretreatment, coagulation and pH conditions
N_p (particle number concentration)	Coagulation addition and flocculation time	Coagulant may add particles, flocculation may reduce N_p and increase d_p
η_T (single collector efficiency)	Diffusion and interception	Minimum η_T for d_p of 1μm
Flotation tank		
d_b (bubble diameter)	Saturator pressure	Small bubbles produce large interfacial areas and surface forces between bubbles and particles. Small bubbles, improve η_T
Φ_b (bubble volume concentration	Saturator pressure and recycle ratio	Large Φ_b ensures collision opportunities and lowering of floc density

Ward (1992) in his article on dissolved air flotation made an improvement on Equation 2.45 by integrating it over the tank depth H from N N_0 at the surface $H=0$ to N n at the tank base H H. Thus the overall particle removal equation becomes:

$$N \quad N_0 e^{\left(\frac{3\alpha_{pb}\eta_T\Phi_b H}{2d_b}\right)} \tag{2.46}$$

Then the overall efficiency is given by:

$$\eta \quad 1-\frac{N}{N_o} \tag{2.47}$$

2.4.2.6 Tank design

The usual design procedure for any flotation unit can be based on Figure 2.10. All the suspended solids in the flotation chamber should have a sufficient rise velocity to travel the effective depth D within the specified detention time T. This means, the rise rate V_T must be at least equal to the effective depth D divided by the detention time T, or equal to the flow divided by the surface area:

$$V_T \quad D\,T \quad Q\,A_S \tag{2.48}$$

where V_T=vertical rise rate of suspended solids, m/sec.

D =effective depth of flotation chamber

T =detention time, sec.

Q influent flow rate, m^3/sec. and

A_S –surface area of flotation chamber

The particles to be removed must also have a horizontal velocity;

$$V_H \quad Q\,A_C \tag{2.49}$$

where V_H horizontal velocity

A_C–cross-sectional area of flotation chamber, m^2

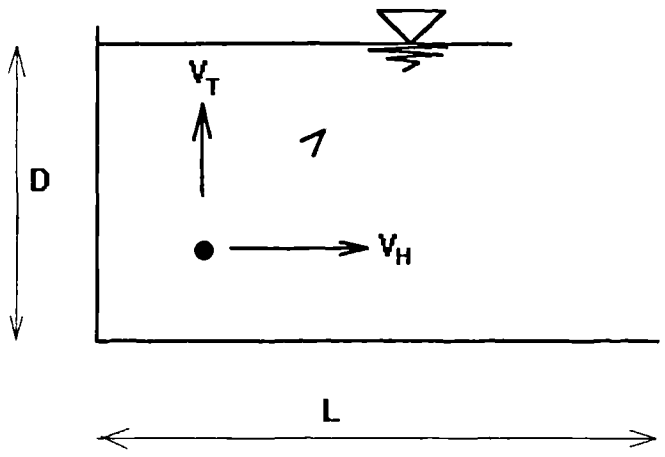

Figure 2.10 - Basic design concept of flotation unit (Source: Wang and Wang, 1989)

If the flotation chamber is in a rectangular shape, then the following equations can be established:

$$W \quad A_C/D \tag{2.50}$$

$$L \quad A_S/W \quad A_S/(A_C/D)$$
$$=V_H D A_S/Q \tag{2.51}$$

where W is the width of the flotation chamber (m), L is the effective length of the flotation chamber, Q is the influent flow rate (m^3/sec.) and the value of D/W is usually between 0.3 to 0.5.

The size of the flotation tank can be reduced if the separation rate is increased (Katz and Wullschleger, 1957). Their studies showed that a particle with a bubble attached to it would increase in its rising rate with an increase in the particle size. This finding is similar to that reported by Packham and Richards (1972a). However other factors such as pressure, recycle ratio, temperature, pH, zeta potential of the particles, number and size of bubbles produced, types of nozzles, flocculation process, flow condition and configuration of the tank are believed to have a significant affect on the separation process (Eckenfelder and O'Connor, 1961; Fukushi *et al.*, 1995; Noone, 1995; Gregory and Zabel, 1990)

Longhurst and Graham (1987) reported that the surface overflow rate (SOR) or rise rate is the fundamental criterion for tank design. It is defined as the flow rate divided by the surface area of the flotation tank. In practice the surface area is based on the interfacial area between clarified water and sludge and not the total area of the flotation tank (Longhurst and Graham, 1987). The characteristics of water and bubble size will determine the air floc aggregate rise velocity. For normal design purposes, rise velocities between 3 and 8 m/hour have been used (Rovel, 1977). For laminar flow the maximum size of bubble is 130 micron, for bubbles less than 130 micron Stokes' Law applies (Gregory and Zabel, 1990) and Equation 2.2 can be used to calculate the rise rate. The maximum bubble size for laminar flow can be calculated from Equation 2.3 by assuming limited laminar flow, Re=1 and using the relationship

between bubble size and rise rate of air bubble which has been established in graphical form (Gregory and Zabel, 1990). A survey done by Longhurst and Graham (1987) showed that the average normal operating SOR is below 6 to 9m/hr with a maximum rate up to 11m/hr.

Bratby and Marais (1975a) in their investigation on the application of dissolved air flotation in activated sludge were of the same opinion as indicated by Longhurst and Graham (1987) regarding the design of flotation units. Instead of SOR, Bratby and co-workers used the term downflow rate which is defined as the total flow into the unit divided by the plan area at the outlet. It is the value of limiting downflow rate (V_L), where the bubble-particle aggromerates are just carried down with the effluent, that controls the design of the tank.

Recently data published by Edzwald (1995) on the design and operation parameters of DAF showed that there were still considerable variations in retention time, hydraulic loading and recycle ratio between different treatment works in different parts of the world. These are shown in Table 2.7.

In terms of shape, Zabel *et al.* (1980) indicated that a rectangular shape has gained greater acceptance due to advantages such as simple design, easy introduction of flocculated water, easy float removal, small area and flexibility of scale-up. In addition to that floc break-up is minimised, hydraulic efficiency is maximised and engineering and construction is simplified (Longhurst and Graham, 1987). A tank with SOR in the range of 6 to 12m/hr would have a depth of 1.2 to 1.6m and a residence time of 5 to 15 minutes (Hyde, 1975). Results from survey works (questionnaire) done by Longhurst and Graham (1987) in Great Britain showed that in practice tank depths range 1 to 3.2m with a mean value of 2.4m, while tank shapes vary from 'squarish' to 'long and thin' and there is a continuing debate in this area. Gregory and Zabel (1990) indicated that tank depth of about 1.5m with an overflow rate of 8 to 12m/hr (depending on the type of water) are normally used. An effective flotation unit could be between 1.5 to 9 feet deep (Wang and Wang, 1989). The angle for the inlet baffle is approximately 60^0 to the horizontal which ensures minimum disturbance to the bubble-floc agglomerate (Zabel, 1985). However Longhurst and

Graham (1987) reported that in theory the baffle angle can range from 45^0 to 90^0 to the horizontal. 'Purac' have used a vertical baffle in the production of the 'Flofilter' tank in order to avoid an eddying current during clarification and hydraulic congestion during filter backwash. But for conventional filter they preferred to use an inclined baffle.

Table 2.7 - Summary of DAF design and operation parameters
(Source: Edzwald, 1995)

Parameter	South Africa	Finland	Nether-lands	UK[1]	UK[2]	Scandi-navia
Flocculation						
Intensity						
Time (min)	4-15	20-127	8-16	20-29	18-20	28-44
Flotation						
Reaction zone·						
Time (min)	1-4		0.9-2 1			
Hyd Load (m/hr)	40-100		50-100			
Separation zone·						
Hyd Load (m/hr)	5-11	2 5-8	9-26			
Total Flotation Area.						
Hyd Load (m/hr)			10-20	5-12	8.4-10	6.7-7
Time (min)					11-18	
Recycle (%)	6-10	5 6-42	6 5-15	6-10	5-10	10
Unpacked Sat.						
Pressure (KPa)	400-600				400-550	460-550
Hyd Load.(m/hr)	20-60					
Time (sec)	20-60					
Packed Sat.						
Pressure (KPa)	300-600				400-500	
Hyd Load.(m/hr)	50-80					
Packing Depth,m	0 8-1.2					
Saturators*						
Pressure (KPa)		300-750	400-800	310-830	480-550	

* Unspecified with respect to unpacked or packed saturator. (1) Longhurst and Graham (1987) and (2) Edzwald *et al.*, 1994.

The depth of water below the water surface is found to vary across treatment plants and greater depths than those recommended by the Water Research Centre of 0.3 to 0.4m are normally used (Longhurst and Graham, 1987). In South Africa the depth varies from 1.5m to 3.5m and in the United Kingdom from 1.0m to 3.2m (Haarhoff and Vuuren, 1995). This means there is still no agreement in practice to the extent with which depth affects the optimisation of design criteria. On the width of the tank, it was observed that widths of between 2.4 to 9.4m are found in practice. However Gregory and Zabel (1990) reported that tank widths are less significant to hydraulic flow and are sometimes restricted by the sludge removing device. A study carried out by Heinanen (1988) on the use of dissolved air flotation for potable water treatment in Finland showed that the design parameters for the process are still far from ideal and this has resulted in high construction costs. He indicated that the situation could be avoided if research institutes had played an important part in the design works.

Recent discussions with Noone (1995) indicated that there is a need to investigate the optimum shape of the tank. This means further investigations would be useful to justify the arrangements of the nozzles, the distance between the inlet and the baffle, the baffle angle, and the depth of water surface from the baffle.

Longhurst and Graham (1987) indicated that if the length of the tank runs only up to point A (Figure 2.11), the tank may be too short and the floc will not achieve its optimum flotation which occurs at point B. At point C, the tank is too long and it will cause the floc to settle down.

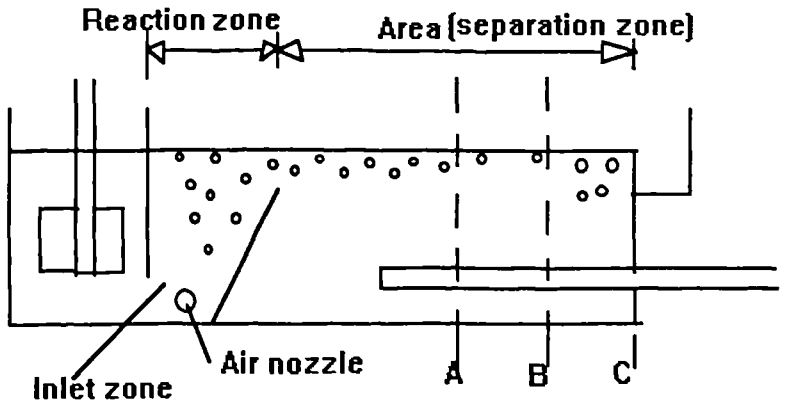

Figure 2.11-Arrangements in flotation tank (Source: Longhurst and Graham, 1987)

Noone (1995) indicated that even in Severn-Trent Water, there is a range of tank sizes with varying rectangular shapes, and different arrangements of air nozzles, baffles, depths and operational procedures with no evidence to prove their effectiveness. Thus it is worth investigating these parameters so that a better fundamental understanding can be developed towards the achievement of an optimisation of tank dimensions and the flotation process in practice. This could result in the saving of power, chemicals, operation times and the development of standard design procedures.

CHAPTER 3

SUMMARY OF LITERATURE AND RESEARCH OBJECTIVES

A survey of literature has indicated that the dissolved air flotation process has gained considerable acceptance and popularity for potable water clarification. DAF is a rapid process compared to conventional gravity settling. A considerable number of water treatment plants using dissolved air flotation are found in the United Kingdom, Netherlands, Australia, Scandinavian countries, the United States, South Africa and in the Far East. Recently an international conference on dissolved air flotation for water clarification held in London (16-18th April, 1997) indicated that more water treatment works will be constructed using the DAF process. A number of sedimentation processes have already been or will be converted to this process in the near future.

In Section 2.4.1.4 (Chapter 2) the performance of dissolved air flotation process was shown to be effective in the removal of algae, colour, turbidity, residual coagulant, bacteria and protozoa. Extensive research has been carried out in the laboratory, pilot plants and full-scale plants on the performance of dissolved air flotation for the removal of the above parameters. Effective removal of algae in the water treatment process is vital because its presence is associated with tastes, odours and the need to clean the filter beds more frequently. Colour in water is due to the presence of impurities from dissolved minerals, plants, animal by-products and industrial wastes. Coloured water may be associated with potability and health hazard. The same problems are true for turbidity. The latter is due to the presence of small particles in water. Small particles hinder the ability of chlorine to kill pathogenic organisms including bacteria and protozoa which may be present within the particles rather than on the surface. Thus the removal of turbidity is important. Noone (1995) indicated that for potable water clarification, a rapid and effective process is needed for the turbidity removal before filtration. This is vital to minimise the risk of pathogenic organisms entering the filter beds. Once the pathogens are in the filters there is a risk that these organisms will enter into the distribution system. Future trends in water

treatment will be more concerned with the removal of undesirable substances rather than disinfection.

To date, studies referenced in the literature on turbidity removal were carried out using samples collected in the flocculation tanks or at the raw water inlet and compared with the turbidity samples collected at the outlet of the flotation tank. Hitherto no study has been undertaken to investigate the variation of turbidity within the flotation tank and to evaluate the effectiveness of the tank physical parameters in relation to turbidity removal and the flow rates within the tank. This indicates there are gaps in knowledge on the understanding of turbidity variation within the separation zone and the effect that the tank physical dimensions have on it.

In Chapter 2, the performance of DAF processes based on the research carried out by numerous workers has been summarised (Table 2.2b). Performance of DAF (as shown in Table 2.2b in Chapter 2) is linked with flocculation processes such as the velocity gradient, requirement for tapered flocculation and the size of flocs. Edzwald and Walsh (1992) indicated that pinpoint size (10 to 30 μm) flocs were favourable for a DAF process in water treatment. Their proposition was in agreement with Klute *et al.* (1995) and Bunker *et al.* (1995) who indicated that floc size in the range of 30 to 45μm was appropriate. From their results (Edzwald and Walsh, 1992; Klute *et al.*,1995; Bunker *et al.*, 1995) an assumption may be made in the full-scale plant operation that for floc sizes below 300μm may be used as a fixed factor to model the performance of the DAF tank.

Section 2.4.2.6 in Chapter 2 also indicated that there is a great variation in the sizes and shapes of DAF tanks (Longhurst and Graham, 1987). However the rectangular shape has gained greater acceptance due to simplicity of design, easy introduction of flocculated water, easy float removal, required small area and flexibility of scale-up (Zabel and Melbourne, 1980). There is also no clear evidence to suggest that a certain aspect ratio (i.e. length to width ratio) is superior to any other. Franklin *et al.* (1997) indicated that in Yorkshire Water aspect ratios of 0.5:1 and 3:1 are used and suggested that the higher aspect ratios work better. Survey work done at Frankley,

Trimpley, Draycote, Cropston, and Melbourne Water Treatment Works of Severn Trent Water showed that each treatment works has different tank configurations. To date no attempt has been made to study the effect of tank dimensions on the velocity distribution within the tank and its effect on turbidity removal except by computer simulation. Discussions with Severn Trent Water and the literature review in Chapter 2 (Section 2.4.2.6) confirmed that there are gaps in knowledge on the appropriate design procedures for the DAF tanks. There are no clear answers to the question of why different shapes are adopted at different treatment plants except by using the surface loading theory. However the latter is based on a constant flow rate whereas in the actual plants the flow rate may be changed from time to time. Details on the actual velocity characteristics within the tank are not known.

The present study was carried out on full scale dissolved air flotation plants run by Severn Trent Water with the main objective being to identify the important design parameters within the separation zone of the DAF tank and their relationships with the velocity and turbidity distributions. In order to achieve the objective several procedures were identified and proposed. These were as follows:

1. To investigate the suitability of the Acoustic Doppler Velocimeter (ADV) to measure low flow in a dissolved air flotation tank by analysing and comparing the collected velocity data using appropriate statistical techniques.

2. To investigate the velocity distributions in the x, y and z directions in the separation zone of the dissolved air flotation tanks at Frankley and Trimpley Water Treatment Works using the ADV probe.

3. To investigate the effects of width, depth, length and the interactions between them on the velocity distributions in the tank using appropriate statistical techniques.

4. To develop statistical models to describe the velocity distribution in the tank and to develop a general statistical model which can be applied to a range of tank sizes and flow rates.

5. To investigate the effectiveness of turbidity removal at different positions within the separation zone of the DAF tank.

6. To compare the performance of DAF tanks at Frankley and Trimpley in terms of turbidity removal within the separation zone of the DAF tanks.

7. To identify any redundancy in the tank dimensions based on the turbidity and flow rate studies on the DAF tanks at the Frankley and Trimpley Water Treatment Works.

CHAPTER 4

EQUIPMENT AND METHODS

4.1. INTRODUCTION

A survey of literature has indicated that the flow in the separation zone of a dissolved air flotation tank is designed to be laminar with Reynolds number normally less than one. The rising velocity of the bubble was reported between 125mm/minute to 500mm/minute (Krofta and Wang, 1989). No direct measurement of specific bubble size rising in a water column was made. Krofta and Wang (1989) only measured the volume of air obtained at a specific interval rising at a specific depth through a water column. An inference was made to the data using Stokes' law to obtain the bubble size and rising rate. The average horizontal velocity (design) of water in the dissolved air flotation tanks is approximately 9.5mm/sec at the Frankley Treatment Works. It is not possible to measure these low velocities with conventional propeller type velocity meters. A survey of instruments to measure low velocity was made from various manufacturers around the world.

There are three types of velocity meter which are capable of measuring low flow. These are as follows:

1. Acoustic Doppler Velocimeter
2. Laser Doppler Velocimeter (LDV)
3. Propeller Vector Averaging Current Meter (VACM)

LDV is quite expensive in the region of £80,000 (Elliott, 1997). It required a complicated set up in a transparent tank and is considered inappropriate for site investigation in concrete tanks at Severn Trent Water. VACM is the cheapest but cannot measure velocity components in the y and z directions. It is not good for low flow measurement especially where there is a sludge blanket in the tank which can disturb the efficiency of the propeller.

4.2 EQUIPMENT

4.2.1 Acoustic Doppler Velocimeter (ADV)

The SonTek Acoustic Doppler Velocimeter was originally developed and tested for velocity measurements at the United States Army Engineer Waterways Experiment Station (Kraus *et al.*, 1994). It can be used for scientific research, hydraulic engineering and general flow problems in environmental science. It has advantages of high sampling rate and requires only a small sampling volume. The latter makes it possible to measure the velocity profile to within a few millimetres from the boundary. When compared to the acoustic travel-time and electromagnetic techniques, it has the advantages of being inherently drift free, not requiring routine recalibration and the acoustic pulses do not suffer the range limitation of optical pulses in turbid water (Lohrmann *et al.*, 1995). In terms of cost, this instrument is much cheaper than the Laser Doppler system. The types of probe used depend on the types of investigation anticipated. For operating in a shallow water, a 2-D side-looking probe would be suitable. A 3-D side-looking probe requires water of at least 6cm depth. To measure flow close to the surface layer a 3-D up-looking probe may be used. A 3-D down-looking probe is ideal for measuring velocity close to the bottom of the boundary layer.

The velocity measuring equipment consists of an ADV sensor, probe, signal conditioning module, high frequency cable and processor in a splashproof box. The ADV sensor has three acoustic receivers and a transmitter. The probe is made up of a sensor, stem and an endbell. The signal conditioning module is placed inside a waterproof housing and holds the receiver. The system used in this study was operated on site using a laptop computer. Software for the operation of the ADV was supplied by the manufacturer. A sketch diagram of the system is shown in Figure 4.1.

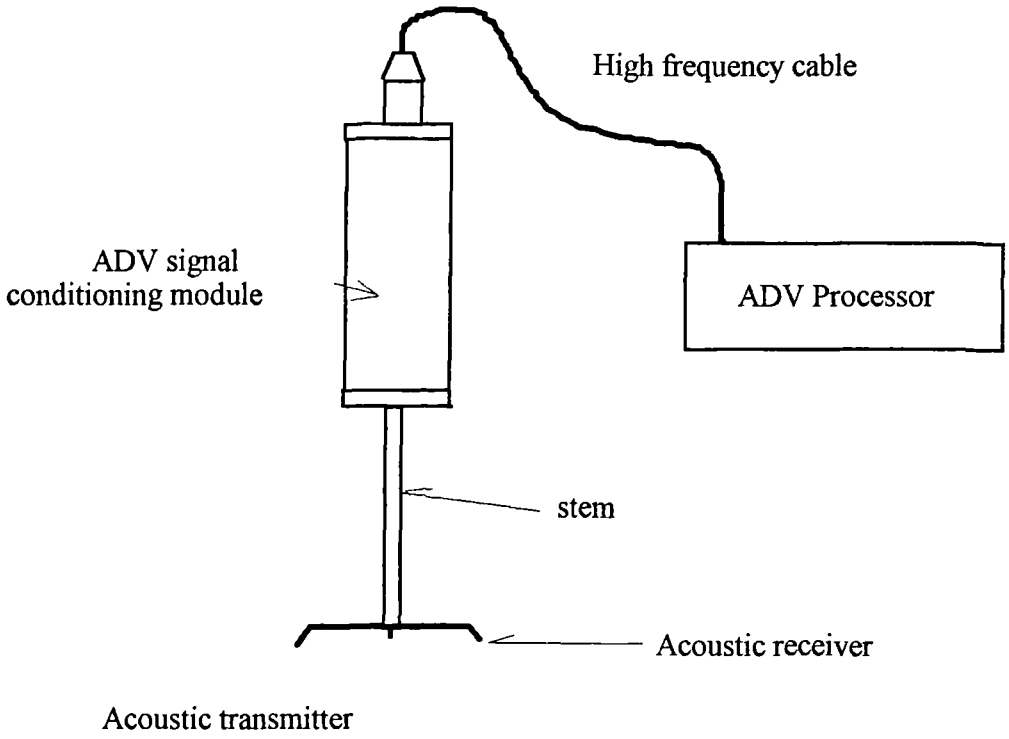

Figure 4.1 - Acoustic Doppler Velocimeter

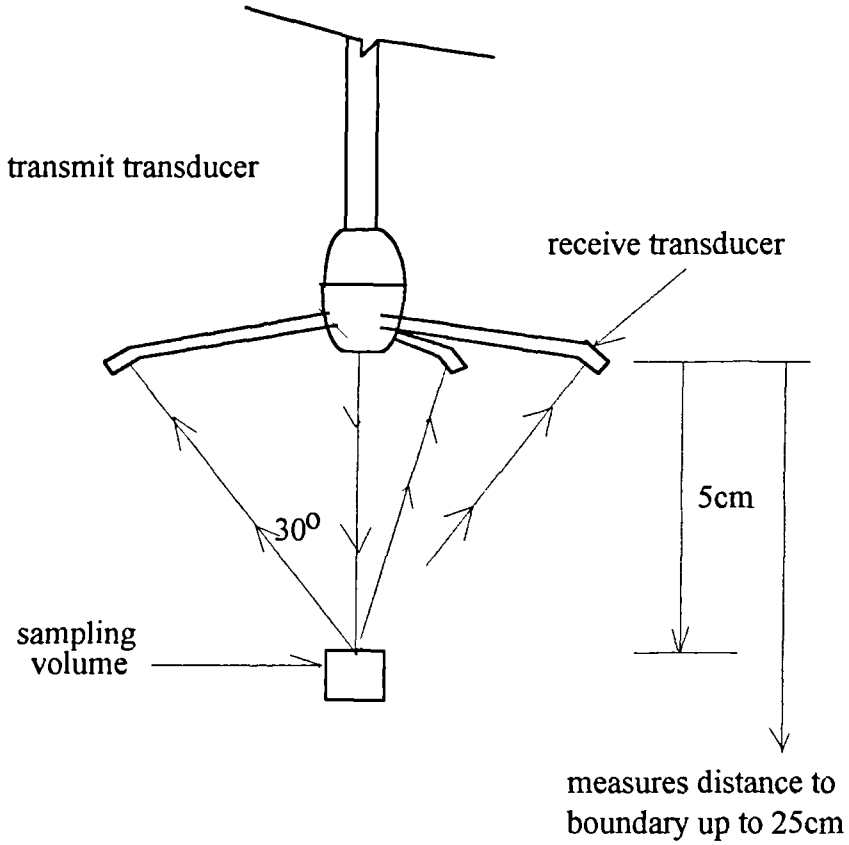

Figure 4.2 - Signal produced by ADV probe

4.2.2 ADV Probe

The probe used in this investigation was a three-dimensional down-looking type consisting of a 5cm sensor mounted on a 40cm stem. The red receiver arm points in the direction of the *x*-axis. The directions of the *y*-axis and *z*-axis are based on the definition of a right-handed co-ordinate system where *z* is pointing upwards. The centre of sampling volume is approximately 5cm below the transmitter. The exact position is encoded in a probe-specific configuration file. The distance to the boundary shown on the computer display is the distance from the middle of the sampling volume to the nearest boundary. Maximum and minimum water depth specified for this equipment is 30m and 60mm respectively. Measurements as close as 5mm from the sampling volume to the boundary can be made but it cannot measure the velocity in the upper 5cm of the water column. The sampling volume is 3-9mm long and approximately 6mm in diameter. It is defined by the interception of the signal beams together with the width of the transmitted pulse. Figure 4.2 indicates the operation mechanism of the transducer. The receive transducers are mounted on short arms around the transmit transducer at 120° azimuth intervals. The angle between each receiver, sampling volume and the transmitter is fixed at 30 degrees. This was developed by the manufacturer based on the balance between probe size and statistically induced variance in the horizontal velocity components (Kraus *et al.*, 1994). The velocity is derived from signals scattered by small particles present in the natural bodies of water. For laboratory models, microscopic bubbles will act as natural seeding. For models which involve clean water, seeding materials must be added at a concentration of about 10mg/l so that signals can be transmitted to the transducers. The acoustic frequency used is at 10 MHz with a velocity range of ±0.03, 0.10, 0.30, 1.0, or ±2.5m/sec and a resolution of 0.1mm/sec. The operating temperature of the probe is between 0 to 40°C. The sampling rate can be programmed from 0.1 to 25Hz. This means at the higher rate one sample reading is recorded at every 0.04 second but the computer screen only displays one sample reading per second.

4.2.2.1 Accuracy of Probe

A comparison of the horizontal component of the wave orbital velocity under random surface waves using three dimensional ADV and Laser Doppler Velocimeter (LDV) showed that good agreement was obtained over a velocity range of 10 to 250cm/sec (Kraus *et al.*, 1994). The slope of the linear regression line from these data gave a value of 1.03. Similar agreement was obtained for the vertical velocity component which had a lower velocity. Validation of slow moving velocity (means of *Vx*, *Vy* and *Vz* were -0.8 cm/s, -2.2cm/s and 0.08cm/s respectively) showed that ADV data were in agreement with qualitative observations of the movement of dye injected near the meter.

Different types of velocity meters which used the same acoustic technique were tested for measuring velocity distribution in a closed conduit (Vermeyen, 1994). The result of the analysis of the path velocities indicated that there was very little cross flow component. Velocities measured on a similar acoustic path agreed very well. However the evaluation of the acoustic velocity meters was carried out at high flow conditions which involved velocities in the regions of 3 to 4m/s. No tests were made at low velocities. Lohrmann *et al.* (1995) reported that a comparison of Reynolds stress was carried out over a velocity range and indicated that at low flows of less than 10cm/s the ADV data has a slight bias.

Direct comparisons of the SonTek ADV with a Vector Averaging Current Meter (VMCM) were reported to have been carried out at the Woods Hole Oceanographic Institute in the United States (Anderson and Lohrmann, 1995). The VMCM is a propeller type current meter capable of recording data internally with an averaging interval of 7.5 seconds. At a low frequency evaluation, data were collected at 1Hz for a period of 43 consecutive hours. The current speed measured used in the study was that of the horizontal velocity vector. The result indicated that the mean current speed from ADV was 23.23 cm/s whereas from VMCM was 23.14 cm/s. A small deviation in velocity could be due to the difference in temperature. The water temperature was 5^0C warmer for the VMCM than as set up in the ADV processing.

When a second comparison for low frequency evaluation was carried out on the two current meters, the result showed that the correlation coefficient between them was 0.955 with a mean difference of 1.8 cm/s. However if the last 50 minutes of the records were used, the mean difference dropped to 0.04 cm/s.

Recently, Brunk *et al.* (1996) indicated that pulse-to-pulse interference can produce an inaccurate result of velocity measurement by using the ADV. This is because ADV analysed the echoes returning from the sonic burst and any interference due to echoes from the apparatus walls may affect the accuracy of velocity readings. However it would be possible to recognise any data arising from pulse-to-pulse interference by looking at any sharp increased in the signal noise level.

Lohrmann *et al.* (1994) indicated that a small deformation in the receiver arm will only result in very small errors in the horizontal velocity. A change in angle as large as $5^{o}{}_{o}$ to the receiver arm produces a calibration error of less than 1%. A simple visual inspection can be made to detect any damage to the receiver arm. Software utilities can also be used for the same purpose. If the signal strength during data collection reduces significantly, there are some problems with the receiver arm. The instrument needs to be calibrated during data collection procedures by entering the actual temperature and salinity of the water. Without this a nominal speed of sound at $1490ms^{-1}$ is used.

Care has to be taken not to damage the sensor. When operating in salt water for a period of more than 24 hours, a zinc-anode has to be mounted on the stem. Physical damage of the probe can be easily detected by simple inspection (Lohrmann *et al.*, 1994). If the receiver is twisted or bent, the receiver elements cannot focus on the sampling volume. Hardware diagnostics can be used to check out whether the sensor is in a correct working order. The output from this test shows the signal strength in each of the three receiver as a function of time. A damaged receiver will display significantly reduced signal strength compared to undamaged receiver arms.

4.2.3 ADV Processor

The ADV processor requires an AT-compatible PC with a 386 processor or higher with one 16-bit full-sized card slot for each processor board installed, VGA colour graphics and a hard disk drive which are installed in a splash-proof box. Data are collected using digital (RS-232) transfer which allows real-time data acquisition. A direct current (DC) supply (12 - 24 volts) is connected to the processor and the battery has to be charged for a duration of at least 11 hours before operating the probe for field investigation. The connector on the splash-proof box is designed to be used with 110 or 220V AC/DC adapters supplied for standard notebook computers. The positive terminal has to be on the inside of the coaxial connector. The power consumption is between 3 to 4 watts depending on the input voltage level.

4.2.3.1 Mechanical Switches

Three circuit boards are installed inside the ADV field enclosure. The upper board consisting of several mechanical switches whose functions are clearly printed with white letters. These switches are intended for setup, mode, sampling rate, velocity range and synchronisation functions. The 'setup' switch can be set to hardware or software positions. If the switch is set to hardware, the CPU will read the switch settings when power is on and data collection will start. At this setting, software communication is not possible. When the switch is set to software control, it will override the mechanical switches. The 'mode' switch determines whether the system is under a normal operation (RUN) or in the calibration mode (CAL). The 'sampling rate' switch has dual functions. If the 'mode' switch is under RUN, the switch sets the sampling rate to either 25Hz, 1Hz, or 0.1Hz. If it is set under CAL, the switch enables the three analog outputs Vx, Vy and Vz to be calibrated. The 'range' is used to set the velocity range to either ±30cm/s, ±100cm/s, or ±250cm/s. The synchronisation switch can be set to either 'asynchronous', for external synchronisation to be disabled, 'start' for starting data collection when the first

synchronisation pulse is received, or 'sample' to get the average velocity between each synchronisation pulse.

The default setting on the mechanical switches is set for software control. The settings override the mechanical switches even after a power down or up. Once the power is connected, the system is run using the 'ADF.EXE' file.

4.2.4 Cables and Connectors

Cables and connectors are basically used for communication, data collection and control lines. Analog outputs (velocities in x, y and z directions) generate voltages proportional to the velocity components measured by the ADV. These outputs are smoothed by a one-pole RC filter with a corner frequency of 25Hz. The output voltage range is 0-5V.

The splash-proof box has three connectors and one power jack. The coaxial power connector is configured with a positive terminal on the inside and negative terminal on the outside. It takes an input power in the range of 12-24V. The diode will light up when the external switch is powered up.

The high frequency cable which is connected to the ADV signal conditioning module has a 25-pin connector plugged onto the splash-proof box. A RS-232 serial cable with a DB-9 connector connects between the computer serial port and the processor board in the splash-proof box. The DB-9 connector provides a number of signals for interfacing the ADV to other instrumentation.

4.2.5 Calibration of Analog Outputs

Calibration of the analog output is required if the system is connected to another data acquisition software or data logger (Shephard, 1997). It is also necessary to recalibrate if the standard cable has been altered in its length or replaced.

No recalibration was required during the data collection period for this thesis, however a description of the required procedure is given in Appendix A for completeness.

4.2.6 ADV Software

The ADV field data acquisition program is supplied together with the equipment. Hardware requirements for field investigation is 33MHZ 386 or 486SX/DX desktop or laptop computer with 640K RAM, hard disk, colour VGA graphics and one serial port per ADV. It has the following functions:

a) To enable the user to set up data collection parameters which include sampling rate, recording file, velocity range, water temperature and salinity, unit system and external synchronisation.
b) To control the operation of up to 8 ADVs simultaneously
c) To provide real-time display in the forms of graphic and alphanumeric for the velocity data, signal to noise ratio, recording file, correlation coefficient for each of the receiver and other information useful to the operator.
d) To record the data into compressed binary files on hard disk.

4.2.6.1. Installation of ADV Software

To install the software into the lap-top computer, the following procedures were carried out in the laboratory at the University of Newcastle:

1. A directory was made for the ADV software in the c-drive. This was done by typing the following commands:

a) C:\>md~sontek(R) where ~ is for space and (R) is for return
b) C:\>cd\sontek(R)
c) C:\sontek>

2. The ADV software disc was copied onto the C drive in the sontek directory by using command copy~a:*.*~c:(R). By using command C:\sontek>dir~/p(R), a list

of files appeared on the screen. One of them was the calibration file 1137.PRO. The latter file has to be deleted because the ADV signal conditioning module which was purchased from SonTek Inc. has a calibration file '1239' stamped on the end plate. File 1137.PRO on the hard disc was deleted and file 1239.PRO was copied onto the C drive. A command dir~/p was made as before to check the right calibration file installed. 'advprobe.def' was edited for the correct probe number.

3. The correct serial port on the lap-top was checked to make sure it was configured. By using a command C:\sontek>type~advprobe.def and pressed return, the output was in the form of PROBE 1 1239.PRO. Number 1 referred to the communication port in use for the computer. Port number 1 of the lap-top was used. This may be required to be edited if another port is used. The term 1239.PRO is the probe number and the calibration file reference. Serial line cable RS232 was used for connection between the computer port and the splash proof box.
4. To check whether the system was working, the probe was lowered into a bucket of water, the power on the splash proof box was switched on and the command C:\sontek>adf was made. It took a few seconds for the system to 'wake up' the probe and then showed a setup mode screen. This screen showed parameters needed to be entered such as water temperature and salinity, sampling rate, velocity range, file name to store the data, date and time of sampling. When the arrow was pointed to the word 'start data collection' and pressed enter, the next screen appeared was 'ADV probe adjustment for boundaries'. By moving the probe in a bucket of water up and down, the screen showed some changes on the distance of the probe tip to the boundary. By pressing the F10 key, initial familiarisation on data acquisition was made.

4.3 TRIMPLEY WATER TREATMENT WORKS

The water treatment works at Trimpley has seven dissolved air flotation tanks for the solid-liquid separation process. These tanks were commissioned in 1995 to incorporate the existing hopper bottom clarifiers. Normally three to four dissolved air

flotation cells are used at a time. The maximum design output from each cell is approximately 7.4 million litres per day (mld).

The raw water is abstracted from River Severn and impounded in a reservoir next to the treatment works. Prior to flotation, the water undergoes coagulation and flocculation processes. In the coagulation process aluminium sulphate is added and hydraulic mixing is employed. Flocculation is done in two stages which involved further mixing of water and chemicals using mechanical flocculators to achieve suitable flocs for the flotation process. A retention time of 30 minutes is allowed in the flocculation tank. Under most circumstances, a retention time of 20 minutes is considered sufficient depending on energy input. In the dissolved air flotation process, air bubbles are injected through 112 air nozzles in the reaction zone of the flotation tank in order to promote the bubble-floc attachment process to take place. The saturator pressures employed in the process is between 4.7 to 6 bar with a recycle ratio of approximately 10% of the outflow. Sludge is removed by the mechanical scraper in a 30 minute sequence for each tank or as deemed necessary depending on the incoming water quality. The effluent from the flotation tank is discharged into rapid gravity filters for final clarification. Finally the filtered water flows into a contact tank for disinfection.

4.3.1 Tank Configuration

All dissolved air flotation tanks at the Trimpley Water Treatment Works have the same configuration. Figure 4.3 shows the tank configuration at Trimpley. The nominal size of the tank is 7870mm length, 5120mm width and 2250mm depth. The nominal depth of water is 1650mm. The tanks were constructed parallel to each other so that the middle tanks share a common T-shape wall. This means both sides have a cantilever platform. The rails of the bridge scraper were built along the cantilevered platform on the dividing wall. The presence of these cantilever structures and the launder at the outflow end of the tank prevent measurement of velocity near the wall. This means that the measurement of velocities across the width of the tank has to be carried out directly from the edge of the cantilever floor. Velocity measurements

along the length at the outlet wall were made at 0.5m from the wall due to the presence of the launder and pipework. This distance was considered safe to prevent any accidental damage to the probe.

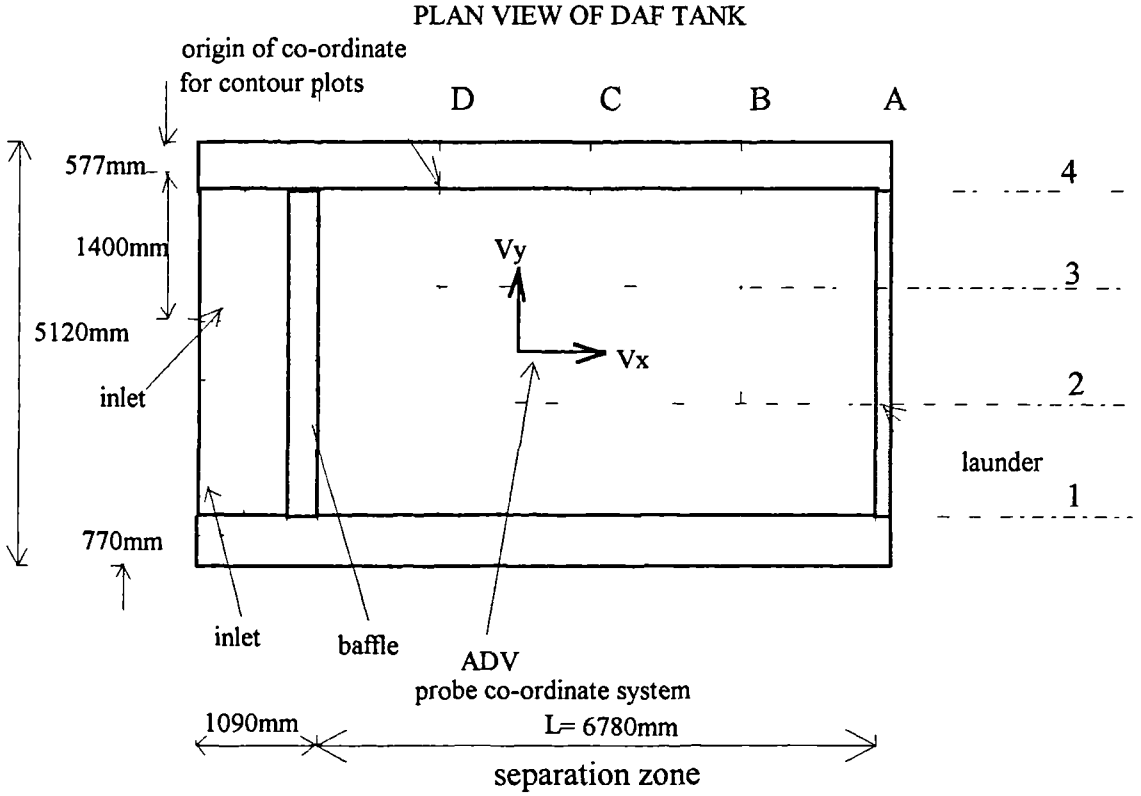

Note: point D4 (in plan view) is the origin of co-ordinate for contour plots in Appendices B1 to B4

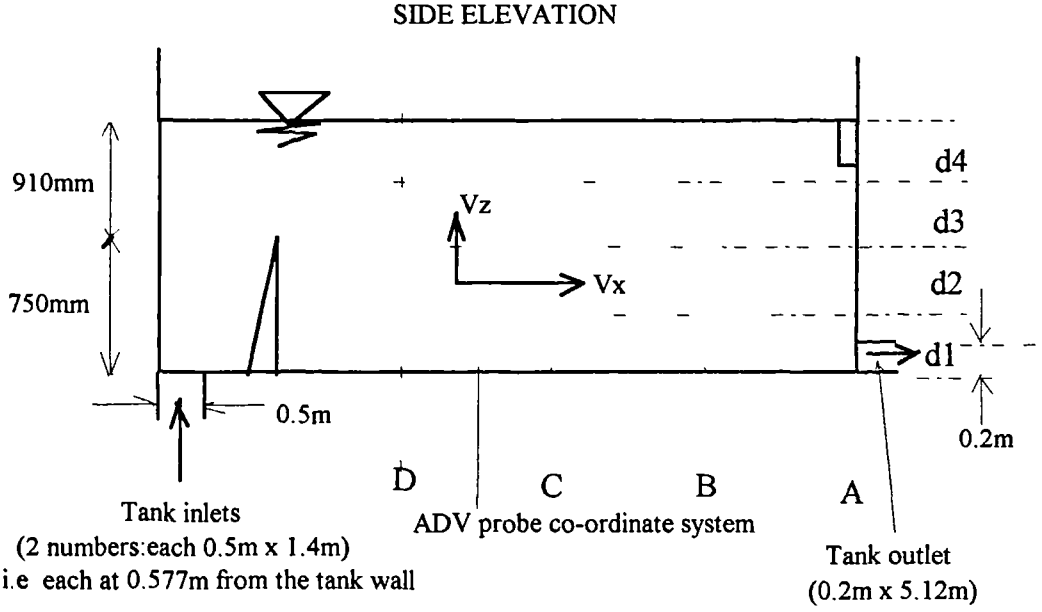

Figure 4.3 - Grid System Used in Dissolved Air Flotation Tank

4.4. FRANKLEY WATER TREATMENT WORKS.

The treatment works has twenty dissolved air flotation cells, each having two sub-tanks with a common inlet but different outlets. Figure 4.4 illustrates the configuration of each cell at the Frankley Treatment Works which indicates the inlet is situated in the middle section of the tank. At this section the flocculated water is saturated with air from the nozzles and subsequently flow over the baffles in two directions towards the flotation tanks. The maximum plant output is 450 million litres per day (mld) with a design average of 365 mld. The raw water is abstracted from the Elan Valley in the mid-Wales and impounded at Bartley and Frankley reservoirs. Additional water demand is met by pumping the raw water at a rate up to 180 mld from the River Severn at Trimpley.

Clarification processes involve hydraulic rapid mixing, flocculation, dissolved air flotation and rapid gravity sand filtration. Lime and/or carbon dioxide may be added to modify the hardness of the water and to ensure that the pH following the addition of coagulant is in the optimum band. Ferric sulphate is used as the main coagulant or alternatively aluminium sulphate or polyaluminium chloride (PAC) may be used.

Three stages of flocculation are employed at this treatment plant to ensure the following objectives:

1. To allow completion of the coagulation reaction and initiate flocculation in the first stage.
2. To promote flocculation in the second stage
3. To encourage final floc development and to produce an equal flow regime across the outlet of the flocculation tank in the third or final stage.

The technical specification for the flocculation process can be summarised as shown in Table 4.1.

Table 4.1 - Technical specification for flocculation

Process Parameters	Specification
Retention time at cell output of 26.4mld	30 minutes
Mean velocity gradient	25-80 per second
Maximum tip speed	1 m/s
Flow pattern	Diagonal

In the dissolved air flotation process 7 to 10 g/m^3 of air is injected through a needle valve which has a double diffuser. The same type of valve is used in the flotation tanks at the Trimpley Water Treatment Works. The saturator is designed with a surface loading of 26.5 $m^3/m^2/h$ to cope with maximum recycle flow of 10%. Air nozzles are spaced at 180mm centres in the reaction zone. The maximum flow through each nozzle is 0.2 litres per second (lps) with a total of 162 nozzles in each cell. However 14 nozzles were shut down during the investigation. The minimum and maximum working pressures of the saturator are 220 and 550kpa respectively.

4.4.1 Tank Configuration

All the tanks at this treatment works have the same configuration. Figure 4.4 shows the configuration of each DAF cell. Measurement on site showed that the width of the dissolved air flotation tank is 7m. The length of the separation zone on each side of the tank is 8.4m. The separation zone is the distance measured in plan view between the outlet of the tank and the top end of the baffle. The reaction zone is 2.37m and in this case it is the distance between the tip of the two baffles. The distance between the foot of the baffles where the nozzles were installed is 780mm. The floor of the tank is constructed at a gradient of 1:84 sloping down from the outlet wall towards the baffles. The nominal depth of water at the outlet end during operating conditions was found to be 2.1m.

The raw water is fed to the DAF cells through two channels where rapid hydraulic mixing occurs. Each raw water channel branched into two smaller channels. Coagulated water from each smaller channel is then fed into the flocculators and DAF

tanks. There are five flocculators laid parallel to each other for every stage of flocculation. The five DAF tanks receiving the flocculated water are also constructed parallel to each other. The method of construction is similar to those at Trimpley as per section 4.3.1 and this presents a similar restriction for velocity measurement.

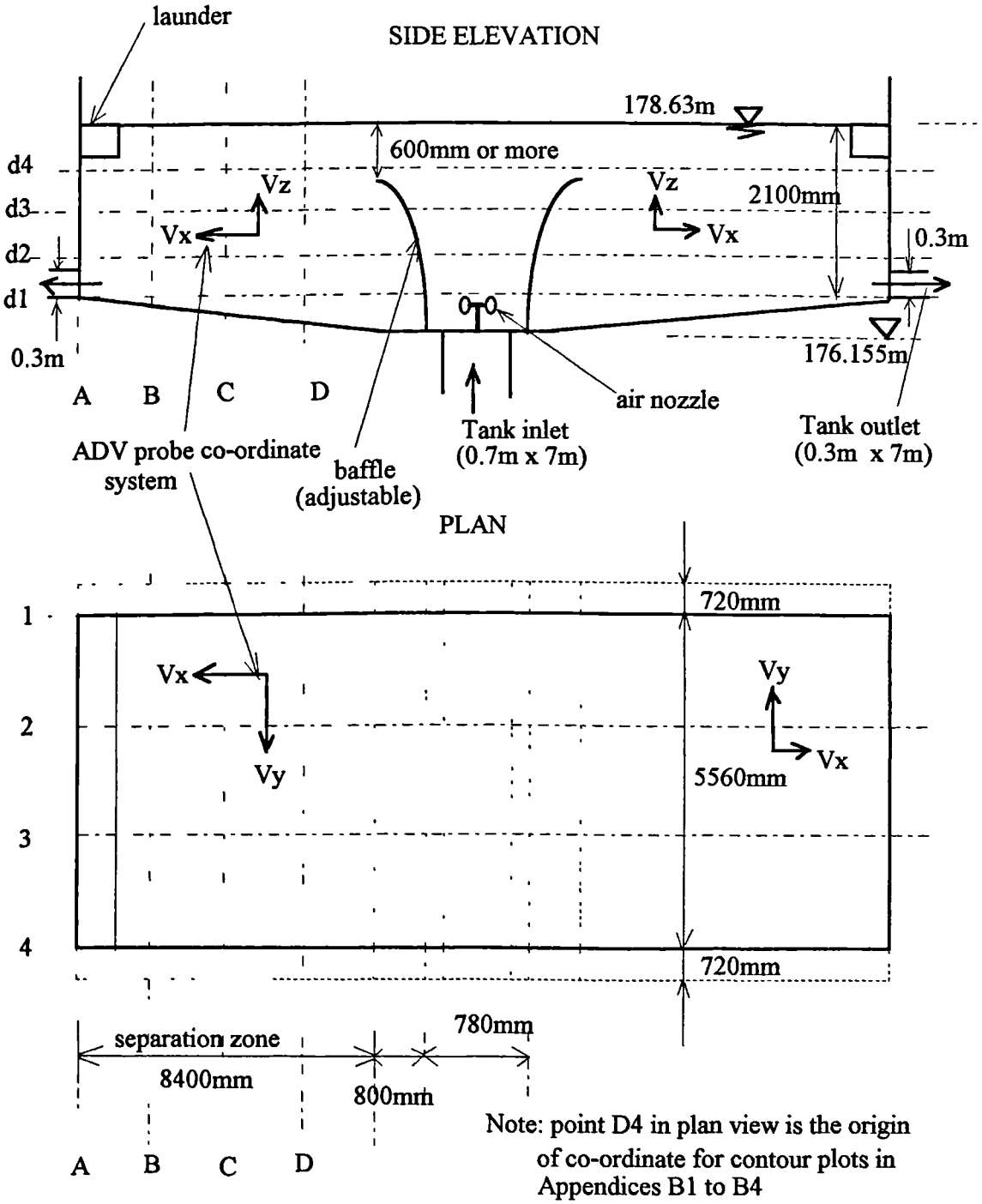

Figure 4.4 - Grid system in a dissolved air flotation tank at Frankley Works

4.5. WATER SAMPLER

A water sampler made from rigid polypropylene with a capacity of 60ml was used to collect water samples from the same points where velocity measurements were taken. Plate 4.1 shows a photograph of the water sampler used in the investigation. It has a heavy weighted base with a spring mechanism attached at the upper section of the equipment. When a sharp pull was made on the cord, the two small inlets situated on the upper part of the bottle opened (was closed initially) and this allowed water to be admitted into the bottle. As the water entered the bottle, air bubbles were displaced from the bottle. The bottle was assumed full when there was no sign of air bubbles on the surface of the tank. The absence of sludge in the water sample may indicate that the sample was acceptable for use in the study.

Minor adjustments were made to the water sampler to achieve maximum performance for collecting 64 samples in one run or set of experiments. A new spring was fabricated in the workshop at the University of Newcastle to replace the original spring supplied with the equipment. The original spring was found to be too soft and snap easily due to extensive use. A plastic bottle cap was found to be invaluable on site. It was installed at the upper end of the spring. It was used to prevent the sludge blanket from getting into the water sample when the sampler was pulled up through the surface of the sludge blanket. Initial work without a bottle cap on the rope showed that the time taken just to take one sample without the interference of sludge was between 10 to 30 minutes. The use of a bottle cap helped to reduce the time taken to take water samples. This would enable a reduction of disturbances on the water body due to less repetition. The diameter of the bottle cap was smaller than the diameter of water sampler and therefore a minimum disturbance to the turbidity distribution in the tank was achieved.

The water sampler was attached to a strong nylon cord. A knot was made on the string to mark the required depths for sampling points to be taken. Initial markings were made by allowing the sampler to be placed in a bucket of water so that its buoyancy would be taken into account.

4.6. STATISTICAL METHODS FOR DATA COLLECTION

4.6.1. Formatting Factors and Levels

Statistically the parameters width, depth and length of the tank can be called 'factors' in the experiment. Once the factors have been established, the experimenter can divide these factors into different 'levels'. In this case the different positions where the velocity and turbidity were measured are called levels. Figures 4.3 and 4.4 clearly indicate that the width, depth and length are assigned at four different levels in accordance to the mesh system. Each level was designated at a distance of one-quarter of each factor. Subsequently for any tank size in the investigation, the level can be considered fixed. The format used in this study to assign three factors, each at four different levels satisfies standard statistical procedure to carry out data analysis such as an analysis of variance (ANOVA) and other techniques.

4.6.2. Experimental Design

In order to obtain meaningful conclusions from the data, a statistical approach to experimental design is essential. Montgomery (1991) defined the statistical design of an experiment as a process of planning the experiment so that appropriate data, that can be analysed by statistical methods, will be collected, resulting in valid and objective conclusions. The experimental design incorporates three basic principles namely replication, randomization and blocking. Replication means a repetition of the basic experiment. For the purpose of this research work the term 'run' has been used for each set of tank data. Three runs were carried out at each tank to provide the required replication. It is an important process due to the following reasons:

1. To obtain an estimate of the experimental error. This estimate will be a basic unit of measurement to determine whether the observed differences in data are really statistically different.

2. To obtain a more precise estimate on the effect of a factor on the sample mean.

During the investigation, two tanks were chosen from each site (Frankley and Trimpley Treatment Works). Velocity measurements from each tank were taken in three different runs. The order of measurement carried out for different points in the tank was based on a randomization procedure over the 16 points in plan view of the tank. The decision not to randomise all the 64 points in the tank was made due to the following reasons:

1. To reduce disturbances to the on-going dissolved air flotation process at the treatment plants.

2. To reduce any risk of contamination or failure to the water supply system and to safeguard Severn Trent Water Company from any complaint.

3. To reduce the time of moving the sludge scraper forwards and backwards in the tank and the danger of running up and down from the control room (to switch on the sludge scraper) to the tank in order to stop the bridge scraper at the required position.

The randomization process can reduce systematic error arising from measurement or investigation being carried out repeatedly in the same order (Chatfield, 1992). It can help in averaging out the effects of factors which have not been or cannot be controlled by the experimenters. Examples of those experiments which cannot be controlled are those involved with raw materials which vary in quality, changes which occurred at different times of the day or with any other environmental conditions.

A technique to increase the precision of the experiment is called blocking. This technique involves making comparisons within matched pairs of experimental data. By having two tanks from each site, the result can be compared using an appropriate statistical test. For example, the average velocities of the two tanks were compared and subsequently the confidence interval on the average velocities were evaluated.

4.6.3. Methods for Velocity Measurements

The methods involved in velocity measurement were divided into three different phases. These can be summarised as follows:

1. Identifying the appropriate statistical technique to be used for data collection
2. Initial preparation works on site before data collection and
3. Data collection

4.6.3.1. Statistical Technique

In order to carry out measurement of the velocity profile along the width, length and depth of the tank, a grid system of equal intervals for each tank dimension was chosen. The distance between the baffle to the outlet wall was divided into four equal intervals. This can be seen from Figures 4.4 and 4.5 (plan view) for the Trimpley and Frankley Water Treatment Works respectively. The length is divided into sections A, B, C and D. The width is divided into sections 1, 2, 3, and 4 with an equal interval between each section. The points of intersection between cross sections and longitudinal sections are those points where velocity measurements were taken. In plan view, there were 16 number of points to be monitored. However the depth is also divided into four equal interval as can be seen from the side elevation view of Figures 4.4 and 4.5. The four different depths are indicated at levels d1, d2, d3 and d4. Thus the total number of points to be investigated for velocity measurement were 64.

The decision to divide the length, width and depth at equal interval was made for the following reasons:

1. It gave a better understanding of the velocity distribution in the tank.

2. It helped to develop a proper statistical model when comparisons were made between different runs or replications. An analysis of variance on the model was readily carried out when there were fixed factors on each tank parameter.
3. It was easy to remember and prevent unnecessary errors during data recording and collection.

4.6.3.2. Preparation Works

Initially drawings of the dissolved air flotation tanks were obtained from the site managers of each treatment works. The dimensions on the drawings were checked based from an available tank which had been emptied.

The difficult problem during site measurement was to transfer points from the floor of the tank to the top wall so that the marking and setting up any dimensions for any particular parameter could be taken. For example it was necessary to measure the length of the mixing zone i.e. in plan view between the tip of the baffle to the outlet wall of the tank. In reality the tip of the baffle was not accessible. It is located within the tank which is below the walking platform. The same problem occurred for the outlet wall of the tank. It was constructed from the floor of the tank to a depth below the walking platform. The solution was made by using a plumb-bob. The positions of any inaccessible points were marked on the upper wall of the tank using a plumb-line. Marking for the different in length position where samplings are required were made on the kerb situated at the upper wall of the tank. For the width of the tank, the marking of the positions were made on the side of the bridge scraper.

The following procedures were undertaken before actual data collection on velocity distribution was made:

1. The batteries of the ADV and lap-top computer were charged. A charger was provided with the ADV equipment and it took at least 10 to 12 hours to get the battery fully charged. The battery of the lap-top computer used in the investigation needed at least 4 hours to be charged. The batteries of the ADV and

lap-top computer can be used for a maximum operation period of 11 and 3 hours respectively.

2. The clamps to hold the ADV probe were installed on the upper and lower side rails of the bridge scraper. The clamps were aligned using a plumb-line. An Allen key was used to screw the clamp to the side rails and to the rod of the ADV probe.
3. A trolley for the ADV processor and the lap-top computer was placed on the platform of the bridge scraper. Connections between the processor and the computer were made accordingly.
4. A bucket of water and a roll of tissue papers were made available on the bridge scraper for cleaning purposes.
5. A log-book was placed on the trolley to record any significant events during data collection.

4.6.3.3. Data Collection

For data collection, the conditioning module was attached with a mounting bracket. This bracket was mounted on the stem made up of galvanised iron pipe of 20mm nominal diameter. The stem was made into segments and joined together by fastening the stud at one end to threaded hole at the other. Experience of using the aluminium cylindrical stem showed that the thread at the joint was easily damaged due to the soft property of aluminium and the extensive connecting and disconnecting of the stem segments. When a steel thread connection was used, it did not create any problem on site. The stem used for data collection was a strong cylindrical hollow tube which is robust, light and easily handled on site. If the stem is too heavy, it is difficult to handle and there is a great possibility that the probe might be dropped into the tank damaging the transmitter and receivers. Plate 4.2 shows how the ADV signal conditioning module was clamped to the bracket and the stem was held in a vertical position by clamping it to the side rails of the bridge scraper. Without the bridge scraper it would be expensive and difficult to carry out any measurement in the middle areas of the flotation tank.

The procedures involved during data collection are described and summarised as follows:

1. The ADV probe was lowered to the prescribed point according to the randomization procedure. The power of the battery at the splash proof box and the computer were switched on. Then the ADV software was operated as described in section 4.2.6.1.
2. The values of water temperature in the tank, the salinity (zero), the sampling rate and the velocity range were entered. In the experiment a sampling rate of 25Hz was used initially at Frankley and 1Hz was used later at Trimpley. A different sampling rate was made because the earlier work at Frankley showed that large quantities of data were captured at a rate of 0.04 second for each reading. This occupied a large amount of hard disk storage capacity. There is a restriction of 140,000 lines if the data is to be transferred onto the EXCEL software. A decision was made to record velocity data at each point for a period of 2 to 3 minutes. A longer recording time was considered inappropriate because initial tests at several points for a period of 25 minutes at each point indicated that there was no significant difference of velocity variation in the time series curves. At the Trimpley Works, a sampling rate of 1Hz was considered appropriate following the first meeting of ADV users within the United Kingdom when it was found that the ADV processor would automatically average the velocity for a period of one second. A velocity range of 3cm/sec was used in the experiment based on the low flow anticipated in the tank of 10mm/sec.
3. The file name of the point to be measured was entered onto the software and the command to start data collection was entered. The file name for each point was based on the grid measurement positions (Figures 4.4 and 4.5) for the Trimpley and Frankley Treatment Works respectively. For example in run number one at the Trimpley Works, a file name of R1A1d1 was made and entered into the software. R1 indicated that it was in run number one, A1 was the point in plan view where the vertical line A met the horizontal line 1 of the grid system and d1 indicated that it was at a depth d1 based from the side elevation view of Figure

4.3. The outflow from the tank was recorded when velocity measurements were taken. This data was used at later stage for data analysis.

4. Any features which may give some impact on the data were normally recorded.
5. No movement on the bridge scraper was made to prevent the probe from being disturbed. The probe is very sensitive and any movement can produce a bias in the result.

4.6.4. Method for Water Sampling

The procedures to identify the water quality sampling points using statistical techniques are the same as those for velocity measurements as per section 4.6.3.1. However the preparation works were different and these can be summarised as follows:

1. A compartment for 64 bottles samples was prepared on the upper tray of the aluminium trolley. A hard cardboard paper was used to separate the sampling bottles. On the sides of the compartment, identification for the sampling points was made based on the rows of bottles to be placed inside the compartment. This helped to avoid mistakes during sampling.
2. Markings on the side and on the top of the bottle cap were made according to the sampling points to be taken. Then the bottles were arranged in a proper order in the compartment. In the experiment, the order of arrangement was made from point A1, A2, A3, A4, B1 and so on. This sequential arrangement was useful to prevent any mistake occurred during sampling operation. For marking purposes a water resistant marker was used.
3. The trolley together with its contents was placed on the platform of the bridge scraper.
4. A bucket of water and a roll of tissue paper were provided on the bridge scraper for cleaning purposes.
5. A log-book was put on the trolley to mark the sampling time for each point.

4.6.4.1. Sampling for Turbidity

During data collection water samples were collected from 64 points in the tank where the velocities were measured. The time of collection of each sample was recorded. At the Trimpley Works, the time and the quantity of outflow from the tank were recorded and monitored automatically by the computer. At the Frankley Works manual recording of the outflow from the tank had to be made because the on-line computer was not programmed to store the outflow data. Water samples from three different stages of flocculation were also taken for each run. Water temperature was recorded in the log-book.

All turbidity measurements were made using a 2100A Hach turbidimeter which was standardised with latex suspension supplied by the manufacturer.

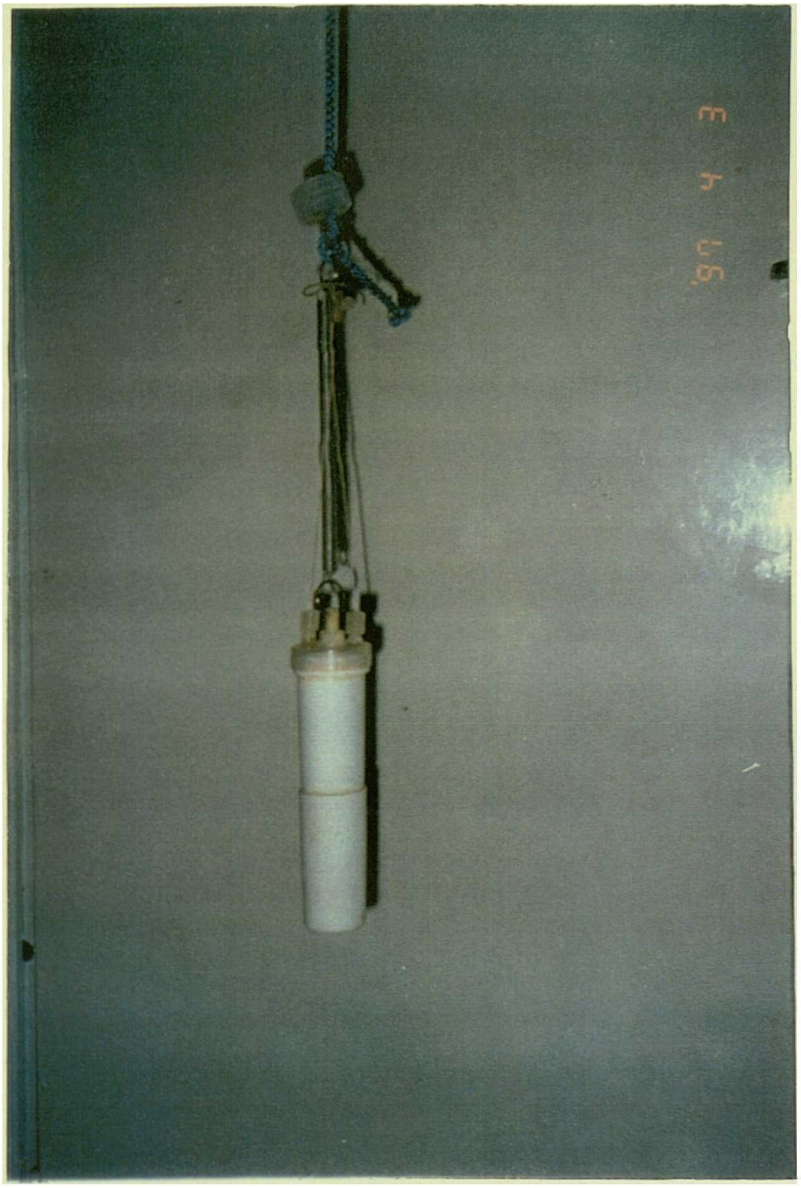

Plate 4.1 - Photograph of bottle sampler used for the investigation

Plate 4.2 - Photograph taken at Trimpley Works showed the ADV was held in position for velocity measurement

CHAPTER 5

A REVIEW OF STATISTICAL METHODS

5.1 INTRODUCTION

In order to achieve the objectives of the study, velocity and turbidity data collected from the two treatment plants at Frankley and Trimpley were analysed using appropriate statistical techniques. Statistical methods employed during data collection have been described in Chapter 4. This chapter provides a review of the statistical approach to data analysis. A detailed explanation of each statistical technique is given in this chapter to provide a clear understanding on the statistical concepts employed. The results of the statistical analysis will be described and explained in Chapters 6, 7 and 8.

A detailed description on how the samples were extracted from the binary files into ASCII files using the WinADV software will also be explained in this chapter. This is followed by a step by step statistical procedure which has been undertaken to analyse the data. Basically this procedure describes the techniques used to analyse the data collected from the field for the purposes of estimation and comparison to test the reliability of the data.

The word 'statistic' can be described as a measure obtained by using the data values from a sample, whereas a measure obtained by using all the data values for a specific population is called a 'parameter' (Bluman, 1992). As statistics are involved with the science of making decisions in the face of uncertainty (Chatfield, 1992), this chapter will consider and discuss the robustness of each statistical method used in the data analysis. The procedures and limitations of each method will be explained. Particular emphasis will be given to data estimation and prediction.

5.2 DATA ESTIMATION

5.2.1 Summarising Velocity Data

Velocity data collected by the ADV software for each point was in the form of a binary file. Each file has an extension of 'adv'. A point A1d1 was put under a file name of R1A1d1 to indicate that the data was collected during 'Run 1'. The default system in the software assigned this point under a file name of 'R1A1d1.adv'. This was converted into an ASCII format by the following procedures:

1. The ADV software, which was named 'Sontek', was run in the C:\cd\sontek directory. To see the files which have been recorded during site investigation, a command C:\sontek>dir was made. The screen showed all the files under 'Sontek' in the C drive.

2. Each file was then converted to an ASCII file using format C:\sontek>getvel~(data file)~(output file)~(probe)~(first sample)~(last sample) where ~ is for space. For example, file R1A1d1 was converted by entering a command C:\sontek>getvel~R1A1d1~1R1A1d1~all. The probe number was not entered because only one probe was used in the investigation. The default system in the software will override it if the word 'all' is used. This is also applicable when it is required to get all the values of the velocity samples in a file.

3. The results of the conversion files in ASCII format were designed to be extracted only by LOTUS or EXCEL software. Using EXCEL software each file was read and saved. Sixty-four files were saved from each run. For a total of four tanks from the Trimpley and Frankley Water Treatment Works, 768 files were saved in EXCEL. These numbers were based on three runs for each tank.

For velocity samples of size $n \geq 30$, an estimate of a population variance, σ^2 is provided by calculating the sample variance s^2. When the sample size increases the sample mean ($\bar{x}$) will get closer to the population mean μ (Chatfield, 1992). For

each point at the Trimpley Treatment Works a sample size of more that 200 was made. As for the Frankley Treatment Works a sample size of not less than 1,000 was collected for every point.

Discussion by Metcalfe (1996) and Martin (1996) has indicated that the velocity data of each point in the file can be considered as a sample of the population and can be analysed by averaging the whole sample. MINITAB software was employed. Basically the calculation was made based on the following equation:

$$\textit{sample mean, } \bar{x} = \frac{\sum_{i=1}^{n} x_i}{n} \qquad (5.1)$$

where x_i is a sample of size n from some population.

Since the sample was random, x_1, x_2....., x_n can be interpreted as n independent random variables. Each sample was also drawn from the same population and thus the expected $E(x_i)=\mu$ and $var(x_i)=\sigma^2$. The proof can be written as follows (Chatfield, 1992):

$$E(\bar{x}) = E\left\{\frac{(x_1 + x_2 + \ldots\ldots\ldots x_n}{n}\right\}$$

$$= E\left(\frac{x_1}{n}\right) + E\left(\frac{x_2}{n}\right) + \ldots\ldots\ldots + E\left(\frac{x_n}{n}\right)$$

$$= \frac{\mu}{n} + \frac{\mu}{n} + \ldots\ldots\ldots \frac{\mu}{n}$$

$$= \mu$$

For the variance of ($\bar{x}$);

$$\textit{variance } (\bar{x}) = var\left(\frac{\sum x_i}{n}\right)$$

$$= \frac{1}{n^2}\left[\text{var}(x_1) + \text{var}(x_2) + \ldots\ldots + \text{var}(x_n)\right]$$

$$-\frac{1}{n}\left(\sigma^2+\sigma^2+.....+\sigma^2\right)$$

$$\sigma^2/n$$

The standard deviation or standard error of $\bar{x}$ is equal to $\sigma/\sqrt{n}$. This indicates that as the number of observations n increases the standard error will decrease. This confirms the idea that the more observations taken the more accurate will be the sample mean.

When the ADV software for velocity data screening was developed by the US Bureau of Reclamation and then supplied to the ADV users, velocity data were screened for poor quality readings. It was found that there was no significant difference in the average velocity between using 'MINITAB' and ADV data screening software. This was due to the fact that during data collection the values of the signal correlation for each of the three receivers were more that 70% and considered good. These values are given as a percent and a value of 100 means a perfect correlation.

Contact was made with the manufacturer (Lohrmann, 1997) of the equipment and the author (Wahl, 1997) of the software for velocity screening (WinADV) on how exactly the correlation parameter was calculated. Lohrmann (1997) indicated that the ADV velocity is estimated by measuring the phase shift between the echo from two successive pulses. According to the manufacturer the phase shift was estimated by a signal processing technique called "complex covariance estimation between pulse-pairs" which generates a covariance function that has a phase and magnitude. The phase is directly proportional to the distance the particles have travelled during the time between the pulses. The magnitude is a measure of the similarity of the echoes described by Lohrmann (1997) in terms of a normalised correlation. If the echo from the two pulses are identical the correlation will be perfect. If the echoes are dissimilar the correlation will be reduced.

By using the WinADV, the quality of each sample was estimated by an autocorrelation parameter. Samples with a value of less than 70 were removed from the series. Samples that were tagged with communications error flags (i.e. samples not properly received by the ADV program) were removed and replaced with interpolated values. The latter was carried out by clicking on the 'Filter out communications errors' option on the filtering options screen of the WinADV. The filtering process that was carried out was based on the average correlation parameter from amongst the three channels. The filtering process can also be based on a minimum correlation parameter for all three channels. Additional filtering techniques were based upon the signal-to-noise ratio, the removal of samples within a specified range, or the removal of data which were marked with communication error flags.

During the filtering process it was found that four out of 768 files were unable to be processed using an autocorrelation parameter. The velocity data of these files were collected from the Trimpley Water Treatment Works. The four files were R2D4d4 of run number 2 from tank C1, R1D4d4 of run number 1 from tank C1, R2D1d4 and R2D4d4 of run number 2 from tank C1. The output from the WinADV screen only stated 'Sampling window does not specify any valid sample for this flag arrangement' and 'Review sampling options'. Since the software indicated that there was a need to review the sampling option, an average signal-to-noise ratio filtering option was tried and was able to filter the velocity data. The signal-to-noise ratio is the ratio of the signal strength to the background acoustic noise level inherent in the ADV instrument. The measurement values are in dB (decibel) relative to the noise level. WinADV specified that for measuring mean velocities the signal-to-noise ratio should be 5dB or higher. Low signal-to-noise ratio indicated that the water sample has low concentration of scatterers (particles in the flow that reflect acoustic signal back to the probe receivers).

The following procedures were carried during the filtering process using WinADV:

1. The WinADV program was opened using 'winadv.exe' from the file manager.

2. Raw data for each file was opened and the screen displayed the unfiltered time series graphs for velocity components in the x, y and z directions. Velocity components in the x, y and z directions were marked in black, blue and red colours respectively. Checking for aliasing in the velocity data was made visually from the output graphs. Aliasing is represented by ADV as a spike in the velocity data that biases the average velocities and makes instantaneous velocity measurements uncertain. To assist in identifying aliasing, WinADV computed the skewness of the velocity distribution for each file and reported the maximum skewness in the '.sum' file. Skewness greater than 1.5 has to be investigated for evidence of aliasing.

3. A filtering command was clicked and this gave the percentage of good data which has been filtered. 100% indicates that all the raw data in the file were good with correlation more than 70%. A 'redraw' command was clicked to see the time series graphs for all velocity components.

4. A 'process' command was made from the screen to process the filtered velocity data so that summary statistics and sample-by-sample files were computed and stored in the C drive. Summary statistics and sample by sample data were given with extension files '.sum' and '.vf' respectively. An output format was clicked under 'EXCEL' so that the above files can be read under EXCEL software.

5.2.2 Comparing Data

In order to reach a subjective conclusion as to whether there is a significant difference of mean velocities between different runs, the use of a descriptive method was employed. For this purpose MINITAB software was used to analyse the data. Velocity data from three different runs in the tank were compared using a boxplot. A rectangular box was plotted for each run which represented the middle 50% of the data. The general extent of the data was represented by lines on both sides of the box. The median value of the data was marked across the box. The outliers or observations which were far from the rest of the data were marked by an asterisk.

MINITAB considers outliers as any value lying between one and a half and three times the spread of the middle 50% of the data above and below the average values. Any more remote value is considered an extreme outlier and marked as '0'.

5.2.3 Analysis of Variance (ANOVA)

The statistical procedure used to compare different components of variation is called the analysis of variance. It is always linked with the analysis of designed experiments. This procedure attempts to analyse the variation of the response variable (the variable to be predicted), which is in this case the velocity and turbidity. The rationale of the problem is that the response variable will only vary because of the variability associated with a set of unknown independent variables. For example, velocity at different points in the tank may vary due to unknown independent variables such as the flow into the tank, the dimension of the tank, the temperature of the fluid and many others. In reality, the experimenter will rarely include all the variables affecting the response in the experiment because of the overall cost, development time or the practicality of the investigation. Hence random variation will also be observed even if all the independent variables considered were held constant. The main objective of ANOVA is to identify the independent variables which cause significant variation in the response variable and to determine how they interact and subsequently affect the response.

During the investigation three runs (treatments) were performed for each tank. The observed response from each of the three runs or treatments was a random variable. The velocity data appeared in the form that can be generally formatted as in Table 5.1.

Table 5.1 - The formatted form of velocity data

	Observations	Total	Sample mean	Population mean	Sample variance
Treatment 1	$x_{11},x_{12},$ .....x_{1n}	T_1	$\bar{x}_1$	μ_1	s_1^2
Treatment 2	$x_{21},x_{22},$.....x_{2n}	T_2	$\bar{x}_2$	μ_2	s_2^2
.....	.....	...	...	...	...
.....	.....	...	...	...	...
Treatment c	$x_{c1},x_{c2},$.....x_{cn}	T_c	$\bar{x}_c$	μ_c	s_c^2

It is useful to describe the observations based on Table 5.1 with the following linear statistical model:

$$x_{ij} = \mu + \tau_i + \varepsilon_{ij} \qquad (5.2)$$

where x_{ij} was the (ij)th observation, μ was a parameter common to all treatments (conditions or processes whatever being compared) called the overall mean, τ_i was a parameter unique to the ith treatment called ith treatment effect and ε_{ij} was a random error component. This model is called one-way or single-factor analysis of variance because only one factor (i.e. the treatment effect) is considered. The model was considered to be a fixed effects model because the treatments or runs have been specifically chosen during the investigation and in this case the experimenter was only trying to see the variation in velocities between different runs from one tank. Montgomery (1991) has indicated that in the fixed effects model the treatment effects τ_i can be defined as deviations from the overall mean where,

$$\sum_{i=1}^{a} \tau_i = 0 \qquad (5.3)$$

where a is the level of the factor.

One-way analysis of variance was performed to test the hypothesis that there was no difference between a number of treatments or runs for velocity data. Here the F test

was used to test a hypothesis concerning the means of three or more populations. The *t* test cannot be used because its application is limited to comparing two means at a time, and the rest of the means under study are ignored (Bluman, 1992). The second reason is that the probability of rejecting the null hypothesis when it is true is increased, since the more the *t* tests are being conducted the greater the chances of getting significant differences by chance alone. The third reason is that a greater number of *t* tests will be required when comparing a large number of means. The assumptions for the *F* test for comparing three or more means are as follows:

1. The underlying sample populations must be normally distributed.
2. The samples must be independent of each other.
3. The variances of the population must be constant.

Under this test two different estimates of the population variance were made. The first estimate of variation was made between runs or treatments by measuring the variability between the run means, $\bar{x}_1, \bar{x}_2 \ldots\ldots \bar{x}_n$. The second estimate of variation was made within each run by computing the variance of all the data and was not affected by differences in the means. For velocity data where there is no difference in the means, the between-run estimate will be approximately equal to the within-run variance estimate and the value of F-test will be 1. However when the means differed significantly the between-run variance will be much larger than within-run variance; consequently the F-test value will be larger than 1 and the null hypothesis will be rejected.

MINITAB software was used for the analysis of variance. The data computed by the software were given in a tabulated format and the calculations were based on the following table:

Table 5.2 - One-way ANOVA (Source: Chatfield, 1992)

Source of variation	Sum of squares	Degrees of freedom	Mean square
Between runs	$n\sum_{i=1}^{c}(\bar{x}_i - \bar{x})^2$	$c-1$	s_B^2
Within runs	$\sum_{i=1}^{c}\sum_{j=1}^{n}(x_{ij} - \bar{x}_i)^2$	$c(n-1)$	s^2
Total variation	$\sum_{i=1}^{c}\sum_{j=1}^{n}(x_{ij} - \bar{x})^2$	$cn-1$	

n= sample size c=run or treatment $\bar{x}$ =sample mean
i=ith run j=jth observation
s_B^2 =estimate of σ^2 based on $(c-1)$ degrees of freedom
s^2 –combined estimate of σ^2 (population variance) from the variation within runs
x_{ij} is the jth observation in the sample from population i, x_i

The mean squares for s_B^2 and s^2 were obtained by dividing the appropriate sum of squares by the appropriate number of degrees of freedom (Ryan and Joiner, 1994). The degrees of freedom are the number of values which are free to vary after a computation on a sample statistic is made, and are associated with the specific curve to be used when a distribution consists of a family of curves. The F ratio was obtained by dividing the mean square between runs with the mean square within runs. The software also produced the significance level denoted as p in the ANOVA table based on the F ratio with the appropriate degrees of freedom.

A 95% confidence interval for the means from three runs were plotted to give a subjective conclusion on the velocity data. This estimation means 95% of the time we have a certain confidence that the interval does contain the mean value. Each confidence interval was calculated based on the following equation:

$$\bar{x}_i - ts_p / \sqrt{n_i} \text{ to } \bar{x}_i + ts_p / \sqrt{n_i} \qquad (5.4)$$

where $\bar{x}_i$ and n_i are the sample mean and sample size for level i , s_p is the pooled standard deviation and equal to the square root of mean square error which is the

pooled estimate of the common standard deviation σ, and t is the value from a t-table corresponding to 95% confidence and the degrees of freedom associated with the mean square error.

5.2.3.1 Model Adequacy

The observations described by the model in Equation 5.2 were based on the assumptions that the errors were normally and independently distributed with mean zero and constant but unknown variance σ^2, i.e. normally written as NID(0,σ^2). If the assumptions were valid then the ANOVA procedure was an exact hypothesis test of no difference in the treatment means. To check that these assumptions were not violated the residuals were investigated. Montgomery (1991) defined the residual for observation j in treatment i for the one-way model as follows:

$$\begin{aligned} e_{ij} &= x_{ij} - \hat{x}_{ij} \\ &= x_{ij} - \bar{x}_i \end{aligned} \qquad (5.5)$$

where $\hat{x}_{ij}$ is an estimate of the corresponding observation x_{ij} and $\bar{x}_i$ is the overall mean in the i treatment. The derivation of the above equation can be found in Montgomery (1991).

The residuals from the ANOVA of each tank were examined for model adequacy. Plots of residuals versus fitted values were made. The model is only valid when the plot shows a structureless pattern. The residuals should be unrelated to any other variable, including the response x_{ij}. If the plot looks like an outward-opening funnel, the implication is that the error or the background noise in the experiment was a constant percentage of the size of the observation. This means that the variance of the observations increases as the number of observations increased.

A check on the normality assumption can be made by constructing a normal probability plot or by plotting a histogram of the residuals. If the NID(0,σ^2)

assumption on the errors is satisfied the normality plot will resemble a straight line. When visualising the straight line more emphasis on the central values of the plot should be made (Montgomery, 1991). As for the histogram plot, it will look like a sample from a normal distribution centred at zero.

Velocity data from the investigation were checked using a normal plot. The residuals from each observation were arranged in the increasing order and a plot of the ordered residuals versus probability was made using MINITAB software. In the fixed effects ANOVA model, moderate departures from normality are of little concern (Montgomery, 1991). An error distribution with thicker or thinner tails than normal will be of greater concern than a skewed distribution whereby the plot showed the right tail longer than the left. A skewed distribution has little effect on the true significance level. However for a random effects model non-normality can severely affect the true significance levels on interval estimates of variance components.

5.2.4 Randomized Block Design

During the investigation two out of several tanks of the same size from each treatment works were randomly selected at the initial stage and then investigated for velocity and turbidity distributions. A measurement for each run or treatment from the same tank was made on different days. Thus the experiments were extended for several days. It is possible that observations made on the same day may show better agreement than those made on different days. In this case there was a danger of introducing a systematic error if only one tank was investigated. Two tanks of the same size were utilised with an equal number of measurements being made in each tank or block, and the order of tests within a block are randomized, then the experiment is called a randomized block experiment. A blocking technique is considered a useful method of increasing the precision of comparative experiments (Chatfield, 1992).

For a randomized block experiment at the Trimpley and Frankley Water Treatment Works, the data collected from each site can generally be described and formatted in a universal form as shown in Table 5.3. In this case the term 'run' which was used in the experiment can be considered as the treatment.

Table 5.3 - General form of data for the randomized block experiment
(Source: Chatfield, 1992)

	Treatment 1.....Treatment c	Row total	Row average
Tank 1	x_{11} .....x_{1c}	$T_{1.}$	$\bar{x}_{1.}$
Tank 2	x_{21} .....x_{2c}	$T_{2.}$	$\bar{x}_{2.}$
Column total	$T_{.1}$ .....$T_{.c}$		
Column average	$\bar{x}_{.1}$ ..... $\bar{x}_{.c}$		

5.2.4.1 Two-way ANOVA

The data in Table 5.3 are classified into two characteristics i.e. treatment (run) and tank. Thus the procedure to analyse the data is called two-way analysis of variance. Three runs or treatments were carried out on each tank. The average velocity of each run was calculated and the value was entered under the 'Treatment' column according to Table 5.3. There were no missing velocity data encountered during the investigation. If there were any missing velocity data the design would be unbalanced. MINITAB software was used to analyse the data. For one average observation of velocity on each run in each tank, the statistical model of the design was as follows:

$$x_{ij} = \mu + \tau_i + \beta_j + \varepsilon_{ij} \qquad (5.6)$$

where i=1,2,...r, j=1,2,....c, μ is the overall mean, τ_i is the effect of the ith run (treatment), β_j is the effect in the jth tank (block) and ε_{ij} is the usual NID(0,σ^2) random error term. Runs and tanks were initially considered as fixed factors. The run and tank effects were defined as deviations from the overall mean so that:

$$\sum_{i=1}^{r} \tau_i = 0$$

and

$$\sum_{j=1}^{c} \beta_j = 0$$

The hypothesis tests involved were to find the equality of the treatment means and then to see any significant difference between the observed run (treatment) effects. The total corrected sum of squares for Equation 5.6 and its derivation can be found in Montgomery (1991). This can be expressed as the total variation in velocity equals the sum of variation due to run, variation due to tank and variation due to random error.

MINITAB software was used for hypothesis testing of the experimental data. This was done using two-way ANOVA with balanced designs. The outputs from the software were based on Table 5.4.

Table 5.4 - Two-way ANOVA (Source: Chatfield, 1992)

Source of variation	Sum of squares (*SS*)	Degrees of freedom(*df*)	Mean squares(*MS*)	F-ratio
Treatments or Runs (columns)	$r\sum_{j=1}^{c}(\bar{x}_{.j} - \bar{x})^2$	*c-1*	$\frac{SS_{treatments}}{df}$	$\frac{Treatment_{MS}}{Residual_{MS}}$
Blocks or Tanks (rows)	$c\sum_{i=1}^{r}(\bar{x}_{i.} - \bar{x})^2$	*r-1*	$\frac{SS_{blocks}}{df}$	$\frac{Block_{MS}}{Residual_{MS}}$
Residuals(error)	$\sum_{ij}(x_{ij} - \bar{x}_{i.} - \bar{x}_{.j} + \bar{x})^2$	*(r-1)(c-1)*	$\frac{SS_{error}}{df}$	
Total	$\sum_{i,j}(x_{ij} - \bar{x})^2$	*rc-1*		

Note: c = runs r = tanks

Model adequacy checks for two-way ANOVA are similar to those procedures found in Section 5.2.3.1. Normal probability plots of residuals were carried out on the data

from both treatment works. Similarly plots of residuals versus fitted values were also made.

5.3 MAKING PREDICTIONS FROM VARIABLES

5.3.1 Factorial Designs

The full-plant study was concerned with the investigation of the effects of width, depth and length on the velocity and turbidity distributions of the DAF tank. The physical parameters of the tank (width, depth and length) were called 'factors' and the fixed positions where the velocities and turbidities have been measured were called 'levels'. In general factorial designs were most efficient for this type of experimentation. By using factorial designs all possible combinations of the levels of the factors were investigated.

The effect of a factor can be defined as the change in response produced by a change in the level of a factor (Montgomery, 1991). Normally this is called the 'main effect' because it refers to the primary factors of interest in the experiment. Factorial designs have the following advantages:

1. To provide a more efficient method of experiment than one-factor-at-a-time.
2. To avoid misleading conclusions on the results when interactions between factors are present.
3. To allow the effects of a factor to be estimated at several levels of the other factors and to give conclusions that are valid over a range of experimental conditions.

5.3.1.1 Multifactor Balanced Designs

In the experiment three factors were investigated. Each factor was set at four different levels. This type of experiment is called the 'three-factor factorial design'.

In general this type of factorial design can be described as having a levels of factor A, b levels of factor B and c levels of factor C. For n replicates of the experiment there will be a total of $abcn$ observations.

For one site where all the tanks have the same size then the physical dimensions are considered fixed. The model to be developed will fall under a category of a fixed effects model. If there are many water treatment sites to be investigated with various tank configurations within each site, and the tanks chosen from each site are based on randomization procedures, then the model to be developed will be called a random effects model. The latter model will enable the experimenter to draw conclusions from a wider population than that covered by the experiment.

When comparisons on the effects of velocity distribution at different levels of width, depth and length are made on the same tank size, then the fixed effects model for the three-factor analysis of variance can be written as follows:

$$x_{ijkl} = \mu + \tau_i + \beta_j + \gamma_k + (\tau\beta)_{ij} + (\tau\gamma)_{ik} + (\beta\gamma)_{jk} + (\tau\beta\gamma)_{ijk} + \varepsilon_{ijkl} \qquad (5.7)$$

where x_{ijkl} is the observed response when factor A is at the ith level (i=1,2,....,a), factor B at the jth level (j=1,2,....,b), factor C at the kth level (k=1,2,....,c) for the lth replicate (l=1,2,....,n), μ is the overall mean, τ_i is the effect of the ith level of factor A, β_j is the effect of the jth level of factor B, γ_k is the effect of the kth level of factor C, $(\tau\beta)_{ij}$, $(\tau\gamma)_{ik}$, $(\beta\gamma)_{jk}$ and $(\tau\beta\gamma)_{ijk}$ are the interaction terms between them and ε_{ijkl} is the random error component.

Multifactor balanced designs were conducted using MINITAB software based on the model in Equation 5.7. For the three-factor fixed effects model, the analysis of variance carried out by the computer package was based on Table 5.5. The detailed equations 'the sum of squares for all factors' and their interactions can be found in Montgomery (1991).

Table 5.5 - ANOVA for the three-factor fixed effect model
(Source: Montgomery, 1991).

Source of variation	Sum of squares	Degrees of freedom (*df*)	Mean square (*MS*)	F-ratio
A	SS_A	*a-1*	$\frac{SS_A}{df}$	$\frac{MS_A}{MS_E}$
B	SS_B	*b-1*	$\frac{SS_B}{df}$	$\frac{MS_B}{MS_E}$
C	SS_C	*c-1*	$\frac{SS_C}{df}$	$\frac{MS_c}{MS_E}$
AB	SS_{AB}	*(a-1)(b-1)*	$\frac{SS_{AB}}{df}$	$\frac{MS_{AB}}{MS_E}$
AC	SS_{AC}	*(a-1)(c-1)*	$\frac{SS_{AC}}{df}$	$\frac{MS_{AC}}{MS_E}$
BC	SS_{BC}	*(b-1)(c-1)*	$\frac{SS_{BC}}{df}$	$\frac{MS_{BC}}{MS_E}$
ABC	SS_{ABC}	*(a-1)(b-1) (c-1)*	$\frac{SS_{ABC}}{df}$	$\frac{MS_{ABC}}{MS_E}$
Error	SS_E	*abc(n-1)*	$\frac{SS_E}{df}$	
Total	SS_T	*abcn-1*		

Note: a = levels of factor A b = levels of factor B c = levels of factor C
n = number of replicate (run)

5.3.2 Analysis of Covariance

This technique is used to improve the precision of the experiment (Montgomery, 1991). During the investigation, the levels of each factor (i.e. width, depth and length) can be controlled. However the discharge from the tank cannot be controlled. The discharge is a covariate or concomitant variable. The analysis of covariance involved adjusting the response variable (i.e. the velocity) for the effect of the discharge. According to Montgomery (1991), the covariate could inflate the error

mean square and make true differences in the response due to treatments difficult to detect.

For the experiment which has three factors with one covariate as described in the previous section (Section 5.3.1), the model for the analysis of covariance can be written as follows:

$$x_{ijkl} = \mu + \tau_i + \beta_j + \gamma_k + (\tau\beta)_{ij} + (\tau\gamma)_{ik} + (\beta\gamma)_{jk} + (\tau\beta\gamma)_{ijk} + \psi(\omega_{ijkl} - \overline{\omega}_{....}) + \varepsilon_{ijkl} \quad (5.8)$$

where all the terms in the equation are the same as in Equation 5.7 except that ω_{ijkl} is the measurement made on the discharge corresponding to x_{ijkl} when factor A is at the ith level, factor B at the jth level, and factor C at the kth level for the lth replicate. $\overline{\omega}_{....}$ is the mean of the ω_{ijkl} values and ψ is a linear regression coefficient indicating the dependency of x_{ijkl} on ω_{ijkl}. The assumptions made (on Equation 5.8) are that the errors ε_{ijkl} are NID(0,σ^2), the slope of $\omega \neq 0$ and the relationship between x_{ijkl} and ω_{ijkl} are linear, the regression coefficients for each treatment are identical, the treatment effects sum is equal to zero and the concomitant variable is not affected by the treatment. Further details regarding this model and the calculations on the sum of squares can be found in Montgomery (1991). The analysis of covariance model (i.e. Equation 5.8) is a combination of the linear model employed in the analysis of variance (see Equation 5.7) and regression.

5.3.3 Regression Analysis

The word 'regression' was first introduced by Sir Francis Galton in his Presidential address of the British Association in 1885 at Aberdeen, Scotland (Draper and Smith, 1981). However the analysis he made at that time would only be called a 'correlation analysis' today. The method used in regression is the same as the method of analysis called the 'method of least squares'. It was reported that this method of analysis was discovered independently by C.F.Gauss and A.M.Legendre (Draper and Smith, 1981).

Regression is a method used to describe the nature of the relationship between variables. There are two types of variables involved in any regression analysis. The first one is called the independent variable or the predictor variable. These variables are those that can be controlled or manipulated, or else take values that can be observed but not controlled. Normally the independent variable is designated as the x variable in a simple linear regression equation. In the case of this investigation the independent variables were the width, depth and length of the tank. The second type of variable is called the dependent or response variable. This variable cannot be controlled or manipulated. The velocity or turbidity data from the full-plant studies were considered as the response variables. For a simple linear regression equation the dependent variable is normally designated as the y variable. In general, the objective of regression analysis is to find out how changes in the predictor variables affect the values of the response variables (Draper and Smith, 1981). The distinction between independent and dependent variables is not always a straightforward or a clear-cut case, but is sometimes arbitrary and depends on the objective of the study.

An overview of a simple linear regression will be described in the next section. The objective is to clarify the basic principle in regression analysis so that the idea of correlation and the coefficient of determination can be explained before moving into a complex method of analysis, where the latter will be used extensively when every regression analysis is carried out. For this reason it is felt that the principle of a simple linear regression has to be reviewed.

5.3.3.1. Linear Regression

Linear regression normally deals with a straight line relationship between two variables. To check whether there is any strength and direction of a relationship between the two variables, a simple test on correlation coefficient (r) can be made by using Equation 5.9. It is meaningless to make a prediction using a regression line when the correlation coefficient is not significant. For a strong positive or negative

relationship between the two variables, the value of r will be close to +1 and -1 respectively.

$$r = \frac{n(\sum xy) - (\sum x)(\sum y)}{\sqrt{\left[n(\sum x^2) - (\sum x)^2\right]\left[n(\sum y^2) - (\sum y)^2\right]}} \qquad (5.9)$$

For a response variable Y and predictor variable X where each has n number of observations, a first-order model can be written as:

$$Y = \beta_0 + \beta_1 X + \varepsilon \qquad (5.10)$$

where ε is the increment by which any individual Y may fall off the regression line (refer to Draper and Smith, 1981).

Referring to Equation 5.10, β_0, β_1 and ε are unknown and in fact ε changes for each observation of Y, but β_0 and β_1 remain fixed and can be found by examining all possible occurrences of Y and X. To give the estimates of b_0 and b_1 of β_0, β_1 from Equation 5.10, the following equation can be written:

$$\hat{Y} = b_0 + b_1 X \qquad (5.11)$$

where $\hat{Y}$ is the predicted value of Y for a given X, when b_0 and b_1 are determined.

For n sets of observations (X_1, Y_1), (X_2, Y_2), (X_3, Y_3),..... (X_n, Y_n), then Equation 5.10 can be written as:

$$Y_i = \beta_0 + \beta_1 X_i + \varepsilon_i \qquad (5.12)$$

where i=1,2,.....n, then the sum of squares of deviation S from the true line is

$$S = \sum_{i=1}^{n} \varepsilon_i^2 = \sum_{i=1}^{n} (Y_i - \beta_0 - \beta_1 X_i)^2 \qquad (5.13)$$

By choosing b_0 and b_1 as the estimate to be the values which, when substituted for β_0, and β_1, will produce the least possible value of S, then b_0 and b_1 can be found by differentiating Equation 5.13 with respect to β_0, and then β_1 and setting the results equal to zero. The details of the differentiation can be found in Draper and Smith (1981). The value of b_1, which is the slope of the fitted straight line, will be as follows:

$$b_1 = \frac{\sum(X_i - \overline{X})(Y_i - \overline{Y})}{\sum(X_i - \overline{X})^2} \qquad (5.14)$$

where $\overline{Y} = \sum Y_i / n$ and $\overline{X} = \sum X_i / n$

The value of b_0 in Equation 5.11 refers to the value at the intercept of $X=0$ of the fitted straight line of the least squares method. This value can be found as follow (Draper and Smith, 1981):

$$b_0 = \overline{Y} - b_1 \overline{X} \qquad (5.15)$$

By substituting Equation 5.15 into Equation 5.11, the estimate of regression equation will be

$$\hat{Y} = \overline{Y} + b_1(X - \overline{X}) \qquad (5.16)$$

For a fitted line as per Equation 5.10, the sum of squares of deviation of the *i*th observation from the overall mean will be equal to the sums of squares of the deviation of the predicted value of the *i*th observation from the mean plus the sum of squares of the deviation of the *i*th observation from its predicted value (Draper and Smith, 1981). This expression can be written with the following equation:

$$\sum(Y_i - \overline{Y})^2 = \sum(\hat{Y}_i - \overline{Y})^2 + \sum(Y_i - \hat{Y}_i) \qquad (5.17)$$

The expression from Equation 5.17 has normally been shortened with the following wording:

Sum of squares about mean	=	*Sum of squares due to regression*	+	*Sum of squares about regression*

In order to check how useful the regression line is as a predictor variable, an assessment has to be made on how much the sum of squares (*SS*) about the mean has fallen into the *SS* due to regression and how much into the *SS* about regression. This is done using the following expression:

$$R^2 - SS \text{ due to regression}/SS \text{ about the mean} \qquad (5.18)$$

where R^2 is called coefficient of determination and often expressed as a percentage.

SS due to regression and *SS* about the mean are sometimes called explained variation and total variation respectively. For a strong relationship between response and predictor variables the ratio of R^2 is not far from unity. In fact the other interpretation of R^2 is the squares of the correlation between the observed y values and the fitted y values.

5.3.3.2. Developing Regression Models

Since the data collected from the full-plant studies consisted of three predictor variables (namely width, depth and length), the use of a simple linear regression with one predictor variable as explained in the previous section is not appropriate. However its basic principle can be extended by having a first-order linear model with three independent variables. This model can be written as follows:

$$Y = \beta_0 + \beta_1 X_1 + \beta_2 X_2 + \beta_3 X_3 + \varepsilon \qquad (5.19)$$

where β_1, β_2, and β_3 are the coefficient for the width X_1, depth X_2, and length X_3 respectively and ε is the random error component.

The basic assumptions behind the multiple regression model of Equation 5.19 can be explained as follows:

1. The underlying population regression line is approximately $Y=\beta_0+\beta_1X_1+\beta_2X_2+\beta_3X_3$.

2. For all values of X_1, X_2 and X_3, the Ys have approximately the same or constant variance, σ^2.

3. The Y values for each X_1, X_2 and X_3, are approximately normal distributions.

4. The Y values are approximately independent.

5. Finally b_0, b_1, b_2, b_3, and s are used for the estimated values of β_0, β_1, β_2, β_3 and σ respectively.

Equation 5.19 was the first initial model developed during regression analysis for each tank. Tests on R^2 showed that the model was not appropriate because the percentage of explained variation was very low and was considered not to fit the data. In order to improve the model, a series of transformations was incorporated into the model. These trials were carried out in an ordered way and the sequence of trials were based on Table 5.6. These trials were found to be unproductive as there was not much improvement on the value of R^2.

Table 5.6 - A series of transformation trials carried out during data analysis:

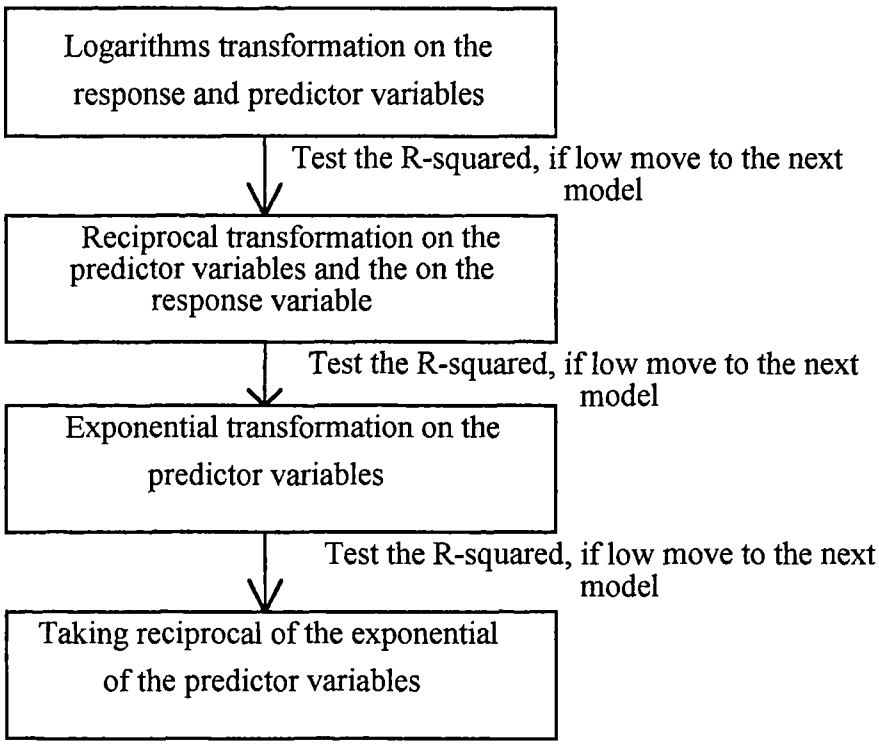

Since the first-order model was found to be unacceptable, a second-order model was postulated. At this stage another predictor variable, i.e. the outflow from the tank, was added thus making the total number of predictor variables into four. The outflow from the tank cannot be controlled during the full-plant studies. Any variation in the flow would affect the velocity and turbidity distributions in the tank. However, without taking the outflow into the model it will violate the basic principle of regression i.e. to develop the relationship of all the known variables in the tank. The following second-order model for four predictor variables was tried:

$$Y = \beta_0 + \beta_1 X_1 + \beta_2 X_2 + \beta_3 X_3 + \beta_4 X_4 + \beta_{11} X_1^2 + \beta_{22} X_2^2 + \beta_{33} X_3^2 + \beta_{44} X_4^2 + \beta_{12} X_1 X_2 + \beta_{13} X_1 X_3 + \beta_{14} X_1 X_4 + \beta_{23} X_2 X_3 + \beta_{24} X_2 X_4 + \beta_{34} X_3 X_4 + \varepsilon \qquad (5.20)$$

where X_1, X_2, X_3, and X_4 are the width, length, depth and the flow out of the tank respectively and all the βs are the coefficients for respective variables.

The basic assumptions of the model in Equation 5.20 were fundamentally the same as the previous model (Equation 5.19). The only difference in this model from the previous one was an increased number of variables to be analysed.

The above model was found to have a better value of R^2 than the first-order model for all the tanks under investigation. A trial was made to improve this model by having a third-order model. However it was found with the latter model that no significant improvement was achieved. Hence the second-order model was adopted.

5.3.3.3 Interpreting the Output

Computations of the response and predictor variables based on the model in Equation 5.19 were made using 'MINITAB' software. The outputs from the software enabled the significance of all the predictor variables to be checked. The results were arranged into five columns. The first column consisted of the predictor variables followed by their coefficients, standard deviations, t-ratio and level of significance. The coefficients were the values of all the βs terms in the model. Tests of significance for each predictor variable were based on the hypothesis that the value of the hypothesised coefficient was zero. This t-test is equivalent to testing whether the population correlation coefficient is zero. This can be written as follows:

$$t = \frac{coefficient - (hypothesised.value)}{(estimated.stdev.of.predictor.\text{var}iable)} \qquad (5.21)$$

where t is given in the column headed 't-ratio'.

The last column denoted by p indicates the level of significance for a particular predictor variable. A step-by-step trial was made to eliminate the first most non-significant predictor variable from the model (Metcalfe, 1997). Then the value of R^2 was checked to see whether any improvement had been made. If there was an improvement, then the next least significant variable was eliminated and again the value of R^2 was checked for the new model. The same procedure was made to the next predictor variable unless no improvement was achieved.

It should be noted that care has to be taken in the use of R^2 as a criterion for judging the quality of the regression equation. Draper (1981) demonstrates that by selecting a sufficient number of variables, the value of R^2 can be made equal to 1. He also demonstrates that an improvement in R^2 can occur simultaneously with an increase in the standard error, which implies a reduction in the precision of the estimate.

The standard deviation of y, or the response variable about the regression line, or the standard error of estimate was carried out by the software based on the following equation:

$$s = \sqrt{\frac{\sum(y - fitted.y)^2}{n-2}} \qquad (5.22)$$

The value of s is a measure of how much the observed y value differs from the corresponding average y value as given by the least square line. The t-test (Equation 5.21) was based on the value of s in Equation 5.22 with (n-2) degrees of freedom.

5.3.3.4 Model Adequacy

An analysis of residuals from a linear regression model is necessary in order to determine the adequacy of the least squares fit (Montgomery, 1991). The residuals can be defined as the differences between what is actually observed and what is predicted by the regression equation. In fact this is the amount which the regression equation has not been able to explain. If the model is correct, then the residual e_i can be treated as the observed errors.

When the regression analysis was carried out, the following assumptions on the errors were made. The errors were independent with mean zero, having constant variance σ^2, and followed normal distribution. If the fitted models were correct, the residuals must exhibit tendencies to confirm the assumptions made. The basic tests that had been carried out were the same as those found in section 5.2.3.1.

CHAPTER 6

VELOCITY DATA CHARACTERISTICS ANALYSIS

6.1 INTRODUCTION

In Chapter 4 statistical techniques were used to carry out velocity measurement on each of the 64 points in the tank. Detailed descriptions on the equipment, DAF tanks, and the way in which the velocity measurements were carried out on site have been described. In Chapter 5 the methods of extracting raw velocity data from the ADV data logger were described. This was followed with the descriptions of the WinADV software to filter the data. The statistical methods to analyse the velocity and turbidity data obtained from the site investigation are also described in Chapter 5, these include comparing the data (velocity or turbidity) between runs, within runs, between tanks, and between sites using the appropriate statistical technique. The techniques of developing suitable models from the velocity and turbidity data were also explained.

This chapter deals with the results obtained from the full-scale plant studies of Trimpley and Frankley Water Treatment Works (WTW) of Severn Trent Water. The first part of the chapter describes and compares the velocity obtained by averaging the observed velocities for each point with the average velocity obtained by a filtering method using the WinADV software. The terms 'average velocity' or 'averaging velocity' described in this chapter refer to the total sum of all velocity samples observed during the investigation divided by the number of observations. The average filtered velocity method described in this chapter refers to the total sum of velocity samples which have been selected according to the filtering criteria of the WinADV divided by the number of filtered velocity samples. The filtering criteria of the WinADV can be found in Chapter 5 (Section 5.2.1).

Velocity data at different depths in the tanks are also analysed and compared by plotting the velocity surface profiles. This method enables the visualisation of the characteristics of each velocity component and thus gives a better understanding of

the flow in the dissolved air flotation tank. In order to facilitate the presentation, the discussion of the results follows after using each method of data analysis.

6.2 CHECKING DATA QUALITY

The ADV probe used to measure velocity distribution in the tank is a new piece of equipment. It has never been used to measure velocity in a dissolved air flotation tank (i.e. at the time when data collection was made). The initial recommendation by the manufacturer was to use a sampling rate of 25Hz for data collection. This has resulted in a large amount of data stored in the hard disk during velocity data collection at the Frankley WTW. During the 'First ADV Users Meeting' within the United Kingdom at the Hydraulic Research Station, Wallingford in September 1996, the problem of requiring large disk space was raised with the manufacturer. The latter suggested that a sampling rate of 1Hz may be used because the probe will average the reading for any sampling rate (Lohrmann, 1996). The suggestion led to the use of a sampling rate (frequency) of 1Hz at the Trimpley WTW. Two tanks were investigated at the Frankley WTW, namely Tanks A3 and C2. For the Trimpley WTW another two tanks were investigated, namely Tanks C1 and C7.

This section checks statistically to see whether the difference in sampling rate affects the quality of velocity data. The software provided with the equipment called the WinADV (for details see Section 4.2.6.1 of Chapter 4) was used to check data quality. Two approaches were used and these are as follows:

1. WinADV identifies the percentage of good data based on a correlation more than 70% as explained in Section 5.2.1 of Chapter 5.

2. WinADV identifies skewness of more than 1.5 for the velocity data as explained in Section 5.2.1 of Chapter 5. Skewness (i.e.more than 1.5) may be due to actual velocity distribution or due to aliasing as explained in Chapter 5.

This section also identifies the positions where the skewness (>1.5) occurs and tries to provide reasons for the occurrence. Finally, this section attempts to relate whether there is any straight line relationship between the skewness and the velocity in the x direction. The process involved in this section can be summarised as shown in Figure 6.1.

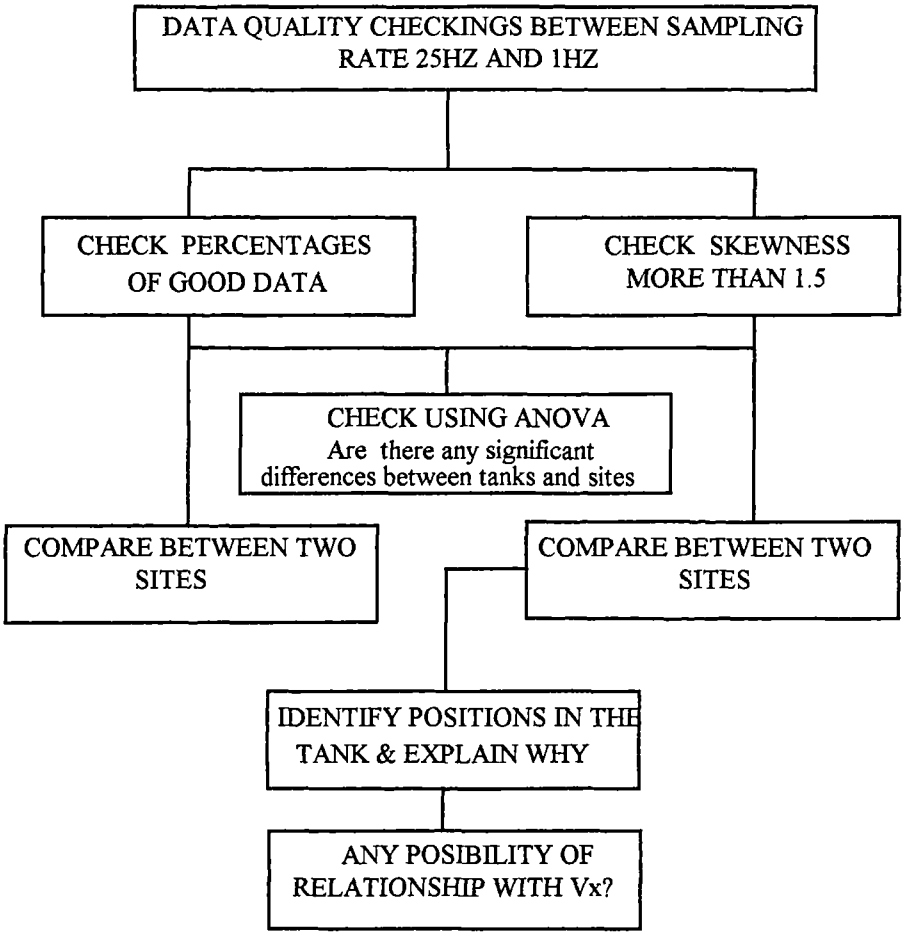

Figure 6.1 - Flow chart for data quality checking

During the full-scale plant studies different numbers of velocity observations were taken at each point in the tank for different runs or replications. These observations have been summarised in Table 6.1. Each run comprises observation at 64 points in the tank. At each point several hundreds of velocity samples were taken. The number of velocity measurements taken at each point was not constant. The average number of observations at each point is the total observations per run divided by 64.

From Table 6.1, it can be seen that the average numbers of velocity readings taken at Frankley were between 1189 to 2899 and at Trimpley between 202 to 207. The higher number of observations at Frankley was mainly due to the use of a higher sampling rate (25Hz) during data collection whereas at Trimpley a lower sampling rate of 1Hz was used.

Table 6.1 - Data on the minimum and maximum numbers of observations carried out at each sampling point conducted at each tank

Frankley	Tank A3			Tank C2		
Run	1	2	3	1	2	3
Maximum observations (number)	2058	2053	4584	4766	4773	10597
Minimum observations (number)	921	866	1027	1165	1592	1663
Average observations (number)	1232	1189	1932	2127	2760	2899
Trimpley	Tank C1			Tank C7		
Run	1	2	3	1	2	3
Maximum observations (number)	257	236	300	236	232	237
Minimum observations (number)	152	199	200	199	200	203
Average observations (number)	203	202	203	207	203	203

Note: 64 points in the tank were investigated for each run (refer to Figures 4.4 and 4.5 of Chapter 4 to see the position of each point in the tank)

Data quality was checked using WinADV software. The detailed procedures and guidelines on data screening using the software can be found in Section 5.2.1 of Chapter 5. Two criteria can be used for the purpose of checking data quality from the two different sampling rates. Firstly, comparing the percentage of good velocity data obtained after data screening may provide an indication of which sampling rate has a lesser number of bad velocity data. The percentage of good velocity data was based on the signal correlation of more than 70 as described in Section 5.2.1 of Chapter 5.

Secondly, by comparing the skewness of the filtered data from the two different sampling rates, it is possible to make an evaluation of which sampling rate can be regarded as more reliable than the other. A maximum skewness of more than 1.5 is regarded as suspicious and uncertain as explained in Chapter 5.

6.2.1 Discussions on the Percentage of Good Data

This section attempts to compare the results of the percentages of good data between Frankley and Trimpley WTW. Sampling rates of 25Hz and 1Hz were used at Frankley and Trimpley WTW respectively. The comparison enables us to suggest which sampling rate has produced better velocity data. This section also discusses the results from the ANOVA (refer to Section 5.2.3 of Chapter 5) of the percentage of good velocity data between tanks and between sites. Here the use of ANOVA is to find out whether there is any significant difference in the percentage of good velocity data between tanks. It is also used to evaluate whether there is a significant difference in the percentage of good velocity data between sites. The former attempts to find out variability of percentage of good velocity data between tanks while the latter attempts to find out whether sampling rates affect data quality (velocity data).

Table 6.2 shows the percentage of good data for each run from Tanks A3, C2, C1 and C7, which were obtained using the WinADV software. There were three runs carried out at each tank. Observed velocity samples for each run are shown in Table 6.1 (Section 6.2). The average percentage of good velocity data collected at the Frankley WTW is 94.33% with a standard deviation of 3.56%. The calculation was made by adding all the percentages of good velocity data obtained at Frankley and then dividing by 6. The same procedure was used to calculate the average percentage of good velocity data at Trimpley. The value at Trimpley is 91.17% with a standard deviation of 2.99%. This indicates that the sampling rate of 25Hz which was used at Frankley WTW has produced a better velocity data than at Trimpley with a sampling rate of 1Hz.

Statistical evaluation using analysis of variance (ANOVA) was also made to see the variability of the percentage of good velocity data between four different tanks. Table 6.3 shows that there are highly significant differences in the percentage of good velocity data collected between the four tanks at Frankley and Trimpley WTW. Also, if comparison is made by blocking (separate the tanks into two sites) the tanks into Frankley and Trimpley WTW, the significance level is 0.126 as shown in Table 6.3. This indicates that for 87% of the time a significant difference in the percentage of good velocity data between the two sites will occur.

6.2.2 Discussion of Skewness (i.e. >1.5)

Skewness is a non-dimensional measure of symmetry calculated by dividing the average cube deviation from the mean by the cube of standard deviation. Skewness values near zero indicate symmetry in the histogram. Large positive values imply a long tail to the right and large negative values indicate a long tail to the left. WinADV calculated the skewness based on the following equation:

$$Skewness_x = \frac{\sum V_x^3 - (3\sum V_x \sum V_x^2)/n - 2(\sum V_x)^3/n}{(n-2)s^3} \qquad (6.1)$$

Checking and discussions of skewness (i.e. >1.5) in this section can be divided into three parts as follows:

1. The first part of this section tries to compare the number of occurrences of skewness (i.e.>1.5) obtained using a sampling rate of 25Hz at the Frankley WTW and that of 1Hz at the Trimpley WTW. The main objective is to find out which sampling rate is better than the other.

2. The second part is to compare the skewness (>1.5) between tanks and between sites. ANOVA was used to find any significant difference of skewness between tanks and between sites. The objective of comparing skewness (>1.5) between tanks is to find out whether skewness is based on real velocity distribution or

experimental error. The objective of comparing skewness (>1.5) between sites is to find out which sampling rate is better than the other.

3. The third part is to identify where and why the skewness (>1.5) occurred in the tank. This part also tries to find out whether there is any possibility of direct relationship between skewness and velocity in the x-direction.

6.2.2.1 Comparison of Occurrence of Skewness (>1.5) Between Two Sites

Table 6.2 shows the characteristics of skewness of velocity samples for each run in each tank at the Frankley and Trimpley WTW. Maximum skewness for each run refers to the maximum amount of skewness at one out of the 64 points observed. The same principle applied for the minimum skewness. The average skewness is the total sum of the skewness of all the points divided by 64. The number of skewness more than 1.5 refers to the number of sampling points in the tank where the skewness (>1.5) occurred during each run out of a total of 64 points observed. The positions of skewness (>1.5) are the points where the skewness (>1.5) occurred in the tank for each run (refer to Figures 4.4 and 4.5 in Chapter 4 for the position of each point).

At Frankley 12 sampling points were found to exhibit skewness (>1.5) in the velocity distribution (Table 6.2). The skewness calculation was based on 12,139 velocity observations spread over the 12 points. At Trimpley 7 sampling points exhibited skewness (>1.5). The latter was based on 1,221 velocity observations spread over 7 points. This suggests that the higher sampling frequency observation (25Hz) at Frankley produces less skewness than the lower sampling frequency (1Hz) at Trimpley. Table 6.2 also shows that the maximum value of skewness at the Trimpley WTW was 14.1 compared with 8.39 at the Frankley WTW. This again indicates the possibility that a sampling rate of 25Hz results in lower values of skewness than at 1Hz.

Table 6.2 - Comparison of data quality between Frankley and Trimpley WTW

Frankley	Tank A3			Tank C2		
Run	1	2	3	1	2	3
%Good	93	92	89	97	97	98
Maximum skewness	8.39	1.86	1.4	3.14	1.21	4.5
Minimum skewness	0.08	0.11	0.09	0.08	0.12	0.03
Average skewness	0.77	0.61	0.65	0.61	0.55	0.60
Skewness No.>1.5	5	2	0	4	0	1
Positions of skewness more than 1.5	C1d1=8.39 D1d1=2.15 A2d2=1.73 D1d2=1.68 C3d1=1.60	A1d2=1.86 A1d3=1.60	nil	D3d1=3.15 D3d2=2.16 B3d2=2.03 B3d1=1.84	nil	D4d1=4.50
Trimpley	Tank C1			Tank C7		
Run	1	2	3	1	2	3
%Good	88	88	90	92	95	94
Maximum skewness	9.27	1.67	1.53	2.42	14.14	1.52
Minimum skewness	0.12	0	0	0.06	0.19	0
Average skewness	0.83	0.58	0.64	0.65	0.79	0.63
Skewness No.>1.5	2	1	1	1	2	1
Positions of skewness more than 1.5	A2d4=9.27 D4d4=7.35	C4d3=1.67	D2d1=1.53	D4d1=2.42	D3d4=14.1 D4d1=1.75	D4d1=1.52

Note: No.=number; 64 points in the tank were investigated for each run (refer to Figures 4.4 and 4.5 of Chapter 4 to see the position of each point in the tank).

6.2.2.2 Comparison of Skewness (>1.5) Between Tanks and Sites

In this section ANOVA is use to identify whether there is a significant difference in the skewness (>1.5) of velocity data between all the tanks at Frankley and Trimpley WTW. ANOVA is also used in an attempt to find any significant difference in the skewness (>1.5) of velocity data between the sites (Frankley and Trimpley). A significant difference indicates that sampling rates may affect velocity data (quality).

Table 6.3 shows that there is no significant difference in the value of skewness of more than 1.5 either between all the tanks or between the tanks from the two sites. However the significant level for the tanks between different sites is nearly half of that between all the tanks from both sites. This may indicate that the difference in skewness could be highly significant if an equal number of observations is made at each site.

Table 6.3 - ANOVA for percentage of good and skewness of velocity data

Tests	Source of variation	Level of significance
Percentage good velocity	Between tanks	0.000
	Between sites	0.126
Skewness>1.5	Between tanks	0.869
	Between sites	0.467

6.2.2.3 Positions of Skewness

From Table 6.2, it can be seen that at the Frankley WTW the skewness (>1.5) occurred at section D of the tank 5 times whereas at the Trimpley WTW it occurred 6 times at D. Section D was located at a quarter length of the mixing zone from the baffle and this position can be found from the diagrams in Figures 4.4 and 4.5 of Chapter 4. The occurrence at section D in the separation zone of DAF tanks at Frankley and Trimpley represents 42% and 75% of the total occurrence (skewness more than 1.5) respectively. Table 6.4 shows that the occurrence tends to be more frequent at depth d1 of section D. The total number of points with excess skewness was 7 at depth d1, two at depth d2, none at depth d3 and two at depth d4. The highest value of skewness was 14.1 at a position D3d4 from run 2 of tank C7 of the Trimpley WTW. This indicated that although the occurrence of skewness was more frequent at depth d1 their values are lower compared with that at depth d4. It can also be seen that the occurrences were greater at position D4, which is near the wall of the tanks.

In order to see whether there is any relationship between higher values of skewness and the velocity in the tank at different positions, a number of graphs were drawn.

Figure 6.2 (DAF tank A3 at Frankley for run 1) indicates that at width D1, the velocity for different depths is mostly in the negative regions. This may be the reason for points D1d1 and D1d2 having skewness of more than 1.5. The same characteristic was found on point D4d1 (width D4) based on run 3 from tank C2 at the Frankley WTW. The latter can be seen from Figure 6.3. Here at depth d1 the velocity *Vx* was highly negative. Further data from Figure 6.4 shows that the same characteristic was encountered for points D3d1 and D4d1 at width D3 and D4 respectively.

Table 6.4 - Positions and number of skewness (>1.5) at section D of the tanks

Positions	Tanks at Frankley	Tanks at Trimpley
Depth d1	3	4
Depth d2	2	0
Depth d3	0	0
Depth d4	0	2
Width D1	2	0
Width D2	0	1
Width D3	2	1
Width D4	1	4

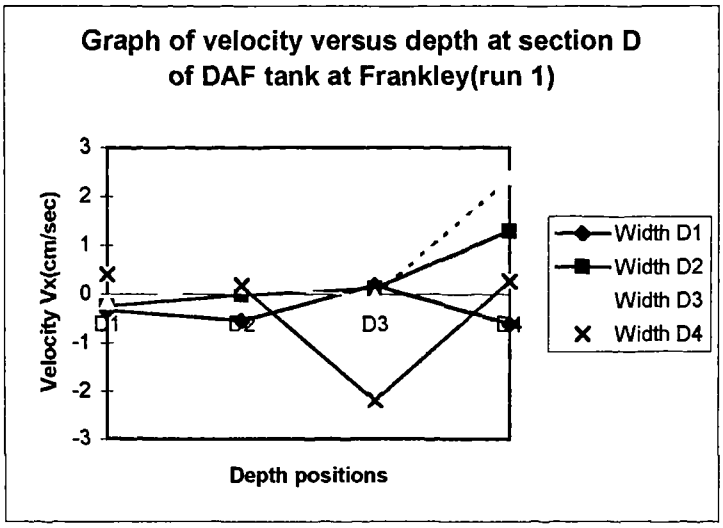

Figure 6.2 - Average velocity in *x* direction at section D of tank A3 at Frankley (run 1)

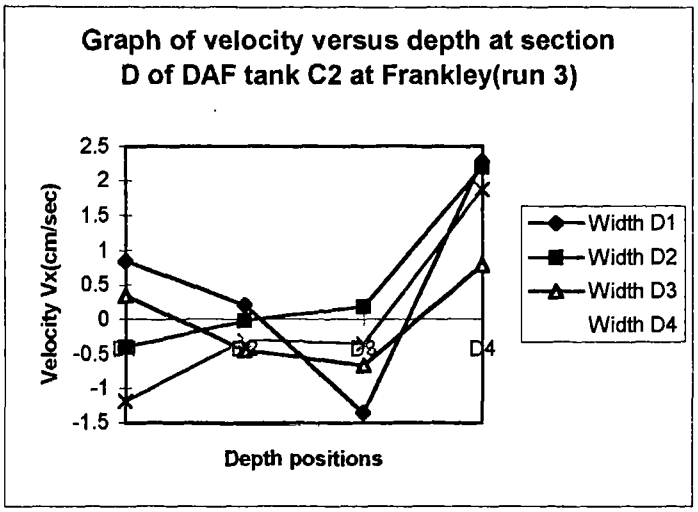

Figure 6.3 - Average velocity in x direction at section D of tank C2 at Frankley (run 3)

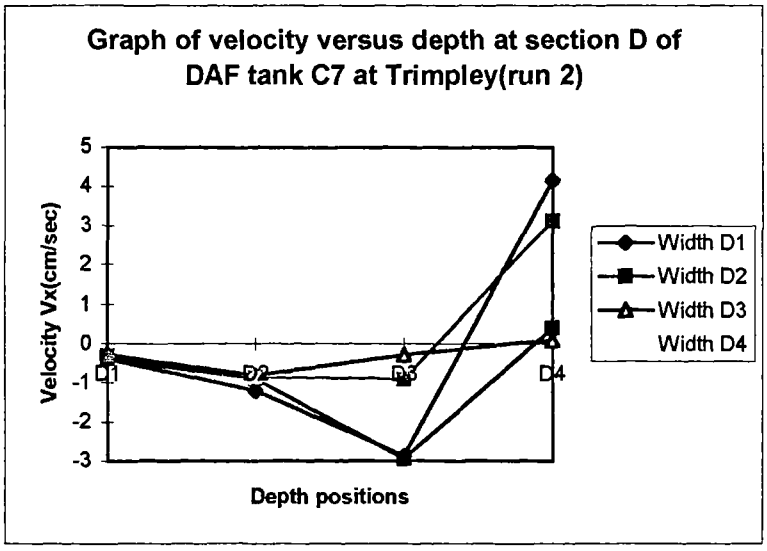

Figure 6.4- Average velocity in x direction at section D of tank C7 at Trimpley (run 2)

Further checks were also made to see whether there is any form of relationship between the skewness and the velocity Vx (velocity in x-direction). The results are as shown in Figures 6.5, 6.6, 6.7 and 6.8. These graphs indicate that there is no evidence to suggest that there is any direct relationship between the velocity Vx and the maximum skewness encountered in the tank. However it can be concluded that the maximum skewness at Frankley WTW occurred at the negative values of Vx whereas at the Trimpley WTW the maximum skewness occurred at a low value of Vx. The low and negative values of Vx and the positions (as discussed earlier) where the

maximum skewness occurred may indicate that the flow at these points was under a transition regime.

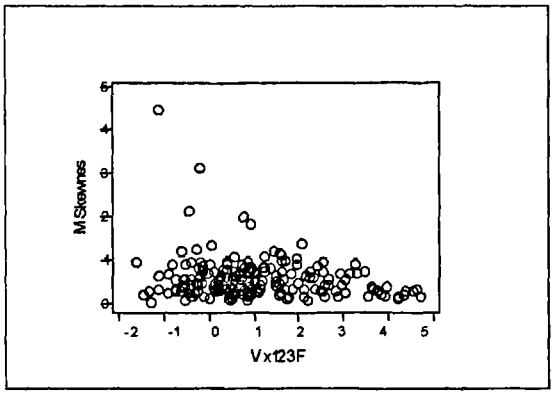

Figure 6.5 - Plot of Maximum skewness versus *Vx* (run 1, 2 and 3) for tank C2, Frankley WTW

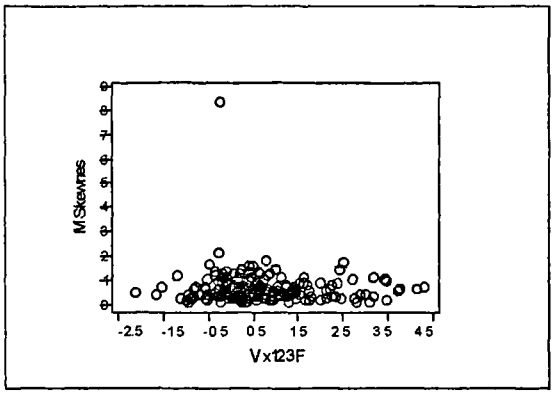

Figure 6.6 - Plot of Maximum skewness versus *Vx* (run 1, 2 and 3) for tank A3, Frankley WTW

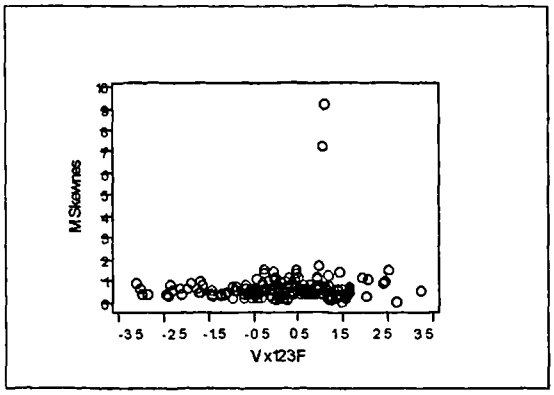

Figure 6.7 - Plot of Maximum skewness versus *Vx* (run 1, 2 and 3) for tank C1, Trimpley WTW

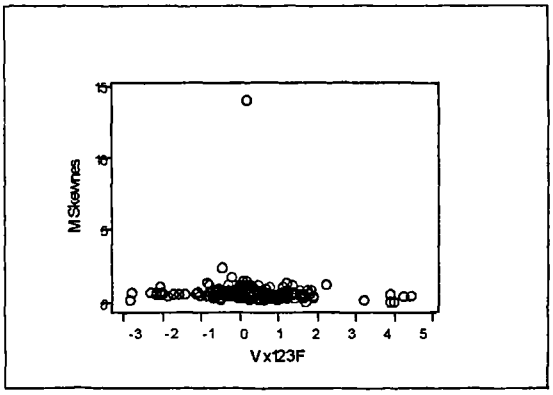

Figure 6.8 - Plot of Maximum skewness versus *Vx* (run 1, 2 and 3) for tank C7 Trimpley WTW

6.3 COMPARING AVERAGE FILTERED AND AVERAGE RAW VELOCITY DATA USING BOXPLOTS

Sixty-four points at different locations in each tank were investigated for each experimental run. At each sampling point several hundreds of velocity readings were taken. During data analysis WinADV was used to filter the velocity data at each point, using the filtering criteria as described in Section 5.2.1 in Chapter 5. The

output from the WinADV programme is called the average filtered velocity data for each point. Samples which do not fulfil the filtering criteria are discarded by the WinADV. The average filtered velocity data of 64 points in the tank for each experimental run is the sum of the average filtered velocity data at each point divided by 64. This is called the average filtered velocity for each run.

Raw velocity data are the actual velocity samples collected during the investigation which are not subjected to the WinADV filtering process and may be called unfiltered velocity data. Section 5.2.1 in Chapter 5 has described the method to extract the raw velocity samples of each point in the tank. The average raw velocity data at each point is the sum of all the velocity samples at each point divided by the number of velocity samples. The average raw velocity data or sample for each run is the sum of the average raw velocity data at each point in the tank divided by 64 (there are 64 points in the tank for each run). This can be called the average unfiltered velocity sample (data) for each run.

The objectives of comparing the average velocity data (filtered and unfiltered) between each experimental run at each tank are as follows:

1. To investigate the variability between the average filtered and unfiltered velocity data of all the average samples within each run and to compare them between different runs in the same tank. To achieve this purpose boxplots diagrams are used (refer to Section 5.2.2 in Chapter 5). The boxplots will show the variation of the average velocity from all the 64 points in the tank and indicate the average velocity for each run based on the 64 points. This enables the velocity data characteristics from the two types of data to be compared and analysed.

2. To investigate the difference between the average filtered and unfiltered velocity data between each run in the same tank. In this section the boxplot method is used. This can provide a subjective impression of the results. ANOVA is carried out in Section 6.5 to confirm the results from the boxplots. If there is no difference in the average data of the filtered and unfiltered velocity samples between different

runs in the same tank, this may imply that the velocity samples collected at each tank are consistent and the performance of the ADV probe is fairly good. This suggests that the probe is suitable to be used for the flow measurement in the dissolved air flotation tank. The other technique which may be used to check the suitability of the probe to be used for flow measurements in a dissolved air flotation tank is checking the overall percentage good data from all the points in the tank. The disadvantage of this technique is that the velocity mean of all the 64 points in each run cannot be compared and the characteristics of the points in the tank cannot be ascertained.

In order to reduce repetition on the technique of presenting results from the data analysis, only the results from tanks C2 and C1 from the Frankley and Trimpley WTW will be presented here. The results from tank A3 of the Frankley WTW can be found in Appendix A1 and the results from tank C7 of the Trimpley WTW are presented in Appendix A2.

6.3.1 Frankley WTW

6.3.1.1 Boxplots

Table 6.1 in Section 6.2.1 indicates that there is a great variability in the numbers of observations taken during the period of data collection. In order to see whether these large variations in the numbers of observations for different runs have any significant effect on the velocity distribution in the tanks, a subjective impression of velocities in the x, y and z directions are made using boxplots. The results of these subjective comparisons of velocities in the x, y, and z directions for tank C2 are shown in Figures 6.9, 6.10 and 6.11 respectively. For the tank A3, the results are shown in Figures A1.1, A1.2 and A1.3 of Appendix A1 for the velocities in the x, y and z directions respectively. It can be seen from all the boxplots that there appears to be no significant difference between the mean velocity of filtered data using WinADV software and that of using the average unfiltered velocity data for tanks C2 and A3 at the Frankley WTW. The variances are approximately the same (i.e.one of the criteria

needed in the F test as mentioned in Section 5.2.3 of Chapter 5). However some outliers can be seen in each of the boxplots. In the context of the application these outliers can be explained as follows:

1. Data collected near the baffle and outlet of the tank normally have higher velocities than at other points due to the presence of constrictions across the cross-sectional area of the tank which hindered the flow. For example in Run 2 (boxplot of Group 3 in Figure 6.9), velocities in the x direction(Vx) at points A1d1 and D2d3 were 4.62 and 4.19cm/sec respectively. These values are found to be significantly higher than those found at other points in the tank. The details of the positions of maximum velocity components in the tank are shown in Table 6.5.

2. The flow in and out of the tank was unsteady. The flow was a function of water demand, filter head-loss, and the cleaning of DAF and filter tanks. This means that at certain times the flow tends to be higher or lower than average and thus affects the velocity in the tank.

The subjective impression from all the boxplots for the velocity components in the x, y and z directions (i.e. Vx, Vy and Vz in Figures 6.9 to 6.11 and Figures A1.1 to A1.3 in Appendix A1) indicates that the velocity range is higher in the x direction, followed by y and z directions respectively.

The velocity component in the z-direction from the boxplots of Figure 6.11 indicates that outliers occur at the top and bottom parts of the boxplots and these represent the positive and negative velocity components respectively. A positive velocity component of Vz implies that the particles in the DAF tank move upward whereas a negative component indicates the particles move towards the floor of the tank. The latter may possibly indicate the following problems:

1. The length of the tank is too long, which may allow the sludge flocs to settle. This has implications for tank design.

2. Desludging is delayed causing the sludge to break-up and settle. This is an operational problem.

3. The water moves out from the tank through the outlet compartment, which is located near the floor of the tank. The area near this outlet will have a negative velocity component of *Vz*.

Table 6.5 indicates that the negative velocity components of *Vz* occurred along the cross-section A, which is at 0.5m from the outlet channel of the tank (see Figure 4.5 in Chapter 4). The occurrences of the maximum negative *Vz* seem to be more frequent at depth d2 which is at one-quarter depth from the floor of the tank (total depth 2.1m). This seems to be plausible since depth d2 is near the outflow chamber.

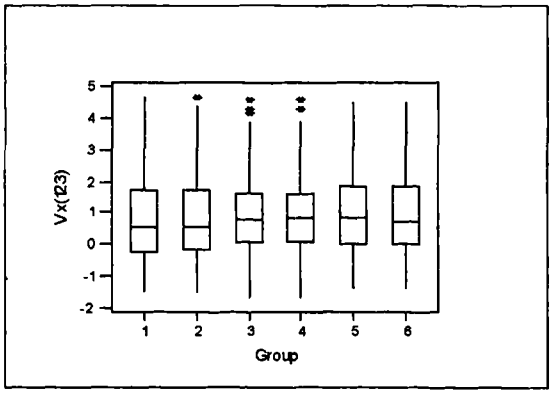

Figure 6.9 - Boxplots for velocity components in *x* direction using filtered and averaging methods for runs 1, 2 and 3 (Cell C2, Frankley)
Note: Groups 1,3 and 5 are the average filtered velocities for runs 1, 2 and 3 respectively and Groups 2, 4 and 6 are the average unfiltered velocities for runs 1, 2 and 3 respectively.

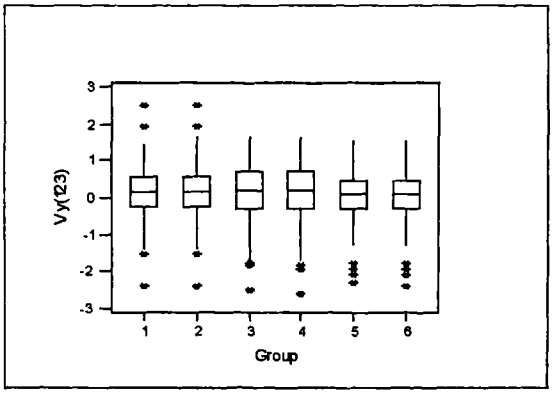

Figure 6.10 - Boxplots for velocity components in *y* direction using filtered and averaging methods for runs 1, 2 and 3(Cell C2, Frankley).
Note: Group s1,3 and 5 are the average filtered velocities for runs 1, 2 and 3 respectively and Group s2, 4 and 6 are the average unfiltered velocities for runs 1, 2 and 3 respectively.

Since the subjective impressions from the boxplots do not show any significant difference between the average filtered and unfiltered velocity data, further analysis may be carried out by using the filtered velocity data which has been obtained using WinADV software. However the results from the boxplots need to be confirmed using the analysis of variance (ANOVA) before conclusions can be made on the

appropriateness of using the filtered velocity data. The analysis will be carried out in Section 6.4 of this chapter.

6.3.1.2 Normal Plots

As described in Section 5.2.3 of Chapter 5, testing of velocity data using an F-test can be made only if the assumptions on the samples are true. One of the assumptions is that the velocity samples are derived from a normal distribution. For this purpose, normal plots were used to validate the assumption on the velocity data. The results for velocity samples in the x, y and z components for different runs for tank C2 are as shown in Figures 6.12, 6.13, 6.14, 6.15, 6.16, 6.17, 6.18, 6.19 and 6.20. The results from tank A3 are as shown in Figures A1.4, A1.5, A1.6, A1.7, A1.8, A1.9, A1.10, A1.11 and A1.12 of Appendix A1. All of these Figures indicate that the velocity samples are derived from normally distributed random variables.

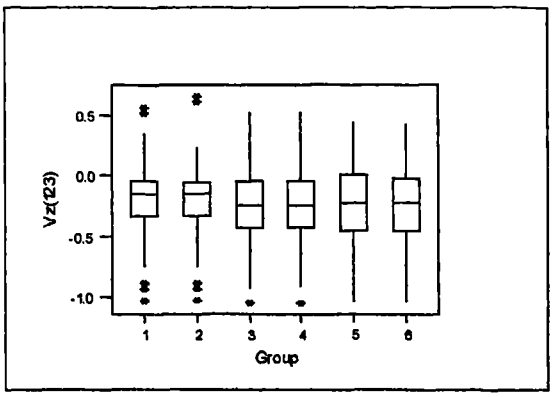

Figure 6.11 - Boxplots for velocity components in z direction using filtered and averaging methods for runs 1, 2 and 3 (Cell C2, Frankley).
Note: Groups 1,3 and 5 are the average filtered velocities for runs 1, 2 and 3 respectively and Group 2, 4 and 6 are the average unfiltered velocities for runs 1, 2 and 3 respectively.

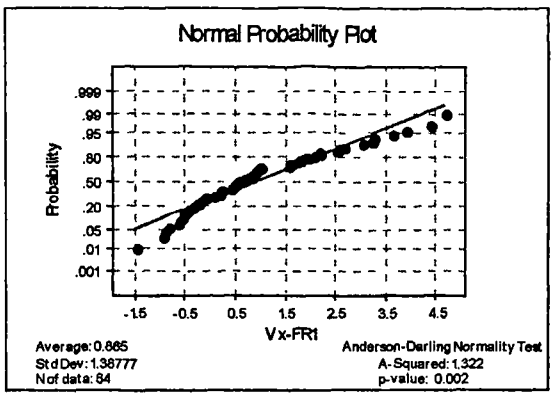

Figure 6.12 - Normal probability plot of velocity in x direction (filtered) for run 1 (Cell C2, Frankley).

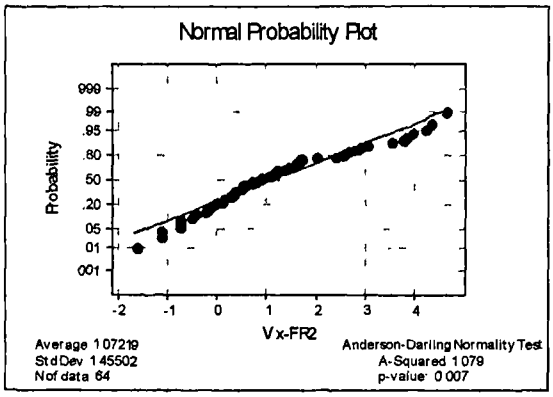

Figure 6.13 - Normal probability plot of velocity in x direction (filtered) for run 2.

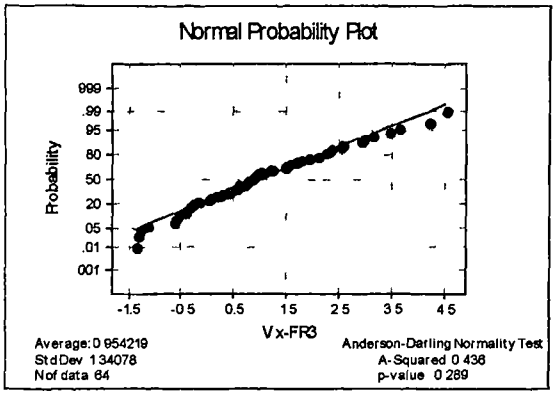

Figure 6.14 - Normal probability plot of velocity in x direction (filtered) for run 3.

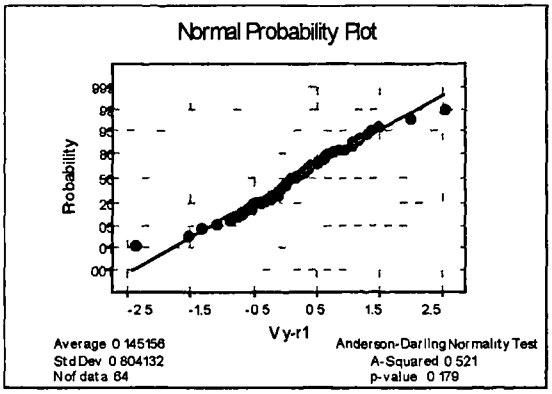

Figure 6.15 - Normal probability plot of velocity (y component) in run 1

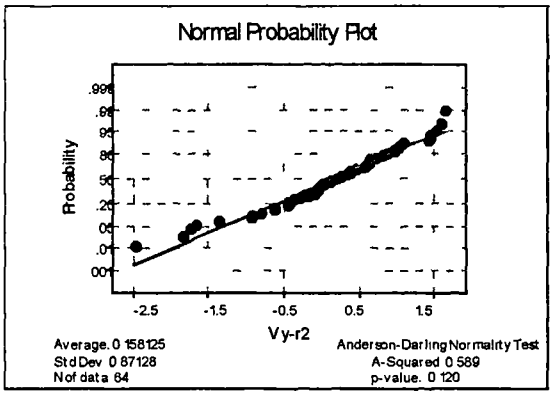

Figure 6.16 - Normal probability plot of velocity (y component) in run 2

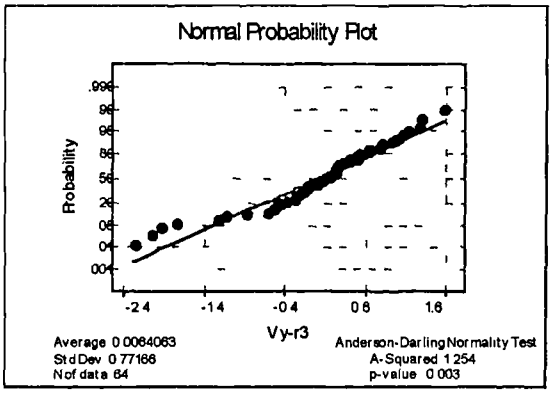

Figure 6.17 - Normal probability plot of velocity (y component) in run 3

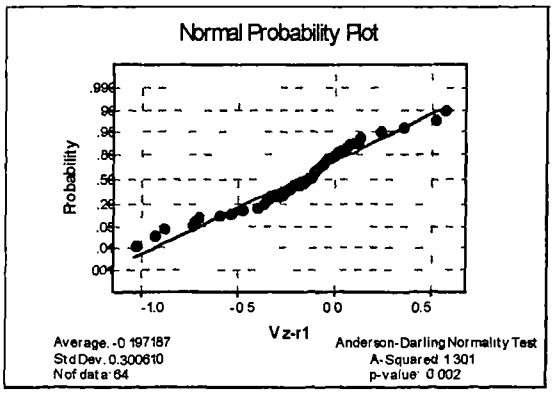

Figure 6.18 - Normal probability plot of velocity (z component) in run 1

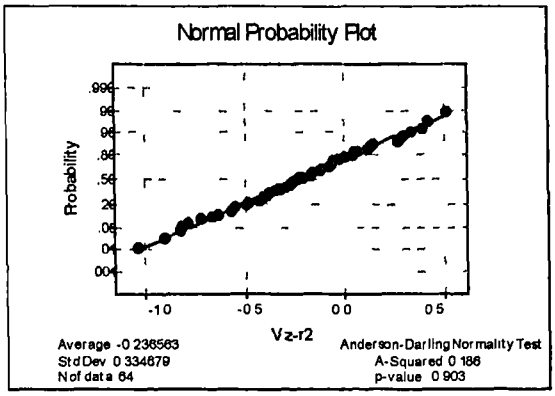

Figure 6.19 - Normal probability plot of velocity (z component) in run 2

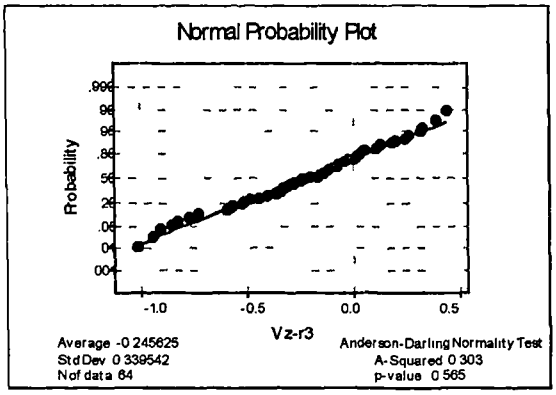

Figure 6.20 - Normal probability plot of velocity (z component) in run 3

Table 6.5 - Details of maximum and minimum velocity in the DAF tank at Frankley WTW

Tanks	Tank A3			Tank C2		
Runs	Run 1	Run 2	Run 3	Run 1	Run 2	Run 3
Max. *Vx*	3.73	3.05	4.26	4.68	4.62	4.5
Pos. of max. *Vx*	A4d1	C4d3	A2d1	A2d1	A1d1	A4d1
Min. *Vx*	-2.17	-1.19	-1.26	-1.50	-1.67	-1.39
Pos. of min. *Vx*	D4d3	D1d2	D1d3	D4d1	C1d3	B1d3
Max. *Vy*	1.89	1.52	2.25	2.51	1.63	1.56
Pos. of max. *Vy*	A4d3	A3d4	A3d4	C3d4	C2d4	B3d3
Min. *Vy*	-1.55	-1.35	-1.91	-2.41	-2.49	-2.29
Pos. of min. *Vy*	C3d4	B2d4	D2d4	A2d4	A2d4	A2d4
Max. *Vz*	0.80	0.54	0.41	0.56	0.51	0.43
Pos. of max. *Vz*	D2d4	C2d4	D3d2	D3d2	B4d2	C3d1
Min. *Vz*	-1.38	-1.30	-1.62	-1.04	-1.05	-1.03
Post. of min. *Vz*	A4d3	A2d2	A4d2	A2d2	A3d2	A3d1

Max.= maximum Min.=minimum Pos. = position

Vx, *Vy* and *Vz* are the velocity in the x, y and z directions measured in cm/sec.

6.3.2 Trimpley WTW

6.3.2.1 Boxplots

Referring to Table 6.1 of Section 6.2.1, there is not much variability in the average observation (value) for velocity carried out at the Trimpley WTW. There is however a need to compare and see whether there is any significant difference between the filtered and averaging velocity data. Subjective comparisons for velocities in the x, y and z directions for three different runs between the filtered and average velocities

were made using boxplots. Figures 6.21, 6.22 and 6.23 for tank C1 indicate that there is no significant difference between the velocity mean of filtered and that of average data. The same criterion was observed from tank C7 based on the boxplots from Figures A2.1, A2.2 and A2.3 in Appendix A2. Some outliers were captured in the boxplots and their presence is due to the reasons explained in Section 6.3.1. Referring to Figures 6.21 and A2.1(Appendix A2), the outliers in the upper side represent the higher velocity encountered during each run. The details of the outliers for *Vx* from each run are as follows:

1. Almost all the highest velocity *Vx* for each run was encountered at section D (one-quarter length of the mixing zone from the baffle) of both tank C1 and C7. The detailed result can be seen from Table 6.6. These results are significantly different from those found at the Frankley WTW where the highest velocity occurred at section A (Table 6.5).

2. All lowest velocity *Vx* was encountered at section D of the tank (Table 6.6). These results are almost identical with those found at the Frankley WTW except for two runs at tank C2.

3. The results of the outliers for *Vx* have the same causes as explained in Section 6.3.1.1.

The boxplots also indicate that the velocity range *Vx* is higher than *Vy* and the latter is higher than *Vz*. These results are similar to those found at the Frankley WTW. The subjective impressions from the boxplots do not show any significant difference between the average filtered and unfiltered velocity data between different runs of the experiment within the same tank. Further analysis may be carried out using the filtered data. In order to confirm the results from the boxplots, hypothesis testing using ANOVA needs to be done. The latter will be described in Section 6.4 onwards.

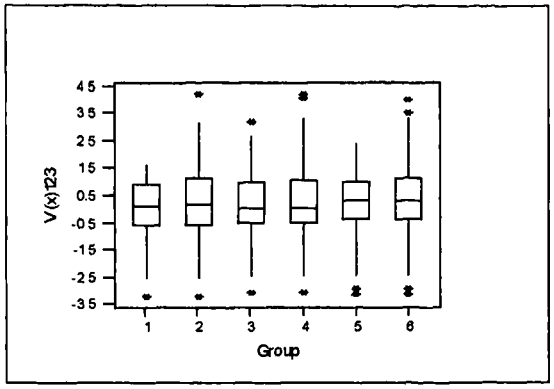

Figure 6.21 - Boxplots for velocity components in x direction using filtered and averaging methods for runs 1, 2 and 3.
Note: Groups 1,3 and 5 are filtered velocities for runs 1, 2 and 3 respectively and Groups 2, 4 and 6 are the average velocities for runs 1, 2 and 3 respectively.

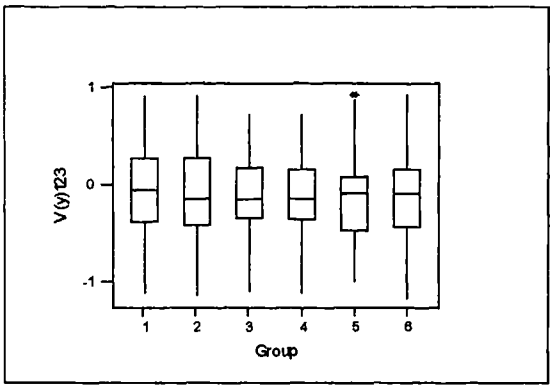

Figure 6.22 - Boxplots for velocity components in y direction using filtered and averaging methods for runs 1, 2 and 3.
Note: Groups 1,3 and 5 are filtered velocities for runs 1, 2 and 3 respectively and Groups 2, 4 and 6 are the average velocities for runs 1, 2 and 3 respectively.

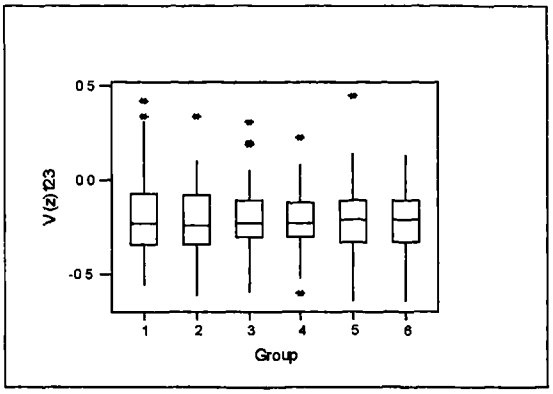

Figure 6.23 - Boxplots for velocity components in z direction using filtered and averaging methods for runs 1, 2 and 3.
Note: Groups 1,3 and 5 are filtered velocities for runs 1, 2 and 3 respectively and Groups 2, 4 and 6 are the average velocities for runs 1, 2 and 3 respectively.

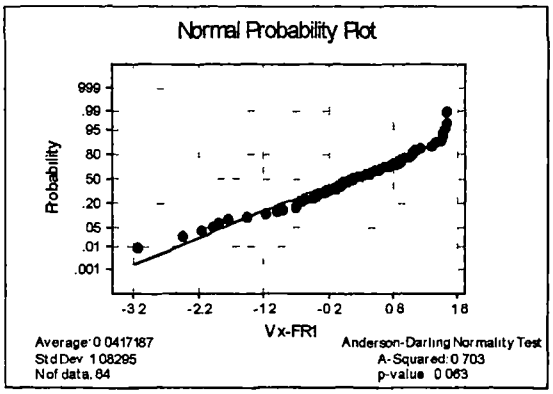

Figure 6.24 - Normal probability plot of velocity in x direction (filtered) for Run 1.

6.3.2.2 Normal Plots

To test the normality of the velocity data as described in Section 6.3.1.2, the same procedure is again used here. Figures 6.24 to 6.32 for tank C1 and Figures A2.4 to A2.12 (Appendix A2) for tank C7 indicate that the velocity samples in the x, y and z

directions for different runs are considered to be derived from normal distributions. This means standard statistical techniques can be used to analyse the velocity data.

Table 6.6 - Details of maximum and minimum velocity in the DAF tank at Trimpley WTW

Tanks	Tank C1			Tank C7		
Runs	1	2	3	1	2	3
Max. *Vx*	1.59	3.19	2.38	4.37	4.18	3.96
Position of max.*Vx*	D1d4	D4d4	D2d4	D1d4	D1d4	C1d4
Min. *Vx*	-3.19	-3.04	-3.09	-2.26	-2.93	-2.37
Position of min.*Vx*	D1d3	D2d3	D1d3	D1d3	D2d3	D2d3
Max. *Vy*	0.89	0.70	0.92	0.87	0.92	1.01
Position of max.*Vy*	D3d3	D2d1	D4d3	A4d4	A4d2	A4d1
Min. *Vy*	-1.12	-1.10	-1.01	-1.31	-1.49	-1.28
Position of min.*Vy*	B3d3	D3d4	B3d4	C3d3	C2d3	C3d3
Max. *Vz*	0.42	0.31	0.45	0.14	0.13	0.19
Position of max.*Vz*	C4d4	D3d4	D3d4	D2d4	C2d4	D4d4
Min. *Vz*	-0.56	-0.60	-0.65	-0.67	-0.58	-0.99
Position of min.*Vz*	A3d1	A1d1	A1d1	A1d1	A2d2	A4d1

Max.= maximum Min.=minimum
Vx, *Vy* and *Vz* are the velocities in the *x*, *y* and *z* directions measured in cm/sec.

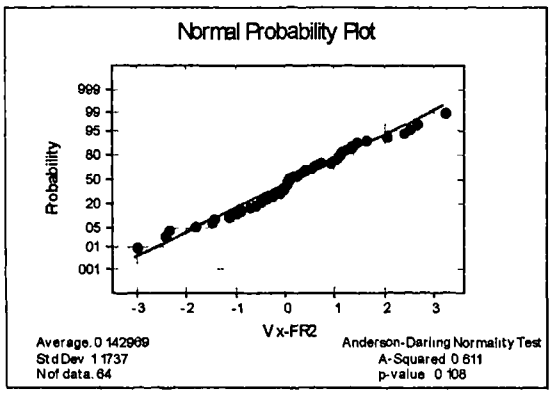

Figure 6.25 - Normal probability plot of velocity in *x* direction (filtered) for run 2.

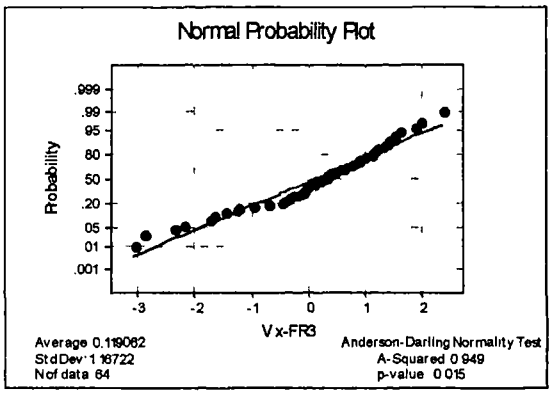

Figure 6.26 - Normal probability plot of velocity in *x* direction (filtered) for run 3.

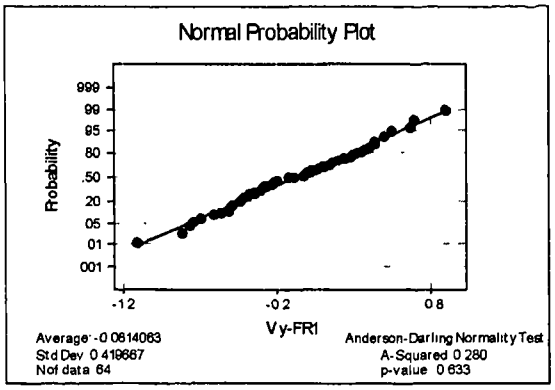

Figure 6.27 - Normal probability plot of velocity in y direction (filtered) for run 1.

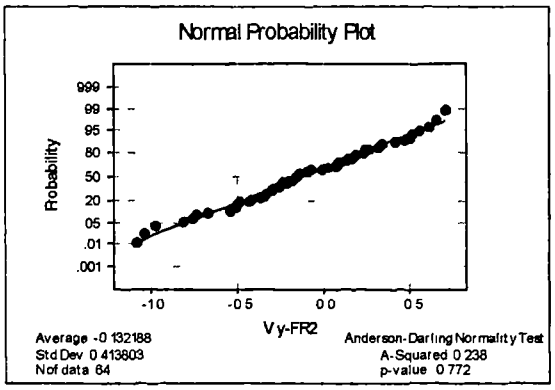

Figure 6.28 - Normal probability plot of velocity in y direction (filtered) for run 2.

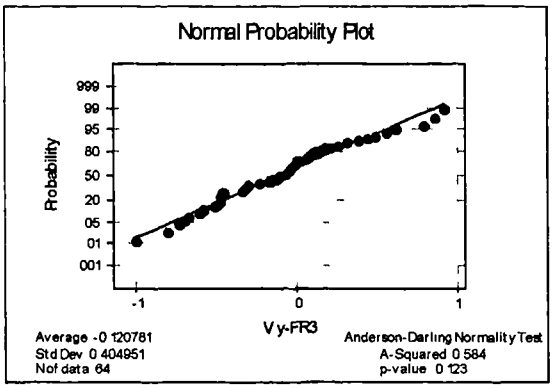

Figure 6.29 - Normal probability plot of velocity in y direction (filtered) for run 3.

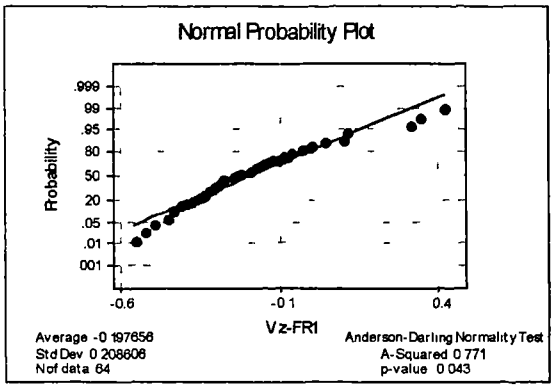

Figure 6.30 - Normal probability plot of velocity in z direction (filtered) for run 1.

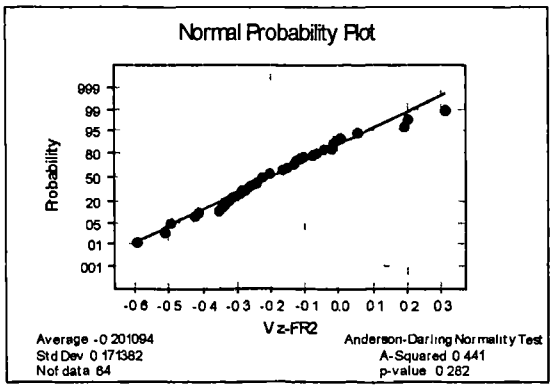

Figure 6.31 - Normal probability plot of velocity in z direction (filtered) for run 2.

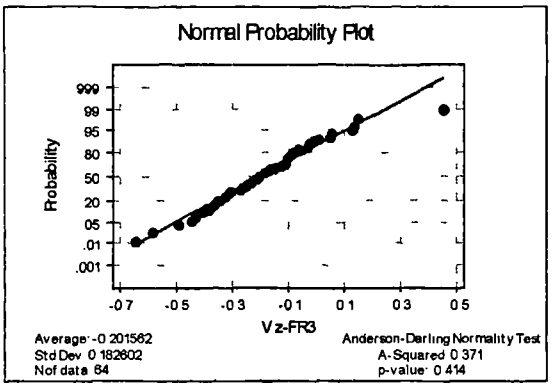

Figure 6.32 - Normal probability plot of velocity in z direction (filtered) for run 3.

6.4 COMPARING AVERAGE FILTERED AND AVERAGE RAW VELOCITY DATA USING ANOVA

In Section 6.3 comparisons of the average filtered and average raw (unfiltered) velocity were made using a boxplot technique. In this section the same data as have been compared using boxplots are analysed again using ANOVA. ANOVA was carried out by comparing the average filtered and the average unfiltered velocity samples of each run. The average filtered and unfiltered data from runs 1, 2 and 3 are set into different 'groups'. The average filtered velocity data from runs 1, 2 and 3 were assigned into groups 1, 3 and 5 respectively whereas average unfiltered velocity data from runs 1, 2 and 3 were put under groups 2, 4 and 6 respectively. This technique (ANOVA) is used to analyse and compare the average filtered and unfiltered velocity data from the Frankley and Trimpley WTW.

The objective of ANOVA is to test the null hypothesis that there is no difference between the mean velocity of each group of data. The ANOVA is used to confirm the subjective impressions from the boxplots.

6.4.1 Frankley WTW

Tables 6.7, 6.8 and 6.9 (results from tank C2) show that the null hypothesis is true, which indicates that there is no significant difference of mean velocity between runs 1, 2 and 3 for the average filtered and the average unfiltered velocities. Similar results are obtained from tank A3 as shown in Tables A1.1, A1.3 and A1.5 (Appendix A1). This test confirmed the earlier subjective impression using boxplots. This test provides an important tool in deciding which velocity data (filtered or unfiltered) to be used for further analysis. Further details on the variability of filtered and unfiltered velocities in the x, y and z directions from runs 1, 2 and 3 are shown in Tables 6.10, 6.11 and 6.12 for tank C2 and in Tables A1.2, A1.4 and A1.6 for tank A3 respectively. These tables show and compare the velocity mean from the average filtered and unfiltered velocities together with their respective 95% confidence intervals based on pooled standard deviation. The word 'pooled' means the standard

deviations from the samples are pooled to get an estimate of the common standard deviation (Ryan and Joiner, 1994). The equation for pooled standard deviation can be found in Ryan and Joiner (1994).

The results from Tables 6.10, 6.11 and 6.12 for tank C2 and Tables A1.2, A1.4 and A1.6 for tank A3 (Appendix A1) show that the values of standard deviations of each run are higher than the velocity mean. This is due to the presence of positive and negative values of velocity mean in the tank. Table 6.5 shows the maximum positive and negative velocities with their positions in the tank.

Since the test does not show any significant difference between the average filtered and unfiltered data, it can be concluded that the ADV probe used is in good condition and there were enough scattered particles in the dissolved air flotation tank for the probe to operate satisfactorily. If there was a significant difference between the two sets of velocity data then there would be some doubts concerning the equipment and the quality of data collected. For further analysis filtered velocity data will be used.

The observations of velocity for each run based on Tables 6.7, 6.8 and 6.9 (or Tables A1.1, A1.3 and A1.5 in Appendix A1) can be described based on a linear statistical model of Equation 5.2 in Chapter 5. In order to check whether this model is appropriate (i.e. the ANOVA procedure is an exact test of no difference between velocity means), a plot of residuals versus fitted values from the ANOVA was made. Figures 6.33, 6.35 and 6.37 show that the residuals from the respective ANOVA of the velocity in the x, y and z directions are unrelated and this indicates the velocity samples have constant variance. Similar results are obtained for tank A3 (Figures A1.13, A1.15 and A1.17 in Appendix A1). In Figures 6.34, 6.36 and 6.38 for tank C2 and Figures A1.14, A1.16 and A1.18 (Appendix A1) for tank A3 the plots of residuals show that the velocity samples were from a normal distribution. Hence these plots confirm that the model from Equation 5.2 in Chapter 5 is appropriate.

Table 6.11 indicates that the velocity mean Vy is rather low and not significant compared with Vx and Vz from Tables 6.11 and 6.12 respectively. Data from

Appendix A1 (Table A1.4) for the tank A3 also indicates that a similar situation was encountered with *Vy*. Since *Vy* in both tanks is not significant compared with *Vx* and *Vz*, it is appropriate to discard it from further analysis. *Vy* is also not significant compared to bubble rise velocity of approximately 2.7mm/sec for bubble size of 70 microns (Fawcett, 1997).

Table 6.7 - ANOVA for velocities (*x* direction) *Vx* in run 1, 2 and 3.

Source	DF	SS	MS	F	p
Group	5	2.74	0.55	0.28	0.925
Error	378	744.97	1.97		
Total	383	747.71			

DF=degrees of freedom SS=sum of squares MS=mean squares
F=ratio using F-test p=level of significance

Table 6.8 - ANOVA for velocities (*y* direction) *Vy* in run 1, 2 and 3.

Source	DF	SS	MS	F	p
Group	5	1.848	0.370	0.55	0.739
Error	378	254.666	0.674		
Total	383	256.514			

Table 6.9 - ANOVA for velocities (*z* direction) Vz in run 1, 2 and 3.

Source	DF	SS	MS	F	p
Group	5	0.175	0.035	0.34	0.891
Error	378	39.495	0.104		
Total	383	39.670			

Table 6.10 - Confidence interval (CI) for velocity mean *Vx*

```
                                  INDIVIDUAL 95% CI'S FOR MEAN
                                  BASED ON POOLED STDEV
LEVEL    N    MEAN    STDEV ---------+---------+---------+------
    1   64   0.865    1.388 (-----------*-----------)
    2   64   0.884    1.401  (-----------*-----------)
    3   64   1.072    1.455        (-----------*-----------)
    4   64   1.088    1.462         (-----------*-----------)
    5   64   0.954    1.341   (-----------*-----------)
    6   64   0.969    1.373    (-----------*-----------)
                              ---------+---------+---------+------
POOLED STDEV =  1.404                0.75      1.00      1.25
```

Note: see note at the end of Table 6.12

Table 6.11 - Confidence interval (CI) for velocity mean *Vy*

LEVEL	N	MEAN	STDEV	INDIVIDUAL 95% CI'S FOR MEAN BASED ON POOLED STDEV
1	64	0.1452	0.8041	(----------*----------)
2	64	0.1567	0.8072	(----------*----------)
3	64	0.1581	0.8713	(----------*----------)
4	64	0.1539	0.8854	(----------*----------)
5	64	0.0064	0.7717	(----------*----------)
6	64	0.0067	0.7781	(----------*----------)
POOLED STDEV = 0.8208				-0.16 0.00 0.16 0.32

Note: see note at the end of Table 6.12

Table 6.12 - Confidence interval (CI) for velocity mean *Vz*

LEVEL	N	MEAN	STDEV	INDIVIDUAL 95% CI'S FOR MEAN BASED ON POOLED STDEV
1	64	-0.1972	0.3006	(----------*----------)
2	64	-0.2003	0.3007	(----------*----------)
3	64	-0.2366	0.3347	(----------*----------)
4	64	-0.2451	0.3263	(----------*----------)
5	64	-0.2456	0.3395	(----------*----------)
6	64	-0.2467	0.3352	(----------*----------)
POOLED STDEV = 0.3232				-0.300 -0.240 -0.180 -0.120

Note: Level 1,3 and 5 are filtered velocity for runs 1, 2 and 3 respectively and Level 2, 4 and 6 are the average velocity for run 1, 2 and 3 respectively.
N = number of observation points in the tank STDEV=standard deviation

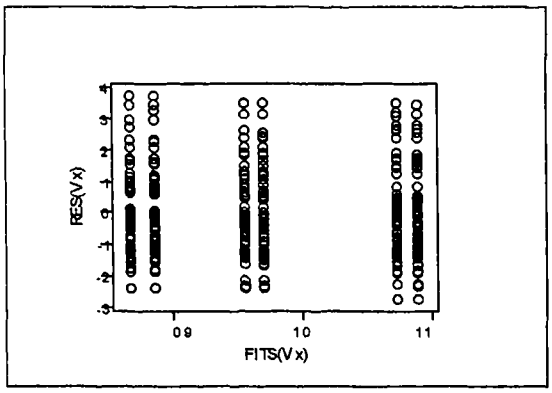

Figure 6.33 - Plot of residual versus fitted values from the ANOVA for velocities (filtered and average) in *x* direction

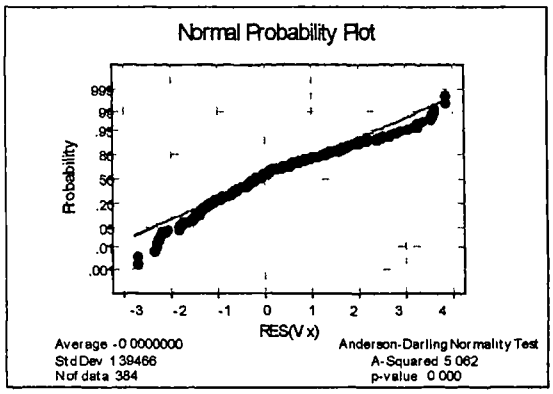

Figure 6.34 - Normal probability plot of residuals from the ANOVA for velocities (filtered and average) in *x* direction

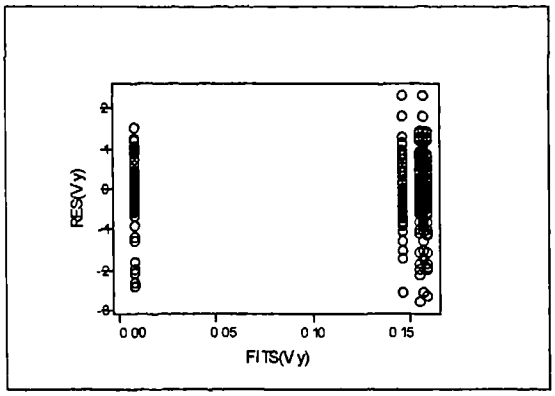

Figure 6.35 - Plot of residual versus fitted values from the ANOVA for velocities (filtered and average) in *y* direction

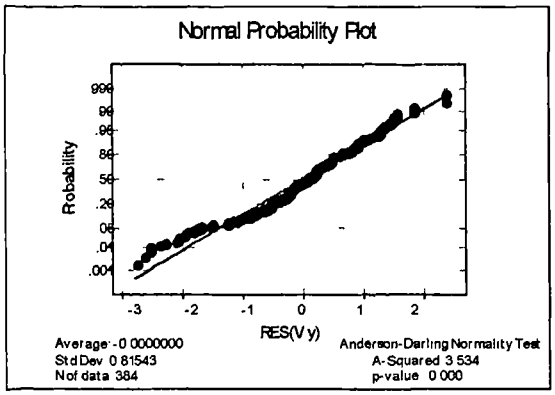

Figure 6.36 - Normal probability plot of residuals from the ANOVA for velocities (filtered and average) in *y* direction

Table 6.13 - Details of velocity and discharge for the tanks at the Frankley WTW

Frankley	Tank A3			Tank C2		
Run	1	2	3	1	2	3
Vx (Max.)	3.73	3.05	4.26	4.68	4.62	4.50
Vx (Min.)	-2.17	-1.19	-1.26	-1.50	-1.67	-1.39
Vy (Max.)	1.89	1.52	2.25	2.51	1.63	1.56
Vy (Min)	-1.55	-1.35	-1.91	-2.41	-2.49	-2.29
Vz (Max.)	0.80	0.54	0.41	0.56	0.51	0.43
Vz (Min.)	-1.38	-1.30	-1.62	-1.04	-1.05	-1.03
Max. Q (mld)	21.47	17.69	21.25	21.80	22.68	21.25
Min. Q (mld)	18.10	15.25	19.66	15.93	15.31	16.41
Average Q(mld)	19.68	16.35	20.83	18.35	20.52	19.76

Vx, *Vy* and *Vx* are the velocities in the *x*, *y* and *z* directions respectively
Max. = maximum Min. = minimum Q = discharge
mld = million litres per day

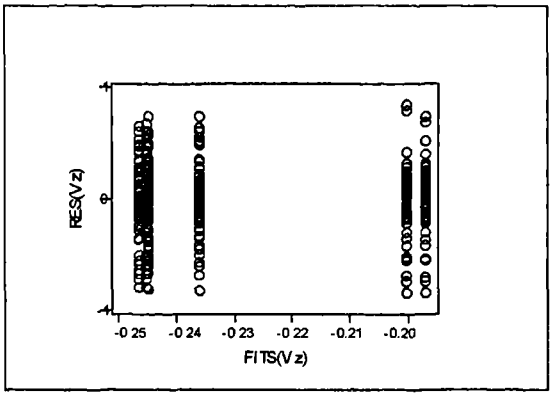

Figure 6.37 - Plot of residual versus fitted values from the ANOVA for velocities (filtered and average) in *z* direction

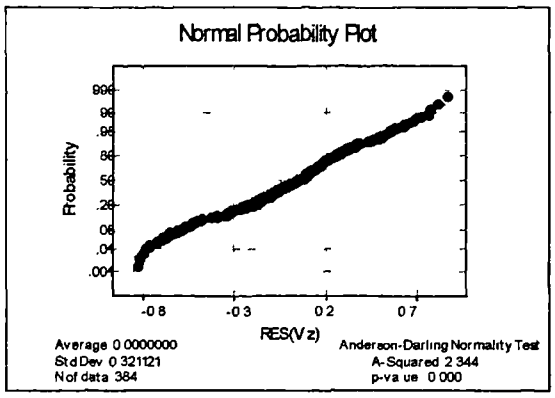

Figure 6.38 - Normal probability plot of residuals from the ANOVA for velocities (filtered and average) in *z* direction

6.4.2 Trimpley WTW

Similar procedures as described in Section 6.4 were used to analyse the average filtered and unfiltered velocity samples from the Trimpley WTW. The results of the ANOVA from tank C1 are shown in Tables 6.14, 6.15 and 6.16 for the velocity components in the *x*, *y* and *z* directions respectively. Additional results from tank C7 are shown in Tables A2.1, A2.3 and A2.5 (Appendix A2). The results from these tables indicate that there is no significant difference in velocity mean between the average filtered and unfiltered velocity data. This confirms the earlier subjective impression of the boxplots. The results also conclude that there is no significant difference of velocity mean between different runs in each tank.

The results of the confidence interval for the velocity mean in the *x*, *y* and *z* directions from Tank C1 (Tables 6.17, 6.18 and 6.19) and Tank C7 (Tables A2.2, A2.4 and A2.6 in Appendix A2) indicate that 95% of the time there is no difference in the velocity mean between different runs in each tank.

In order to check whether the observation on velocity is following the linear statistical model as described in Equation 5.2 of Chapter 5, similar checks as described in Section 6.4.1 were made. Figures 6.39 to 6.44 (tank C1) and Figures A2.13 to A2.18 (Appendix A2 for tank C7) confirm that the underlying velocity samples have constant variance and are derived from a normal distribution.

Table 6.14 - ANOVA for velocities (*x* direction) *Vx* in run 1, 2 and 3.

Source	DF	SS	MS	F	p
Group	5	3.77	0.75	0.46	0.808
Error	378	623.35	1.65		
Total	383	627.12			

Table 6.15 - ANOVA for velocities (*y* direction) *Vy* in run 1, 2 and 3.

Source	DF	SS	MS	F	p
Group	5	0.115	0.023	0.13	0.985
Error	378	65.204	0.172		
Total	383	65.318			

Table 6.16 - ANOVA for velocities (*z* direction) Vz in run 1, 2 and 3.

Source	DF	SS	MS	F	p
Group	5	0.0527	0.0105	0.34	0.890
Error	378	11.8041	0.0312		
Total	383	11.8568			

Table 6.17 - Confidence interval (CI) for velocity mean *Vx*

```
                                    INDIVIDUAL 95% CI'S FOR MEAN
                                    BASED ON POOLED STDEV
LEVEL    N    MEAN    STDEV  -+---------+---------+---------+-----
    1   64   0.042    1.083  (-----------*----------)
    2   64   0.255    1.369            (----------*-----------)
    3   64   0.143    1.174       (-----------*----------)
    4   64   0.306    1.435             (----------*-----------)
    5   64   0.119    1.167       (-----------*----------)
    6   64   0.300    1.431             (-----------*-----------)
                                -+---------+---------+---------+-----
POOLED STDEV =  1.284          -0.25     0.00      0.25      0.50
```

Note: Level 1,3 and 5 are filtered velocity for runs 1, 2 and 3 respectively and Level 2, 4 and 6 are the average velocity for run 1, 2 and 3 respectively.
N = number of observation points in the tank STDEV=standard deviation

Table 6.18 - Confidence interval (CI) for velocity mean *Vy*

				INDIVIDUAL 95% CI'S FOR MEAN BASED ON POOLED STDEV
LEVEL	N	MEAN	STDEV	----+---------+---------+---------+--
1	64	-0.0814	0.4197	(----------*----------)
2	64	-0.0922	0.4425	(----------*----------)
3	64	-0.1322	0.4138	(----------*----------)
4	64	-0.1164	0.3905	(----------*----------)
5	64	-0.1208	0.4050	(----------*----------)
6	64	-0.1132	0.4187	(----------*----------)
				----+---------+---------+---------+--
POOLED STDEV =		0.4153		-0.210 -0.140 -0.070 0.000

Note: Level 1,3 and 5 are filtered velocity for runs 1, 2 and 3 respectively and Level 2, 4 and 6 are the average velocity for run 1, 2 and 3 respectively.
N = number of observation points in the tank STDEV=standard deviation

Table 6.19 - Confidence interval (CI) for velocity mean *Vz*

				INDIVIDUAL 95% CI'S FOR MEAN BASED ON POOLED STDEV
LEVEL	N	MEAN	STDEV	---------+---------+---------+-------
1	64	-0.1977	0.2086	(----------*----------)
2	64	-0.2313	0.1779	(----------*----------)
3	64	-0.2011	0.1714	(----------*----------)
4	64	-0.2131	0.1564	(----------*----------)
5	64	-0.2016	0.1826	(----------*----------)
6	64	-0.2176	0.1582	(----------*----------)
				---------+---------+---------+-------
POOLED STDEV =		0.1767		-0.245 -0.210 -0.175

Note: Level 1,3 and 5 are filtered velocity for runs 1, 2 and 3 respectively and Level 2, 4 and 6 are the average velocity for run 1, 2 and 3 respectively.
N = number of observation points in the tank STDEV=standard deviation

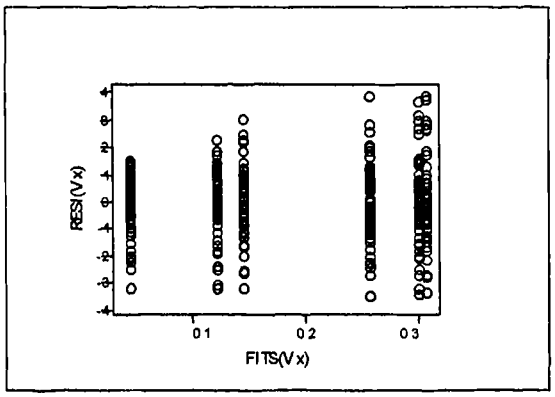

Figure 6.39 - Plot of residual versus fitted values from the ANOVA for velocities (filtered and average) in x direction

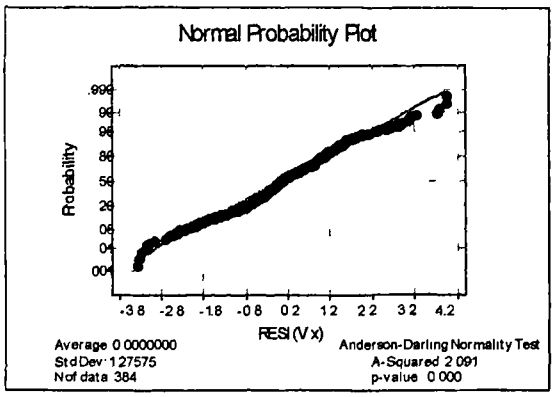

Figure 6.40 - Normal probability plot of residuals from the ANOVA for velocities (filtered and average) in x direction

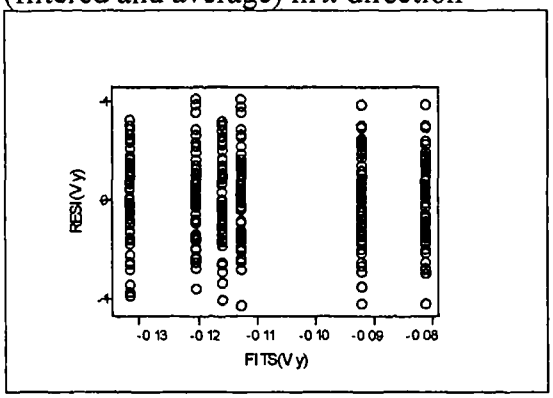

Figure 6.41 - Plot of residual versus fitted values from the ANOVA for velocities (filtered and average) in y direction

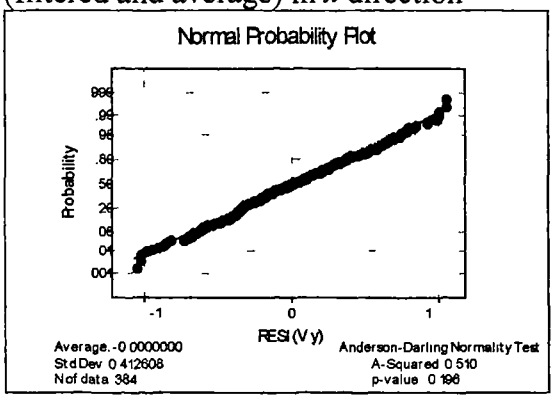

Figure 6.42 - Normal probability plot of residuals from the ANOVA for velocities (filtered and average) in y direction

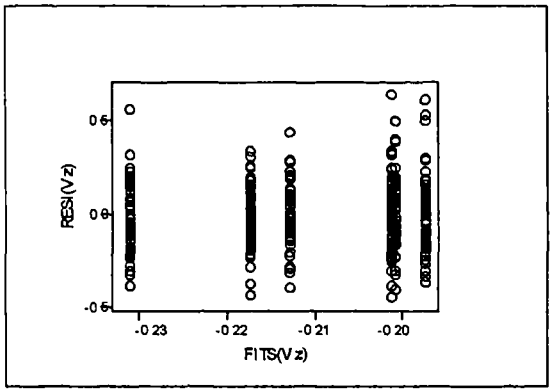

Figure 6.43 - Plot of residual versus fitted values from the ANOVA for velocities (filtered and average) in z direction

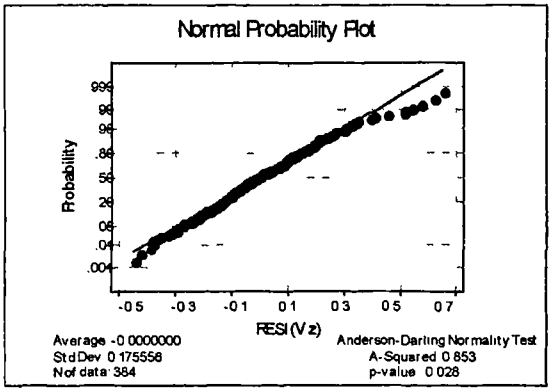

Figure 6.44 - Normal probability plot of residuals from the ANOVA for velocities (filtered and average) in z direction

6.5 COMPARISON OF TANK VELOCITY DISTRIBUTION

6.5.1 Frankley WTW

6.5.1.1 Velocity Distribution *Vx* (velocity in *x* direction)

Further analysis of velocity data *Vx* was made by comparing the filtered velocity distribution for each run at four different levels of depth. The same average filtered velocity data at each point of the tank as described in Section 6.4 are used to plot the velocity distribution for each run. Four different levels of depth refer to depths d1, d2, d3 and d4, which correspond to 2.125m, 1.650m, 1.100m and 0.550m from the top water level of the dissolved air flotation tank. The contour diagrams of the average filtered velocity are as shown in Appendix B1 and B2 for tanks C2 and A3 respectively. Comparisons of velocity distribution *Vx* at depth d1 for different runs from tank C2 indicate a similar flow pattern. These can be seen from Figures B1.4, B1.8 and B1.12 of Appendix B1. The higher velocity values are found near the outlet of the tank. This confirms the earlier impression from the boxplots. Velocity distribution *Vx* at depth d2 (Figures B1.3, B1.7 and B1.11 in Appendix B1) are found to have an approximately similar pattern between each run. At depth d3 (Figures B1.2, B1.6 and B1.10 in Appendix B1), only velocity distribution from runs 2 and 3 can be considered to have an approximately similar pattern. At depth d4 (Figures B1.1, B1.5 and B1.9 in Appendix B1), there appears to be some differences in velocity distributions (*Vx*) between different runs. These diagrams however indicate overall that the velocity *Vx* was higher across one diagonal of the tank (in plan view) and lower at the other diagonal. These velocity distributions confirm that the flow at depth d4, which is at 0.55m (one-quarter of the depth of the tank) from the surface of the tank, was not uniform. This suggests that the effect of unsteady flow into the tank is effectively experienced in the upper one-quarter depth of the tank.

If comparisons of velocity distributions *Vx* are made between tank C2 and A3, the results indicate that at depth d3 and d4 the velocity distributions of the two tanks are not similar. These comparisons are based on the diagrams in Figures B1.1, B1.2,

B1.5, B1.6, B1.9 and B1.10 from Appendix B1, and B2.1, B2.2, B2.5, B2.6, B2.9 and B2.10 from Appendix B2. At depths d1 and d2, the velocity distributions *Vx* from both tanks can be approximately considered to have some similar patterns (Figures B1.3, B1.4, B1.7, B1.8, B1.11 and B1.12 from Appendix B1, and B2.3, B2.4, B2.7, B2.8, B2.11 and B2.12 from Appendix B2).

6.5.1.2 Velocity Distribution *Vy* (velocity in *y* direction)

Comparison of *Vy* for different runs at different depths within tank C2 based on Figures B1.13 to B1.24 (Appendix B1), indicates that there appears to be no similarity in velocity patterns except for runs 2 and 3 at depths d3 and d4. In the case of tank A3, Figures B2.13 to B2.24 (Appendix B2) indicate that there is no similar velocity distribution between different depths in the tank for three different runs. In the contour diagrams (Appendices B1 to B4) the positions of *Vy* were plotted at a specific distance from the wall of the tank (refer to Figures 4.3 and 4.4 in Chapter 4).

6.5.1.3 Velocity Distribution *Vz* (velocity in *z* direction)

Figures B1.25 to B1.36 and B2.25 to B2.36 (Appendices B1 and B2) show the velocity distributions Vz for tanks C2 and A3 respectively. At depth d4, the overall positive *Vz* covers only a small proportion of the surface area of the tank. This means fewer particles moving upward in the upper one-quarter depth of the tank. The flow distributions between tanks C2 and A3 at different depths do not show any significant similarity.

6.5.2 Trimpley WTW

6.5.2.1 Velocity Distribution *Vx* (velocity in *x* direction)

Velocity distributions *Vx* for tanks C1 and C7 are as shown in Figures B3.1 to B3.12 and Figures B4.1 to B4.12 in Appendices B3 and B4 respectively. There are some similarities in the flow patterns at depths d1, d2 and d3 between runs 1, 2 and 3 for

tank C1. Higher *Vx* dominates the flow near the outlet of the tank whereas low *Vx* appears near the baffle of the tank. At depth d4, Figures B3.1, B3.5 and B3.9 indicate that there is no similarity in the flow pattern between runs 1, 2 and 3. This may be due to unstable conditions prevailing at depth d4.

In the case of tank C7, there appears to be some similarity in the flow pattern at depths d1, d2, d3 and d4 between runs 1, 2 and 3 except at depth d4 run 3. These velocity distributions can be seen from Figures B4.1 to B4.12 in Appendix B4.

6.5.2.2 Velocity Distribution *Vy* (velocity in *y* direction)

Figures B3.13 to B3.24 and B4.13 to B4.24 in Appendices B3 and B4 show the velocity distributions *Vy* for tanks C1 and C7 respectively. For tank C1, there appear to be no distinctive flow patterns between three different runs for various depths except as follows:

1. At depth d1, runs 1 and 2 can be considered to follow an approximately similar pattern.
2. At depth d3, runs 1 and 2 show a weak form of similarity.

The results from tank C7 (Figures B4.13 to B4.24 in Appendix B4) indicate that only velocity distributions *Vy* at depth d3 from runs 1 and 2 are similar.

6.5.2.3 Velocity Distribution *Vz* (velocity in *z* direction)

Velocity distributions *Vz* for tank C1 and C7 are as shown in the diagrams in Appendices B3 and B4 respectively. For the tank C1, it can be said that at depths d2 and d3 for runs 1, 2 and 3 there exists a poor similarity in the flow patterns between different runs (Figures B3.27, B3.31 and B3.25 at depth d2, and Figures B3.26, B3.30 and B3.34 at depth d3). Positive velocity at depth d4 (Figures B3.25, B3.29 and B3.33) appears to cover a small surface area of the tank and seems to be predominantly near the baffle of the tank. The same condition applies for tank C7

(Figures B4.25, B4.29 and B4.33 in Appendix B4). However the latter does not seem to have any form of similarity in its flow patterns between different runs for a specified depth.

6.5.3 Discussions on Velocity Distributions

The overall results from both treatment plants indicate that at depth d1 (i.e. the flow in the *x*-direction) similar patterns of velocity distributions were observed. At the outlet of the tank the velocity *Vx* is higher (positive) whereas near the baffle the velocity *Vx* is negative. This result is in agreement with the works of O'Neill *et al.* (1997) which used a CCTV camera to monitor the flow from a physical model of a dissolved air flotation tank. However it is not in agreement with the Computational Fluid Dynamics (CFD) model (Fawcett, 1997; Ta and Brignal, 1997). The latter indicated that a simple flow pattern (i.e. no recirculation of flow in the *x* direction) was encountered within the depth d1. Fawcett's work was based on a model simulation of two-dimensional flow in a dissolved air flotation tank based on uniform discharge. In reality it is in a three-dimensional flow regime with an unsteady flow rate. If the diagrams of velocity distributions *Vx* and *Vz* at depth d1 are analysed together (i.e. Figures B1.4, B1.8, B1.12, B1.28, B1.32 and B1.36), the resultant velocity components for different runs are not the same.

For the velocity in the *z*-direction, the overall results from this investigation are not in agreement with O'Neill *et al.* (1997) and Fawcett (1997). The former indicated that the flow below the datum of the baffle (datum refers to the horizontal elevation of the upper end of the baffle) is in the downwards direction except in the area near the baffle (i.e between the tip of the baffle and the floor). The results from this study however indicate that a more complex situation occurred in the tank (i.e. Figures B1.25 to B1.36 in Appendix B1). Although *Vz* is moving upwards near the baffle, it does not occur at all sections across the width of the tank. The CFD model (Fawcett, 1997) indicated that the flow at the far end of the tank is in the downward direction. The result is in agreement with the velocity distribution observed at Frankley and Trimpley.

6.6 COMPARING AVERAGE FILTERED VELOCITY VARIATIONS BETWEEN RUNS, TANKS AND SITES

Velocity data from the average filtered velocity at each point in the tank as described in Section 6.3 were used to compare the velocity variations between different runs, between different tanks and between different sites. Only *Vx* and *Vz* were used for the analysis (Section 6.4.1 indicates *Vy* is not significant). In order to compare the average filtered velocities between different runs and between different tanks of the same size from the same site, the average filtered velocity at each of the 64 points in the tank from each run was used in accordance with the statistical procedures described in Section 5.2.4 of Chapter 5.

Two-way analysis of variance (ANOVA) was carried out to see the effects of tanks and runs on the observed velocity obtained during the experiments. Two-way ANOVA calculated the total variation in the average velocity data based on the sum of variation from several sources:

Total variation in average velocity = (variation due to different tanks)
+(variation due to different runs)
+(variation due to random error)

If the variation due to different tanks is much greater than the variation due to random error, there will be statistically significant evidence of a difference in velocity between the two tanks at the same site. Similarly, if the variation due to different runs is much greater than the variation due to random error, there will be statistically significant evidence of a difference in velocity between runs.

Statistical tests were conducted on the average filtered velocity data at Frankley and Trimpley WTW. The main objectives of the tests were to answer the following questions:

1. Is the difference in the velocity means (if any) due to the tanks effects?

2. Is the difference in velocity means (if any) due to the runs effects?

In order to compare the average filtered velocity between different sites (i.e at Frankley and Trimpley), the same velocity data which were used to compare different runs were used. The analysis was carried out using one-way ANOVA (Section 5.2.3 in Chapter 5). The factor used in the ANOVA was the sites (i.e. using the MINITAB software). A one-way ANOVA attempts to calculate the total variation in the average filtered velocity based on the variation due to sites and the variation due to random error. If the variation due to sites is much greater than the variation due to random error, there will be statistically significant evidence of a difference between sites (Frankley and Trimpley). The objective of the test is to see whether there is any significant difference in the velocity mean between different sites. In other word this test is trying to answer the question, "Do different sites have different velocity means?".

The analysis carried out in this section can be summarised as shown in Figure 6.45.

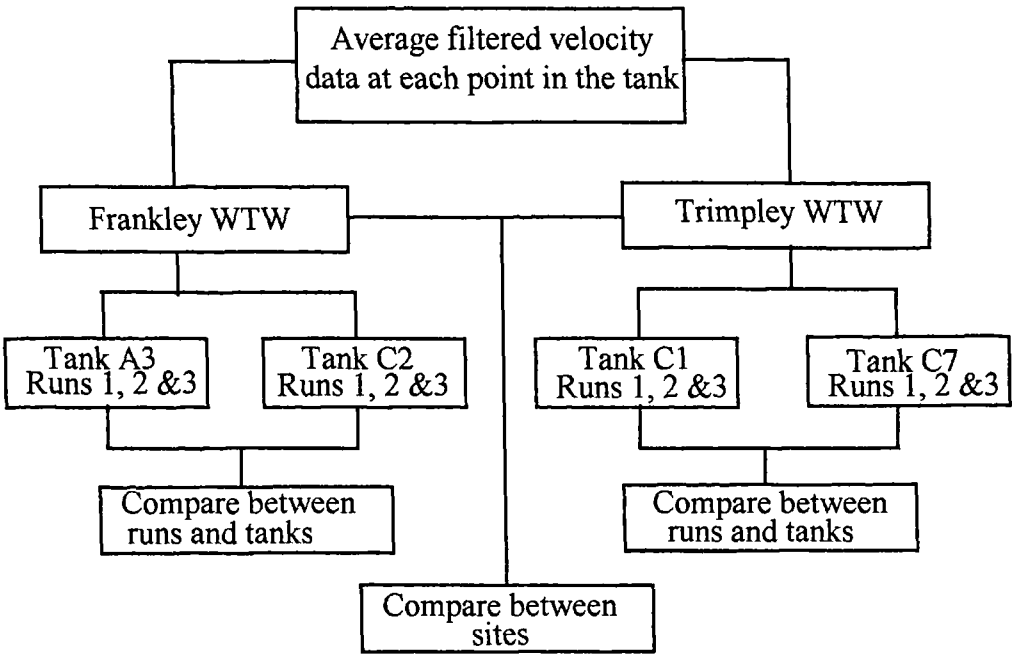

Figure 6.45 - Schematic diagram of the analysis to compare variation of velocity mean between runs, tanks and sites

6.6.1 Frankley WTW

The results of the tests for velocity components in the x and z directions are shown in Tables 6.20 and 6.21 respectively. Table 6.20 indicates that there was a significant difference of velocity mean between different tanks (Tanks A3 and C2). This result suggests that the tank physical parameters may affect the velocity mean and the velocity distribution in the tank. The velocity mean Vx for Tank A3 was 0.632cm/sec whereas for Tank C2 was 0.964cm/sec. However there is no evidence to suggest any significant difference in velocity mean between different runs (Table 6.20). This result implies that different runs which were carried out on different days did not influence the velocity mean in the tank.

The results for velocity components in the z direction (Table 6.21) indicate that there was no significant difference in velocity mean between the tanks and between different runs. The results suggest that different tanks of the same site and different runs carried out at different times do not contribute any changes in velocity mean in the dissolved air flotation tanks. The velocity means Vz for tanks A3 and C2 were-0.256 cm/sec and -0.226 cm/sec respectively.

A linear statistical model on the average observation of velocity on each run in each tank is described in Equation 5.6 of Chapter 5. To check whether this model is appropriate with the ANOVA as tabulated in Tables 6.20 and 6.21, model adequacy checking is made. Figures 6.46, 6.47, 6.48 and 6.49 indicate that the model is appropriate for velocity components in the x and z directions.

Table 6.20 - Two-way ANOVA (balanced design) for Vx based on runs 1,2 and 3

Source	DF	SS	MS	F	p
Tanks	1	10.547	10.547	6.52	0.011
Runs	2	3.600	1.800	1.11	0.330
Error	380	614.410	1.617		
Total	383	628.557			

p = level of significance

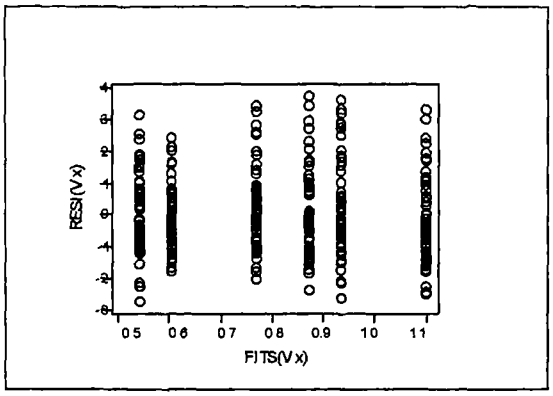

Figure 6.46 - Plot of residual versus fitted values from two-way ANOVA for *Vx*

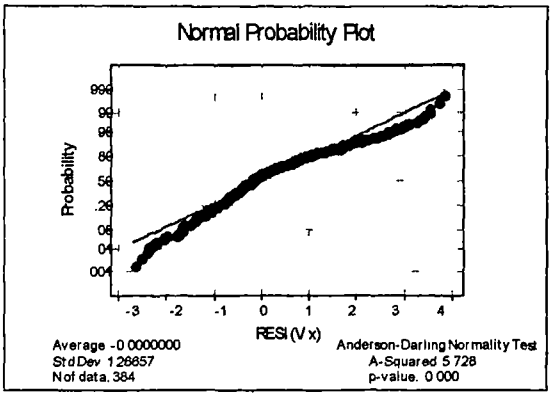

Figure 6.47 - Normal probability plot of residuals from two-way ANOVA for *Vx*

Table 6.21 - Two-way ANOVA (balance design) for *Vz* based on runs 1,2 and 3

Source	DF	SS	MS	F	P
Tanks	1	0.0814	0.0814	0.67	0.414
Runs	2	0.0081	0.0040	0.03	0.967
Error	380	46.1854	0.1215		
Total	383	46.2749			

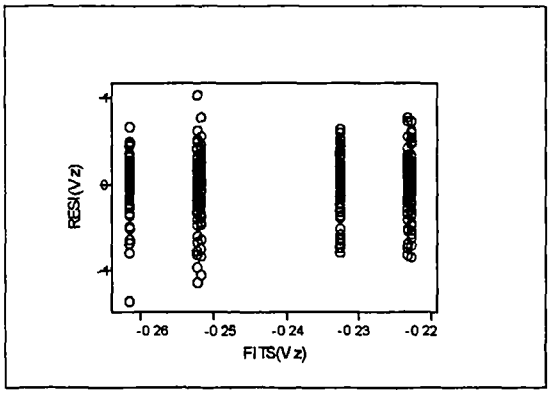

Figure 6.48 - Plot of residual versus fitted values from two-way ANOVA for *Vz*

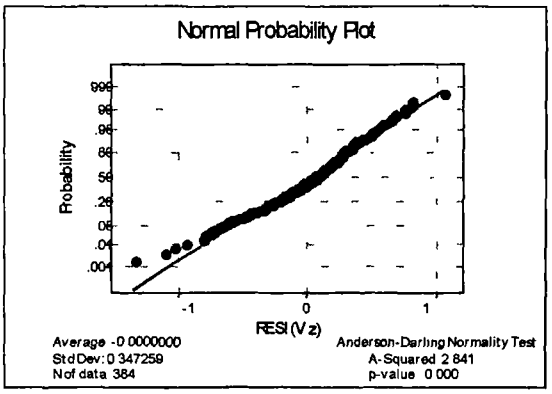

Figure 6.49 - Normal probability plot of residuals from two-way ANOVA for *Vz*

6.6.2 Trimpley WTW

Similar procedures as described in the previous section (Section 6.6.1) were carried out to find the effects of tanks and runs on the observed velocity from the full-plant studies at the Trimpley WTW. The results from Tables 6.22 and 6.23 indicate there was no significant difference of velocity means between tanks and between runs for

the velocity components in the x and z directions respectively. The observed velocity means of Vx for tanks C1 and C7 were 0.101cm/sec and 0.241cm/sec respectively. In the case of Vz, the velocity mean for the tank C1 was -0.200cm/sec whereas tank C7 was -0.232cm/sec.

Figures 6.50 to 6.53 indicate that the linear statistical model as described in Equation 5.6 of Chapter 5 and Section 6.6.1 is appropriate for velocity components in the x and z directions.

Table 6.22 - Two-way ANOVA (balance design) for Vx based on runs 1,2 and 3

Source	DF	SS	MS	F	P
Tanks	1	1.876	1.876	1.44	0.231
Runs	2	0.095	0.048	0.04	0.964
Error	380	495.391	1.304		
Total	383	497.362			

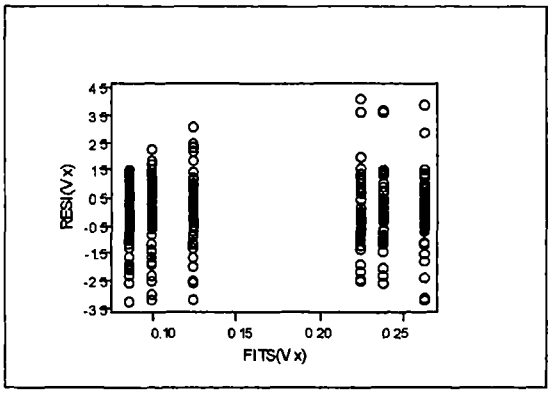

Figure 6.50 - Plot of residual versus fitted values from two-way ANOVA for Vx

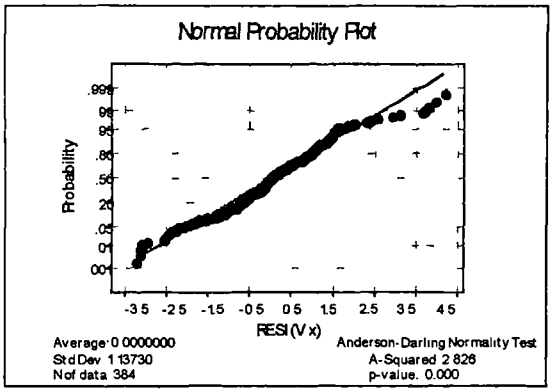

Figure 6.51 - Normal probability plot of residuals from two-way ANOVA for Vx

Table 6.23 - Two-way ANOVA (balance design) for Vz based on runs 1,2 and 3

Source	DF	SS	MS	F	P
Tanks	1	0.09882	0.09882	2.66	0.104
Runs	2	0.01051	0.00525	0.14	0.868
Error	380	14.13517	0.03720		
Total	383	14.24450			

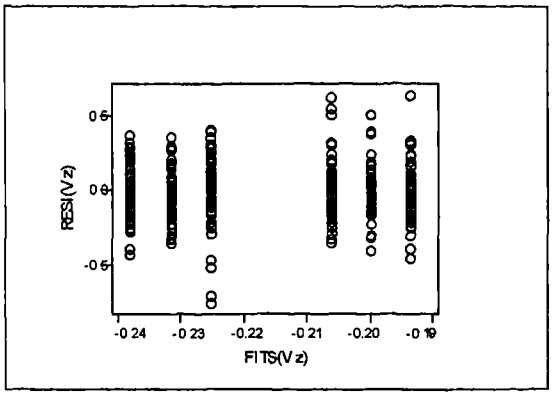

Figure 6.52 - Plot of residual versus fitted values from two-way ANOVA for *Vz*

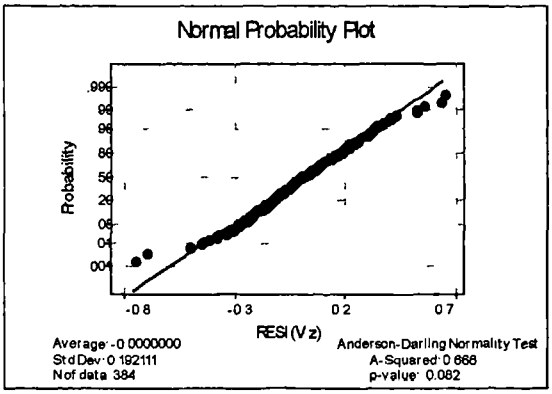

Figure 6.53 - Normal probability plot of residuals from two-way ANOVA for *Vx*

6.6.3 Comparison Between Two Sites

Comparison of velocity means between the tanks at Frankley and Trimpley WTW was made. Table 6.24 shows that variation of velocity mean *Vx* between Frankley and Trimpley WTW was highly significant. Velocity means at Frankley and Trimpley WTW were at 0.798cm/sec and 0.171cm/sec respectively. This result is plausible because from the empirical calculations based on the average flow rate divided by the cross-sectional area for the tanks at Frankley and Trimpley indicated that the average velocity at Frankley was higher than at Trimpley (Table 6.26). Comparisons of the average flow rate and the average velocity for the tanks at Frankley and Trimpley are shown in Table 6.26.

For the velocity in the *z* component, Table 6.25 indicates that there is no evidence to suggest any significant difference of the velocity mean between the two sites. Velocity mean *Vz* at Frankley was at -0.241cm/sec and at Trimpley was -0.216cm/sec. This result shows that the average velocity mean *Vz* at Frankley and Trimpley was in a downwards direction. Although the flow rate (Table 6.26) at Frankley and Trimpley differed significantly, both sites have negative *Vz*.

Comparisons of velocity means based on data obtained from the ADV probe and that of using the average flow rate divided by the average cross-sectional area of the tanks (hereinafter called a simplified method) were also made. Table 6.26 indicates that

there were significant differences in velocity means of *Vx* between that obtained by using the ADV probe and the simplified method for all the tanks at Frankley and Trimpley. The differences are plausible since the boxplots (Figures 6.9 to 6.11, 6.21 to 6.23, A1.1 to A1.3 in Appendix A1 and A2.1 to A2.3 in Appendix A2) indicate that there was a large variation in the velocity mean for each run of the experiment. Table 6.26 also indicate that there was a considerable variation in the flow rate for each run. This demonstrates that a simplified method cannot be used to ascertain the value of *Vx* for design purposes.

Table 6.24 - ANOVA for *Vx* to identify variation between sites

Source	DF	SS	MS	F	P
Sites	1	75.46	75.46	51.34	0.000
Error	766	1125.919	1.470		
Total	767	1201.382			

Table 6.25 - ANOVA for *Vz* to identify variation between sites

Source	DF	SS	MS	F	P
Sites	1	0.1188	0.1188	1.50	0.221
Error	766	60.5194	0.0790		
Total	767	60.6382			

Table 6.26 - Variation of discharge during velocity data collection

Frankley	Tank A3			Tank C2		
Vol.(m^3)	134.5			134.5		
Run	1	2	3	1	2	3
Max. Q_2 (mld)	21.47	17.69	21.25	21.80	22.68	21.25
Min. Q_2 (mld)	18.10	15.25	19.66	15.93	15.31	16.41
Average Q_2 (mld)	19.68	16.35	20.83	18.35	20.52	19.76
Average Q_1 (mld)	9.840	8.175	10.415	9.175	10.260	9.880
$RT_{Average}$ (minutes)	19.7	23.7	18.6	21.1	18.9	19.6
Average *Vx* (cm/sec)*	0.711	0.591	0.753	0.663	0.742	0.714
Average *Vx* (cm/sec)**	0.537	0.454	0.906	0.865	1.072	0.954
Trimpley	Tank C1			Tank C7		
Vol.(m^3)	66.50			66.50		
Run	1	2	3	1	2	3
Max. Q (mld)	6.00	5.87	6.40	5.90	6.90	7.57
Min. Q (mld)	5.05	4.22	4.40	5.31	5.13	5.11
Average Q (mld)	5.50	5.96	5.40	5.67	5.93	5.60
$RT_{Average}$ (minutes)	17.4	16.1	17.7	16.9	16.1	17.1
Average *Vx* (cm/sec)*	0.641	0.694	0.629	0.661	0.691	0.653
Average *Vx* (cm/sec)**	0.042	0.143	0.119	0.266	0.241	0.216

Max. = maximum Min. = minimum mld = million litre per day
Q_2 =f low based on two tanks Q_1 = flow based on one tank
Q = flow based on one tank $RT_{Average}$ = average retention time
*Vx** = average flow rate divided by the average cross-sectional area of the tank
*Vx*** = velocity mean obtained using an ADV probe

6.7 SUMMARY OF RESULTS AND FINDINGS

1. Comparisons of velocity data collected using sampling rates of 25Hz and 1Hz were made. The results indicate that the velocity data collected at 25Hz has a higher percentage of good velocity data than at 1Hz. In terms of skewness (>1.5), the

results suggest that the higher sampling frequency observation (25Hz) at Frankley produce less skewness than the lower sampling frequency (1Hz) at Trimpley. Velocity data exhibiting higher skewness occurred at a lower or negative velocity which may suggest that the flow is under a transition regime. The occurrence of the skewness (>1.5) is predominantly at depth d1 (at one quarter depth of the tank) and d2 (at half depth of the tank) at a distance of one-quarter length of the tank from the baffle.

2. Comparisons of the variation of the average filtered and average raw velocity data indicate that there is no significant difference between data at Frankley or Trimpley WTW. This suggests that the raw data was as good as the filtered data and the ADV probe is suitable to be used for flow measurements in the separation zone of the dissolved air flotation tank. In fact it can be claimed that this is the first research work which has measured and analysed the velocity distribution in the separation zone of DAF tanks using appropriate statistical techniques.

3. Comparison of measured velocity distribution in the tank with the output from Computational Fluid Dynamics (CFD) models produced by Fawcett (1997) and Ta and Brignal (1997) indicates that there are some differences in the flow patterns except near the tank outlet (the works of Fawcett, Ta and Brignal cannot be reproduced here but can be found as indicated in the reference). Present CFD models are based on two dimensional flow with the assumptions that the flow in the y direction is uniform (zero), a constant inflow into the tank and the velocity patterns are independent of time. In reality the inflow into the tank is unsteady. The inflow into the tank is subjected to the desludging of other tanks, cleaning of the filters and changes in water demand. When one of the DAF cells is under a desludging process, the outlet gate will be closed which results in the increase of the water level in the tank. At the same time the sludge scraper will move forward to push the sludge into the collecting channel. During this process (desludging), the other tanks will be subjected to a higher input flow rate. In fact it has been observed that during the collection of velocity and turbidity data at the Frankley and Trimpley WTW, the output flow rate of each tank changes every second.

Tables 6.5 and 6.6 indicate that the velocities in the x, y and z directions were very low, which suggests that the flow within the tank was laminar. The plan view of contour diagrams in Appendices B1 to B4 (i.e. based on the measured velocity) showed that significant variations in time occurred within the tank for the velocities in the x, y and z directions. These variations may induce short circuiting and indicate a non-uniform spatial flow and also with respect to time. The significance of velocity variation Vx at depth d4 may affect the performance of the DAF tank in terms of turbidity removal. For example in Figures B1.1 and B1.25 (in Appendix B1) at depth d4 (one quarter depth from the surface), higher values of Vx were related to positive values of Vz (i.e. on the right hand side of the baffle). Positive values of Vz indicate that the flow moved upward. This suggests that the particles were moving up toward the surface of the tank. The results from the research work suggest that this is the first work which enables us to show the actual three-dimensional velocity distribution in a DAF tank and also helps to analyse the effective positions of turbidity removal within the separation zone. Future CFD approaches should have stochastic input and output for good representation of tank velocity distribution.

4. The plan view contour diagrams of Vz indicate that the flow is predominantly moved downwards at depths d1, d2, d3 and d4 (Figures 4.4 and 4.5 in Chapter 4). This suggests that the separation process in the separation zone is only effective in the upper one-quarter depth of the tank. Particles not captured in this zone will exit with the bulk flow.

5. At the Frankley WTW, it was found that there was no significant difference of velocity in the x direction (Vx) for different runs for each tank but there was a significant difference of Vx between the tanks of the same size. This suggests that there was a significant difference in the flow rates between the tanks at Frankley. The results at the Trimpley WTW show that there was no significant difference of Vx between runs and between tanks.

6. There was no significant difference of velocity mean in the z direction (Vz) between different runs and between different tanks of the same size at Frankley and Trimpley WTW. This may suggest that the velocity mean in the vertical component of any DAF tank may be approximately the same. The present results were based on two tanks of different sizes. There is a need to investigate more tanks of different sizes to confirm this hypothesis.

7. Comparisons of velocity components in the x direction between the tanks at Frankley and Trimpley indicate that there was a significant difference of Vx between both sites. The difference in Vx may be due to a higher flow rate at Frankley than Trimpley.

CHAPTER 7

ANALYSIS OF THE RELATIONSHIP BETWEEN TANK DIMENSIONS, FLOW AND VELOCITY DISTRIBUTION

7.1 INTRODUCTION

In Chapter 5 statistical techniques using factorial designs and regression analysis have been explained. These techniques have been used in this chapter to develop the relationship between tank dimensions, flow rate and velocity distribution in the tank. Chapter 5 also explained the initial steps which have been taken during data analysis prior to developing second-order models in the regression analysis. These include an attempt to use first-order linear regression and a series of logarithmic, reciprocal and exponential transformations to develop relationships between the predictor and response variables.

In Chapter 6 the quality of velocity data at each of the 64 points in the tank for each run was checked. Velocity samples at each point were averaged. Extensive statistical techniques were used to compare the average velocity data (from each point in the tank) between different sampling rates, between different runs, between tanks, between sites and between different velocity components. The results indicate that the velocity samples collected at each point were normally distributed and have constant variance. The average filtered velocity sample distributions were consistent with the average unfiltered velocity sample distributions. Statistical tests on the velocity data indicate that the velocity samples were reliable and hence can be used for the development of models to describe the velocity distribution in the tank. The velocities in the x and z directions were more significant than in the y direction.

This chapter examines the velocity component in the x and z directions. Statistical techniques such as the analysis of variance (ANOVA), analysis of covariance (ANCOVA) and regression analysis are used to develop models to describe the velocity distribution in the tank. The process of developing the models required the velocity data to be analysed in stages. The stages can be summarised as follows:

1. To check the effects of tank dimensions on the velocity distribution in the tank using ANOVA with an appropriate statistical model. If the physical tank dimensions were found to have a significant effect on the velocity distribution in the tank, checks on the model adequacy were made (Section 5.2.3.1 in Chapter 5).

2. To check whether the discharge may affect the velocity distribution in the tank. Since the discharge was a concomitant variable which was continuous in nature, another test statistic called ANCOVA was used.

3. The final stage was to use regression analysis to develop suitable models to describe the velocity distribution in the tank. The ANOVA and ANCOVA which were used at the previous stage were important so that comparison can be made on the relative significance of the predictor variables between different methods.

7.2 CHECKING THE EFFECTS OF TANK DIMENSIONS ON VELOCITY

7.2.1 Velocity in the x Direction

A fixed effects model as described in Section 5.3.1.1 was investigated for its suitability to describe velocity distribution based on the data collected during the investigation. The main objective was to find out whether the tank physical parameters, i.e. width, depth and length, have any significant effect on the velocity distribution in the dissolved air flotation tank. Since there are three factors (width, depth and length) to be investigated in this research work, three-factor analysis of variance with interaction terms as described in Section 5.3.1.1 of Chapter 5 was used to analyse the data. The fixed effects model applies only to the tanks from which the data was collected. Some of the variation in velocity is due to the fluctuation in flow rate over the sampling period.

Tables 7.1, 7.2 and C1.2 (Appendix C) indicate that the effects of width, depth, length and all the interaction terms have a highly significant effect on the velocity

component in the x direction. However the results from Tank A3 at Frankley indicate that all the physical dimensions and the interaction terms are highly significant except the interaction term between width and depth. The results are shown in Table C1.1 (appendix C). This means the cross-sectional area of the dissolved air flotation tank at A3 does not show any significant effect on the velocity distribution in the tank based on the three runs carried out during the investigation. There is no apparent reason why there was a difference in the result between Tank C2 and A3 at the Frankley WTW. The analysis of variance (Table 7.3) did not show any significant difference of flow rate between both tanks.

The statistical model describing the observed velocity in the x direction as shown in equation 5.7 of Chapter 5 will be appropriate if the checks on model adequacy satisfy the requirements as set up in Section 5.2.3.1 of Chapter 5. Figures 7.1 to 7.4, C1.1, C1.2, C1.3 and C1.4 (Appendix C) indicate that the requirements are satisfied. The plots of residual versus fitted values and normal probability plots of residuals indicate the underlying velocity samples have constant variance and are normally distributed.

Table 7.1 - Analysis of variance for velocities in x direction (runs 1,2 & 3) using multifactor balanced designs (Tank C2, Frankley WTW)

Source	DF	SS	MS	F	P
Width	3	5.2637	1.7546	5.54	0.001
Depth	3	35.3713	11.7904	37.24	0.000
Length	3	78.6516	26.2172	82.81	0.000
Width*Depth	9	18.1186	2.0132	6.36	0.000
Width*Length	9	23.0394	2.5599	8.09	0.000
Depth*Length	9	129.4741	14.3860	45.44	0.000
Width*Depth*Length	27	38.9051	1.4409	4.55	0.000
Error	128	40.5219	0.3166		
Total	191	369.3457			

Note: * is for interaction

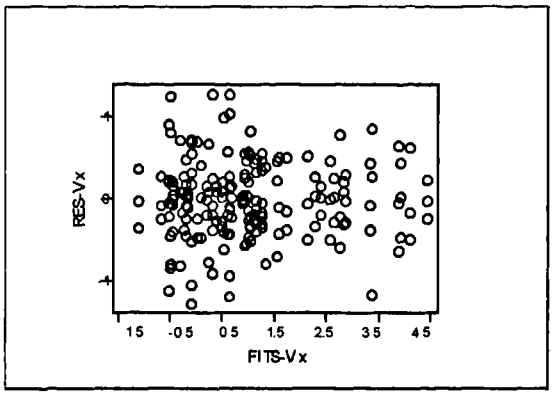

Figure 7.1 - Plot of residuals versus fitted values from the analysis of variance for velocities in x direction (Tank C2, Frankley WTW)

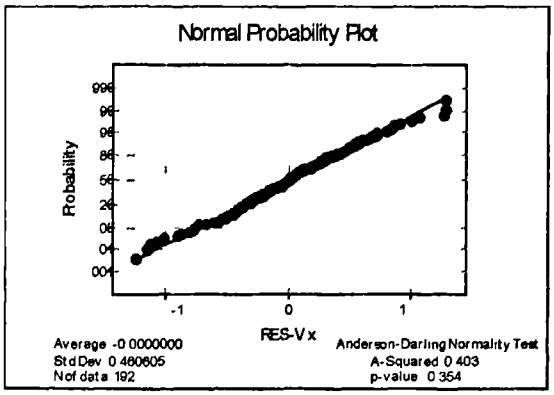

Figure 7.2 - Normal probability plot of residuals from the analysis of variance for velocities in x direction (Tank C2, Frankley WTW)

Table 7.2 - Analysis of variance for velocities in x direction (runs 1,2 & 3) using multifactor balanced designs (Tank C1, Trimpley WTW)

Source	DF	SS	MS	F	P
Width	3	14.7350	4.9117	26.70	0.000
Depth	3	129.7573	43.2524	235.13	0.000
Length	3	19.7734	6.5911	35.83	0.000
Width*Depth	9	6.6063	0.7340	3.99	0.000
Width*Length	9	7.3864	0.8207	4.46	0.000
Depth*Length	9	35.1050	3.9006	21.20	0.000
Width*Depth*Length	27	9.9521	0.3686	2.00	0.005
Error	128	23.5460	0.1840		
Total	191	246.8615			

Note: * is for interaction

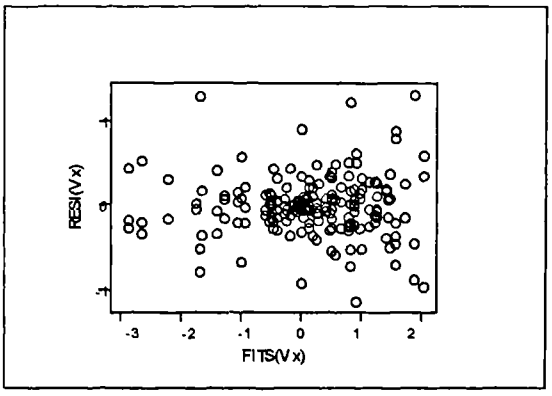

Figure 7.3 - Plot of residuals versus fitted values from the analysis of variance for velocities in x direction (Tank C1, Trimpley WTW)

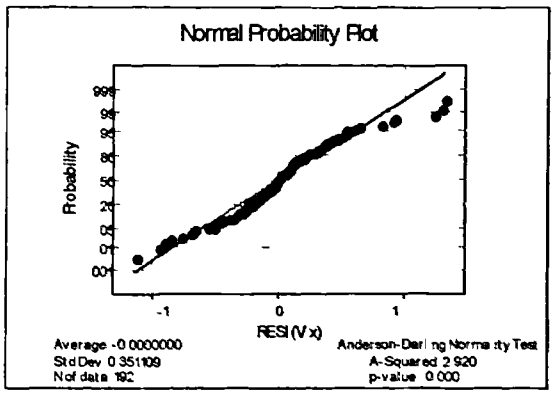

Figure 7.4 - Normal probability plot of residuals from the analysis of variance for velocities in x direction (Tank C1, Trimpley WTW)

Table 7.3 - ANOVA on the flow rate between Tanks C2 and A3 at Frankley WTW

Source	DF	SS	MS	F	P
Tanks	1	0.131	0.131	0.16	0.712
Error	4	3.313	0.828		
Total	5	3.444			

7.2.1.1 Analysis of Covariance (*Vx*)

Since the output flow from the dissolved air flotation tank is a continuous process and cannot be controlled during the investigation, an attempt to find out whether the output flow has any relationship with the velocity distribution in the tank has to be made by using an analysis of covariance. This method enables the effect of the continuous variable (output flow or discharge) to be analysed alongside the fixed variables (width, depth and length of the tank). Section 5.3.2 in Chapter 5 explained further details on the analysis of covariance.

The results for velocity in the *x*-direction on Tank C2 and A3 at Frankley WTW are shown in Tables 7.4 and C1.3 (Appendix C) respectively. These results indicate that the discharge (covariate) from the tank is affecting the velocity distribution in the tank.

Table 7.4 - Analysis of Covariance for *Vx* (Tank C2, Frankley WTW)

Source	DF	ADJ. SS	MS	F	P
Covariate(discharge)	1	2.8960	2.8960	9.78	0.002
Width	3	4.9613	1.6538	5.58	0.001
Depth	3	35.0584	11.6861	39.44	0.000
Length	3	76.7177	25.5726	86.32	0.000
Width*Depth	9	18.1335	2.0148	6.80	0.000
Width*Length	9	23.5030	2.6114	8.81	0.000
Depth*Length	9	129.9672	14.4408	48.74	0.000
Width*Depth*Length	27	38.1224	1.4119	4.77	0.000
Error	127	37.6259	0.2963		
Total	191	369.3457			

Note: * is for interaction

The results for the Trimpley WTW are shown in Table 7.5 for Tank C1 and Table C1.4 (Appendix C) for Tank C7. These results are not in as good agreement as those for the tanks at Frankley WTW. The covariates or the discharges from both tanks are not significant. The reason may be due to the low variability of the discharges between different runs during the investigation. Boxplots in Figures 7.5 and 7.6 indicate that the ranges overlap to a large extent between different runs for each tank indicating no significant difference in the discharge between each run.

Table 7.5 - Analysis of Covariance for *Vx* (Tank C1, Trimpley WTW)

Source	DF	ADJ. SS	MS	F	P
Covariates	1	0.0179	0.0179	0.10	0.757
Width	3	12.8033	4.2678	23.04	0.000
Depth	3	129.7680	43.2560	233.49	0.000
Length	3	19.7745	6.5915	35.58	0.000
Width*Depth	9	6.6117	0.7346	3.97	0.000
Width*Length	9	7.3714	0.8190	4.42	0.000
Depth*Length	9	35.1165	3.9018	21.06	0.000
Width*Depth*Length	27	9.9155	0.3672	1.98	0.006
Error	127	23.5281	0.1853		
Total	191	246.8615			

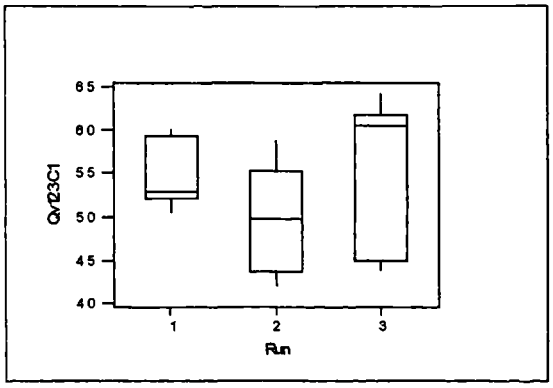

Figure 7.5 - Boxplots for discharge at different runs (Tank C1, Trimpley WTW)

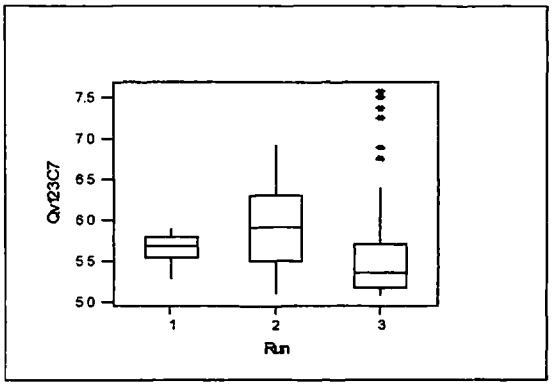

Figure 7.6 - Boxplots for discharge at different runs (Tank C7, Trimpley WTW)

7.2.2 Velocity in the *z* Direction

A similar procedure as in Section 7.2.1 was carried out on the velocity data in the *z* direction to see the effects of the tank physical parameters on *Vz*. The results of the analysis are shown in Tables 7.6 and C1.5 (Appendix C) for the tanks at Frankley WTW and in Tables 7.7 and C1.6 (Appendix C) for the tanks at Trimpley. Table 7.8

is a summary of the results from all the tanks under the investigation. Table 7.8 indicates that the factors depth and length and the interaction between them have a significant effect on *Vz*. Thus it can be concluded that the upward and downward velocity in the tank is affected by the depth and length and the interaction between them.

Table 7.6 - Analysis of variance for velocities in *z* direction (runs 1,2 & 3) using multifactor balanced designs (Tank C2, Frankley WTW)

Source	DF	SS	MS	F	P
Width	3	0.25169	0.08390	1.66	0.178
Depth	3	3.06513	1.02171	20.27	0.000
Length	3	5.10617	1.70206	33.77	0.000
Width*Depth	9	0.78739	0.08749	1.74	0.087
Width*Length	9	0.67401	0.07489	1.49	0.160
Depth*Length	9	1.55491	0.17277	3.43	0.001
Width*Depth*Length	27	2.20649	0.08172	1.62	0.040
Error	128	6.45200	0.05041		
Total	191	20.09779			

Note: * is for interaction

Table 7.7 - Analysis of variance of velocities (*z* direction) for runs 1, 2 and 3 using multifactor balanced designs (Tank C1, Trimpley WTW).

Source	DF	SS	MS	F	P
Width	3	0.07517	0.02506	2.32	0.078
Depth	3	1.93422	0.64474	59.81	0.000
Length	3	2.05779	0.68593	63.63	0.000
Width*Depth	9	0.12704	0.01412	1.31	0.238
Width*Length	9	0.25492	0.02832	2.63	0.008
Depth*Length	9	0.49534	0.05504	5.11	0.000
Width*Depth*Length	27	0.36885	0.01366	1.27	0.191
Error	128	1.37987	0.01078		
Total	191	6.69320			

Note: * is for interaction

Table 7.8 - Summary of results on significant effects of tank physical parameters

Sites	Frankley WTW		Trimpley WTW	
Sources	Tank C2	Tank A3	Tank C1	Tank C7
Width	0	0	0	0
Depth	x	x	x	x
Length	x	x	x	x
Width and depth	0	0	0	0
Width and length	0	0	x	0
Depth and length	x	x	x	x
Width,depth and length	x	0	0	0

Note: Symbol '0' is not significant whereas 'x' is highly significant.

Model adequacy evaluations were made with the same procedures as described in the previous section (Section 7.2.1). Figures 7.7 to 7.10, C1.5, C1.6, C1.7, and C1.8 (Appendix C) indicate that the observed velocity in the z direction can be described according to Equation 5.7 of Chapter 5. Plots of residuals versus fitted values from the ANOVA have constant variance and normal probability plots of residuals indicate the underlying assumption that velocity samples *Vz* were derived from normal distributions is satisfied.

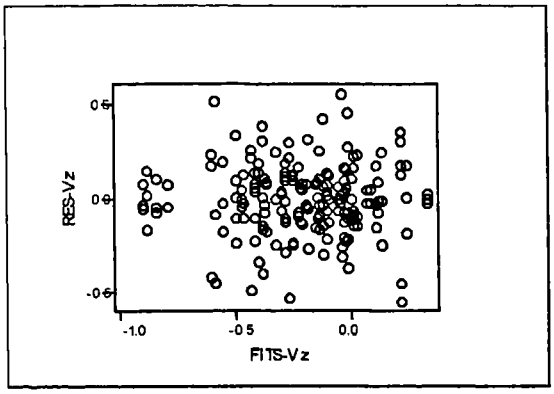

Figure 7.7 - Plot of residuals versus fitted values from the analysis of variance for velocities in *z* direction (Tank C2, Frankley WTW)

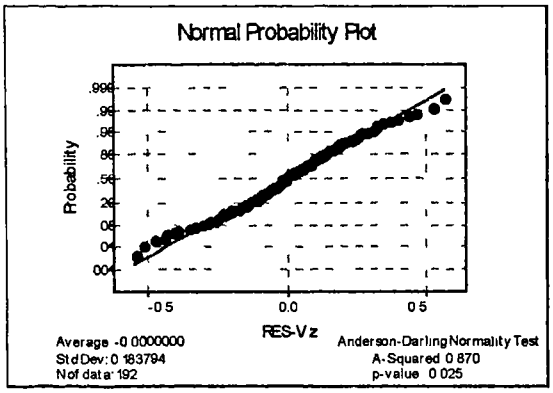

Figure 7.8 - Normal probability plot of residuals from the analysis of variance for velocities in *z* direction (Tank C2, Frankley WTW)

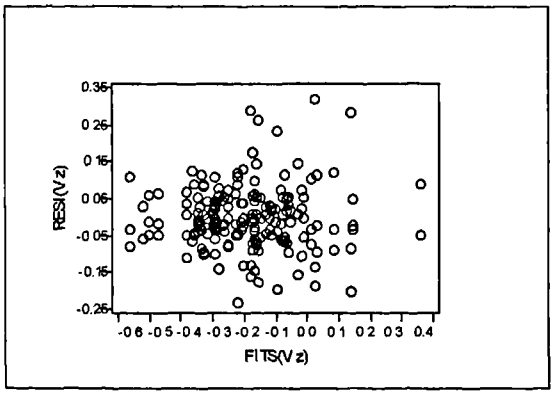

Figure 7.9 - Plot of residuals versus fitted values from the analysis of variance for velocities in *z* direction (Tank C1, Trimpley WTW)

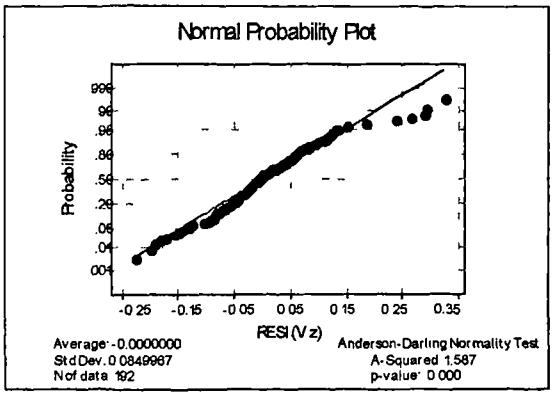

Figure 7.10 - Normal probability plot of residuals from the analysis of variance for velocities in *z* direction (Tank C1, Trimpley WTW)

7.2.2.1 Analysis of Covariance (*Vz*)

A similar statistical technique to that described in Section 7.2.1.1 was used to check whether the discharge from the tank affects the velocity in the *z* direction. The results from Tanks C2 and A3 at Frankley show that the discharge does not affect the velocity distribution in the *z* direction (Table 7.9 and Table C1.7 in Appendix C). The same result was obtained for Tank C1 at the Trimpley WTW (Table 7.10). However the result from Tank C7 (Trimpley WTW) from Table C1.8 in Appendix C is surprisingly different. The discharge appears to affect the velocity in the *z* direction. Table 7.11 indicates that the correlation coefficient between *Vz* and the discharge in Tank C7 was -0.346. This tank also has a less significant correlation coefficient between *Vx* and *Vz* as shown in Table 7.11.

Table 7.9 - Analysis of Covariance for *Vz* (Tank C2, Frankley WTW)

Source	DF	ADJ. SS	MS	F	P
Covariates	1	0.00844	0.00844	0.17	0.684
Width	3	0.24363	0.08121	1.60	0.193
Depth	3	3.06492	1.02164	20.14	0.000
Length	3	5.11448	1.70483	33.60	0.000
Width*Depth	9	0.78683	0.08743	1.72	0.090
Width*Length	9	0.64411	0.07157	1.41	0.190
Depth*Length	9	1.54831	0.17203	3.39	0.001
Width*Depth*Length	27	2.20800	0.08178	1.61	0.042
Error	127	6.44356	0.05074		
Total	191	20.09779			

Table 7.10 - Analysis of Covariance for *Vz* (Tank C1, Trimpley WTW)

Source	DF	ADJ. SS	MS	F	P
Covariates	1	0.00491	0.00491	0.45	0.502
Width	3	0.07971	0.02657	2.45	0.066
Depth	3	1.93198	0.64399	59.48	0.000
Length	3	2.05561	0.68520	63.29	0.000
Width*Depth	9	0.12836	0.01426	1.32	0.234
Width*Length	9	0.25773	0.02864	2.65	0.008
Depth*Length	9	0.49403	0.05489	5.07	0.000
Width*Depth*Length	27	0.36862	0.01365	1.26	0.196
Error	127	1.37495	0.01083		
Total	191	6.69320			

Table 7.11 - Correlation coefficient between *Vx*, *Vz* and the discharge.

Tanks	Correlation coeff. *Vx* and *Vz*	Correlation coeff. Vz and discharge
Tank C2(Frankley)	-0.065	0.034
Tank A3(Frankley)	-0.187	-0.016
Tank C1(Trimpley)	0.235	0.079
Tank C7(Trimpley)	-0.005	-0.346

Note: coeff. is for coefficient

7.3 DEVELOPING SUITABLE MODELS FROM REGRESSION ANALYSIS

In Section 7.2 the effects of tank dimension on velocity distribution in the tank were analysed for each tank site, namely Frankley and Trimpley Water Treatment Works. Since the physical dimensions of the tank have significant effects on the velocity in the tank (as found in Section 7.2), it is important to express their relationship by developing suitable models, which have been discussed in Section 5.3.2.2 of Chapter 5. This Section will focus on the results of data analysis based on the regression model as discussed in Chapter 5.

To get a good estimate of regression analysis, there is a need to look for a strong relationship between the response and predictor variables. Higher values of R^2 as

described in Section 5.3.2.1 of Chapter 5 are an indication of a strong relationship. Several attempts were made to develop suitable regression models for Tanks C2, A3, C1 and C7 from the Frankley and Trimpley WTW. Tests were made using up to 4^{th} order models with interactive response variables. The value of R^2 was used to evaluate the predictive ability of each model. However with higher-order models it becomes difficult to interpret the physical meaning of the interactive response variables. Velocity in the x and z directions are used as the response variables in the models. The order of the predictor variables used in the analysis is shown in Table 7.12.

Table 7.12 - Predictor variables used for regression analysis

Predictors	Order used in regression analysis			
Width, W	W	W^2	W^3	W^4
Depth, D	D	D^2	D^3	D^4
Length, L	L	L^2	L^3	L^4
Interaction	All possible interaction of predictor variables			

Several different approaches are available for determining appropriate combinations of predictive variables. Some of these approaches are summarised below.

1. The actual width, depth and length co-ordinates of each sampling point relative to a datum may be used. This approach is called 'Method 1' in this chapter.

2. The sampling points may be referenced to the datum by a simple numerical ranking system (at different levels) in each dimension based on factorial design theory. There were four different levels of each factor. The point nearest to the reference datum was marked as level 1 and the furthest was marked as level 4. This method may reduce the precision of the estimate due to higher cumulative values when the order of the regression model is increased. This approach is called 'Method 2' in this chapter.

3. Using a transformation of the numerical levels in approach (2) above. For example levels 1, 2, 3 and 4 may be represented by -3, -1, +1 and +3. This approach

eliminates errors in the regression. This approach is called 'Method 3' in this chapter.

Approaches 1 and 3 above are presented in this chapter.

7.3.1 Velocity in the x Direction (Vx)

Filtered velocities in the x-direction from runs 1, 2 and 3 of each tank were used to develop an appropriate model using regression analysis. A combination of 40 predictor variables with their interactions based on Table 7.12 were used in the regression analysis. The results of regression analysis for velocity in the x-direction using 40 combinations of predictor variables are shown in Tables 7.13. It can be seen that Method 3 produced a better value of R^2 (coefficient of determination) than Method 1. The significant variables based on the regression analysis from both methods are not consistent but vary considerably for the same velocity data. However the 'depth' factor seems to be significant in most cases. Results from Method 2 have not been presented because of large cumulative errors as noted earlier (Section 7.3).

The source of velocity data has a considerable influence on the value of R^2 in the regression analysis. Velocity data for each point in the tank which has been averaged over the three runs gives better R^2 than the use of separate velocity data values from runs 1, 2 and 3 regressed together. For example in Table 7.13, Tanks A3 and C2 have an R^2 of 67.3% from Method 1 based on the separate velocity data values from runs 1, 2 and 3. The R^2 value improves to 77.7% using the average data from the three runs. Although this value was better than for Method 1 it was decided not to pursue this approach because the independent variables used were not seen to be helpful in assisting in the tank design process. Method 3 was used to demonstrate that R^2 can be improved by suitable choice of independent variables, which gives confidence in the use and interpretation of the regression analysis. At this stage Method 1 was felt to be appropriate since the tank dimensions had been substituted directly into the model to describe the observations carried out during the investigation.

Table 7.13 - Results from the various techniques and velocity data in the regression analysis of *Vx* using a combination of 40 predictor variables.

Tanks	Methods	Velocity data	R^2	*s*	Variables highly significant
A3 and C2 (Frankley)	1	Runs 1, 2 & 3 for both tanks	67.3%	0.7577	W, D, W^3, D^3, DL^2, LD^2, LD^4, L^2D^2, DQ_v, Indv.
A3 and C2 (Frankley)	3	Runs 1, 2 & 3 for both tanks	68.3%	0.7536	D, W^2, D^2, D^3, DL, DL^2, DQ_v, Indv.
C1 and C7 (Trimpley)	1	Runs 1, 2 & 3 for both tanks	66.2%	0.6872	W, D, W^3, D^3, LD^2, LD^4.
C1 and C7 (Trimpley)	3	Runs 1, 2 & 3 for both tanks	75.3%	0.5917	W, L, W^2, D^2, D^3, L^2, WD, WD^2, WD^3, DW^2, DL, LD^2, LD^3.
A3 and C2 (Frankley)	1	Average from runs 1,2 &3 for both tanks	77.7%	0.6275	W^3, LD^4, Indv.
A3(Frankley)	1	Average from runs 1,2 &3 for the one tank	88.3%	0.4265	W^3, LD^2, LD^3.
C2(Frankley)	1	Average from runs 1,2 &3 for the one tank	83.1%	0.6645	D^3, DL^2, LD^4, L^2D^2, WQ_v.
C1 and C7 (Trimpley)	1	Average from runs 1,2 &3 for both tank	72.7%	0.6434	W^3, L^2, L^3, WD^3, LD^2.
C1(Trimpley)	1	Average from runs 1,2 &3 for the one tank	82.4%	0.5580	LD^4, DQ_v.
C7(Trimpley)	1	Average from runs 1,2 &3 for the one tank	74.5%	0.6992	W^3.

Note: R^2 = coefficient of determination *s* = standard deviation of the errors.
W, D, L, and Qv are the width, depth, length , discharge of the tank respectively
Indv. = indicator variable

Table 7.13 indicates that if each tank is modelled separately (using an average velocity from runs 1, 2 and 3), the values of R^2 seem to be improved compared with modelling together two tanks of the same size. It can be seen that the value of R^2 is 77.7% when Tanks A3 and C2 were used together but when the tanks were analysed separately the values of R^2 improve to 88.3% and 83.1% for Tanks A3 and C2 respectively. The same characteristic also was observed for the tanks at Trimpley WTW.

The regression analysis using 40 predictor variables was carried out to see if a better description of tank performance could be obtained compared with a simpler second-order model as described in Equation 5.18 (Chapter 5). The higher-order model order is difficult to interpret from a design point of view and was discarded in favour of the second-order model which is described below. A regression analysis using an indicator variable was used to model the velocity in the x direction. The results of the analysis for second-order models of Tank A3 and C2 at the Frankley WTW and Tanks C1 and C7 at the Trimpley WTW are shown in Equations 7.1 and 7.2 respectively. The indicator variables (refer to Draper and Smith 1981 or Metcalfe, 1994) are applied for Tanks C2 (Frankley) and C7 (Trimpley).

$$V_x = -82.4+1.28W-11.1D-3.16L+9.85Q_v-0.0771W^2+1.24D^2+0.0489L^2 -0.277Q_v^2+0.060WD-0.0009WL-0.0406WQ_v+0.482DL +0.275DQ_v+0.118LQ_v+0.363VAR \quad (7.1)$$

$$V_x = -19.1-3.05W-8.30D+1.09L-5.20Q_v+0.0984W^2+4.26D^2-0.0398L^2 +0.490Q_v^2-0.100WD+0.0058WL+0.456WQ_v+0.395DL -0.402DQ_v-0.191LQ_v-0.065VAR \quad (7.2)$$

where W, D, L and Q_v are the width, depth, length in metres for each point and flow rate in million litres per day of the dissolved air flotation tank respectively. VAR is the indicator variable where its coefficient is used to describe the velocity in the appropriate tank (only applicable for Tank C2 or C7). The value of R^2 for Equations 7.1 and 7.2 are 69.5% and 67.2% respectively and the corresponding standard

deviations of the errors are 0.6964 and 0.6665. The details of the results of Equations 7.1 and 7.2 are tabulated in Tables 7.14 and 7.15 respectively.

Comparison of velocities at individual points relative to the regression line identified certain points with large differences between the observed and predicted values (standard residuals). The points with large standard residuals are as follows:

1. At Frankley points C3d4 and D1d4 from Tank A3 and points B1d4, B4d4, C1d4 and D2d4 from Tank C2
2. At Trimpley points C1d3, D1d3, D2d3 and D2d4 from Tank C1 and points C2d3, D1d3, D1d4, D2d3 and D4d4 from Tank C7.

At Frankley all these points are at depth d4 which is in the observed high horizontal velocity zone of the tank. At Trimpley the majority of high standard residuals occurred at d3, with some at d4. This may be due to the smaller depth of Trimpley tanks which create a relatively larger zone of higher velocities in the upper layer of the tank.

Table 7.14 and 7.15 summarise the regression analyses which show the effects of each predictor variable based on the Student t-test. The interpretation of the low t-ratio for the flow (Tables 7.14 and 7.15) is that the coefficients are not determined with much precision. Earlier tests using analysis of covariance (Table 7.4) indicated that the flow or discharge was highly significant. The covariate model has a t-value of 3.127 with a coefficient of 0.08027 (standard deviation 0.0257) and the regression model has t-value of 1.23 with a coefficient of 9.854 (standard deviation 7.983). This is not contradictory. The covariate model involves many terms, high-order interactions and levels are treated independently as an individual category rather than on a continuous scale. The problems with the full covariate model are difficult to interpret physically and more importantly it does not appear to generalise compared to the second-order model (regression analysis).

Table 7.14 - Summary of results from regression analysis based on Equation 7.1 for the Frankley WTW

Predictor	Coefficient	Std. deviation	t-ratio	p
Constant	-82.35	77.94	-1.06	0.293
Width(m)	1.283	1.594	0.81	0.422
Depth(m)	-11.051	3.712	-2.98	0.004
Length(m)	-3.162	1.192	-2.65	0.009
Flow Qv(mld)	9.854	7.983	1.23	0.220
$Width^2$	-0.07709	0.02343	-3.29	0.001
$Depth^2$	1.2350	0.2269	5.44	0.000
$Length^2$	0.04890	0.01777	2.75	0.007
Q_v^2	-0.2770	0.2056	-1.35	0.181
Width*depth	0.06003	0.05147	1.17	0.246
Width*length	-0.00091	0.01418	-0.06	0.949
Width*Qv	-0.04061	0.07838	-0.52	0.605
Depth*length	0.48237	0.04796	10.06	0.000
Depth*Qv	0.2751	0.1891	1.45	0.149
Length*Qv	0.11835	0.06041	1.96	0.053
Indicator variable	0.3625	0.1507	2.40	0.018

Note: * is the interaction term std. = standard t = t-test
p = level of significance

Table 7.15 - Summary of results from regression analysis based on Equation 7.2 for the Trimpley WTW

Predictor	Coefficient	Std. deviation	t-ratio	p
Constant	19.15	14.59	1.31	0.192
Width(m)	-3.054	1.407	-2.17	0.032
Depth(m)	-8.301	2.374	-3.50	0.001
Length(m)	1.0873	0.7386	1.47	0.144
Flow Qv(mld)	-5.198	5.119	-1.02	0.312
$Width^2$	0.09844	0.04703	2.09	0.039
$Depth^2$	4.2572	0.3456	12.32	0.000
$Length^2$	-0.03981	0.02640	-1.51	0.134
Q_v^2	0.4898	0.4738	1.03	0.303
Width*depth	-0.0996	0.1034	-0.96	0.337
Width*length	0.00583	0.03074	0.19	0.850
Width*Qv	0.4562	0.2323	1.96	0.052
Depth*length	0.39547	0.07520	5.26	0.000
Depth*Qv	-0.4015	0.3954	-1.02	0.312
Length*Qv	-0.1908	0.1250	-1.53	0.130
Indicator variable	-0.0645	0.1679	-0.38	0.702

Note: * is the interaction term std. = standard t = t-test
p = level of significance

Model adequacy checking (Figures 7.11, 7.12, 7.13 and 7.14) for Equations 7.1 and 7.2 indicates that the sample population for velocity in both cases are of constant variances and from normal distribution. Thus the modelling approach for each equation is valid. This confirms that the assumptions underlying the residuals are correct.

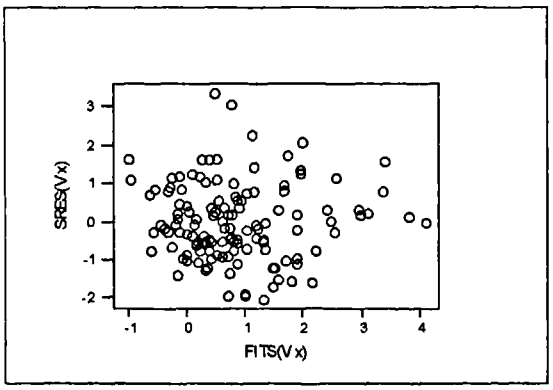

Figure 7.11 - Plot of standard residual versus fitted values from regression analysis of *Vx* (Tanks A3 and C2)

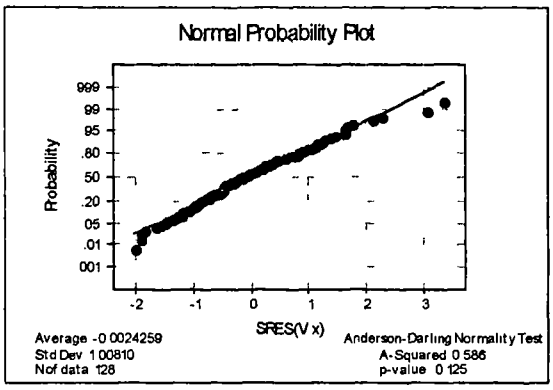

Figure 7.12 - Normal probability plot of standard residuals from regression analysis of *Vx* (Tanks A3 and C2)

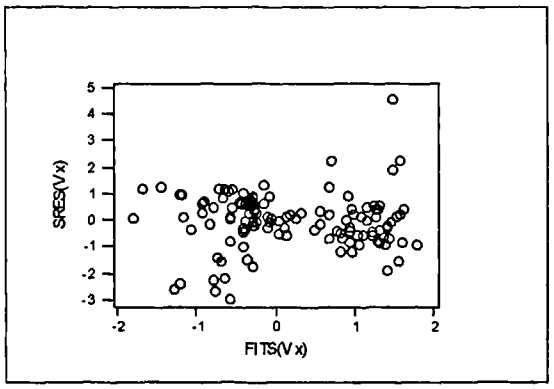

Figure 7.13 - Plot of standard residual versus fitted values from regression analysis of Vx(Tanks C1 and C7)

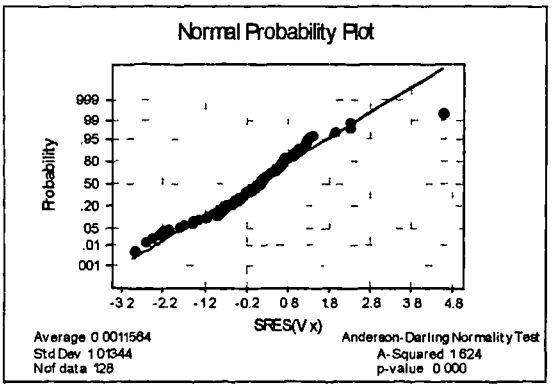

Figure 7.14 - Normal probability plot of standard residuals from regression analysis of Vx(Tanks C1 and C7)

7.3.2 Velocity in the z Direction(Vz)

Similar procedures to analyse the velocity in the x direction as described in Section 7.3.1 are used in the regression analysis of the response variable in the z direction. The summary of the results of regression analysis of Vz are shown in Table 7.16. Again Method 3 produces a better value of R^2 than Method 1 for velocity data from runs 1, 2 and 3. If these data are averaged so that only one set of data is used in the regression analysis, the values of R^2 are considerably increased. These results are in agreement with the previous analysis on the velocity in the x direction. If however comparisons of R^2 are made between the tanks at the same site on whether Vx and Vz have the same trend (i.e. R^2 at Tank A3 or C1 is always higher than at Tank C2 or C7), the results are not in agreement. This indicates that a good relationship of Vx with the predictor variables in a particular tank is not necessarily true for Vz. The significant variables obtained from the regression analysis of Vz are also found not to be in agreement with the significant variables from the analysis of Vx. The differences of significant variables either from the regression of Vx or Vz (in Table 7.13 or 7.16) may be due to the standard deviations of errors within a tank being less than the standard deviations of errors between tanks. So the assumptions that the errors (ε_i) have a common variance may not be satisfied. In practical terms the runs within tanks are less informative than runs using different tanks. Also as for the Vz, the 4^{th} order analysis will tend to lead to too many statistically significant variables, which are physically difficult to interpret.

Table 7.16 - Results from the various techniques and velocity data in the regression analysis of *Vz* using a combination of 40 predictor variables.

Tanks	Methods	Velocity data	R^2	*s*	Significant variables
A3 and C2 (Frankley)	1	Runs 1, 2 & 3 for both tanks	51.3%	0.2508	Constant, W^3, D^3, L^3, DL^4, LD^2.
A3 and C2 (Frankley)	3	Runs 1, 2 & 3 for both tanks	53.5%	0.2477	Constant, W^2, D^2, L^2, L^3, DL^2, DL^3, D^2L^2, Q_v, Q_v^2.
C1 and C7 (Trimpley)	1	Runs 1, 2 & 3 for both tanks	69.1%	0.1113	DL, DL^2, LD^2, D^2L^2, Q_v, Q_v^2, Indv.
C1 and C7 (Trimpley)	3	Runs 1, 2 & 3 for both tanks	69.5%	0.1113	Constant, W, D^2, L^2, DL^2, LD^2, D^2L^2.
A3 and C2 (Frankley)	1	Average from runs 1,2 &3 for both tanks	75.1%	0.1645	W, W^3, L^2, L^3, DL^4, LQ_v.
A3(Frankley)	1	Average from runs 1,2 &3 for the one tank	83.6%	0.1585	W, W^3.
C2(Frankley)	1	Average from runs 1,2 &3 for the one tank	75.6%	0.1625	D, D^3, L^3, DW^2, DW^3, DL^2, DL^4, LD^2.
C1 and C7 (Trimpley)	1	Average from runs 1,2 &3 for both tank	84.2%	0.07808	Constant, DL, DL^2, LD^2, D^2L^2, Q_v, Q_v^2.
C1(Trimpley)	1	Average from runs 1,2 &3 for the one tank	88.5%	0.06970	DL, DL^2, LD^2, D^2L^2, Q_v.
C7(Trimpley)	1	Average from runs 1,2 &3 for the one tank	89.6%	0.07321	Constant, D^3, L^3, DL, DL^2, LD^2, D^2L^2.

Note: R^2=coefficient of determination *s*=standard deviation of the errors.
W, D, L, and Qv are the width, depth, length and discharge of the tank respectively
Indv.=indicator variable

In order to simplify the model for the velocity in the *z*-direction, a similar technique to that described in Section 7.3.1 was used. The results of the second-order regression

analysis of *Vz* are shown in Equations (7.3) and (7.4) for the dissolved air flotation tanks at Frankley(Tanks A3 and C2) and Trimpley(Tanks C1 and C7) respectively. The regression analysis of both tank sites(Frankley and Trimpley WTW) indicate that the same predictor variables namely width, depth, length, discharge and the interaction of the discharge with the dimension of the tanks are highly correlated with other predictor variables.

$$V_z=-29.5+0.751W-3.19D-0.722L+3.27Q_v-0.0208W^2+0.465D^2-0.0197L^2 -0.0888Q_v^2+0.0185WD+0.00342WL-0.0332WQ_v+0.0155DL +0.0940DQ_v+0.0419LQ_v-0.0066VAR \quad (7.3)$$

$$V_z=-0.52-0.455W-0.579D+0.024L+0.6Q_v+0.00575W^2+0.384D^2-0.00873L^2 -0.0787Q_v^2-0.0068WD+0.00322WL+0.0719WQ_v-0.0271DL -0.0370DQ_v+0.0006LQ_v-0.0152VAR \quad (7.4)$$

where *W*, *D*, *L* and Q_v are the width, depth, length in metres at each point in the tank and flow rate in million litres per day of the dissolved air flotation tank respectively. *VAR* is the indicator variable where its coefficient is used to describe the velocity *Vz* in the appropriate tank (applicable for Tank C2 or C7).

The value of R^2 from Equation 7.3 for the tanks at Frankley is 66% with the standard deviation of the errors 0.1826. For the tanks at Trimpley the value of R^2 from Equation 7.4 is 74.9% and the standard error of the estimate is 0.09315. The results for *Vz* indicate that the velocity data collected at the Trimpley WTW produce better results than at the Frankley WTW. The low value of the standard deviation of the errors at Trimpley is mainly due to a lower range of *Vz* encountered at the Trimpley WTW. The models for Equations 7.3 and 7.4 are only valid for the dissolved air flotation tanks, which have the same size and flow rates as at the Frankley and Trimpley WTW respectively.

Tables 7.17 and 7.18 are the summary of the results of the regression analysis which correspond to Equations 7.3 and 7.4. Inspection of Table 7.17 indicates that at Frankley the width , depth and length are fairly significant. Table 7.18 (for Trimpley)

shows width and depth are fairly significant. The expected variables affecting *Vz* are width and length rather than width and depth (surface loading theory Section 2.4.2.6 in Chapter 2). The reason for the difference may be due to the sampling at Trimpley not giving the same quality of data as Frankley (Section 6.2 in Chapter 6). Thus the 'noise' in the experimental data has masked the relationship between length and velocity to such an extent that it cannot be confirmed statistically.

It is fairly reasonable to say that Equation 7.3 has some form of relationship with Equation 2.48 of Section 2.4.2.5 in Chapter 2 where the vertical rise rate of the suspended solids depends on the influent flow rate and the surface area of the flotation chamber. Equation 7.3 demonstrates that there is some evidence that the surface area (i.e. width x length) and the discharge are fairly significant. The significance of the indicator variable is fairly low which means there is no difference in *Vz* between Tanks A3 and C2. Thus Equation 7.3 can be used to predict *Vz* for the tanks at the Frankley WTW but cannot be used for other sizes of tank.

Table 7.17 - Summary of the results from regression analysis based on Equation 7.3 for the Frankley WTW

Predictor	Coefficient	Std. deviation	t-ratio	p
Constant	-29.52	20.44	-1.44	0.151
Width(m)	0.7506	0.4180	1.80	0.075
Depth(m)	-3.1880	0.9731	-3.28	0.001
Length(m)	-0.7222	0.3124	-2.31	0.023
Flow Qv(mld)	3.268	2.093	1.56	0.121
$Width^2$	-0.020822	0.006143	-3.39	0.001
$Depth^2$	0.46468	0.05950	7.81	0.000
$Length^2$	-0.019745	0.004659	-4.24	0.000
Q_v^2	-0.08875	0.05390	-1.65	0.102
Width*depth	0.01853	0.01350	1.37	0.173
Width*length	0.003417	0.003719	0.92	0.360
Width*Qv	-0.03318	0.02055	-1.61	0.109
Depth*length	0.01553	0.01258	1.23	0.219
Depth*Qv	0.09403	0.04959	1.90	0.061
Length*Qv	0.04194	0.01584	2.65	0.009
Indicator variable	-0.00660	0.03952	-0.17	0.868

Note: * is the interaction term std.=standard t = t-test
p=level of significance

The results from Table 7.18 indicate that the effects of width and depth of the tank on *Vz* are fairly significant for a simple model of Equation 7.4. The length seems to be not significant. However by using more predictor variables, the results of regression analysis based on Table 7.16 indicate that the length is highly significant. Thus it is reasonable to say that Equation 7.4 can be used to describe the tanks at the Trimpley WTW and can be generalised for other tanks of the same size, since the indicator variable does not show any significant difference between the Tanks C1 and C7.

Model adequacy checking for Equation 7.3 and 7.4 are shown in Figures 7.15 to 7.18. The results from these figures indicate that the validation of the models is satisfactory.

Table 7.18 - Summary of the results from regression analysis based on Equation 7.4 for the Trimpley WTW

Predictor	Coefficient	Std. deviation	t-ratio	p
Constant	-0.520	2.039	-0.25	0.799
Width(m)	-0.4549	0.1967	-2.31	0.023
Depth(m)	-0.5793	0.3318	-1.75	0.084
Length(m)	0.0240	0.1032	0.23	0.816
Flow Qv(mld)	0.5996	0.7154	0.84	0.404
$Width^2$	0.005750	0.006572	0.87	0.384
$Depth^2$	0.38356	0.04830	7.94	0.000
$Length^2$	-0.008728	0.003690	-2.37	0.020
Q_v^2	-0.07870	0.06621	-1.19	0.237
Width*depth	-0.00675	0.01445	-0.47	0.641
Width*length	0.003218	0.004296	0.75	0.455
Width*Qv	0.07193	0.03246	2.22	0.029
Depth*length	-0.02712	0.01051	-2.58	0.011
Depth*Qv	-0.03697	0.05526	-0.67	0.505
Length*Qv	0.00058	0.01746	0.03	0.973
Indicator variable	-0.01515	0.02347	-0.65	0.520

Note: * is the interaction term std.=standard t = t-test
p=level of significance

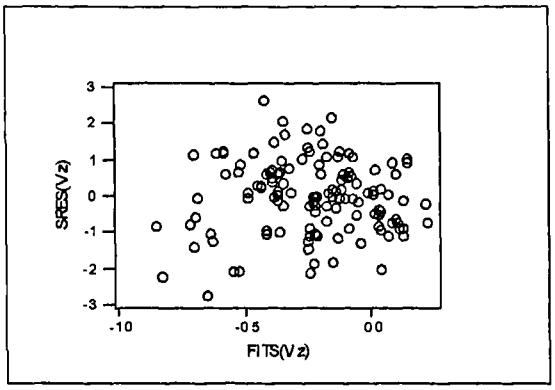

Figure 7.15 - Plot of standard residual versus fitted values from regression analysis of *Vz* (Tanks A3 and C2)

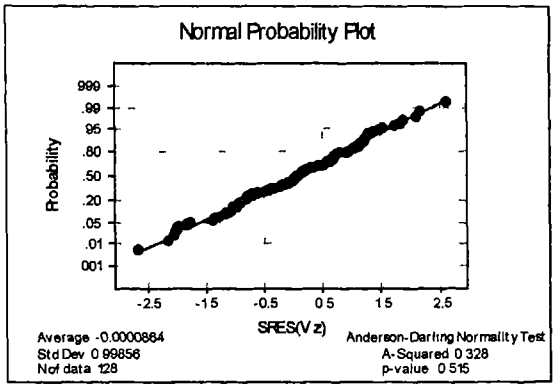

Figure 7.16 - Normal probability plot of standard residuals from regression analysis of *Vz* (Tanks A3 and C2)

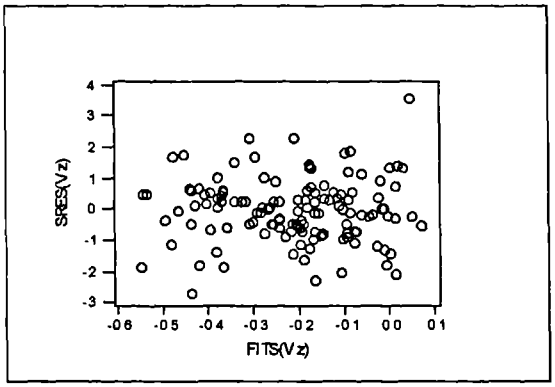

Figure 7.17 - Plot of standard residual versus fitted values from regression analysis of *Vz* (Tanks C1 and C7)

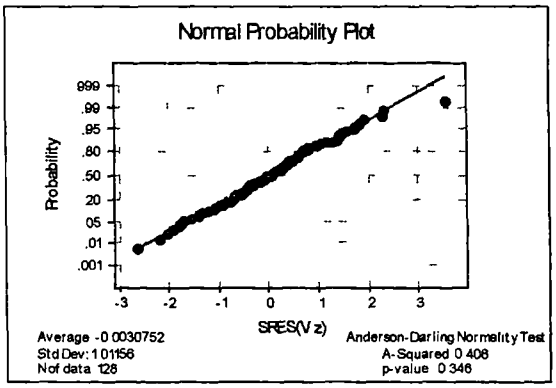

Figure 7.18 - Normal probability plot of standard residuals from regression analysis of *Vz* (Tanks C1 and C7)

7.3.3 Random Effects Model

In the previous sections (i.e. Sections 7.3.1 and 7.3.2) the development of the physical models from the full-plant studies of the dissolved air flotation tanks were mainly concentrated on the fixed effects models. This means the model can only be applied on the same tank size with the same operating conditions, assuming the liquid in the tank has the same temperature, bubble size and baffle configuration. However by having two sites of rectangular tanks of different sizes and baffle configurations, it is possible to make a prediction of the velocity based on a suitable model if the following criteria are fulfilled:

1. Randomisation procedures as described in Chapter 5 are done.
2. Data collected are normally and independently distributed with constant variance.

3. Data collected from different sizes of tanks.
4. There is no external condition which gives significant impact on the performance of the tanks for example extreme differences in operating temperatures or different types of fluid. Any predictor variables which may have a large significant effect on the velocity may influence the suitability of the model.

For the velocity in the x direction, Table 7.19 indicates that variability exists between the tanks. The variance of any observation of velocity in the x direction calculated from Table 7.19 is equal to 3.40. This test concluded that there is a great variation of Vx between the four tanks at Frankley and Trimpley WTW. In the case of Vz, Table 7.20 indicates that there is no evidence to suggest any significant variation of velocity in the z direction between the tanks at Frankley and Trimpley WTW.

Table 7.19 - Analysis of variance for Vx

Source	DF	SS	MS	F	p
Tanks	3	29.23	9.74	7.53	0.000
Error	252	326.08	1.29		
Total	255	355.32			

Table 7.20 - Analysis of variance for Vz

Source	DF	SS	MS	F	p
Tanks	3	0.0996	0.0332	0.57	0.638
Error	252	14.8006	0.0587		
Total	255	14.9002			

In order to develop a model which could describe all the tanks within the range of sizes and flow rates as those found at the Frankley and Trimpley WTW, regression analysis was carried out for the velocity in the x and z directions. The results are shown in Equations 7.5 and 7.6 for Vx and Vz respectively.

$$V_x = -1.04 + 0.043W - 6.14D - 0.48L + 0.442Q_v - 0.0413W^2 + 2.07D^2 + 0.0257L^2 - 0.00532Q_v^2 + 0.019WD + 0.0015WL + 0.0132WQ_v + 0.456DL - 0.0799DQ_v - 0.00792LQ_v + 2.78VAR \quad (7.5)$$

$$V_z = -0.842 + 0.0088W - 1.01D + 0.0476L - 0.0891Q_v - 0.00952W^2 + 0.437D^2 - 0.016L^2 + 0.00357Q_v^2 + 0.0099WD + 0.00099WL + 0.00271WQ_v + 0.00476DL - 0.0102DQ_v + 0.00116LQ_v - 0.055VAR \quad (7.6)$$

where W, D, L and Q_v are the width, depth, length in metres at each point in the tank and flow rate in million litres per day respectively of the dissolved air flotation tank. VAR is the indicator variable where its coefficient is used to describe the velocity at the Trimpley WTW. The R^2 for Equations 7.5 and 7.6 are 58.5% and 63.4% with the corresponding standard deviations of the errors of 0.7841 and 0.1508 respectively.

Tables 7.21 and 7.22 are the detailed results from the regression analysis of velocity in the x and z directions respectively. In Table 7.21 the first-order predictor variables which are highly significant are the depth, length, the interaction of depth and length and the interactions between the discharge with the width and with the depth of the tank. This result subsequently indicates that for the velocity in the x direction there is a need for caution when designing these factors. If the tank were too long and too deep or too short and too shallow then it would affect the velocity distribution and hence the performance of the dissolved air flotation tank. The interactions between the output flow rate (discharge) of the tank with the width, depth and length are fairly significant (Table 7.21). Thus in mathematical terms the products (i.e. multiplication) between each tank dimension and the discharge would have a significant effect on Vx in Equation 7.5. The second-order predictor variables are difficult to interpret but are important factors in the development of a suitable model.

Table 7.21 - Summary of the results from regression analysis based on Equation 7.5 for velocity in the x direction.

Predictor	Coefficient	Std. deviation	t-ratio	p
Constant	-1.043	2.992	-0.35	0.728
Width(m)	0.0433	0.1340	0.32	0.747
Depth(m)	-6.1363	0.4920	-12.47	0.000
Length(m)	-0.4805	0.1385	-3.47	0.001
Flow Qv(mld)	0.4415	0.2953	1.50	0.136
$Width^2$	-0.04132	0.01840	-2.25	0.026
$Depth^2$	2.0663	0.2159	9.57	0.000
$Length^2$	0.02572	0.01619	1.59	0.113
Q_v^2	-0.005316	0.008639	-0.62	0.539
Width*depth	0.01903	0.05045	0.38	0.706
Width*length	0.00154	0.01362	0.11	0.910
Width*Qv	0.013248	0.005529	2.40	0.017
Depth*length	0.45638	0.04575	9.98	0.000
Depth*Qv	-0.07988	0.01738	-4.60	0.000
Length*Qv	-0.007916	0.004637	-1.71	0.089
Indicator variable	2.779	1.675	1.66	0.098

Note: * is the interaction term std.=standard t = t-test
p=level of significance

For the velocity in the z-direction, Table 7.22 indicates that the first-order predictor variables of the depth and the interaction between the discharge with the width and the discharge with the depth of the tank are highly significant. The interpretation of the results implies that the depth of the tank greatly affects the velocity in the vertical direction (Vz) of the dissolved air flotation tank. The ADV probe was able to operate with the presence of small particles or air bubbles in the body of the liquid (Section 4.2.2 Chapter 4). If the assumption is made that the probe is also measuring the movement of the small particles in the liquid then Vz is related to the movement of the particles in the dissolved air flotation tank. This may suggest that Equation 7.6 is also describing the movement of the particles in the vertical direction. If this hypothesis is true, it implies that if the tank were too shallow or too deep, the removal of particles would be affected (since the depth is significant in Equation 7.6).

Table 7.22 - Summary of the results from regression analysis based on Equation 7.6 for velocity in the *z* direction.

Predictor	Coefficient	Std. deviation	t-ratio	p
Constant	0.8417	0.5754	1.46	0.145
Width(m)	0.00181	0.02578	0.07	0.944
Depth(m)	-1.01246	0.09463	-10.70	0.000
Length(m)	0.04760	0.02664	1.79	0.075
Flow Qv(mld)	-0.08913	0.05680	-1.57	0.118
$Width^2$	-0.009519	0.003540	-2.69	0.008
$Depth^2$	0.43683	0.04153	10.52	0.000
$Length^2$	-0.015976	0.003114	-5.13	0.000
Q_v^2	0.003574	0.001662	2.15	0.032
Width*depth	0.009904	0.009704	1.02	0.308
Width*length	0.000994	0.002620	0.38	0.705
Width*Qv	0.002711	0.001064	2.55	0.011
Depth*length	0.004756	0.008799	0.54	0.589
Depth*Qv	-0.010181	0.003342	-3.05	0.003
Length*Qv	0.0011552	0.0008919	1.30	0.197
Indicator variable	-0.0550	0.3222	-0.17	0.865

Note: * is the interaction term std.=standard t = t-test
p=level of significance

By assuming the tanks at both sites (Frankley and Trimpley) working satisfactorily, Equations 7.5 and 7.6 may be applicable to the DAF tanks which have an output flow rate of 4.64 to 10.22 million litres per day. For design purposes the mean velocity of *Vz* should be between -0.20 and -0.25cm/sec and the mean velocity of *Vx* should be between 0.1 and 0.9cm/sec. The mean velocities for *Vz* and *Vx* were obtained based on the mean velocities found at Frankley and Trimpley WTW. The limitation on the mean velocities have to be used as a guideline because a departure from these figures may effect the flow in the DAF tank. If the flow were affected there would be a possibility that the turbidity removal may be affected.

For design purposes, the application of Equations 7.5 and 7.6 involves the following procedures:

1. Identify the proposed dimensions of the tank and the flow rate.

2. Divide the tank into a grid system that has 64 point as shown in Figures 4.3 and 4.4 (Chapter 4).

3. Calculate the values of Vx and Vz at each of the 64 points in the tank using Equations 7.5 and 7.6. The calculation can be carried out by inserting the values of the width, depth and length at each point in the tank for each value of Vx or Vz . A constant value of flow rate can be used for each point.

4. Calculate the average velocity means of Vx and Vy based on the 64 points in the tank and compare with the recommended velocities range proposed (as mentioned earlier) in this chapter.

The problem with Equations 7.5 and 7.6 is the low values of R^2 (58.5% for Equation 7.5 and 63.4% for Equation 7.6). This suggests that the unexplained variations for Equation 7.5 and 7.6 are 41.5% and 36.6% respectively. Large percentages of unexplained variations indicate that both equations are not accurate but fairly empirical. The values of R^2 can be improved by increasing the number of predictor variables as discussed and described in Sections 7.3.1 and 7.3.2. However this procedure lends itself to a complicated model rather than simple models to describe the velocity observation in the tank. In order to refine or improve the model so that R^2 will be more than 90% the following methods for data collection may be recommended:

1. Using a constant flow rate at each point in the tank throughout the experiment. Ideally at least two runs are required for each constant flow rate. Three values of constant flow rate (namely at maximum, minimum and average flow rates) may be required so that the model to be developed can be applied for a wider range of flow rate.

2. Using 64 ADV probes to monitor the velocity at each point in the tank. In this case the flow can be subjected to variation. The problem of using this method is

the cost of the probes. It is too expensive to have 64 probes for the investigation since each probe is approximately at £14,000.

3. Increasing the levels of the tank physical dimensions (width, depth and length) from the existing one (at 4 levels) to 5 or more. For a tank dimension at 5 level each, the total number of points to be investigated will be 125. By having more points in the tank, the velocity profile in each component (*Vx*, *Vy* and *Vz*) can be described more explicitly and will improve on the precision of the estimate (regression analysis).

Method 1 above has been proposed but was not accepted by the Severn Trent Water due to operational problems and the reasoning that in reality the flow in the DAF tank is not constant, and hence modelling of fictitious conditions may not be an appropriate undertaking.

Although Equations 7.5 and 7.6 are not perfectly precise, it has been shown that a standard statistical approach is possible to analyse and model the flow problems in a DAF tank. The unexplained variations in the regression analysis may be due to several other factors which may not be taken into account during data collection. These factors may be the concentrations of particles and bubbles in the water, the water temperature and 'noise' from the desludging of other tank during data collection. The latter may be apparent because the acoustic signal may be slightly disturbed due to some noise generated during the desludging process in the neighbouring tanks.

Normal procedures for model adequacy checking were made for Equations 7.5 and 7.6 and the results from Figures 7.19 to 7.22 indicate that the assumptions on constant variance and normality of the velocity samples were satisfied.

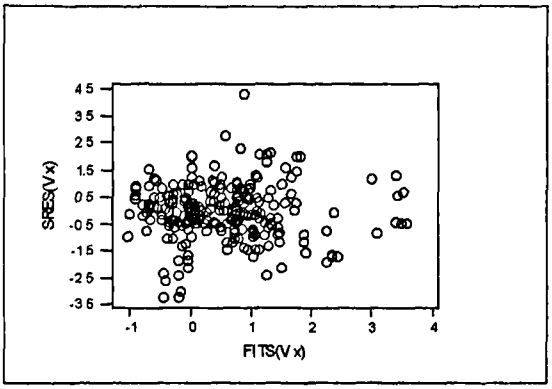

Figure 7.19 - Plot of standard residual versus fitted values from regression analysis of *Vx* (Tanks at Frankley and Trimpley WTW)

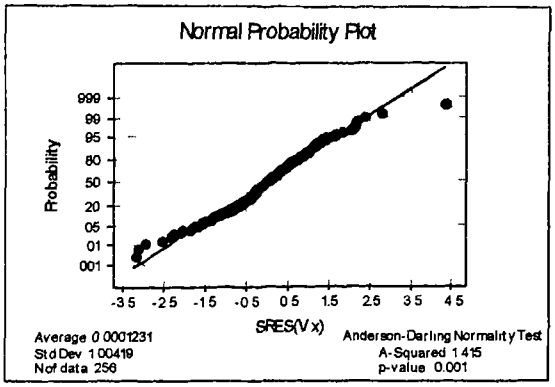

Figure 7.20 - Normal probability plot of standard residuals from regression analysis of *Vx* (Tanks at Frankley and Trimpley WTW)

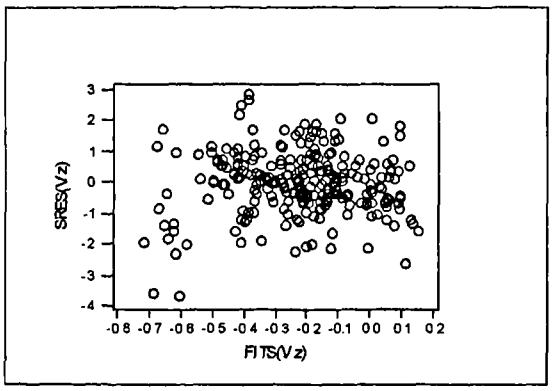

Figure 7.21 - Plot of standard residual versus fitted values from regression analysis of *Vz* (Tanks at Frankley and Trimpley WTW)

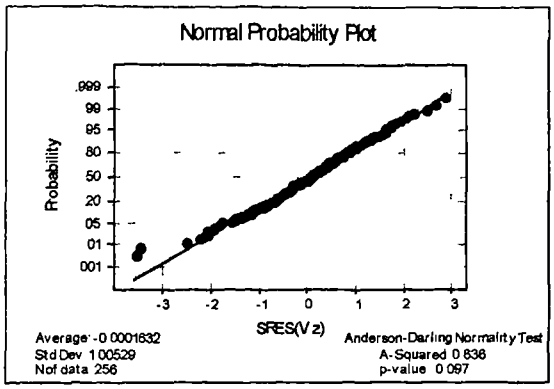

Figure 7.22 - Normal probability plot of standard residuals from regression analysis of *Vz* (Tanks at Frankley and Trimpley WTW)

7.4 SUMMARY OF RESULTS AND FINDINGS

1. Analysis of variance for *Vx* indicates that the tank physical dimensions (width, depth and length) and the interactions between them are highly significant. These terms may affect the velocity distribution in the tank. However the only exception is Tank A3 at Frankley where the interaction between the width and the depth is not significant. Analysis of variance for *Vz* indicates that the depth and length of all the tanks are highly significant. The results suggest that the tank physical dimensions are affecting the velocity in the *x*-direction and are important criteria for design purposes.

2. Analysis of covariance indicates that the flow rate of the dissolved air flotation tanks at Frankley has a significant effect on the velocity in the x-direction but not in the z-direction. The discharge is not significant for both velocity components at the Trimpley WTW except for Vz in Tank C7. The results indicate that the significance of the flow rate depends on its variability. Low variation in the flow rate does not affect the velocity distribution in the tank.

3. Fixed effects models for the tanks at the Frankley and Trimpley WTW from the regression analysis are shown in Equations 7.1 to 7.4. These models are only applicable to the same tank configuration and flow conditions as found at Frankley and Trimpley.

4. Generalised and more flexible models which can be applied within the ranges of tank sizes and the flow rate found at both sites (Frankley and Trimpley WTW) are as presented in Equations 7.5 and 7.6. The R^2 for Equations 7.5 and 7.6 are 58.5% and 63.4% with the corresponding standard deviations of the errors of 0.7841 and 0.1508 respectively. This suggests that the unexplained variations for Equations 7.5 and 7.6 are 41.5% and 36.6% respectively. Higher values of unexplained variation are associated with the models because these models have been simplified. Earlier models using ANOVA and ANCOVA, which used higher order interactions and independent predictor variables, indicate that the physical dimensions of the tank and the interaction between them are highly significant (Tables 7.6 to 7.10). The problem with higher-order interactions between the predictor variables is the difficulty in interpreting them. A simple model is more plausible and appropriate for design purposes than a complicated model. Equations 7.5 and 7.6 may be used to design the appropriate dimensions of a DAF tank. Caution has to be taken if these models are to be applied outside the range of sizes and flow rates mentioned in this thesis. It is also important to check that the overall velocity means in the x and z directions are within the specified ranges as described in Section 7.3.3, when these models are adopted.

5. Although Equations 7.5 and 7.6 are not exactly precise in describing the velocity distribution in the dissolved air flotation tank, the standard statistical techniques used for data analyses are found to be useful for comparing the velocity data from the dissolved air flotation tanks. Statistical techniques are also an important tool in developing an appropriate model to describe the velocities observed in a DAF tank. The present work with the CFD model found in the literature is limited to modelling uniform inflow into the dissolved air flotation tank, as described and discussed in Section 6.7 (Chapter 6).

CHAPTER 8

TURBIDITY DISTRIBUTION IN DISSOLVED AIR FLOTATION TANKS

8.1 INTRODUCTION

In Chapter 6 velocity data from 64 points in the tank were analysed and compared using statistical techniques to determine the quality and the characteristics of the velocity data. Statistical tests were made to find out whether different runs, tanks and sites contribute to any significant variation in the velocity distribution in the tanks.

In Chapter 7 the effects of tank dimensions and the discharge on the velocity distribution in the tanks were analysed using balanced designed ANOVA (analysis of variance) and ANCOVA (analysis of covariate). Since the above factors are significant, models have been developed to describe the velocity distribution in the tanks. The models may be appropriate if they were related and applicable to the turbidity removal in the tank. Thus it is necessary to find out the characteristics of the turbidity distribution in the tank within the investigated flow regime.

This chapter is concerned with the presentation of the results of data analysis on the turbidity distribution at the Frankley and Trimpley Water Treatment Works. The points in the tanks where the turbidity data were collected are at the same points where the velocity were observed. The position of these points have been described in Chapter 4. The effects of discharge (the output flow rate) on the turbidity variation in the tank were analysed so that the characteristics of the turbidity at various points in the tank can be understood. Turbidity removals at different depths and lengths in the dissolved air flotation tanks were also analysed and compared. The objective of the analysis is to find out whether the tank dimension has any significant effect on the turbidity removal in the tank.

8.2 COMPARING TURBIDITY DATA

There were sixty-four points (refer to Figures 4.4 and 4.5 in Chapter 4 for the positions of the 64 points) in each tank where the samplings of turbidity were taken. Three runs were carried out in each tank. A total of four tanks were investigated, two at Frankley and two at the Trimpley Water Treatment Works (WTW). For each run of the experiment in each tank, one sample of turbidity at each point was taken. Hence the number of samples collected at each point was different from the velocity measurements as discussed and presented in Chapters 6 and 7. The main reason that the procedure similar to velocity sampling was not carried out is due to the unavailability of the equipment to monitor the turbidity readings in-situ within a resolution of ±0.1 NTU. The only option is to collect more than one turbidity sample from each point during each run. This is a perfect option but not appropriate to be applied on site due to the following reasons:

1. During the collection of the first sample, there was a disturbance in the area within the point where the sample was collected. Since the flow within each point was laminar and the Reynolds number was normally less than one as described in Chapter 2 (Section 2.4.2.1), it will take sometime for the same point to recover from the disturbance. There is also uncertainty about the size of the area under the disturbance and the duration it takes to recover. If a retention time of 20 minutes were used as an approximate basis for the recovery period then it will take 200 minutes to have 10 turbidity samples from one point in the tank.

2. It was not always possible to collect a turbidity sample in one operation. Sometimes the sludge was trapped in the sampling bottle and the sample had to be discarded. To collect the replacement sample, it would need at least an interval of 15 minutes so that the area around the sampling point in the tank stabilised.

Since only one turbidity sample was collected at each point, the sample cannot be tested for its normality and variability at each point in the tank. This suggests that it is not appropriate to develop a model to describe the observation of turbidity in the

tank. However the turbidity samples can be analysed by comparing the characteristics of the turbidity data between different runs, between different depths and between different lengths in the tank.

The analyses carried out in this section can be summarised as follows:

1. To compare the variation of turbidity samples between different runs in each tank. The main aim is to check the characteristics of turbidity samples between different runs.

2. To find out the effects of the discharge on the turbidity characteristics in the tank. The was made by comparing the variations of turbidity and discharge between the tanks. Subjective comparisons were made using boxplots.

3. To compare the turbidity at different depths of the tank for each run. The objective is to find out whether there was a significant difference in turbidity removal between different depths for each run in the tank.

4. To compare the turbidity samples between different runs and between different depths for each tank. The main aim is to establish whether there is any relationship between runs and between depths on the turbidity distribution in each tank.

5. To compare turbidity removal at different lengths in tanks based on all the runs carried out during the investigation. The main aim is to assess the effectiveness of turbidity removal at different stages along the length of the tank.

8.2.1 Comparing Between Runs

1. In order to see the variation of turbidity between different runs in each tank, boxplots were drawn. Turbidity data at each point in the tank from each run was used to compare the variation of turbidity between different runs. Figures 8.1 to

8.4 indicate that the variations of turbidity for different runs within the same tank at Frankley and Trimpley were significant. The results are plausible in the context of the application. Tables D1.1 to D1.4 (Appendix D) indicated that there were significant differences in the flow rate between different runs. This suggests that the variation in turbidity between different runs may be due to the variation of flow rate between runs.

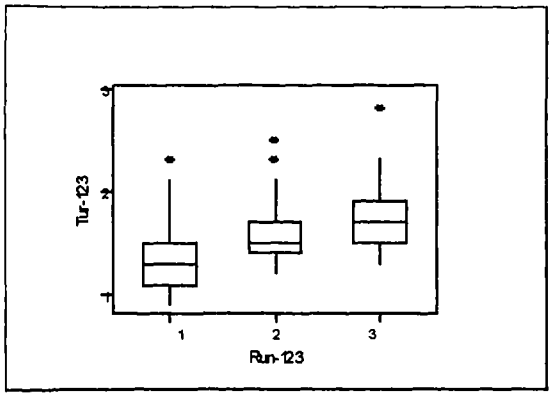

Figure 8.1 - Boxplots of turbidity for different runs at Tank A3 (Frankley WTW)

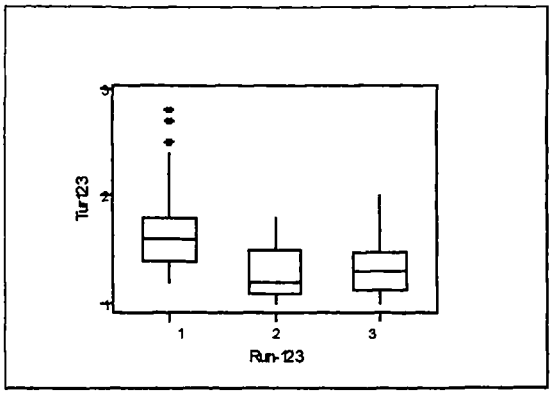

Figure 8.2 - Boxplots of turbidity for different runs at Tank C2 (Frankley WTW)

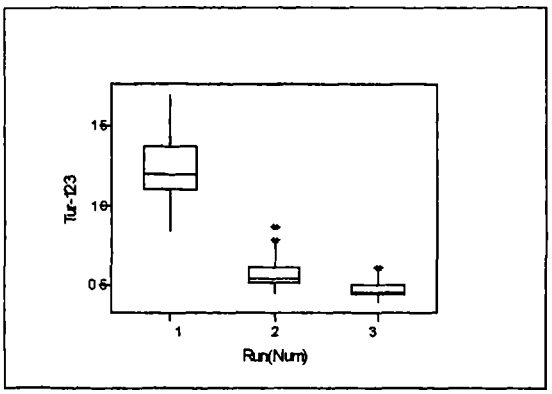

Figure 8.3 - Boxplots of turbidity for different runs at Tank C1(Trimpley WTW)

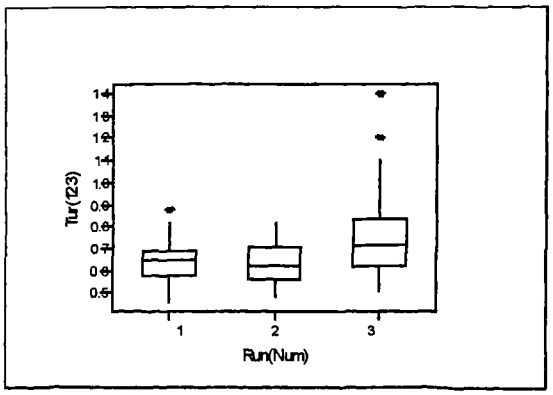

Figure 8.4 - Boxplots of turbidity for different runs at Tank C7(Trimpley WTW)

8.2.2 Turbidity and Discharge Between Tanks

Turbidity readings at the same point from runs 1, 2 and 3 in each tank were averaged. Since in each run there was only one turbidity reading at each point in the tank, the average turbidity for each point from the three runs was calculated based on three turbidity readings. Turbidity data from all the 64 points in the tank were averaged

according to this procedure. Then the average turbidity data of the 64 points in each tank from the same site was compared. The objectives are to see the overall variation of turbidity within the same tank and the difference in the turbidity mean between two tanks of the same size. The results are shown in Figure 8.5 for the tanks at the Frankley WTW and in Figure D1.1 of Appendix D for the tanks at the Trimpley WTW. The results indicate that there are significant differences in turbidity means between the two tanks of the same size at Frankley and Trimpley.

The next step of the analysis was to compare the average discharge which occurred during turbidity sampling between different tanks from the same site. The characteristics of the average discharge were compared with the characteristics of the average turbidity in order to find out any relationship between them. During the sampling of turbidity at each point, at least five discharge readings were taken at Frankley. These readings which corresponded to a point in the tank were averaged. At Trimpley the discharge from each tank was monitored through an on-line computer. To obtain the discharge when the turbidity sampling was taken at each point, the time and duration of the sampling were recorded and then matched with the readings of time versus discharge produced by the computer. Then the discharge readings during the turbidity sampling were averaged. These procedures enable the average discharge to be compared at the time when the turbidity sample was taken. The objectives are to find out the difference in the discharge between the tanks and the relationship between the variations of discharge and turbidity distribution in the tank.

The results are shown in Figure 8.6 for the tanks at Frankley and in Figure D1.2 (Appendix D) for the tanks at Trimpley. The results indicate that there was a significant difference in the mean discharge between the tanks of the same size when samplings of turbidity were carried out.

When the boxplots of turbidity and their respective discharge at the same site are compared (i.e. Figures 8.5 with 8.6 and Figures D1.1 with D1.2 in Appendix D), there is some evidence that higher turbidity was related to a higher range of discharge. This

result may not be in agreement with Shawcross *et al.* (1997). He and co-workers indicated that different surface loading rates (15m/hr, 20m/hr and 25m/hr) would not effect the effluent turbidity of the plant. Their studies were limited to measuring the turbidity readings at the outlet of the DAF plant. There was no indication that a study on the effects of the variation of discharge on turbidity was carried out. Measuring of turbidity at the outlet may not give the same indication as measurement of turbidity at various points in the tank. As reported in Section 2.4.1.1 of Chapter 2, literature review indicated that there has been no previous study to find out the effect of the variability of discharge on the turbidity removal in the tank. These results can be regarded as new findings but must be treated cautiously because only two different sizes of dissolved air flotation tanks were studied. Furthermore the results were limited to the conditions and parameters as explained in the next paragraph.

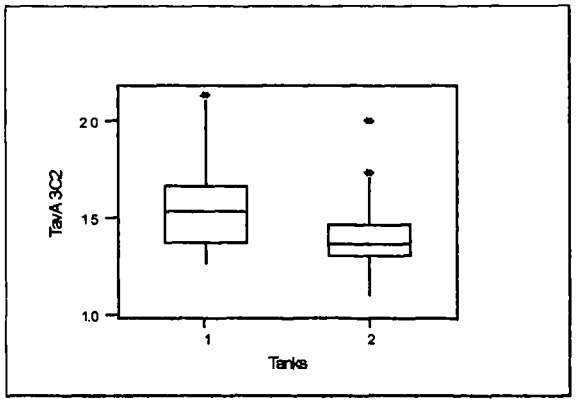

Figure 8.5 - Boxplots of turbidity between Tanks A3 and C2 (Frankley WTW)
Note: Tank 1=Tank A3, Tank 2=Tank C2 and y-axis=turbidity in NTU

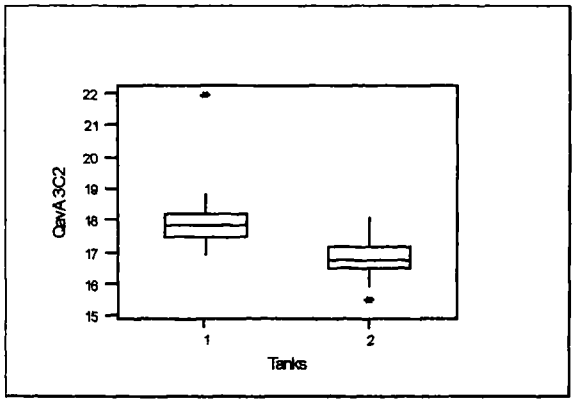

Figure 8.6 - Boxplots of discharge between Tanks A3 and C2 (Frankley WTW)
Note: Tank 1=Tank A3, Tank 2=Tank C2 and y-axis=discharge in million litres per day.

The flocs entering the dissolved air flotation tanks at the Frankley and Trimpley WTW during the investigation were approximately below 300μm. This type of floc is found to be favourable for the solid-liquid separation process to take place (Edzwald *et al.*, 1992; Edzwald, 1995; Klute *et al.*, 1995; Bunker *et al.*, 1995). The relationship between the discharge and the turbidity removal which was obtained from this study is limited to pinpoint-size floc with an average water temperature of 11°C at Frankley and 20°C at the Trimpley WTW. The results are based on the parameters within the specified range as shown in Table 8.1.

Table 8.1 - Parameters used during the data collection for turbidity removal

Parameters	Frankley WTW	Trimpley WTW
Surface area (separation zone)	8400mmX7000mm	6780mmX5120mm
Surface area (flotation cell)	9550mmX7000mm	7870mmX5120mm
Depth of water (m)	2.1m(outlet),2.475m(inlet)	2.23m(outlet),1.65m(inlet)
Volume (m^3)-separation zone	134.5	67.3
Minimum flow (mld)	13.13(1) or 6.57(2)	3.9
Maximum flow (mld)	27.83(1) or 13.92(2)	8.187
Average flow (mld)	17.36(1) or 8.68(2)	5.749
Minimum SL (m/hr)	4.10 or 4.65*	4.03 or 4.68*
Maximum SL (m/hr)	8.67 or 9.86*	8.47 or 9.83*
Average SL (m/hr)	5.41 or 6.15*	5.94 or 6.90*
Minimum DT (minutes)	13.9	11.8
Maximum DT (minutes)	29.5	24.8
Average DT (minutes)	22.3	16.9
Flocs size required	Pinpoint	Pinpoint
Saturator pressure (bar)	4.3 to 5.9	4.7 to 5.27
Recycle ratio**	6 to 10%	6 to 10%
Air dose rate (g/m^3)**	7 to 10	7 to 10
Flow from one nozzle**	0.2 lps (maximum)	0.2 lps (maximum)
Number of nozzles	162 (14 were not used)	112

Note: * is the surface loading based on the surface area in the separation zone and ** is the specifications given by John Brown Engineering (1991), (1) = two tanks, (2) = one tank, lps = litre per second
DT = detention time in the separation zone of the flotation tank = volume/flow
SL = surface loading in the flotation cell = flow/surface area of flotation unit

The results from the boxplots (Figures 8.5, 8.6; D1.1 and D1.2 in Appendix D) indicated that the overall turbidity is relatively lower at a lower range of flow rate. An increase in the flow rate will also result in a decrease of detention time in the tank. A smaller detention time may suggest that the particles within the separation zone do not have enough time to be floated but are dragged down to the tank outlet or initially recirculated within the tank before leaving through the tank outlet.

The average bubble size was expected approximately at 64μm, 66μm and 68μm for saturation pressures of 60 (4.14 bar), 70 (4.83 bar) and 80 (5.52 bar) pound per square inch (psi) respectively. This was based on the results of the investigation carried out in the laboratory by Sebau (1997) for the same type of nozzle used on site. The actual

bubble size in the treatment plants may be in the smaller range because the measurement in the laboratory was done over a period of 15 minutes during which the bubble will generally be expanded.

8.2.3 Turbidity Removal at Different Depths for Individual Run

Data analysis of turbidity removal at different depths was carried out by averaging the turbidity observation across the width of the tank based on each run. For example in run 1, for a point at length B and depth d4 (Figures 4.4 or 4.5 of Chapter 4), the turbidity was calculated by averaging the values of the observed turbidity across the width B of the tank. The same procedures were used for the other points on the longitudinal section (length) of the tank. The idea is to simplify data analysis by using only average values from one longitudinal section of the tank rather than analysing at four longitudinal sections. The term 'longitudinal section of the tank' is defined as the section which shows the length of the tank on the horizontal axis and the depth of the tank on the vertical axis.

The values of the average turbidity for each run at different depths were analysed to see the characteristics of turbidity removal along the length of the tanks. The turbidity readings were compared based on the source turbidity observed at the inlet of the tank. The results of turbidity readings at different depths for each run along the length of the tank are shown in Figures 8.7 to 8.10 for the tanks at Frankley and in Figures D1.3 to D1.6 (Appendix D) for the tanks at the Trimpley WTW. The turbidity readings at the inlet of the dissolved air flotation tank shown in the graphs (Figures 8.7 to 8.10) is labelled with length '0'.

It can be seen from Figures 8.7 to 8.10 that the turbidity readings at the inlet of the dissolved air flotation tanks at the Frankley WTW varied considerably from 1.6 to 5.1 NTU. However the removal of the turbidity was almost the same for all depths for each different run of the experiment. This result may not be in agreement with the results from the laboratory work obtained by Katz and Wullschleger (1957). The laboratory flotation cell used in their experiments was 40 cm deep by 9 cm long and 4

cm wide. The results from Katz and co-worker implied that the removal of particles was higher at the bottom than at the upper part of the flotation cell. Smaller particles were found at the lower part of the tank whereas the larger at the upper section. The measurements of particle size were made between 3 to 11 inches (i.e. 75mm to 275mm) from the bottom of the flotation cell.

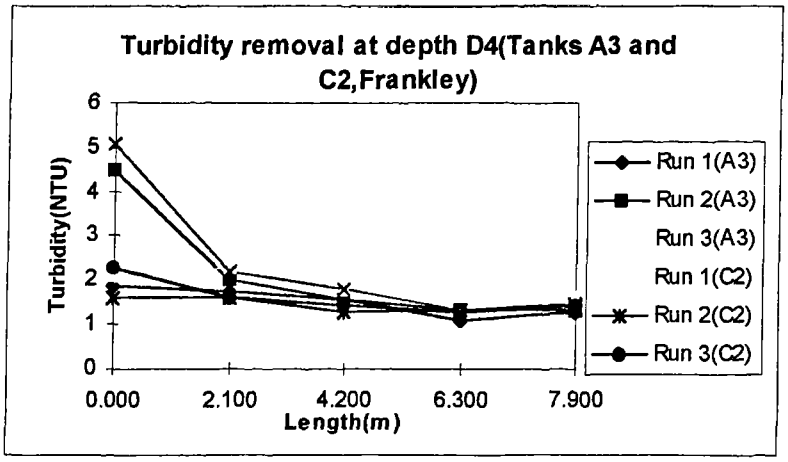

Figure 8.7 - Turbidity removal along the length of the tank at depth d4, Frankley WTW

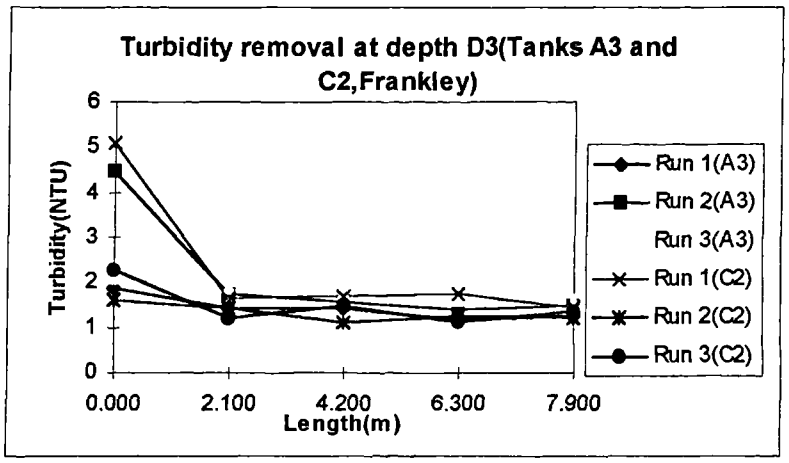

Figure 8.8 - Turbidity removal along the length of the tank at depth d3, Frankley WTW

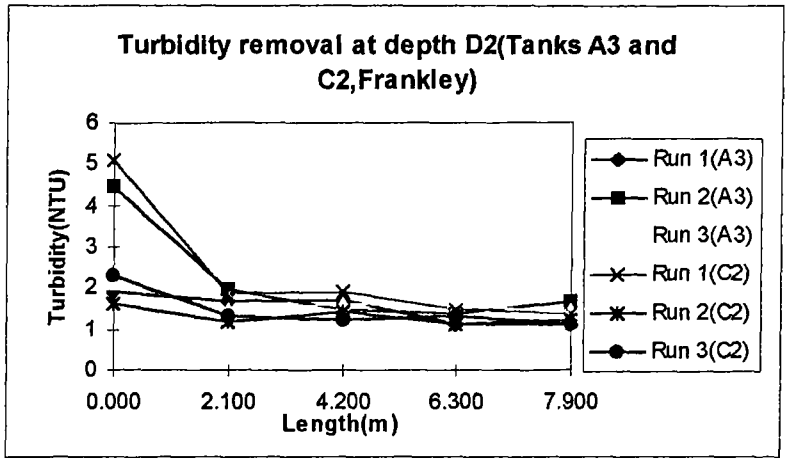

Figure 8.9 - Turbidity removal along the length of the tank at depth d2, Frankley WTW

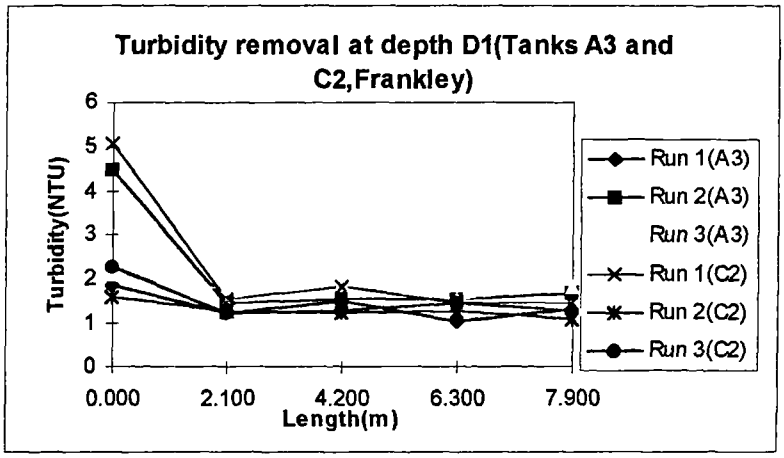

Figure 8.10 - Turbidity removal along the length of the tank at depth d1, Frankley WTW

Since the water at the inlet of the flotation tanks at the Frankley WTW was predominantly a low turbid water, the results of the above analysis are restricted to the water within the turbidity regime under consideration. The results of turbidity removal may be different if a high turbidity were found at the inlet of the tank. Hence the limitation of the results at the Frankley WTW are within the specified inlet turbidity, the range of flow rate and the other parameters as specified in Table 8.1.

Further analysis was carried out on the turbidity removal (at different depths) at the Trimpley WTW. The results indicate that the turbidity levels at different depths for each different run were approximately the same (Figures D1.3 to D1.6 in Appendix D). The range of turbidity at the inlet of the tank was from 1.4 to 3.5 NTU. The

levels of turbidity at the inlets of the dissolved air flotation tanks at Trimpley were lower than those found at the Frankley WTW. Again the results are applicable for less turbid water. In fact the raw water turbidity (0.55 to 0.76 FTU) from the impounding reservoirs at Frankley and Trimpley was normally less than the turbidity at the inlets of the tanks. The turbidity is normally increased due to the coagulation and flocculation process. Longhurst and Graham (1987) reported that the raw water turbidity in the range of 0.5 to 29 NTU was reduced to 0.5 to 8.5 NTU after flotation, but they made no comparison between the level of turbidity at different depths of the tank for particular range of inlet turbidity. Table 8.2 confirms the evidence from the graphs (Figures 8.7 to 8.10 and D1.3 to D1.6 in Appendix D) that there was no significant difference in turbidity between different depths for any individual run.

Table 8.2 - Results on the tests of significance for turbidity on depth.

Runs and Tanks	Levels of significance
Frankley	Between depth
Run 1 (Tank A3)	0.499
Run 2 (Tank A3)	0.904
Run 3 (Tank A3)	0.129
Run 1 (Tank C2)	0.903
Run 2 (Tank C2)	0.291
Run 3 (Tank C2)	0.423
Trimpley:	
Run 1 (Tank C1)	0.936
Run 2 (Tank C1)	0.687
Run 3 (Tank C1)	0.057
Run 1 (Tank C7)	0.076
Run 2 (Tank C7)	0.158
Run 3 (Tank C7)	0.709

Although there was no statistical evidence of any significant difference of turbidity removal at different depths of the tank for each run, inspection of Figures D1.3 to D1.6 (Appendix D) indicate that the removal from Run 1 (Tank C1) was less than the removal from the other five runs. The plotted graph of turbidity removal from Run 1 (Tank C1) did not follow the general trend of line patterns as plotted from the other runs. During Run 1 (Tank C1), the turbidity at the inlet of the tank was 3.5 NTU and

this was the highest turbidity level occurred at the Trimpley WTW during the investigation. However this value is still considered low when compared with the inlet turbidity at the Frankley WTW. Inspection of results from Figures 8.7 to 8.10 for the Frankley WTW indicate that even with a higher inlet turbidity (i.e. more than 3.5 NTU), the graphs show that the line patterns were similar, which suggest that there was no significant difference in the turbidity removal between different runs.

The second highest turbidity reading at the inlet of the flotation tank at the Trimpley WTW was 3.2 NTU (refer to Figures D1.3 to D1.6 in Appendix D). This reading came from Tank C2 but the results of turbidity removal still follow the general trend (similar lines patterns in the graphs as from the other runs) from the other runs. This means higher turbidity at the inlet of the flotation chamber cannot be used as evidence to substantiate the reason for inefficient turbidity removal. Further analysis was made to find out whether a higher turbidity range may contribute to inefficient turbidity removal during Run 1. The results are as shown in Figures D1.7 to D1.10 (Appendix D). These results indicate that the turbidity range (range between maximum and minimum) was not significantly high which may affect the average turbidity readings. The only reason which may cause this problem was the variability of the discharge during Run 1. The results of data analysis show that the standard deviations of the discharge during Run 1, 2 and 3 were 0.6528, 0.4690 and 0.0329 respectively. Run 1 seems to have a higher standard deviation and hence higher variability which results in less efficient turbidity removal. The latter seems to be in agreement with the results from the boxplots in Figures 8.5 and 8.6 which have been described in Section 8.2.2. It can be concluded that higher variability in the discharge or flow rate may cause less efficient turbidity removal in the dissolved air flotation tank.

8.2.4 Turbidity Removal Between Different Runs and Between Different Depths

Further analysis was made to find out whether there is any significant difference in turbidity removal between different runs and between different depths of the tank. The test statistics were made by comparing the turbidity sample mean between

different runs for each tank and simultaneously comparing the turbidity mean at each depth of the tank based on the samples obtained from all the three runs.

The results of the test statistics are shown in Table 8.3 and Tables D1.5, D1.6 and D1.7 in Appendix D. The results indicate that there is a difference in the mean turbidity between different runs for each tank. However the results indicate that there is no significant difference of turbidity mean between different depths in the tank. The results from all the tanks are in agreement to each other. The outcome of the results implies that for a given range of turbidity (1.9 to 5.1 NTU at Frankley and 1.4 to 3.5 NTU at Trimpley) at the inlets of the dissolved air flotation tanks, there is no significant difference in the average turbidity readings at different depths of the tank.

Table 8.3 - ANOVA between runs and depths for Tank A3 (Frankley WTW)

Source	DF	SS	MS	F	P
Run	2	0.98602	0.49301	11.18	0.000
Depth	3	0.06785	0.02262	0.51	0.676
Error	42	1.85164	0.04409		
Total	47	2.90551			

8.2.5 Turbidity Removal at Different Lengths

The approach of the analysis on the turbidity removal at different lengths of the tank is divided into four parts. The length specified in this section is defined as a measurement made from the baffle towards the outlet of the tank. The end of the tank is defined as the positions at cross-section A in plan view of Figures 4.3 and 4.4 in Chapter 4. The first part of the analysis is done by comparing the turbidity readings between three-quarter length of the tank and at the extreme end (near the outlet of the tank) of the tank. The second part of the analysis is to compare the turbidity readings between half length and three-quarter length of the tank. The third part of the analysis is to compare the turbidity readings between one-quarter length and half length of the tank. Comparisons of turbidity readings are made by visual interpretation of the results obtained from the graphs (i.e. Figures 8.7 to 8.10 and

Figures D1.3 to D1.6 in Appendix D). These results are checked using appropriate statistical techniques. The final part is to discuss and compare the overall performance of the dissolved air flotation tanks at Frankley and Trimpley WTW.

8.2.5.1 Turbidity Between Three-quarter Length and the Extreme End

Graphs drawn in Figures 8.7 to 8.10 (in Section 8.2.3) and in Figures D1.3 to D1.6 (Appendix D) can be used to evaluate the effect of the length of the flotation tanks on the turbidity removal for the tanks at the Frankley and Trimpley WTW respectively. In Figure 8.7, at depth d4 (one-fourth of the total depth from the surface), the turbidity removal at 6.3m from the baffle seems to be as effective as at the end of the tank. However the variation of turbidity is more at the length 6.3m due a less effective turbidity removal from Run 3 (Tank A3) and a more effective turbidity removal from Run 1 (Tank A3). It can be concluded that at depth d4 (Frankley WTW), the removal at length 6.3m can be as effective as the removal at the end of the tank. For the Trimpley WTW, Figure D1.3 indicates that the result is the same as for the Frankley WTW except for the turbidity removal from Run 1 (Tank C1) where the problem is isolated and has been explained in Section 8.2.3.

At depth d3 (at one-half of the total depth of the tank), Figure 8.8 indicates that the turbidity readings at a distance of three-quarter length from the baffle (6.3m length) are more varied than at the end of the tank. As for the depth d2 and d1 (Figures 8.9 and 8.10) the turbidity readings at length 6.3m are the same as at the end of the tank. For the tanks at the Trimpley WTW, Figure D1.4 (Appendix D) indicates that the turbidity readings at three-quarter length from the baffle (in the separation zone) were as good as at the end of the tank with the exception of Run 1 (Tank C1). The same results occurred at depths d2 and d1.

The interpretation of the results from the graphs (turbidity removal along the length of the tanks) indicates that the removal of turbidity at a distance of three-quarter length from the baffle for different depths is similar to the end of the tank. Comparison of findings from other workers cannot be made with these results because in most

publications (Longhurst and Graham, 1987; Malley and Edzwald, 1991a; Edzwald, 1997; Shawcross *et al.*,1997) the turbidity readings were reported before and after the flotation process.

Visual interpretation of the results from the graphs by comparing the turbidity readings at 6.3m from the baffle and at the end of the tank may subject to debate. Hence a statistical technique using the analysis of variance was used to find out whether there was any significant difference between the turbidity at 6.3m from the baffle and at the end of the flotation tank. The average turbidity at three-quarter length from the baffle was compared with the average turbidity at the end of the tank. The results are shown in Tables 8.4 and 8.5 for the turbidity at Frankley and Trimpley WTW respectively. The null hypothesis test indicates that there was no difference in turbidity readings between three-quarter length and at the extreme end of all the tanks (i.e. at Frankley and Trimpley).

Table 8.4 -ANOVA on turbidity readings between the turbidity at three-quarter length and at the end of the tank for the tanks at the Frankley WTW.

Source	DF	SS	MS	F	P
Length	1	0.0092	0.0092	0.43	0.536
Error	6	0.1278	0.0213		
Total	7	0.1370			

Table 8.5 -ANOVA on turbidity readings between the turbidity at three-quarter length and at the end of the tank for the tanks at the Trimpley WTW.

Source	DF	SS	MS	F	P
Length	1	0.00128	0.00128	0.63	0.456
Error	6	0.01214	0.00202		
Total	7	0.01342			

8.2.5.2 Turbidity Between Half Length and Three-quarter Length

Figures 8.7 to 8.10 and D1.3 to D1.6 (Appendix D) show the results of turbidity readings at the Frankley and Trimpley WTW respectively. From these Figures there

is compelling evidence that some differences in turbidity existed between those found at half length from the baffle and those at three-quarter length from the baffle.

A statistical approach was used to confirm the interpretation of the results from the graphs. Turbidity data obtained at four positions across the width of the tank was averaged according to each depth and length. Comparison of all the average turbidity data (from runs 1, 2 and 3) between the half length and three-quarter length from the baffle was made using ANOVA. The results of the analysis are shown in Tables D1.8 to D1.11 in Appendix D. The results indicate that the difference in turbidity readings between the two positions (at half and three-quarter length of the tank) for all the tanks are highly significant. This suggests that there was a significant difference in mean turbidity between half length and three quarter length from the baffle.

8.2.5.3 Turbidity Between One-quarter Length and Half Length

The same graphs which were used in the previous section (Section 8.2.5.2) are used again to analyse the turbidity removal in the tank between one-quarter length and half length of the tank from the baffle. Figure 8.7 provides some indications of a significant difference in turbidity between the two positions in the tanks at the Frankley WTW. However the differences at depth d3, d2 and d1 are difficult to identify from Figures 8.8, 8.9 and 8.10 respectively. It is more likely that there is no difference in the average turbidity readings between the two positions at depth d3, d2 and d1. For the tanks at the Trimpley WTW, Figures D1.3 to D1.6 in the Appendix D were used to differentiate the difference in turbidity readings between the two positions in the tanks. It is rather difficult to identify any significant difference between them.

To verify the interpretation from the graph, an analysis of variance was carried out. The results are shown in Tables D1.12 to D1.15 (Appendix D). There are no significant differences in turbidity readings between one-quarter length and half length of the tank except for the Tank A3 (Frankley WTW). Velocity readings from the latter position indicated that these positions may be under unstable conditions.

8.2.6 Discussions on the Overall Performance of DAF Tanks

Comparison on the performance of the dissolved air flotation tanks at the Frankley and Trimpley WTW can also be made based on Figures 8.7 to 8.10 and Figures D1.3 to D1.6 (Appendix D). It can be seen from Figures 8.7 to 8.10 that the turbidity removal at the Frankley WTW was less efficient for low turbid water (1.6 to 2.3 NTU). At the final stage of the turbidity removal, the average turbidity was still between 1.1 to 1.6 NTU (Table D1.16 in Appendix D). The thoroughness of the investigation and data analysis provide strong evidence that the minimum residual turbidity achievable at the Frankley WTW was between 1.1 to 1.6 NTU for low turbid water.

The performance of the dissolved air flotation tanks at the Trimpley WTW to treat low turbid water was better than at Frankley (Figures D1.3 to D1.6). Water with a turbidity of 1.4 to 2.2 NTU was reduced to 0.48 to 0.68 NTU at the extreme end of the tank (Table D1.17). Since both treatment works have the same types of nozzles, the same range of bubble sizes and floc characteristics, it may be assumed that the amount of bubbles used in each tank and the design criteria (such as the flow and the tank dimensions) may affect the turbidity removal.

Table 8.1 indicates that the number of air nozzles used at Frankley was 148 and at Trimpley was 112. These nozzles are of the same type and size. The discharge for the tank at Frankley was from 13.13 to 27.83 mld (flow rate for two tanks with 148 air nozzles) and at Trimpley from 3.9 to 8.187 mld (Table 8.1). This demonstrates that the flow rate at Frankley was 240% more than at Trimpley (calculated based on the maximum flow rate observed from both treatment plants). However the number of air nozzles used at Frankley was only 32% more than Trimpley. This may be one of the reasons that the turbidity removal at Frankley was less efficient than at Trimpley. Recent discussions with Meher (1997) indicated that the air flow rate at Frankley was increased to a range of 9 to 16 mg/litre and the residual turbidity was reported to be improved down to 0.5 NTU.

Table 8.1 indicates that the maximum flow rate from the nozzle is 0.2 litres per second. This suggests that the maximum recycle flow rate from 148 nozzles at the Frankley WTW will be 2.56 mld. For a 10% recycle ratio, the output from each flotation cell cannot exceeded 25.6 mld. If the flow rate from the flotation tank exceeded this figure then the amount of dissolved air required has to be adjusted. During the investigation the flow rate was varied from 13.13 to 27.83 mld (Table 8.1) and the air dose was between 7 to 10 g/m^3. To have an air dose of 10 g/m^3 with a recycle ratio of 10% based on a flow rate of 27.83 mld would be impossible. This is because the maximum amount of water that can be delivered from the nozzles is limited to 2.56 mld. This means the air dose in the recycle flow has to be increased.

The minimum vertical rise rate of suspended solids at Frankley and Trimpley were found to be identical. Table 8.6 indicates that the minimum vertical rise rate of suspended solids (based on the depth divided by the average detention times) at Frankley was 1.293 mm/sec and at Trimpley was 1.300 mm/sec. The maximum vertical rise rates of suspended solids between Frankley and Trimpley were 2.74 mm/sec and 2.73 mm/sec respectively. These values were also identical. If the evaluation were made by dividing the average flow rate with the surface area of the tank, the minimum vertical rise rates of suspended solids at Frankley and Trimpley were 1.709 and 1.917 mm/sec respectively. These results indicate that the average of vertical rise rates of suspended solids at both sites were different. Under the design criteria established by Wang and Wang (1989), the vertical rise rate of suspended solids is equal to the depth of the water in the tank divided by the detention time (refer to equation 2.48 in Chapter 2) and this also equals to the flow rate divided by the surface area of the flotation chamber. The results in Table 8.6 for each tank site are in agreement with equation 2.48 in Chapter 2.

The term 'vertical rise rate of suspended solids' used by Wang and Wang (1989) is similar to the overflow rate used by Edzwald and Walsh (1992) or the surface loading used by Shawcross *et al.* (1997). This is because the overflow rate or the surface loading is calculated based on the flow rate divided by the surface area of the flotation tank. Hence the results from Table 8.7 imply that the minimum and

maximum surface loadings at Frankley were quite similar to that at Trimpley. However the average surface loading at Frankley was 6.25 m/hr and at Trimpley was 6.90 m/hr (from Table 8.7). The average surface loading at Frankley was 12% less than at Trimpley. This result indicates that the DAF plant at Frankley was less efficient in term of surface loading compared with Trimpley. Furthermore the surface loadings at both treatment works were found to be at the lower end of the range compared with the surface loadings reported by Edzwald (1995). Table 2.6 in Chapter 2 indicates that the surface loading of DAF plants in the United Kingdom was between 5 and 12 m/hr and in the Netherlands was between 10 to 20 m/hr.

Table 8.6 - Comparison of vertical rise rate of suspended solids

Parameters	Frankley	Trimpley
Average depth D (m)	2.2875	1.94
Vol. in Separation zone (m^3)	134.505	67.344
Min. detention time T (sec)	835 (13.9minutes)	711 (11.9minutes)
Max. detention time T (sec)	1769 (29.5minutes)	1492 (24.9minutes)
Aver. detention time T (sec)	1339 (22.3minutes)	1012 (16.9minutes)
Qmin. (m^3/sec)	0.076 (6.57mld)	0.045 (3.90mld)
Qmax. (m^3/sec)	0.161 (13.92mld)	0.095 (8.19mld)
Qaver. (m^3/sec)	0.100 (8.68mld)	0.067 (5.75mld)
Separation surface area (As)	58.8	34.714
Vt = D/Tmin.(mm/sec)	2.740 (9.86m/hr)	2.730 (9.83m/hr)
Vt = D/Tmax. (mm/sec)	1.293 (4.65m/hr)	1.300 (4.68m/hr)
Vt = D/Taver.(mm/sec)	1.709 (6.15m/hr)	1.917 (6.90m/hr)
Vt = Qmin./As(mm/s)	1.293 (4.65m/hr)	1.300 (4.68m/hr)
Vt = Qmax./As (mm/s)	2.740 (9.86m/hr)	2.730 (9.83m/hr)
Vt=Qaver./As (mm/s)	1.709 (6.15m/hr)	1.917 (6.90m/hr)

Note: min. = minimum max. = maximum aver. = average
Q = flow rate Vt = minimum vertical rise rate of suspended solids
As = surface area of flotation tank D = depth of water in the tank

The average flow rate at Frankley was 8.68 mld and at Trimpley was 5.75 mld. The average flow rate and the surface area of the tank at Frankley were more than Trimpley by 51% and 66% respectively (Table 8.1). Since the average surface loading at Frankley was lower than at Trimpley, this suggests that the surface area of the DAF tanks at Frankley was rather large which results in a lower surface loading rate. Section 8.2.5.1 indicates that there was no significant difference in turbidity

between three quarter length of the tank from the baffle and at the extreme end of the tank (Table 8.4). There was also no significant difference in the turbidity between different depths of the tank (Table 8.2). The results from the turbidity studies between three quarter length of the tank from the baffle and at the extreme end of the tank suggest that the surface area of the tank can be decreased by decreasing the length of the tank so that the surface loading between Frankley and Trimpley are the same.

The minimum detention time at Trimpley was 18% lower than at Frankley (Table 8.1). The minimum detention time at Trimpley was 11.8 minutes and at Frankley was 13.9 minutes. The average detention times at Frankley and Trimpley were 22.3 and 16.9 minutes respectively (i.e. a difference of 32%). There is a possibility to decrease the detention time at Frankley so that the vertical rise rate of the suspended solids between Frankley and Trimpley is the same. It is expected that with the same rise rate of suspended solids between Frankley and Trimpley the variation of turbidity will be within the turbidity levels shown in Figures 8.7 to 8.10 (i.e. within the turbidity level found during the investigation).

8.3 COMPARING DISCHARGE DURING SAMPLINGS OF VELOCITY AND TURBIDITY

This section compares the variation of discharge (flow rate) observed during the sampling of velocity at each of the 64 points in the tank with the variation of discharge observed during the sampling of turbidity at each of the 64 points in each tank. The objective of the comparison is to determine whether there is a significant difference in the range of discharge during the sampling of velocity and turbidity. If the range of discharge were approximately the same, this suggests that the regression models (the models which described velocity observation in the tank) developed in Chapter 7 can be related to the turbidity observed in the tank.

During the sampling of velocity and turbidity data at each point, the discharge readings from the tanks were recorded. At Frankley the discharge readings were

recorded manually whereas at Trimpley the readings were recorded automatically by an on-line computer. For the manual readings, at least five readings were registered for each point and then these readings were averaged. The discharge readings from the computer were produced in a graphical print out of time versus discharge and also in a tabulated form of an average discharge over a period of 15 minutes. In order to match the discharge occurring at each point during the sampling of velocity and turbidity, the discharge data was averaged based on the time and duration of the sampling at each point in the tank.

The average discharge readings at each point in the tank from runs 1, 2 and 3 during velocity and turbidity samplings for each tank were compared. The results are shown in Figures 8.11 to 8.14. Figures 8.11 and 8.12 indicate that the ranges of average discharge were overlapped to a large during the samplings of velocity and turbidity. The same characteristics were observed in Figures 8.13 and 8.14 for the tanks at Trimpley. The results suggest that the regression models developed in Chapter 7 can be used to predict the turbidity removal in the tank within the turbidity range found in this chapter (Chapter 8). In other words by having the same parameters as specified in Table 8.1, the expected turbidity in the tank may be based on the velocity distribution as described by equations 7.1 to 7.6 in Chapter 7. However if the raw water quality is different, the expected turbidity in the tank may be different from the turbidity data found in this Chapter.

In Chapter 6 (Sections 6.6.1 and 6.6.2) the velocity means, *Vz*, for Tanks C2, A3, C1 and C7 were -0.226, -0.256, -0.200, and -0.232 cm/sec respectively. Negative velocities indicate that the overall particles within the study regime are moving down. For a bubble to move up it requires a terminal velocity higher than *Vz*. Fawcett (1977) reported that a bubble with a diameter of 70μm has a vertical rise rate of 0.267 cm/sec. This means the presence of such bubbles in the separation zone may not be capable of carrying some particles to the surface of the tank. The evidence from the diagrams for the flow contours of *Vz* in Appendix B1 to B4 (Chapter 6) indicate that at one quarter depth of the tank from the surface, *Vz* was predominantly in a

downward direction. Hence it can be confirmed that the area within the study regime did not have enough bubbles which could float the particles.

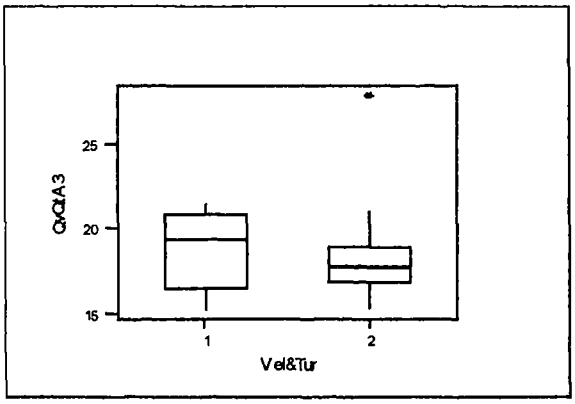

Figure 8.11 - Boxplots of discharge during velocity and turbidity samplings at Frankley (Tank A3). Refer to 'Note' below Figures 8.13 and 8.14 for further details on the boxplots

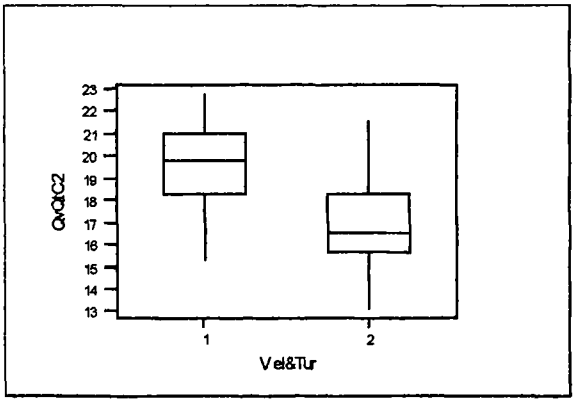

Figure 8.12 - Boxplots of discharge during velocity and turbidity samplings at Frankley (Tank C2). Refer to 'Note' below Figures 8.13 and 8.14 for further details on the boxplots

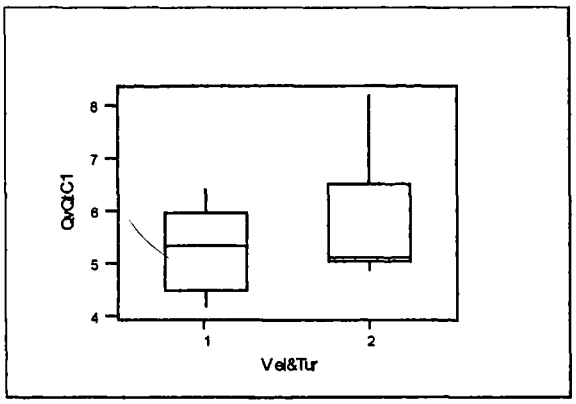

Figure 8.13 - Boxplots of discharge during velocity and turbidity samplings at Trimpley (Tank C1). Refer to 'Note' below Figures 8.13 and 8.14 for further details on the boxplots

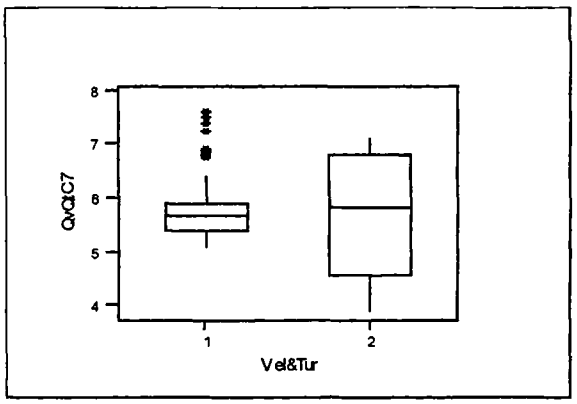

Figure 8.14 - Boxplots of discharge during velocity and turbidity samplings at Trimpley (Tank C7). Refer to 'Note' below Figures 8.13 and 8.14 for further details on the boxplots

Note: On x-axis, 1 = discharge when velocity data was collected and 2 = discharge when turbidity data was collected. On y-axis, discharge in mld.

8.4 SUMMARY OF RESULTS AND FINDINGS

1. Turbidity data for all 64 points in each tank were averaged to obtain a single value for each run. It was found from the boxplot analysis that the differences in the

average values between runs were significant. The results suggest that there were significant variations of turbidity during the course of the experiment. The possible reason may be due to the significant variation of flow rates between each run during samplings. Boxplots of flow rates showed that the flow rates varied significantly between different runs (Tables D1.1 to D1.4 in Appendix D). It is therefore reasonable to conclude that the main variation in turbidity between different runs was due to the variation of flow rate during each run.

2. In order to investigate the overall effect of flow rate on the turbidity removal in the tank, the values of turbidity at each point were averaged from data collected in three separate runs. Each of the 64 points was treated in the same way. As each turbidity sample was gathered 5 discharge readings were taken. These readings were averaged over the 3 runs to obtain an average discharge reading associated with each average turbidity reading. Inspection of the boxplots in Figures 8.5 to 8.6 and D1.1 to D1.2 in Appendix D demonstrates that high average discharge rates are associated with high average turbidity readings. Also the range of turbidity readings exhibit the same characteristics. A high flow variation would seem to imply a high variation in turbidity. This suggests that turbidity removal is sensitive to the applied flow rate. The model in Chapter 7 takes account of the variability in the discharge in the context of turbidity removal. The above findings are also relevant to the attempts in the literature to develop CFD models of DAF systems. At present the CFD models have assumed constant inflow to develop velocity distributions in the tank. The CFD models also considered that the multiphase flow regime was comprised of air and water. However the presence of particles in the flow regime have not been considered. Predictions have been made on the characteristics of air in the flow regime rather than the actual particles. Such predictions may be of limited value because of the lack of stochastic input to the modelling process. Also the literature review found that all published papers to date are based on average turbidity concentration in the tank inflow and outflow.

3. ANOVA and graphical techniques were used simultaneously to find out the differences in the average turbidity readings between different depths in the tank.

The results from the analyses indicate that there was no significant difference in the average turbidity readings between different depths of all the tanks under the investigation. This result suggests that the depth of the tank in the separation zone is not critical for design purposes. This may be in agreement with the literature. Fawcett (1997) indicated that in the literature, tank depth greater than 1 m did not give significant improvement for solids removal. However in practice most of the tanks are more than 1m depth (Haarhoff and Vuuren, 1995). Fawcett (1997) reported that when the depth of the tank was reduced to 1m the CFD model demonstrated that the velocities were increased in the separation zone with a greater recirculation flow pattern. It may be possible that higher velocities could disrupt the floated sludge.

4. Comparisons of the average turbidity readings at different lengths of the tanks from the baffles indicate that there was no significant difference in the average turbidity between the positions at three quarter length from the baffles and at the extreme end of the tanks. Some differences in turbidity readings were observed between half length and three quarter length of the tank from the baffle. The same differences were also observed between one quarter length and half length of the tank from the baffle. Comparison of findings from others cannot be made because in the published papers the turbidity reading were reported before and after the flotation process.

5. The performance of DAF tanks at Frankley was inferior to Trimpley when dealing with a low turbid water. At Frankley the inlet water turbidity of 1.6 to 2.3 NTU was reduced to only 1.1 to 1.6 NTU. At Trimpley the inlet water turbidity was reduced to 0.48 and 0.68 NTU from an inlet turbidity range of 1.4 to 2.2 NTU. Data analysis and discussions in Section 8.2.6 indicated that the average flow rate and the number of nozzles at Frankley was 240% and 32% more than Trimpley respectively. For a maximum flow rate at Frankley, the capacity of the nozzles cannot delivered a 10% recycle ratio with an air dose of 10 g/m^3. Recent communication with Meher (1997) indicated that the air dose has been increased between 9 to 16 g/m^3 and the outlet water quality was reported to be increased up

to 0.5 NTU. This suggest that during the investigation there were not enough air bubbles at the Frankley WTW.

6. The average surface loading (Q/A) at Frankley was 12% less than Trimpley. The average flow rate (Q) and the surface area (A) at Frankley were 51% and 66% more than Trimpley. These comparisons suggest that the surface area in the separation zone at the Frankley WTW may be reduced to 15% which is the same with the difference in the percentage of the average flow rate between Frankley and Trimpley (i.e. at 51%). Earlier discussions (in summary of result number 4 above) indicated that there was no significant difference in turbidity data between three quarter length of the tank from the baffle and that at the extreme end of the tanks at Frankley and Trimpley. This suggests that the length of the tank may be reduced by 1.4m (i.e. based on a reduction of 15% of the surface area with a constant width of 7m). If the length was reduced by 1.4m, the new surface loading would be 6.34 m/hr (1.761 mm/sec). The reduction in length was calculated based on one side of the tank at Frankley. Since each tank was made up of two sides as shown in Figure 4.4 (Chapter 4), the total reduction in length for each tank will be 2.8m. The average surface loading encountered during the investigation was 6.15 m/hr (Table 8.6). Table 8.6 indicates that the new surface loading of 6.34 m/hr is within the surface loading range found at Frankley. The reduction in length may also not interfere with the turbidity removal because in the previous discussions there was not enough air bubbles found in the separation zone to lift the particles (Section 6.7, Chapter 6).

7. The average detention time at Frankley was 32% more than Trimpley. There is also a possibility to decrease the detention at Frankley so that the 'vertical rise rate of suspended solids' (i.e. depth/detention time) or the surface loading at Frankley and Trimpley will be the same (Table 8.6). However there is a need to monitor the turbidity at the outlet of the tank if this suggestion is to be adopted.

CHAPTER 9

CONCLUSIONS AND SUGGESTION FOR FURTHER RESEARCH

9.1 CONCLUSIONS

The main objective of the research was to investigate the relative importance of the design parameters within the separation zone for the dissolved air flotation (DAF) tank. To date, the literature review has indicated that there is no concrete evidence to substantiate the relationship between tank dimensions and the velocity and turbidity distributions in the tank. In order to develop the design parameters extensive works were carried out to understand the flow and turbidity patterns within the separation zone of the DAF tank. Extensive flow and turbidity measurements within the tank were made. Since the liquid velocity within the separation zone is very small and the flow is laminar, an appropriate velocity meter was required. An Acoustic Doppler Velocimeter (ADV) was used for this purpose. The instrument was adopted after a long search for appropriate equipment within the United Kingdom, United States, Canada, Continental Europe and Japan. Its application in the field of flotation during the investigation was new, based on discussions in the first meeting of the ADV users within the United Kingdom which was held on October 1996 at HR Wallingford. No physical velocity measurement within the separation zone was reported in the literature, hence its appropriateness was to be proven.

A summary of results and findings from this research work can be found at the end of Chapters 6, 7 and 8. The overall conclusions can be summarised as follows:

1. The ADV probe was found to be suitable to measure low velocity in the separation zone of the DAF tank. A sampling rate of 25 Hz exhibited a higher percentage of good velocity data than at 1 Hz. Statistical tests on the skewness (>1.5) of velocity samples indicated that samples collected with sampling frequency of 25 Hz produced less skewness than with 1 Hz. The presence of skewness (>1.5) may be due to 'aliasing' or the actual situation within the flow regime. In Chapter 5, the

term 'aliasing' was used by the manufacturer of the WinADV software to describe a spike in the velocity data that biased the average velocities and made the instantaneous velocity measurements uncertain. Velocity data exhibiting higher skewness occurred at a lower or negative velocity which may suggest that the flow is under a transition regime.

Comparisons of the variation of the average filtered and average raw velocity data indicated that there was no significant difference between data at Frankley or at the Trimpley Water Treatment Works (WTW). This suggests that the raw data was as good as the filtered data and hence the ADV probe is suitable to be used for velocity measurement in a DAF tank. The results on the quality of velocity data indicated that only 2.6% of the data has a higher skewness (>1.5). This demonstrates that the quality of velocity data collected was good. The statistical procedure called randomization was used during velocity data collection to reduce systematic error arising from measurement or investigation carried out repeatedly in the same order. A method called blocking has enable velocity data to be compared between tanks of the same size and subsequently skewness or average velocities can be compared and evaluated. It can be concluded that in order to obtain a representative velocity data statistical methods of randomization and blocking may be useful. The appropriateness of data collection not only came from the equipment but also from the methodology and procedures involved during the data collection. Comparison on the used of ADV probe with other users within the flotation field cannot be made due to unavailable reference in the literature.

2. Plan view contour diagrams for velocities in the *x*, *y* and *z* directions for different runs were developed based on the average velocity at each point in the tank (Appendices B1, B2, B3 and B4). The diagrams for each run were based on 64 points set at four different width, depth and length of the tank (Figures 4.4 and 4.5 in Chapter 4).

   For velocity in the *x* direction (*Vx*) at the Frankley and Trimpley WTW, the velocity distributions from three different runs of each tank at depths d1, d2 and d3

were identical. However at depth d4 (one quarter depth from the surface of the tank) the velocity distributions in the x direction were irregular and difficult to interpret. This may suggest that the area within one quarter depth from the surface of the tank was unstable. For the velocity in the y direction (Vy), plan view contour plots indicated that there were irregularities in the flow patterns at different depths for different runs. It can be concluded that there is no relationship between Vx and Vy for all the tanks under the investigation. Velocity in the z direction (Vz) indicated that the flow predominantly moved downwards at depth d1, d2, d3 and d4. Vz is also associated with the movement of the particles or bubbles within the tank. This is because the measurement of velocity using the ADV probe is based on the scattered particles or bubble presence in the water. It can be concluded that the studied area within the tank does not have enough bubbles to lift the particles and therefore is not effective for the solid liquid separation process to take place. It was found that at depth d4 some higher values (positive values) of Vx were related with positive values of Vz, only at certain positions. In general at the baffle there was no relationship between Vx and Vz across the width of the tank. This suggests that fundamentally the solid liquid separation process took place at the reaction zone of the flotation cell and only a small fraction of positive separation occurred in the separation zone.

Computational Fluid Dynamic (CFD) models (Fawcett, 1997; Ta and Brignal, 1997) found in the literature were compared with the results from this study. There were some differences in the flow patterns except at the outlet of the tank. The present CFD models (Fawcett, 1997) describe the flow in two dimensions with a constant flow rate and a uniformity of flow across the width of the tank. The contour plots (plan view) from this research indicate that there was no uniformity of velocity across the width of the tank especially at depth d4 (i.e. at one quarter depth of the tank from the surface). Within one quarter depth from the surface of the tank, the CFD model produced by Fawcett (1977) indicated that the velocity in the x direction was uniform with the same magnitude and moving horizontally all the way along the length of the tank except near the baffle and at the extreme end

of the tank. This result (CFD model) is not in agreement with the results produced in this research as shown in diagrams in Appendices B1, B2, B3 and B4.

At Frankley there was no significant difference in the velocity mean of *Vx* between different runs in each tank but there was significant difference of the velocity mean of *Vx* between different tanks. There was also significant difference of *Vx* between Frankley and Trimpley. This suggests that there was a significant difference in the flow rate between the tanks and between the sites. *Vx* was higher at Frankley than Trimpley due to a higher flow rate. It can be concluded that the contour plots of velocity mean *Vx* were based on a significant variation of flow rate in the DAF tanks. The plots represent the actual full plant operational characteristics within the limited range of tank sizes. The repetition work based on three runs at each tank is more than enough to suggest strong evidence and representation of velocity distribution from Frankley and Trimpley WTW.

Vy was found to have a lower mean velocity than *Vx* and *Vz* and hence can be considered to have a lesser impact on the movement of particles within the separation zone. In terms of *Vz*, it was found that there was no significant difference of *Vz* between Frankley and Trimpley. This suggests that the difference in tank dimensions and *Vx* between the two sites does not affect *Vz*. An inference can be made that *Vz* for different sizes of tanks may be identical. Further tests on different sizes of tank are required to prove this hypothesis.

3. Analyses of variance (ANOVA) and covariance (ANCOVA) for *Vx* indicated that the tank physical dimensions i.e. width, depth and length and the interactions between them are highly significant and affect the velocity distribution in the *x* direction. Only the interaction between the width and the depth for Tank A3 was not significant. However the results from three other tanks indicated that the interaction between the width and depth were significant. The possible reason for Tank A3 to behave differently may be due to the present of greater number of skewed (>1.5) velocity data (Table 6.2 indicates that Tank A3 has 7 number of skewness (>1.5) and the occurrence was greater than other tanks). In ANCOVA

the continuous variable (i.e. the flow rate) was modelled together with the tank physical dimensions. The results indicated that the flow rate at Frankley was significant but not at Trimpley. The significance in the flow rate depends greatly on its variability. Table 6.24 (Chapter 6) indicates that the average flow rate at Frankley varied from 8.175 to 10.145 mld (24.1%) whereas at Trimpley from 5.40 to 5.96 mld (10.4%). It can be concluded that low variation in the flow rate at Trimpley does not effect the velocity distribution in the tank.

The statistical model represented by equation 5.7 in Chapter 5 is found to be appropriate to describe the velocity observed in the tank based on statistical tests on the standard residuals versus fitted values and the normality of the standard residuals.

4. Fixed effects models were developed and applicable to the tanks which have the same configuration and flow conditions as found at Frankley and Trimpley (i.e. equations 7.1 to 7.4 in Chapter 7). Generalised and more flexible models were also developed to describe the velocity distribution in the tank within the sizes and flow rates found at Frankley and Trimpley (i.e. equations 7.5 to 7.6 in Chapter 7). The R^2 for equation 7.5 and 7.6 are 58.5% and 63.4% respectively. This suggests that the unexplained variations for equations 7.5 and 7.6 are 41.5% and 36.6% respectively. Higher values of unexplained variations are due to the fact that the models have been simplified into the second-order models. Regression analysis using 40 predictor variables in a higher order model was found to have higher R^2. ANOVA and ANCOVA indicated that the tank physical dimensions are highly significant by using higher order interactions with an independent predictor variables. The problem with the higher order model is the difficulty to interpret the results. It can be concluded that a simple model is more plausible and appropriate for design purposes than a complicated model.

   Equations 7.5 and 7.6 described the velocity at each point in the tank within the range of tank sizes and flow conditions found at Frankley and Trimpley. For design purposes the overall average velocity of Vx based on the 64 points in the

tank must be within 0.101 cm/sec and 0.964 cm/sec. The overall average velocity of *Vz* based on 64 points in the tank must be between -0.2 cm/sec and -0.256 cm/sec. The flow rate must be between 4.64 to 10.22 million litres per day.

Although equations 7.5 and 7.6 do not fully describe the velocity distribution in a DAF tank, this research has shown that standard statistical techniques which have never been applied before to study the velocity in a DAF tank are useful and relevant to describe the velocity observed in the tank.

5. The relationship between the variations in the average flow rate and the average turbidity in the tank was analysed. Inspection of boxplots indicate that high average flow rates are associated with high average turbidity readings. Also the variation or range of turbidity readings exhibit the same characteristics. A high average flow variation seems to imply a high variation in turbidity (refer to Figures 8.5 and 8.6 in Chapter 8 and Figures D1.1 and D1.2 in Appendix D for further details). It can be concluded that the average turbidity removal is sensitive to the applied flow rate. The model in Chapter 7 takes account of the variability in the flow rate in the context of turbidity removal. At present the CFD models described in the literature assume a constant flow rate and the prediction may be limited due to lack of stochastic input.

   To date, no extensive turbidity measurements have been carried out in the separation zone of the DAF tank. In this study turbidity readings from 64 points in the tank were investigated (refer to Figures 4.3 and 4.4 in Chapter 4). There were four different depths or layers within the tank. Each depth or layer comprised of 16 points. Turbidity reading at each point was averaged based on turbidity readings from the three runs. This study indicates that there were no significant differences in average turbidity readings between different depths in each tank. The study also indicates that there was no difference in the average turbidity between different depths for each run at each tank. It can be concluded that turbidity removal is not effective within the studied area (i.e. from the floor of the tank to one quarter depth from the surface of the tank) and it can also be suggested

that there is not enough air bubble within the studied area to lift the particles. The presence of significant amount of air bubbles may be attributed to the difference in the average turbidity readings between different depths. The result which indicated no difference in the average turbidity for different depth also suggests that the sampling procedure used during the investigation by taking one sample at each point for each run can be considered adequate since the average turbidity readings are identical.

The turbidity readings were also averaged based on each length position (see Figures 4.3 and 4.4 to see the positions for different lengths along the tank) along the tank. Each length has 16 points at four different depth. The turbidity readings at each length in the tank were averaged based on three different runs. The four different lengths were identified as one quarter length from the baffle, half length from the baffle , three quarter length from the baffle and at the extreme end of the tank. The study indicates that there was no differences in the average turbidity readings between three quarter length from the baffle and at the extreme end of the tank. However there were some differences in average turbidity readings between the other three positions of different lengths (i.e. one quarter, half and three quarter lengths from the baffle). This suggests that the length of the tank may be reduced but can only be confirmed when the results from the analysis are presented later in the conclusion (i.e. in conclusion 7).

6. The performance of DAF tanks at Frankley was less efficient than Trimpley for low turbid water where the turbidity was between 1.6 and 2.3 NTU. The turbidity was reduced to only 1.1 to 1.6 NTU. Earlier data analysis indicated that the average flow rate and number of nozzles at Frankley were 240% and 32% more than Trimpley. The number of nozzles at Frankley cannot meet the required 10% recycle ratio with an air dose of 10 g/m^3 based on the maximum flow rate occurred. This suggests that at the maximum flow rate not enough air was injected through the nozzles. Recent communication with Meher (1997) indicated that the air dose at Frankley is now between 9 to 16 g/m^3 and the turbidity reading at the tank outlet has improved to 0.5 NTU. It can be concluded that enough amount of

air must be injected through the nozzles for an efficient solid liquid separation process to take place.

7. The average flow rate and surface area at Frankley were 51% and 66% more than Trimpley. However the average surface loading at Frankley was 12% less than Trimpley. This suggests that the surface area at Frankley may be reduced up to 15%. A reduction in 15% of the surface area implied that the length of the tank at Frankley can be reduced by 1.4m (based on one side of each tank). A 15% reduction in length does not affect the surface loading (Chapter 8). The reduction in length may also not interfere with the turbidity removal because from the previous discussions there was not enough air bubbles in the separation zone to lift the particles. In terms of saving, a reduction of 2.8m length from each tank could save a total of 56m length by 7m width of dissolved air flotation tank at Frankley (based on a total of 20 tanks found at Frankley WTW).

9.2 SUGGESTION FOR FURTHER RESEARCH

Since one of the results in the conclusions (refer to conclusion 5) indicated that the area within the studied regime was not efficient for the turbidity removal, this suggests that the separation zone was acting as a sludge collecting chamber and also as a stilling basin to maintain the flow within an appropriate velocity regime to prevent the breaking up of the flocs. For further improvement of the flotation tank design, the following proposals may be worth considering:

1. Since the separation zone is not efficient for turbidity removal and has the same property as found in the sedimentation tank (i.e. the presence of any particles within this zone may descend to the floor or be carried away with the effluent), it may be appropriate to introduce a series of inclined plates a few centimetres from the floor to at least one-quarter depth of the tank. Further studies are needed before this suggestion can be put into practice. For future construction of the same type of tanks found at Frankley, it may be appropriate to reduce the length of the tank as suggested in this thesis.

2. It can been seen from this study that much of the area within the separation zone was redundant. In order to optimise the area within the separation zone, it may be possible to improve the existing tanks (or for any tanks to be constructed in the future) by having a series of inclined baffles or vertical baffles across the width of the tank with the air nozzles installed between these baffles (Figure 9.1). The influent water can be introduced from the side of the tank or from the bottom of the floor. The effluent can be collected through perforated pipes or a channel constructed below the floor level of the tank. The average velocity range over the baffle may be based on the velocity found at the Frankley WTW, that is between 0.038 m/sec and 0.021 m/sec (John Brown Engineering, 1991). For a given influent flow rate Q_I through each set of baffles, the discharge over each baffle may be designed as $Q_I/2$. The range of velocity over the baffle may be calculated as $Q_I/2A$, where A is the cross-sectional area between the tip of the baffle and the mean water level in the tank.

The above suggestion has the same concept as the counter-current DAF used by Thames Water at Walton, London (Eades *et al.*, 1977). However in a counter-current DAF the influent water flows upward into the DAF tank through a number of conical structures (act as baffles) and air bubbles are injected from outside these structures. The effluent is directed down so that as the water moves down the air bubbles will move up against the flow.

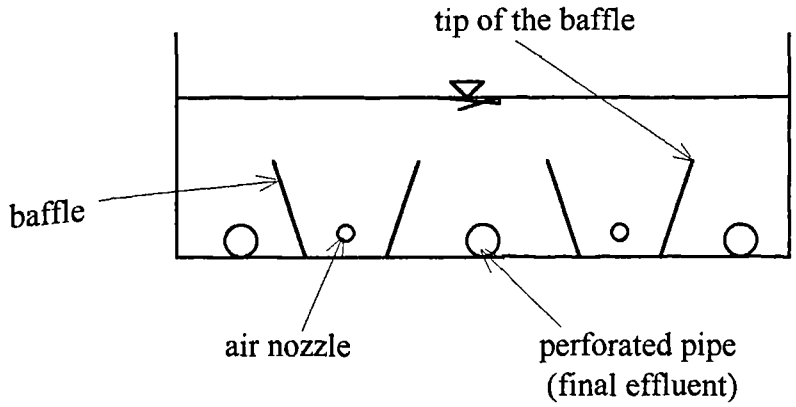

Figure 9.1 - Flotation tank with two sets of inclined baffles

3. Further improvement may be made by incorporating rapid sand filters (either as an initial filter or as a final filtration process) into the flotation tank (Figure 9.2). This concept is parallel to the DAF tanks found at Walton, Thames Water. The initial filtration is carried out using dual-filter media before final filtration using slow sand filters (Eades *et al.*, 1997). In the case of Frankley, filtered water may be collected through a series of pipes installed underneath the sand filters or through a clear water channel constructed below the filters. The typical loading rate of rapid sand filters is between 4.68 m/hr and 14.4 m/hr (Barnes *et al.*, 1981). This value is within the range of the surface loading rate of the flotation tanks found at Frankley and Trimpley (refer to Table 8.1 in Chapter 8). Hence the introduction of a rapid sand filter within the flotation tank may be possible. The use of vertical baffles can be considered if there is any operational problem with the inclined baffles.

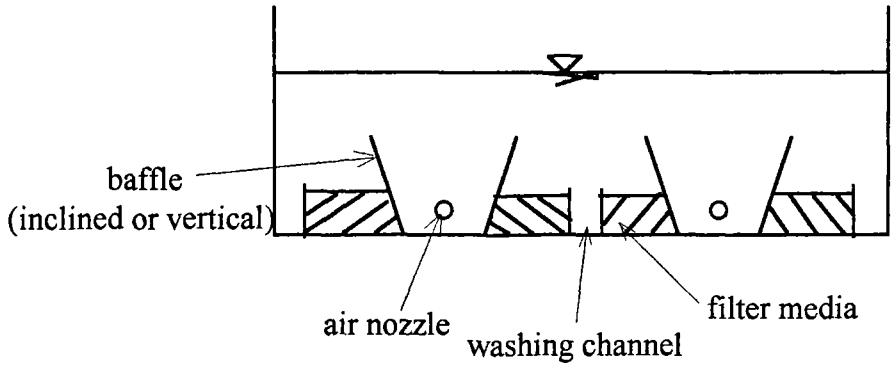

Figure 9.2 - DAF tank with filtration process

Further suggestions for future research based on the effects of tank dimensions on the velocity and turbidity distribution within the tank can be summarised as follows:

Further research should be carried out to refine the existing works by increasing the number of levels for each factor (i.e. tank physical dimension). The existing study was based on 4 different levels of width, depth and length. If the levels are increased, the precision of the estimate (statistical modelling) may be increased. In addition to that it may be useful to investigate more closely the area between one quarter depth from the surface of the tank to the surface of the tank in order to understand the behaviour of the particles within this regime.

This research work also indicated that only two different sizes of tank were investigated. An investigation should be carried out with more tanks of different sizes so that better model with a higher range of tank sizes and flow rate can be developed.

The use of CFD models should be considered to look at the in-tank variation of turbidity in relation to the independent variable such as the variation of flow rate. The CFD model should be in three dimensions since this study indicated that the velocity across the width of the tank was not uniform. Further research should also be carried out to compare the CFD model in the reaction zone with the stochastic model based on full plant studies in the reaction zone.

The separation zone was found to be ineffective for solid liquid separation to take place. Future stochastic modelling also should be concentrated in the reaction zone of the flotation cell. The controlled variables may be the velocity gradient, air dose, baffle angles and the physical dimensions of the reaction zone. Flocs size range may be used as a fixed variable. The possible use of ADV probe should be considered for the investigation.

It was claimed in the literature (Rees *et al.*, 1979, 1980) that an air dose of 8 to 10 g/m^3 is favourable in the mixing zone. However lessons learnt from the Frankley WTW indicate that the increase of air dose produces a better effluent. This result indicates the need for further research to determine the optimum air dose within the mixing zone.

Lastly but not least, further research for novel solutions to the tank configuration should be carried out, especially those of counter-current DAF used by Thames Water and the tank configurations suggested in Figures 9.1 and 9.2.

REFERENCES

Anderson S. and Lohrmann A. (1995) Open water test of the sontek acoustic doppler velocimeter. *Proc. of the IEEE Fifth Working Conf. on Current Measurement,* pp 188-192, St. Petersburg, Florida.

Atkins P. W. (1994) *Physical Chemistry,* Chap. 7. Oxford University Press.

Backhurst J. R., Harker J. H. and Porter J. E. (1974) *Problems in Mass Transfer.* Edward Arnold Ltd., London.

Barnes D., Bliss P. J. , Gould B. W. and Vallenrine H. R. (1981) *Water and Wastewater Engineering Systems,* Chap. 8. Pitman Books Ltd., London.

Barrett F. (1975) Electroflotation-development and application. *Wat. Pollut. Control* **74**, 59-62.

Batchelor G. K. (1988) *An Introduction to Fluid Dynamics.* University press, Cambridge.

Bluman A.G. (1992) *Elementary Statistics: A Step by Step Approach.* Wm. C. Brown Publ., United States.

Bratby J. and Marais G. v. R. (1974) Dissolved air flotation. *Filtration & Separation* **11**, 614-624.

Bratby J. and Marais G. v. R. (1975a) Dissolved air (pressure) flotation - an evaluation of inter-relationships between process variables and their optimisation for design. *Wat. S.A.* **1**, 57-69.

Bratby J. and Marais G. v. R. (1975b) Saturator performance in dissolved-air (pressure) flotation. *Wat. Res.* **9**, 929-936.

Bratby J. and Marais G. v. R. (1977) Flotation, In *Solid/Liquid Separation Equipment Scale-up* (Edited by Purchas D.B.) Chap. 5. Uplands Press Ltd.

Brunk B., Shirk M. W., Jensen A., Jirka G. and Lion L. W. (1996) Modelling natural hydrodynamic systems with a differential-turbulence column. *J. Hydraul. Engng* **122**, 373-380.

Bunker D. Q. Jr., Edzwald J. K., Dahlquist J. and Gillberg L. (1995) Pretreatment considerations for dissolved air flotation:water type, coagulants and flocculation. *Wat. Sci. Tech.* **31**, 63-71.

Cassell E. A., Matijevic' E., Mangravite F. J., Buzzell T. M. and Blabac S. B. (1971) Removal of colloidal pollutants by microflotation. *J. Am. Inst. Chem. Eng.* **17**, 1486-1492.

Cassell E. A., Kaufman K. M. and Matijevic' E. (1975) The effects of bubble size on microflotation. *Wat. Res.* **9**, 1017-1024.

Chatfield, C. (1992) *Statistics for Technology.* 3rd. ed., Chapman & Hall, London.

Childs A. R., Burnfield I. and Rees A. J. (1977) Operational experience with the 2300 m^3/day pilot plant of the Essex Water Company. *Papers and Proc. of the WRC Conf.:Flotation for Water and Waste Treatment.*

Cholton F. (1967) *Textbook of Fluid Dynamics*, Chap. 8. D.van nostrand co. Ltd.,London.

Clift R., Grace J. R. and Weber M. E. (1978) *Bubbles, Drops, and Particles.* Academic press, New York.

Collin G. L. and Jameson G. J. (1976) Experiment on the flotation of fine particles: The influence of particle size and charge. *Chem. Engng. Sci.* **31**, 985-991.

Collin G. L. and Jameson G. J. (1977) Double-layer effects in the flotation of fine particles. *Chem. Engng. Sci.* **32**, 239-246.

Coulson J. M., Richardson J. F., Backhurst J. R. and Harker J. H. (1991) *Chemical Engineering*, Vol. 2, Chap. 1. Pergamon Press, Oxford.

Degremont (1991) *Water Treatment Handbook*, vol.1 , 6th edition.

Draper N. R. and Smith H. (1981) *Applied Regression Analysis.* 2nd. Ed., John Wiley & Sons, New York.

Eades A. and Brignal W. J. (1995) Counter-current dissolved air flotation/filtration. *Wat. Sci. Technol.* **31**, 173-178.

Eades A., Jordan D. and Scheidler S. (1997) Counter-current dissolved air flotation COCO-DAFF. *Proc. of the CIWEM Int. Conf.: Dissolved Air Flotation,* London, 323-340.

Eckenfelder W. W. Jr. and O'Connor D .J. (1961) *Biological Waste Treatment,* Chap. 5. Pergamon Press, London.

Eckenfelder W. W. Jr., Rooney T. F., Burger T. B. and Gruspier J. T. (1958) Studies on dissolved air flotation on biological sludges, In *Biological Treatment of Sewage and Industrial Wastes, Vol. 2* (Edited by McCabe B.S. and Eckenfelder W.W.) pp 241-250, Reinhold Publishing Corp., New York.

Edwards W. M. (1984) Mass transfer and gas absorption, In *Perry's Chemical Engineers' Handbook* (Edited by Green D.W.), 6th edition. McGraw-Hill Inc.

Edzwald J. K. (1997) Contact zone modeling and the role of pretreatment in dissolved air flotation performance. *Proc. of the CIWEM Int. Conf.: Dissolved Air Flotation,* London, 9-23.

Edzwald J. K. (1996) Personal communication.

Edzwald J. K. (1995) Principles and applications of dissolved air flotation. *Wat. Sci. Tech.* **31**, 1-23.

Edzwald J. K., Bunker D. Q., Dahlquist J., Gillberg L. and Hedberg T. (1994) Dissolved air flotation: pretreatment and comparison to sedimentation. *Proc. of the 6th International Symposium on Chemical Treatment,* Gothenburg, Sweden.

Edzwald J. K. and Wingler B. J. (1990) Chemical and physical aspects of dissolved air flotation for removal of algae. *J. Wat. Supply and Technol.-Aqua* **29**, 24-35.

Edzwald J. K., Malley J.P. and Yu C. (1990) A conceptual model for dissolved air flotation in water treatment. *Wat. supply* **9**, 141-150.

Edzwald J. K. and Walsh J. P. (1992) *Dissolved Air Flotation: Laboratory and Pilot Plant Investigation.* AWWA Research Foundation and AWWA.

Edzwald J. K., Walsh J. P., Kaminski G. S. and Dunn H. J. (1992) Flocculation and requirement for dissolved air flotation. *J. Am. Wat. Wks Ass.* **84**, 92-100.

Elliott J. (1997) Personal communication (Hydraulic Research Station, Wallingford).

Ettelt G. A. (1964) Activated sludge thickening by dissolved air flotation. *Proc. 19th Ind. Waste Conf.*, Purdue Univ., 210-244.

Fair G. M., Geyer J. C. and Okun D. A. (1968) *Water and Wastewater Treatment Engineering-Volume 2*, chapter 26. John Wiley.

Fawcett N. S. J. (1997) The hydraulics of flotation tanks: computational modelling. *Proc. of the CIWEM Int. Conf.: Dissolved Air Flotation,* London, 51-71.

Flint L. R. and Howarth W. J. (1971) The collision efficiency of small particles with spherical air bubbles. *Chem. Eng. Sci.* **26**, 1155-1168.

Franklin B. C., Wilson D. anf Fawcett N. S. J. (1997) Ten years experience of dissolved air flotation in Yorkshire Water. *Proc. of the CIWEM Int. Conf.: Dissolved Air Flotation,* London, 141-160.

Friedlander S. K. (1967) Particle diffusion in low speed flows. *J. Colloid Interface Sc.* **23**, 157-164.

Fukushi K., Tambo N. and Kiyotsuka M. (1985) An experimental evaluation of kinetic process of dissolved air flotation. *J. Japan Wat. Wks Ass.* **607**, 32-41.

Fukushi K., Tambo N. and Matsui Y. (1995) A kinetic model for dissolved air flotation in water and wastewater treatment. *Wat. Sci. Technol.* **31**, 37-47.

Gaudin A. M. (1939) *Principles of Mineral Dressing,* Chap. VIII. McGraw-Hill Book Company, London.

Gerrard W. (1980) *Gas Solubilities Widespread Applications*, Chap. 1. Pergamon Press, UK.

Gochin R. J. (1990) Flotation, In *Solid-Liquid Separation* (Edited by Svarovsky L.), pp. 591-613, 3rd Edition, Butterworths, London.

Gregory R. (1997) Summary of general developments in DAF for water treatment since 1976. *Proc. of the CIWEM Int. Conf.: Dissolved Air Flotation,* London, 1-8.

Gregory R. and Zabel T. F. (1990) Sedimentation and flotation, In *Water Quality and Treatment: A Handbook of Community Water Supply/American Waterworks Ass.* (Edited by Pontius F.W.), pp. 367-453, 4th edition, McGraw Hill, Inc.

Gulas V., Benefield R. L., Lindsey R. and Randall C. (1980) Design considerations for dissolved air flotation. *Wat. & Wastewatet Sew. Wks.* **127**, 30-31,42.

Haarhoff J. and Vuuren L. R. J. van (1995) Design parameters for dissolved air flotation in South Africa. *Wat. Sci. Technol.* **31**, 203-212.

Harper J. F. (1972) The motion of bubbles and drops through liquids, In *Advances in Applied Mechanics* (Edited by Chia S. Y.) **12**, pp. 59-129, Academic Press, New York.

Heinanen J. (1988) Use of dissolved air flotation in potable water treatment in Finland. *Aqua Fennica* **18**, 113-123.

Hemming M. L., Cottrell W. R. T. and Oldfelt S. (1977) Experiences in the treatment of domestic sewage by microflotation process. *Papers and Proc. of the WRC Conf.:Flotation for Water and Waste Treatment.*

Ho C. C. and Chan C. Y. (1986) The application of lead dioxide-coated titanium anode in the electroflotation of palm oil mill effluent. *Wat. Res.* **20**, 1523-1529.

Ho C. C. and Tan Y. K. (1989) Comparison of chemical flocculation and dissolved air flotation of anaerobically treated palm oil mill effluent. *Wat. Res.* **23**, 395-400.

Hopper S. H. (1945) Water purification by flotation. *J. Am. Wat.Wks Ass.* **37**, 302.

Hopper S. H. and McCowen M. C. (1952) A floation process for water purification. *J. Am. Wat. Wks. Ass.* **44**, 719-726.

Howe R. H. L. (1958) A mathematical interpretation of flotation for solid-liquid separation, In *Biological Treatment of Sewage and Industrial Wastes, Vol. 2* (Edited by McCabe B.S. and Eckenfelder W.W.) pp 241-250, Reinhold Publishing Corp., New York.

Hudson H. E. Jr. and Wolfner J. P. (1967) Design of mixing and flocculating basins. *J. Am. Wat.Wks Ass.* **59**, 1257-1267.

Hyde R. A. (1975) Water clarification by flotation-4, design and experimental studies on a dissolved air flotation plant treating 8.2 m^3/hr of River Thames water. WRC Tech. Report TR13, Medmenham.

Hyde R. A., Miller D. G., Packham R. F. and Richards W. N. (1977) Water clarification by flotation. *J. Am. Wat. Wks Ass.* **69**, 369-374.

Jameson G. J. (1984) Experimental techniques in flotation, In *The Scientific Basis of flotation* (Edited by Ives, K. J.) pp. 53-78, NATO ASI Series, Martinus Nijhoff Publisher, The Hague.

John Brown Engineering(1991) Project report entitled: *Birmingham Water Supply Frankley Redevelopment Contract Number 1 Clarification Plant and Associated Works.*

Jones A. D. and Hall A. C. (1981) Removal of metal ions from aqueous solutions by dissolved air flotation. *Filtration & Separation* , 386-390.

Kalinske A.I.(1958) Flotation in waste treatment, In *Biological Treatment of Sewage and Industrial Wastes, Vol.2.* (Edited by McCabe B.S. and Eckenfelder W.W.) Reinhold Publishing Corp., New York.

Karamanev G. K.(1994) Rise of bubbles in quiescent liquids. *J. Am. Inst. Chem. Eng.* **40**, 1418-1421.

Katz W. J. and Wullschleger R. (1957) Studies of some variables which affect chemical flocculation when used with dissolved air flotation. *Proc.12th Purdue Ind. Waste Conf.*, Purdue Univ.,466-479.

Kaur K., Bott T. R., Heathcote G. R., Keay G. and Leadbeater B. S. C. (1994) Treatment of algal-laden water: pilot plant experiences. *J. Inst. Wat. Environ. Management* **8**, 22-32.

Kawamura S. (1976) Consideration on improving flocculation. *J. Am. Wat. Wks Ass.* **68**, 328-336.

King R. P. (1982) Flotation of fine particles, In *Principles of flotation* (Edited by King R.P.) pp 215-225, South African Institute of Mining and Metallurgy, Johannesburg.

Kitchener J. A. (1984) The froth flotation process: post and present and future-in brief, In *The scientific basis of flotation* (Edited by Ives K .J .), pp. 3-52, Nato ASI series, Martinus Nijhoff Publishers, The Hague.

Klassen V. I. and Mokrousov V. A. (1963) *An Introduction to the Theory of Flotation.* Butterworths, London.

Klute R., Langer S. and Pfeifer R. (1995) Optimization of coagulation processes prior to DAF. *Wat. Sci. Technol.* **31**, 59-62.

Kolbe F. (1997) Design and operation of six DAF installations in South Africa. *Proc. of the CIWEM Int. Conf.: Dissolved Air Flotation,* London, 429-437.

Kraus C. K., Lohrmann A. and Cabrera R. (1994) New acoustic meter for measuring 3D laboratory flow. *J. Hydraul. Engng* **120**, 406-412.

Krofta M. and Wang L. K. (1982) Potable water treatment by dissolved air flotation. *J. Am. Wat. Wks Ass.* **74**, 305-310.

Krofta M. and Wang L. K. (1985) Application of dissolved air flotation to the Lenox, Massachusetts Water Supply: water purification by flotation. *J. New England Wat. Wks Ass.* **99**, 249-264.

Krofta M., Guss D. and Wang L. K. (1987) Development of low-cost technology and systems for wastewater treatment. *Proc. 42nd Purdue Ind. Waste Conf.*, Purdue Univ., 185-195.

Krofta M., Wang L. K. and Pollman C. D. (1988) Treatment of seafood processing wastewater by dissolved air flotation, carbon adsorption and free chlorination. *Proc. 42rd Purdue Ind. Waste Conf.*, Purdue Univ.,535-550.

Krofta M. and Wang L. K. (1989) Bubble dynamics and air dispersion mechanisms of air flotation process systems, Part B:air dispersion. *Proc. 44th Purdue Ind. Waste Conf.*, Purdue Univ., 505-511.

Letterman R. D., Quon J. E. and Gemmell R. S. (1973) Influence of rapid-mix parameters on flocculation. *J. Am. Wat. Wks. Ass.* **65**, 716-722.

Levich V. G. (1962) *Physicochemical Hydrodynamics.* Prentice-hall, Inc., Englewood Cliffs, N.J.

Li W. H. and Lam S. H. (1964) *Principles of Fluid Mechanics.*Addison-Wesley Publ. Co.,Inc.Massachusetts.

Lister A. R. (1982) A study of bubble-floc attachment process in dissolved air flotation. Unpublished Ph.D. thesis, Manchester Univ.

Lohrmann A. (1996) Personal communication.

Lohrmann A. (1997) Personal communication.

Lohrmann A., Cabrera R. and Kraus C. K. (1994) Acoustic-doppler velocimeter(ADV) for laboratory use, In *Fundamentals and Advancements in Hydraulic Measurements and Experimentation* (Edited by Pugh C.A.) pp 351-365, ASCE.

Lohrmann A., Cabrera R., Gelfenbaum G. and Haines J. (1995) Direct measurements of Reynolds stress with an acoustic doppler velocimeter. *Proc. of the IEEE Fifth Working Conf. on Current Measurement,* pp 205-210, St. Petersburg, Florida.

Longhurst S. J. and Graham J. D. (1987) Dissolved air flotation for water treatment: a survey of operational units in Great Britain. *The Pub. Health Eng.* **14**, 71-76.

Lovett D. A. and Travers S. M. (1986) Dissolved air flotation for abattoir wastewater. *Wat. Res.* **20**, 421-426.

Lundgren H.(1976) Theory and practice of dissolved air flotation. *Jour. of filtration and separation* **13**, 24-28.

MacConell G. S., Harrison D. S., Kirby K. W., Lee H., Mousavipour F., Hazen and Sawyer (1991) Centrifuges vs. dissolved air flotation. *Wat. Envir. & Technol.* **3**, 60-65.

Malley J. P. Jr. (1988) A fundamental study of dissolved air flotation for treatment of low turbidity waters containing natural organic matter. Unpublished Ph.D. diss., Univ. of Massachusetts, Amherst, Mass.

Malley J. P. Jr. and Edzwald J. K. (1991a) Concepts for dissolved air flotation treatment of drinking waters. *Aqua* **40**, 7-17.

Malley J. P. Jr. and Edzwald J. K. (1991b) Laboratory comparison of DAF with conventional treatment. *J. Am. Wat. Wks Ass.* **83**, 56-61.

Mangravite F. J. Jr., Buzzell T. D., Cassell E. A., Matijevic and Saxton G. B. (1975) Removal of humic acid by coagulation and microflotation. *J. Am. Wat. Wks. Ass.* **67**, 88-94.

Martin E.B. (1996) Personal communication.

Meher K. (1997) Personal communication (Process Advisor, Severn Trent Water Ltd.).

Merrill C. W. and Pennington J. W. (1962) The magnitude and significance of flotation in the mineral industries of the United States, In *Froth Flotation 50th Anniversary Volume* (Edited by Fuerstenau D. W.) Chapter 4. The American Institute of Mining, Metallurgical, and Petroleum Engineers, Inc. New York.

Metcalfe A.V. (1996) Personal commucation.

Metcalfe A.V. (1997) Personal commucation.

Metcalfe, A. V. (1994) *Statistics in Engineering: A Practical Approach.* Chapman & Hall, London.

Montgomery, D.C. (1991) *Design and Analysis of Experiments.* 3rd. ed., John Wiley & Sons, Singapore.

Nickols D., Moerschell G. C. and Broder M. V. (1995) The first DAF water treatment plant in the United States. *Wat. Sci. Technol.* **31**, 239-246.

Noone G. (1995) Personal communication.

Φdegaard H. (1995) Optimisation of flocculation/flotation in chemical wastewater treatment. *Wat. Sci. Tech.* **31**, 73-82.

O'Neill S., Yeung H. and Oddie G. (1997) Physical modelling study of the dissolved air flotation process. *Proc. of the CIWEM Int. Conf.: Dissolved Air Flotation,* London, 75-86.

Offringa G. (1995) Dissolved air flotation in Southern Africa. *Wat. Sci. Technol.* **31**, 159-172.

O'Melia C. R. (1980) Aquasol: The behaviour of small particles in aquatic systems. *Envir. Sci. Technol.* **14,** 1052-1060.

O'Melia C. R. (1985) Particles, pretreatment and performance in water filtration. *J. of Environ. Engng.* **111**, 874-890.

Packham R. F. and Richards W. N. (1972a) Water clarification by flotation 1; a survey of the literature. WRA Tech. Paper TP87, Medmenham.

Packham R. F. and Richards W. N. (1972b) Water clarification by flotation 2; a laboratory study of the feasibility of flotation. WRA Tech. Paper TP88, Medmenham.

Packham R. F. and Richards W. N. (1975) Water clarification by flotation 3; treatment of Thames Water in a pilot-scale flotation plant. WRC Tech. Report TR2, Medmenham.

Plummer J. D., Edzwald J. K. and Kelley M. B. (1995) Removing *cryptosporidium* by dissolved-air flotation. *J. Am. Wat. Wks Ass.* **87**, 85-95.

Puffelen J. van, Buijs P. J., Nunn P. A. N. M. and Hijnen W. A. M. (1995) Dissolved air flotation in potable water treatment: the Dutch experience. *Wat. Sci. Technol.* **31**, 149-157.

Ramirez E. R. (1980) Comparative physicochemical study of industrial waste water treatment by electrolytic, dispersed and dissolved air flotation technologies. *Proc.34th Ind. Waste Conf.*, Purdue Univ., 699-709.

Reay D. and Ratcliff G. A. (1973) Removal of fine particles from water by dispersed air flotation. *The Can. J. Chem. Engng.* **51**, 178-185.

Reay D. and Ratcliff G. A. (1975) Experimental testing of the hydrodynamic collision model of fine particle flotation. *The Can. J. Chem. Engng.* **53**, 481-486.

Rees A. J., Rodman D. J. and Zabel T. F. (1979) Water clarification by flotation 5. Tech. Report TR114, Medmenham.

Rees A. J., Rodman D. J. and Zabel T. F. (1980) Dissolved air flotation for solid/liquid separation. *J. Separ. Proc. Technol.* **1**, 19-23.

Repanas K. (1992) A study of bubble generation and hydrodynamics in dissolved air flotation. Unpublished Ph.D.thesis, Univ. of Newcastle Upon Tyne.

Rosen B. and Morse J.J. (1977) Practical experience with dissolved air flotation on various waters in Sweden and Finland. *Papers and Proc. of the WRC Conf.:Flotation for Water and Waste Treatment.*

Rovel J. M. (1977) Experiences with dissolved air flotation for industrial effluent treatment. *Papers and Proc. of the WRC Conf.:Flotation for Water and Waste Treatment.*

Rubin A. J. and Lackey S. C. (1968) Effect of coagulation on the microflotation of *Bacillus Cereus. J. Am. Wat. Wks Ass* **60**, 1156-1166.

Ryan B. F. and Joiner B. L. (1994) *Minitab Handbook*, 3rd. Ed., Duxbury Press, California.

Rykaart E. M. and Haarhoff J. (1995) Behaviour of air injection nozzles in dissolved air flotation. *Wat. Sci. Technol.*, **31**, 25-35.

Schofield T., Perkins R. and Simms J.S. (1991) Frankley Water Treatment Works redevelopment pilot-scale studies. *J. Inst. Wat. Environ. Management*, **5**, 370-380.

Schofield T. (1995a) Birmingham Frankley Water Treatment Works redevelopment. *Wat. Sci. Technol.*, **31**, 213-223.

Schofield T. (1995b) Design and operation of the world's largest dissolved air flotation water treatment. *IAWQ Yearbook 1995-96*, pp.10-13.

Sebau A. U. (1997) An investigation of design characteristics of dissolved air flotation tanks. Unpublished Msc dissertation, Univ. of Newcastle Upon Tyne.

Shannon W. T. and Buisson D. H. (1980) Dissolved air flotation in hot water. *Wat. Res.* **14**, 759-765.

Shaw D. J. (1991) *Introduction to Colloid and Surface Chemistry,* Chap.1, 4th ed. Butterworth-Heinemann Ltd.

Shawcross J., Tran T., Nickols D. and Ashe C. R. (1997) Pushing the envelope: dissolved air flotation at ultra-high rate. *Proc. of the CIWEM Int. Conf.: Dissolved Air Flotation,* London, 121-139.

Shephard I. (1997)Personal communication (Hydraulic Research Station, Wallingford).

Spielman L. A. and Goren S. L. (1970) Capture of small particles by London forces from low-speed liquid flows. *Envir. Sci. Technol.* **4**, 135-140.

Spielman L. A. and Goren S. L. (1971) Capture of small particles by London forces from low-speed liquid flows. *Envir. Sci. Technol.* **5**, 254.

Spielman L. A. and Fitzpatrick J. A. (1973) Theory for particle collection under London and gravity forces. *J. Coll. Interface Sci.* **42**, 607-623.

Stork P. F. (1977) The flockation process:investigation and results obtained by treating river and well water for potable supply. *Papers and Proc. of the WRC Conf.:Flotation for Water and Waste Treatment.*

Sutherland K. L. (1948) Kinetics of the flotation process. *J. Phys. Colloid Chem.*, **52**, 394-425.

Swailes S. R. (1979) The application of dissolved air flotation to the treatment for potable use of stored eutrophic river water. Unpublished M.Phil. thesis, Essex Univ.

Ta C. T. and Brignal W. J. (1997) Application of single phase Computational Fluid Dynamics techniques to dissolved air flotation tank studies. *Proc. of the CIWEM Int. Conf.: Dissolved Air Flotation,* London, 471-487.

Tagart A. F. (1945) *Handbook of Mineral Dressing, Ores, and Industrial Minerals,* 2nd. ed., Wiley, New York.

Takahashi T., Miyahara T. and Mochizuki H. (1979) Fundamental study of bubble formation in dissolved air pressure flotation. *J. Chem. Engng. Japan* **12**, 275-280.

Tibke S. and Beaumont F. (1993) Dissolved air flotation for potable water. *Bulletin, The Inst. of Engrs. Malaysia*, Perak Branch.

Travers S. M. and Lovett D. A. (1985) Pressure flotation of abattoir wastewaters using carbon dioxide. *Wat. Res.* **19**, 1479-1482.

Usui S. and Sasaki H. (1978) Zeta potential measurements of bubbles in aqueous surfactant solutions.

Usui S., Sasaki H. and Matsukawa H. (1981) The dependence of zeta potential on bubble size as determine by Dorn effect. *Jour. of Colloid and Interface Sci.* **81**, 80-84.

Urban M. R. (1978) Aspects of bubble formation in dissolved air flotation. Unpublished Ph.D. thesis, Imperial College, London.

Vermeyen T. (1994) Laboratory and field evaluation of acoustic velocity meters, In *Fundamentals and Advancements in Hydraulic Measurements and Experimentation* (Edited by Pugh C.A.) pp 43-52, ASCE.

Vosloo P. B. V., Williams P. G. and Rademan R. G. (1986) Pilot and full-scale investigations on the use of combined dissolved-air flotation and filtration(DAFF) for water treatment. *Wat. Pollut. Control* **85**, 114-121.

Vrablik E. R. (1959) Fundamental principles of dissolved-air flotation of industrial wastes. *Proc.14th Ind. Waste Conf.*, Purdue Univ., 743-779.

Vuuren L. R. J. van, Meiring P. G. J., Henzen M. R. and Kolbe F. F. (1965) The flotation of algae in water reclamation. *Int. J. Air Wat. Pollut.* **9**, 823-832.

Vuuren L. R. J. van, Stander G. J., Henzen M. R., Meiring P. G. J. and Blerk S. H. V. van (1967) Advance purification of sewage works effluent using a combine system of lime softening and flotation. *Wat. Res.* **1**, 463-474.

Wahl T.L. (1997) Personal communication (United States Bureau of Reclaimation).

Wang L. K. and Wang M. H. S. (1989) Bubble dynamics and air dispersion mechanisms of air flotation process systems. Part A: materials balances. *Proc.44th Purdue Ind. Waste Conf.*, Purdue Univ.,493-504.

Wang L. K., Wang M. H. S. and Mahoney W. J. (1989) Treatment of storm runoff by oil-water separation, flotation, filtration and adsorption. Part B: waste and sludge management. *Proc.44th Purdue Ind. Waste Conf.*, Purdue Univ., 667-673.

Wang L. K. and Mahoney W. J. (1989) Treatment of storm runoff by oil-water separation, flotation, filtration and adsorption. Part A:wastewater treatment. *Proc.44th Ind. Waste Conf.*, Purdue Univ., 655-665.

Ward A. S. (1992) Dissolved air flotation for water and wastewater treatment. *Process Safety and Environ. Protection* **70**, 214-218.

Woodburn E. T., King R. P. and Colborn R. P. (1971) The effect of particle size distribution on the performance of a phosphate flotation process. *Met. Trans.*, **2**,3163-3174.

Yao K. M., Habibian M. T. and O'Melia C. R. (1971) Water and waste water filtration:Concept and applications. *Environ.Sci.Technol.* **5**, 1105-1112.

Zabel T. F. and Hyde R. A. (1977) Factors influencing dissolved air flotation as applied to water clarification. *Papers and Proc. of WRC Conf.:Flotation for Water and Waste Treatment.*

Zabel T. F. (1978) Flotation. Twelfth International Water Supply Congress, Kyoto, Japan.

Zabel T. F. and Melbourne J. D. (1980) Flotation. *Development in Water Treatment-1*, Applied Sci. Publ., London.

Zabel T. F. (1985) The advantage of dissolve air flotation for water treatment. *J. Am. Wat. Wks Ass.* **77**, 42-46.

Calibration of the analog output.

Calibration of the analog outputs is divided into two parts. The first part deals with the conversion from output voltage to velocity. This is done by scaling the velocity range set by the operator in the 'Main menu' of the ADV/ADF software or changing the mechanical switches in the ADVField processor module. The following equation is used to calibrate the velocity:

$$v = \frac{V - [(V\max - V\min)/2]}{(V\max - V\min)/2} \times Vrange \qquad (1)$$

where v is the velocity, V is the voltage output, $Vmax$ is the maximum voltage, $Vmin$ is the minimum voltage and $Vrange$ is the velocity range set by the operator in the 'Main Menu' of the ADV data acquisition software or by using mechanical switches in the ADVField system. The velocity ranges in the software are 3, 10, 30, 100 or 250cm/s whereas by using mechanical switches the ranges are 30, 100 and 250cm/s. The output voltage range as indicated from the previous section is 0-5 Volt. For example, the velocity range is set to ±10cm/s, a 3 Volt output from the ADVField means the velocity can be computed as follows:

$$v = \frac{3 - [(5-0)/2]}{(5-0)/2} \times 10 = 2cm/s$$

There is a possibility that there is a slight difference in voltages between the user-supplied A/D system and the output from ADV. This may be due to temperature changes or to variations in the impedance of cables and the digitising circuit. This leads to the second part to the calibration of analog outputs which can be performed by running the program ADVCALAQ.EXE. The analog outputs are set to three predetermined voltage settings that correspond to the maximum negative velocity, zero and maximum positive velocity. In the data acquisition system, the voltages of these settings can be designated as V_{neg}, V_{zero} and V_{pos}. The voltages measured during data collection (V_{mes}) can be converted to velocity by using equation 2.

$$Velocity(cm/\sec) = \frac{(2 \times V_{mes} - V_{neg} - V_{pos})}{(V_{pos} - V_{neg})} \times V_{range} \quad (2)$$

This is done by combining the correction for the voltage drop over the cable with the conversion from voltage output to velocity (equation 1). The actual output of voltage is measured by either a central data acquisition system or an accurate voltmeter/multimeter. Checking on the linearity of the analog outputs is done by running the zero-velocity calibration in ADVCALAO.EXE provided with the software. The result was checked using the following expression:

$$V_{zero} - 0.5(V_{pos} - V_{neg}) \angle \frac{V_{pos}}{2048} \quad (3)$$

Results from tank A3 of Frankley WTW

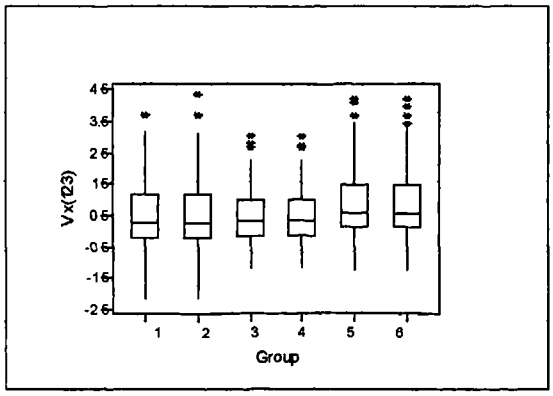

Figure A1.1 - Boxplots for velocity component in x-direction using filtered and averaging methods for run 1, 2 and 3. Note: Group 1, 3 and 5 are filtered velocity for run 1, 2 and 3 respectively and Group 2, 4 and 6 are the average velocity for run 1, 2 and 3 respectively.

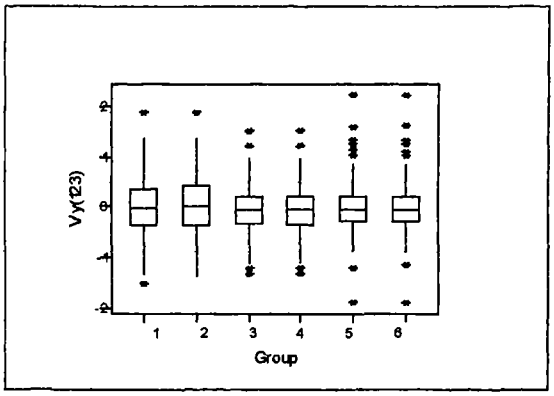

Figure A1.2 - Boxplots for velocity component in y-direction using filtered and averaging methods for run 1, 2 and 3. Note: Group 1, 3 and 5 are filtered velocity for run 1, 2 and 3 respectively and Group 2, 4 and 6 are the average velocity for run 1, 2 and 3 respectively.

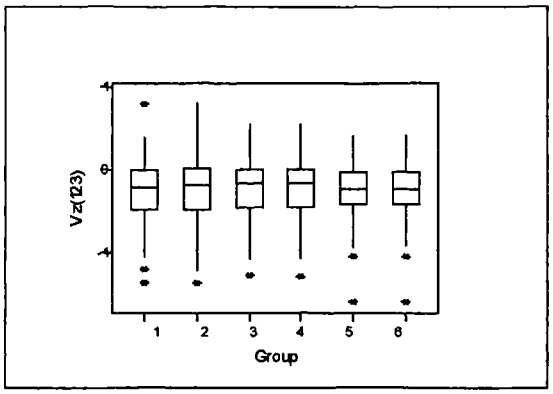

Figure A1.3 - Boxplots for velocity component in z-direction using filtered and averaging methods for run 1, 2 and 3. Note: Group 1, 3 and 5 are filtered velocity for run 1, 2 and 3 respectively and Group 2, 4 and 6 are the average velocity for run 1, 2 and 3 respectively.

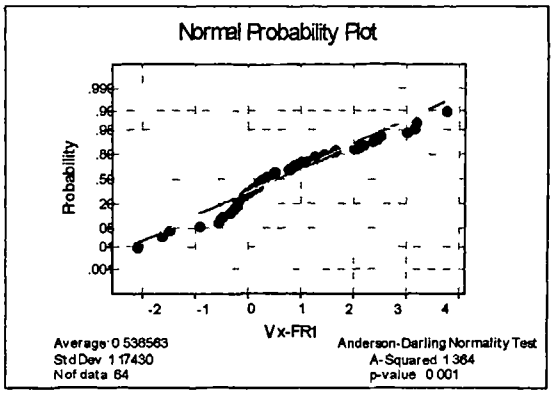

Figure A1.4 - Normal probability plot of velocity in x-direction(filtered) for Run 1

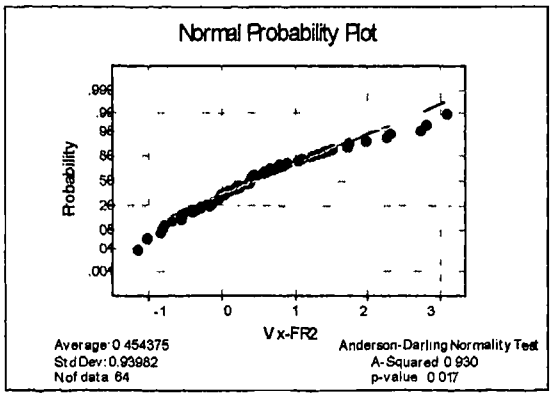

Figure A1.5 - Normal probability plot of velocity in x-direction(filtered) for Run 2

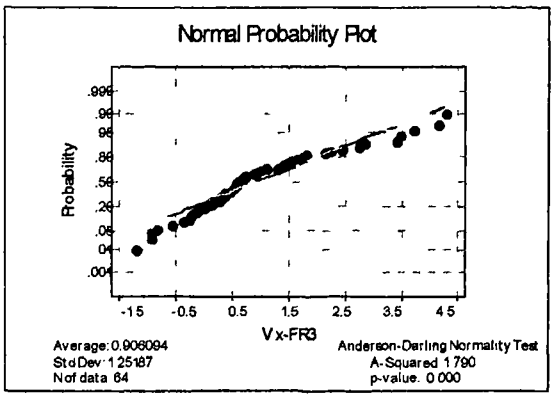

Figure A1.6 - Normal probability plot of velocity in x-direction(filtered) for Run 3

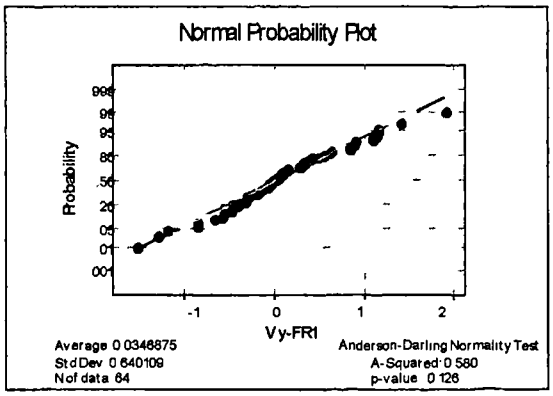

Figure A1.7 - Normal probability plot of velocity in y-direction(filtered) for Run 1.

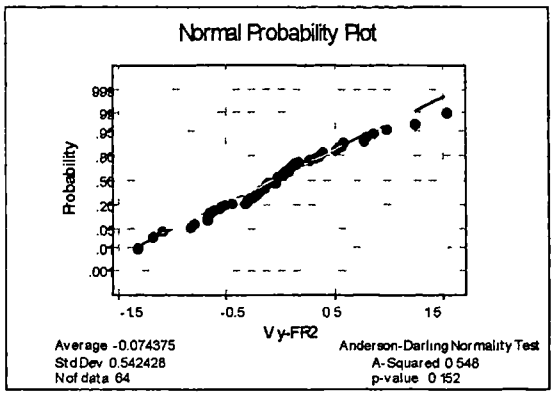

Figure A1.8 - Normal probability plot of velocity in y-direction(filtered) for Run 2.

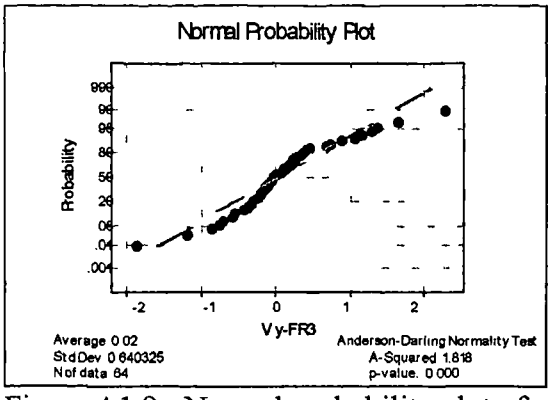

Figure A1.9 - Normal probability plot of velocity in y-direction(filtered) for Run 3

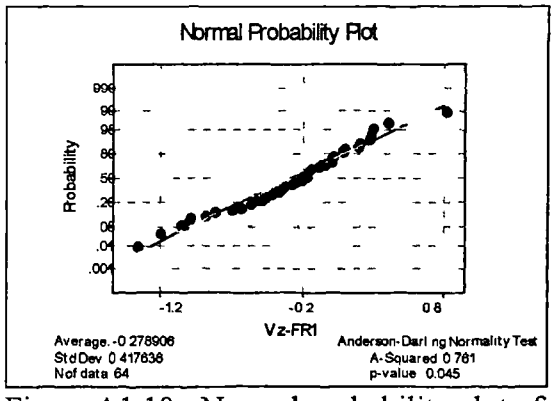

Figure A1.10 - Normal probability plot of velocity in z-direction(filtered) for Run 1.

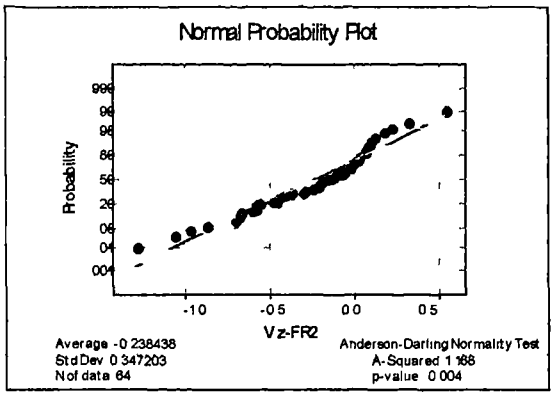

Figure A1.11 - Normal probability plot of velocity in z-direction(filtered) for Run 2.

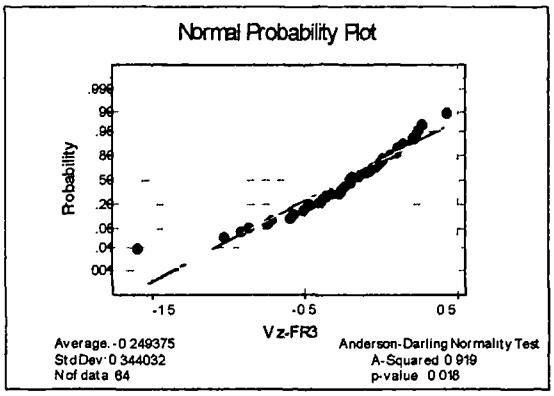

Figure A1.12 - Normal probability plot of velocity in z-direction(filtered) for Run 3.

Table A1.1 - ANOVA for velocities(x-direction)Vx in run 1, 2 and 3.

Source	DF	SS	MS	F	p
Group	5	14.51	2.90	2.20	0.054
Error	378	498.70	1.32		
Total	383	513.22			

Table A1.2 - Confidence interval for velocity mean Vx

INDIVIDUAL 95% CI'S FOR MEAN
BASED ON POOLED STDEV

LEVEL	N	MEAN	STDEV	-----+---------+---------+---------+-
1	64	0.537	1.174	(---------*--------)
2	64	0.562	1.285	(---------*--------)
3	64	0.454	0.940	(--------*---------)
4	64	0.457	0.936	(--------*---------)
5	64	0.906	1.252	(--------*---------)
6	64	0.907	1.248	(--------*---------)

POOLED STDEV = 1.149 -----+---------+---------+---------+-
0.30 0.60 0.90 1.20

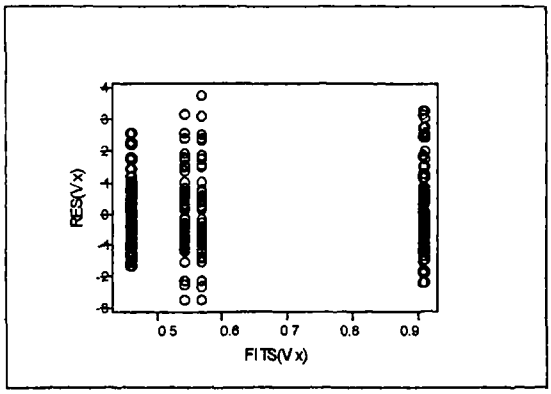

Figure A1.13 - Plot of residual versus fitted values from the ANOVA for velocities(filtered and average) in x-direction.

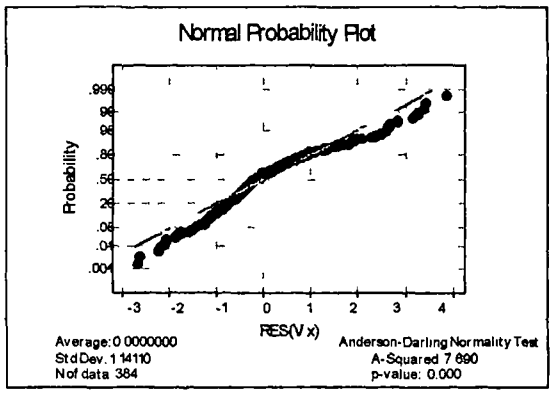

Figure A1.14 - Normal probability plot of residuals from the ANOVA for velocities(filtered and average) in x-direction.

Table A1.3 - ANOVA for velocities(*y*-direction)*Vy* in run 1, 2 and 3.

Source	DF	SS	MS	F	p
Group	5	0.984	0.197	0.52	0.760
Error	378	142.716	0.378		
Total	383	143.700			

Table A1.4 - Confidence interval for velocity mean *Vy*

```
                                    INDIVIDUAL 95% CI'S FOR MEAN
                                    BASED ON POOLED STDEV
LEVEL    N    MEAN    STDEV ---------+---------+---------+-------
    1   64  0.0347   0.6401          (-----------*-----------)
    2   64  0.0471   0.6709           (-----------*-----------)
    3   64 -0.0744   0.5424 (-----------*-----------)
    4   64 -0.0752   0.5414 (-----------*-----------)
    5   64  0.0200   0.6403          (-----------*-----------)
    6   64  0.0218   0.6389          (-----------*-----------)
                             ---------+---------+---------+-------
POOLED STDEV =  0.6145             -0.12     -0.00      0.12
```

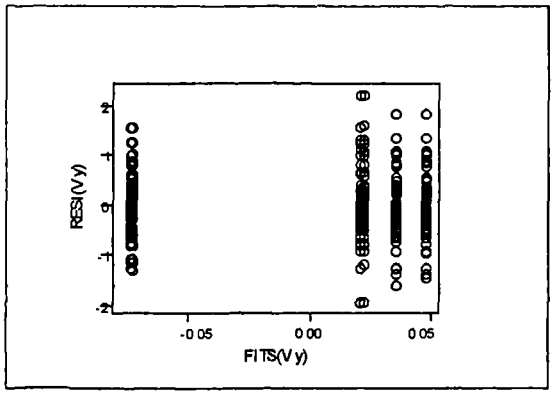

Figure A1.15 - Plot of residual versus fitted values from the ANOVA for velocities(filtered and average) in *y*-direction.

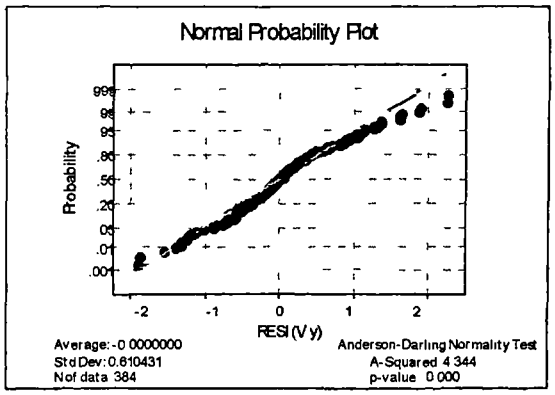

Figure A1.16 - Normal probability plot of residuals from the ANOVA for velocities(filtered and average) in *y*-direction.

Table A1.5 - ANOVA for velocities(y-direction)Vz in run 1, 2 and 3.

Source	DF	SS	MS	F	p
Group	5	0.077	0.015	0.11	0.990
Error	378	52.599	0.139		
Total	383	52.676			

Table A1.6 - Confidence interval for velocity mean *Vz*

LEVEL	N	MEAN	STDEV	INDIVIDUAL 95% CI'S FOR MEAN BASED ON POOLED STDEV
1	64	-0.2789	0.4176	(----------*----------)
2	64	-0.2587	0.4277	(----------*----------)
3	64	-0.2384	0.3472	(----------*----------)
4	64	-0.2372	0.3473	(----------*----------)
5	64	-0.2494	0.3440	(----------*----------)
6	64	-0.2476	0.3435	(----------*----------)

POOLED STDEV = 0.3730 -0.350 -0.280 -0.210 -0.140

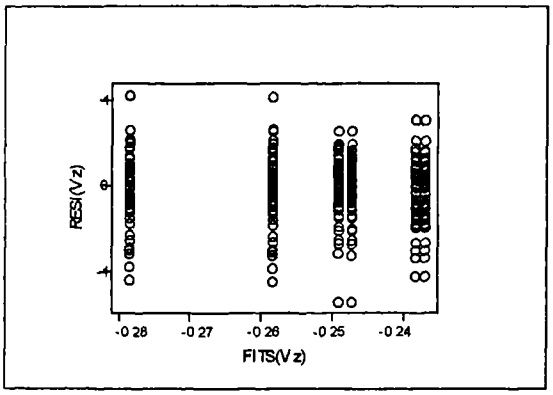

Figure A1.17 - Plot of residual versus fitted values from the ANOVA for velocities(filtered and average) in *z*-direction.

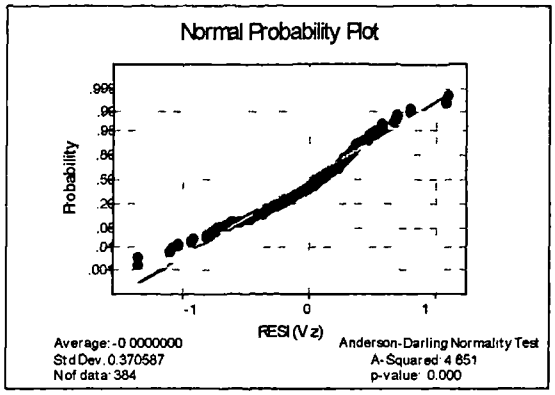

Figure A1.18 - Normal probability plot of residuals from the ANOVA for velocities(filtered and average) in z-direction.

Table A1.7 - Analysis of variance for velocities in x-direction(run 1,2 & 3) using multifactor balanced designs

Source	DF	SS	MS	F	P
Width	3	14.8351	4.9450	11.59	0.000
Depth	3	30.4302	10.1434	23.77	0.000
Length	3	54.6521	18.2174	42.69	0.000
Width*Depth	9	2.0466	0.2274	0.53	0.848
Width*Length	9	12.1903	1.3545	3.17	0.002
Depth*Length	9	61.2139	6.8015	15.94	0.000
Width*Depth*Length	27	18.5612	0.6875	1.61	0.042
Error	128	54.6166	0.4267		
Total	191	248.5461			

Note: * is for interaction

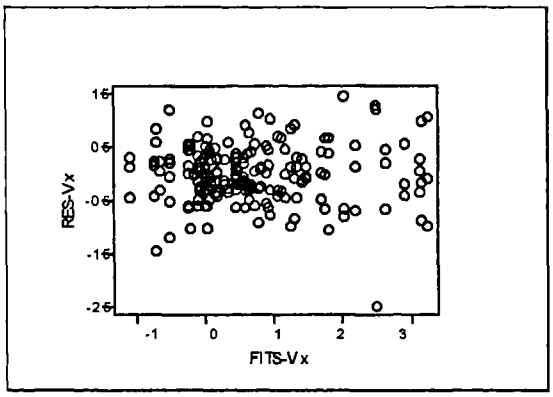

Figure A1.19 - Plot of residuals versus fitted values from the analysis of variance for velocities in x-direction

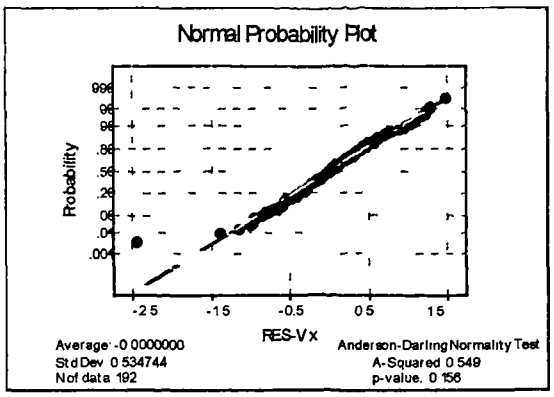

Figure A1.20 - Normal probability plot of residuals from the analysis of variance for velocities in x-direction

Table A1.8 - Analysis of Covariance for Vx

Source	DF	ADJ. SS	MS	F	P
Covariates	1	3.6043	3.6043	9.28	0.003
Width	3	17.4492	5.8164	14.97	0.000
Depth	3	33.7177	11.2392	28.93	0.000
Length	3	51.4815	17.1605	44.16	0.000
Width*Depth	9	2.2111	0.2457	0.63	0.768
Width*Length	9	12.9697	6.9993	18.01	0.000
Depth*Length	9	62.9935	6.9993	18.01	0.000
Width*Depth*Length	27	16.4179	0.6081	1.56	0.052
Error	127	49.3467	0.3886		
Total	191	248.6640			

Note: * is for interaction

Table A1.9 - Analysis of variance for velocities in z-direction(run 1,2 & 3) using multifactor balanced designs

Source	DF	SS	MS	F	P
Width	3	0.18217	0.06072	0.96	0.414
Depth	3	2.50115	0.83372	13.17	0.000
Length	3	8.90787	2.96929	46.90	0.000
Width*Depth	9	0.78527	0.08725	1.38	0.205
Width*Length	9	0.64891	0.07210	1.14	0.340
Depth*Length	9	3.08185	0.34243	5.41	0.000
Width*Depth*Length	27	1.49904	0.05552	0.88	0.642
Error	128	8.10347	0.06331		
Total	191	25.70972			

Note: * is for interaction

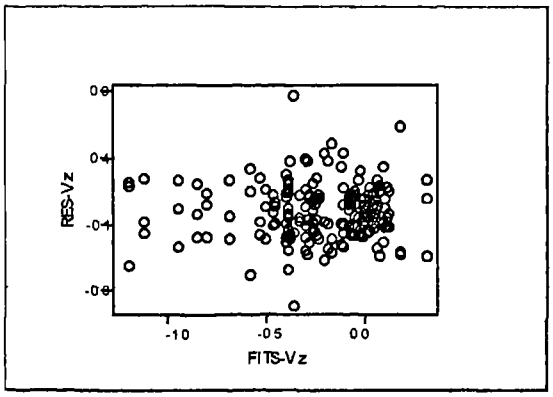

Figure A1.21 - Plot of residuals versus fitted values from the analysis of variance for velocities in z-direction

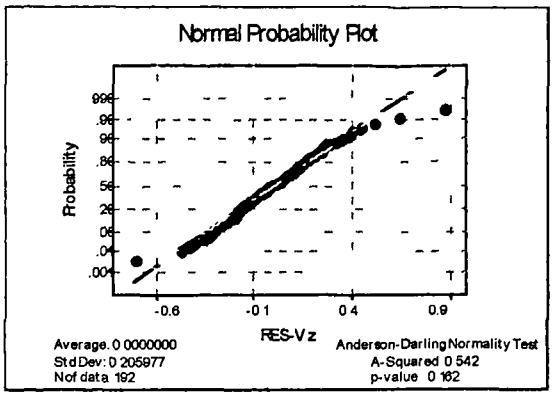

Figure A1.22 - Normal probability plot of residuals from the analysis of variance for velocities in z-direction

Table A1.10 - Analysis of Covariance for Vz

Source	DF	ADJ. SS	MS	F	P
Covariates	1	0.00672	0.00672	0.12	0.724
Width	3	0.36977	0.12326	2.29	0.081
Depth	3	3.09192	1.03064	19.15	0.000
Length	3	10.28514	3.42838	63.70	0.000
Width*Depth	9	0.51924	0.05769	1.07	0.388
Width*Length	9	0.66775	0.07419	1.38	0.204
Depth*Length	9	2.76413	0.30713	5.71	0.000
Width*Depth*Length	27	1.54876	0.05736	1.07	0.390
Error	127	6.83501	0.05382		
Total	191	26.09574			

Note: * is for interaction

Results from tank C7 of Trimpley WTW

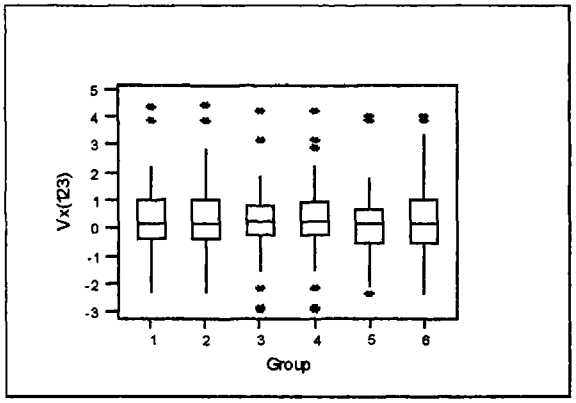

Figure A2.1 - Boxplots for velocity component in x-direction using filtered and averaging methods for run 1, 2 and 3.
Note: Group 1, 3 and 5 are filtered velocity for run 1, 2 and 3 respectively and Group 2, 4 and 6 are the average velocity for run 1, 2 and 3 respectively.

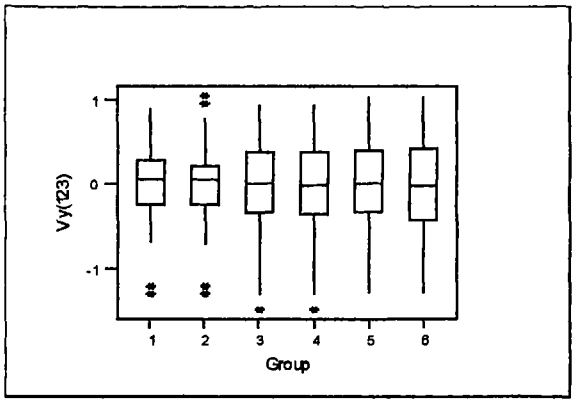

Figure A2.2 - Boxplots for velocity component in y-direction using filtered and averaging methods for run 1, 2 and 3.
Note: Group 1, 3 and 5 are filtered velocity for run 1, 2 and 3 respectively and Group 2, 4 and 6 are the average velocity for run 1, 2 and 3 respectively.

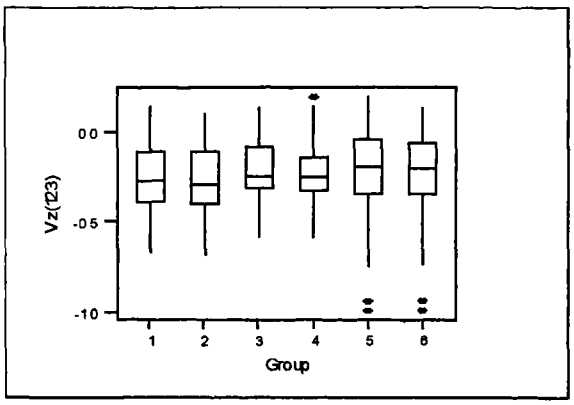

Figure A2.3 - Boxplots for velocity component in z-direction using filtered and averaging methods for run 1, 2 and 3.
Note: Group 1, 3 and 5 are filtered velocity for run 1, 2 and 3 respectively and Group 2, 4 and 6 are the average velocity for run 1, 2 and 3 respectively.

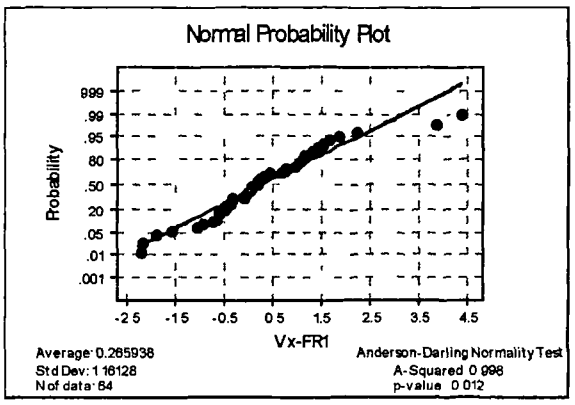

Figure A2.4 - Normal probability plot of velocity in x-direction(filtered) for Run 1

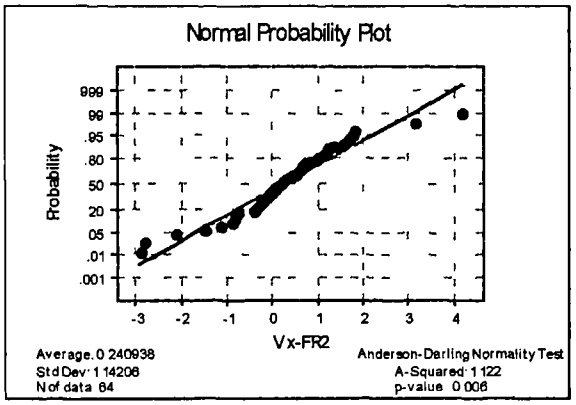

Figure A2.5 - Normal probability plot of velocity in x-direction(filtered) for Run 2

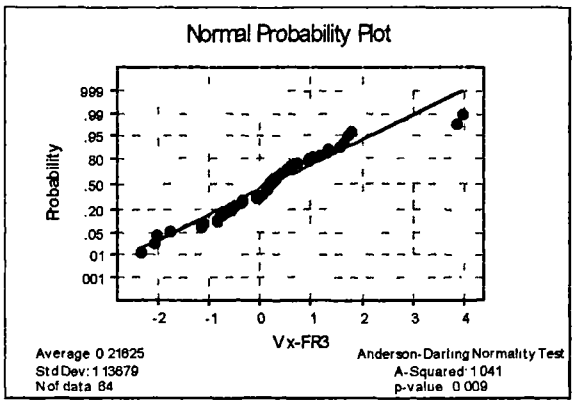

Figure A2.6 - Normal probability plot of velocity in x-direction(filtered) for Run 3

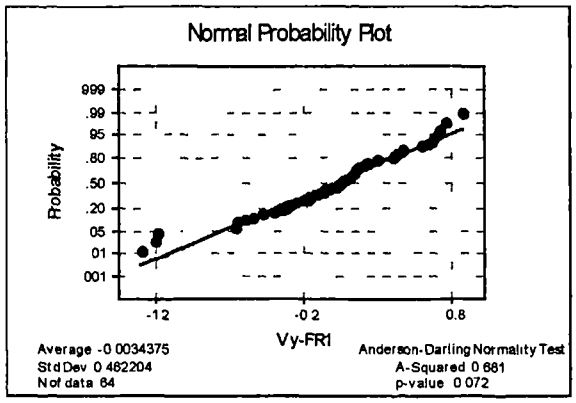

Figure A2.7 - Normal probability plot of velocity in y-direction(filtered) for Run 1.

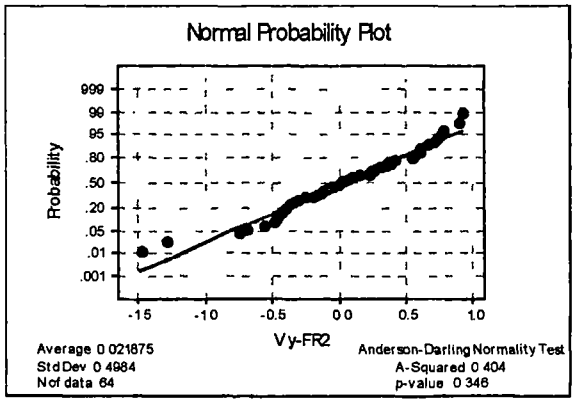

Figure A2.8 - Normal probability plot of velocity in y-direction(filtered) for Run 2.

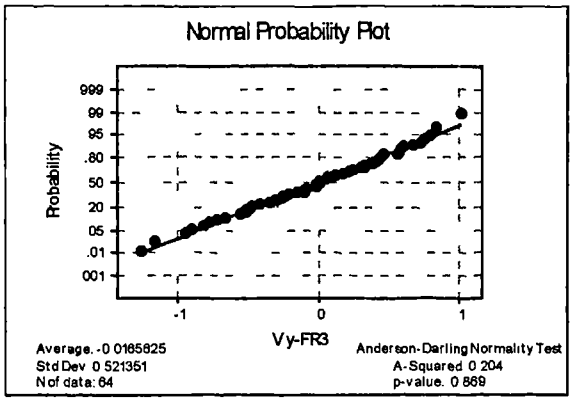

Figure A2.9 - Normal probability plot of velocity in y-direction(filtered) for Run 3

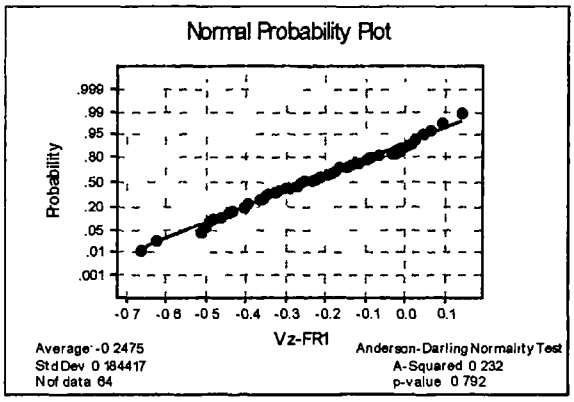

Figure A2.10 - Normal probability plot of velocity in z-direction(filtered) for Run 1

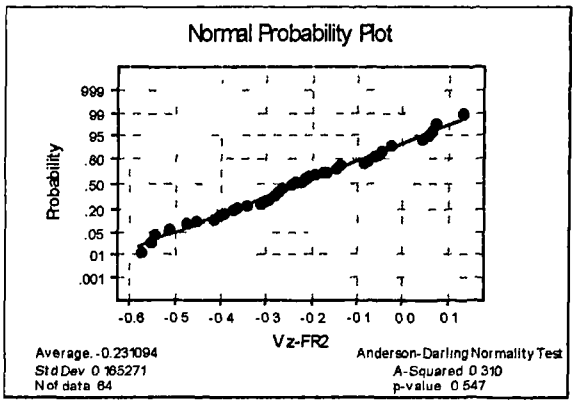

Figure A2.11 - Normal probability plot of velocity in z-direction(filtered) for Run 2

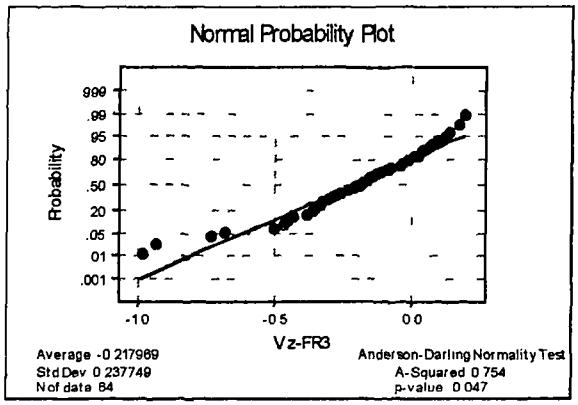

Figure A2.12 - Normal probability plot of velocity in z-direction(filtered) for Run 3.

Table A2.1 - ANOVA for velocities(x-direction)Vx in run 1, 2 and 3.

Source	DF	SS	MS	F	p
Group	5	0.80	0.16	0.11	0.990
Error	378	545.19	1.44		
Total	383	546.00			

Table A2.2 - Confidence interval for velocity mean Vx

LEVEL	N	MEAN	STDEV	INDIVIDUAL 95% CI'S FOR MEAN BASED ON POOLED STDEV
1	64	0.266	1.161	(----------*----------)
2	64	0.343	1.265	(----------*----------)
3	64	0.241	1.142	(----------*----------)
4	64	0.330	1.251	(----------*----------)
5	64	0.216	1.137	(----------*----------)
6	64	0.298	1.242	(----------*----------)
POOLED STDEV =		1.201		0.00 0.20 0.40 0.60

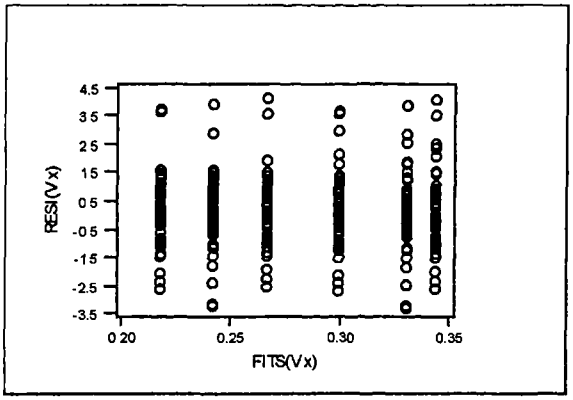

Figure A2.13 - Plot of residual versus fitted values from the ANOVA for velocities(filtered and average) in x-direction.

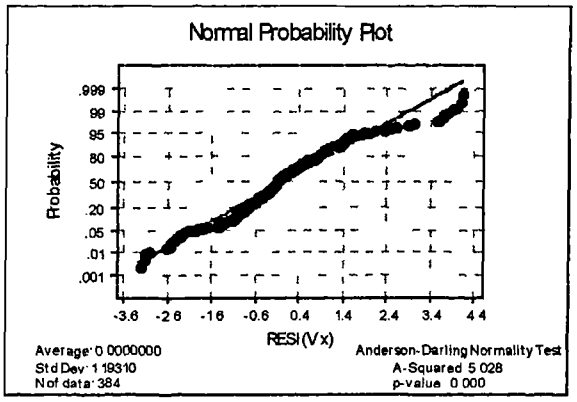

Figure A2.14 - Normal probability plot of residuals from the ANOVA for velocities(filtered and average) in x-direction.

Table A2.3 - ANOVA for velocities(y-direction)Vy in run 1, 2 and 3.

Source	DF	SS	MS	F	p
Group	5	0.081	0.016	0.06	0.997
Error	378	94.291	0.249		
Total	383	94.371			

Table A2.4 - Confidence interval for velocity mean Vy

```
                                    INDIVIDUAL 95% CI'S FOR MEAN
                                    BASED ON POOLED STDEV
LEVEL    N    MEAN     STDEV  ---------+---------+---------+-------
    1   64  -0.0034    0.4622    (---------------*---------------)
    2   64  -0.0031    0.4788    (---------------*---------------)
    3   64   0.0219    0.4984      (---------------*---------------)
    4   64   0.0077    0.4954      (---------------*---------------)
    5   64  -0.0166    0.5214   (---------------*---------------)
    6   64  -0.0216    0.5368   (---------------*---------------)
                                 ---------+---------+---------+-------
POOLED STDEV =  0.4994            -0.080    0.000    0.080
```

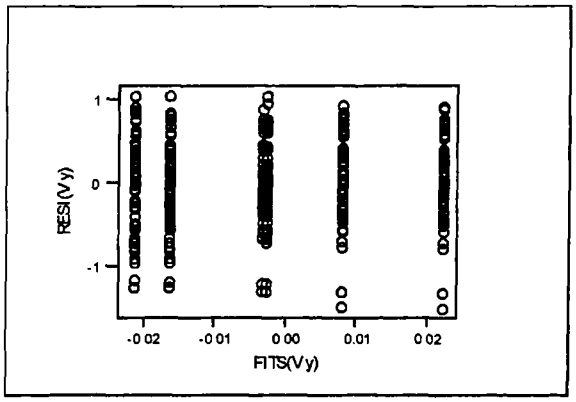

Figure A2.15 - Plot of residual versus fitted values from the ANOVA for velocities (filtered and average) in y-direction.

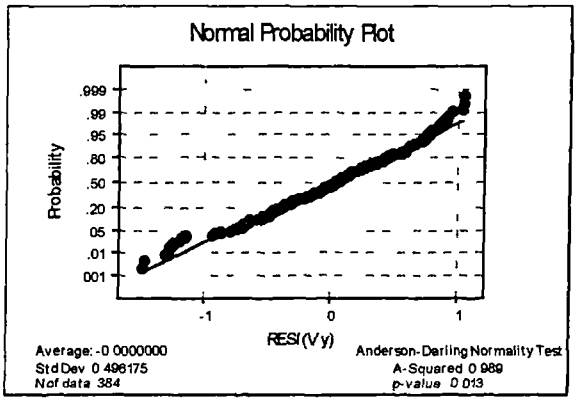

Figure A2.16 - Normal probability plot of residuals from the ANOVA for velocities (filtered and average) in y-direction.

Table A2.5 - ANOVA for velocities(y-direction)Vz in run 1, 2 and 3.

Source	DF	SS	MS	F	p
Group	5	0.0647	0.0129	0.33	0.893
Error	378	14.6767	0.0388		
Total	383	14.7414			

Table A2.6 - Confidence interval for velocity mean *Vz*

LEVEL	N	MEAN	STDEV	INDIVIDUAL 95% CI'S FOR MEAN BASED ON POOLED STDEV
1	64	-0.2475	0.1844	(----------*----------)
2	64	-0.2588	0.1845	(----------*----------)
3	64	-0.2311	0.1653	(----------*----------)
4	64	-0.2350	0.1684	(----------*----------)
5	64	-0.2180	0.2377	(----------*----------)
6	64	-0.2320	0.2296	(----------*----------)

POOLED STDEV = 0.1970 -0.280 -0.240 -0.200

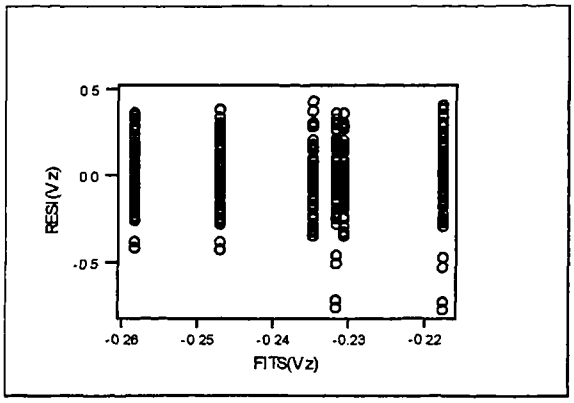

Figure A2.17 - Plot of residual versus fitted values from the ANOVA for velocities (filtered and average) in *z*-direction.

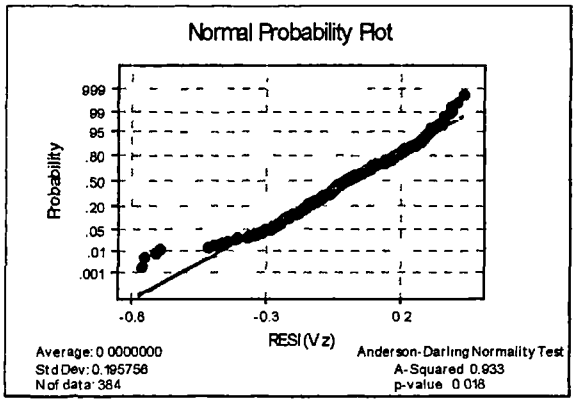

Figure A2.18 - Normal probability plot of residuals from the ANOVA for velocities (filtered and average) in *z*-direction.

Table A2.7 - Analysis of variance for velocities in x-direction(run 1,2 & 3) using multifactor balanced designs

Source	DF	SS	MS	F	P
Width	3	9.3473	3.1158	21.85	0.000
Depth	3	101.8784	33.9595	238.14	0.000
Length	3	15.3661	5.1220	35.92	0.000
Width*Depth	9	20.9559	2.3284	16.33	0.000
Width*Length	9	3.2435	0.3604	2.53	0.011
Depth*Length	9	48.6216	5.4024	37.88	0.000
Width*Depth*Length	27	30.9588	1.1466	8.04	0.000
Error	128	18.2530	0.1426		
Total	191	248.6246			

Note: * is for interaction

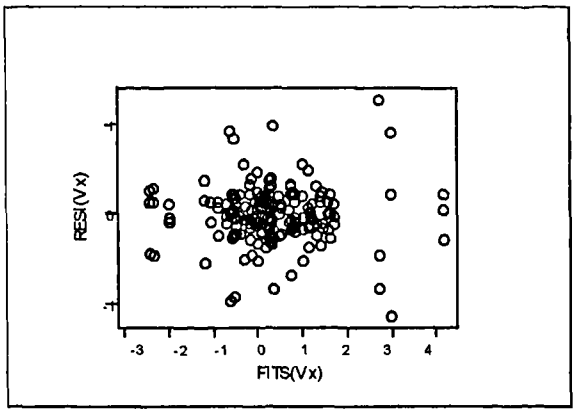

Figure A2.19 - Plot of residuals versus fitted values from the analysis of variance for velocities in x-direction

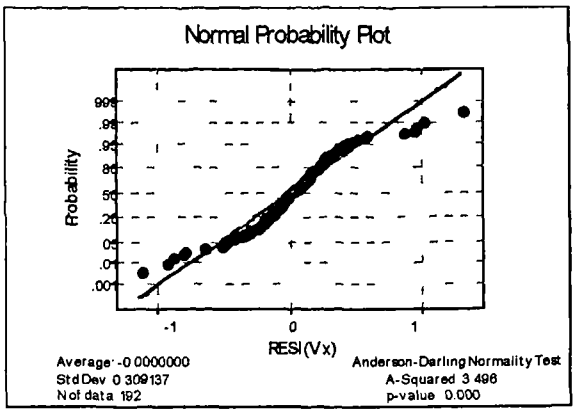

Figure A2.20 - Normal probability plot of residuals from the analysis of variance for velocities in x-direction

Table A2.8 - Analysis of Covariance for Vx(Tank C7)

Source	DF	ADJ. SS	MS	F	P
Covariates	1	0.0091	0.0091	0.06	0.802
Width	3	9.3537	3.1179	21.70	0.000
Depth	3	101.8875	33.9625	236.42	0.000
Length	3	14.8565	4.9522	34.47	0.000
Width*Depth	9	20.9599	2.3289	16.21	0.000
Width*Length	9	3.0053	0.3339	2.32	0.019
Depth*Length	9	48.6069	5.4008	37.60	0.000
Width*Depth*Length	27	30.8971	1.1443	7.97	0.000
Error	127	18.2439	0.1437		
Total	191	248.6246			

Note: * is for interaction

Table A2.9 - Analysis of variance for velocities in z-direction(run 1,2 & 3) using multifactor balanced designs

Source	DF	SS	MS	F	P
Width	3	0.061385	0.020462	2.07	0.107
Depth	3	0.990994	0.330331	33.45	0.000
Length	3	3.286790	1.095597	110.96	0.000
Width*Depth	9	0.202352	0.022484	2.28	0.021
Width*Length	9	0.346073	0.038453	3.89	0.000
Depth*Length	9	0.833481	0.092609	9.38	0.000
Width*Depth*Length	27	0.467540	0.017316	1.75	0.020
Error	128	1.263867	0.009874		
Total	191	7.452481			

Note: * is for interaction

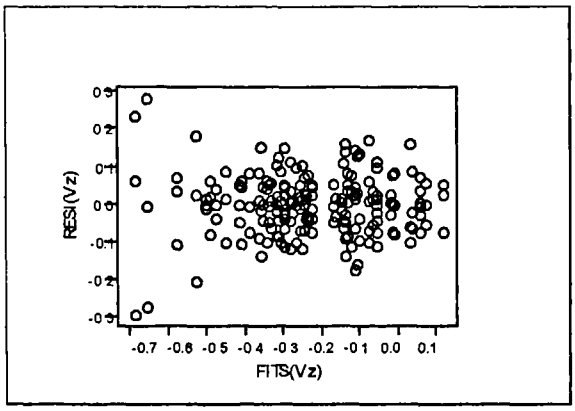

Figure A2.21 - Plot of residuals versus fitted values from the analysis of variance for velocities in z-direction

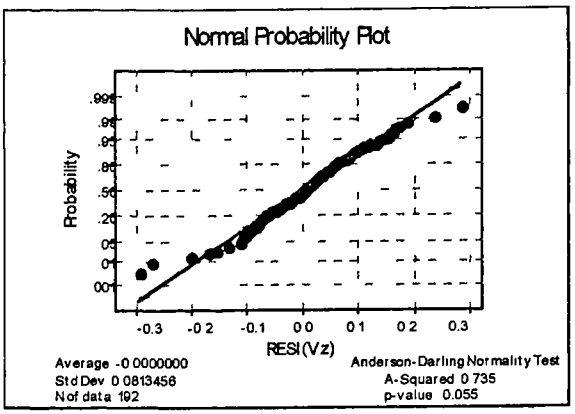

Figure A2.22 - Normal probability plot of residuals from the analysis of variance for velocities in z-direction

Table A2.10 - Analysis of Covariance for Vz(Tank C7,Trimpley WTW)

Source	DF	ADJ. SS	MS	F	P
Covariates	1	0.24166	0.24166	30.02	0.000
Width	3	0.04785	0.01595	1.98	0.120
Depth	3	0.98564	0.32855	40.82	0.000
Length	3	2.73531	0.91177	113.28	0.000
Width*Depth	9	0.21156	0.02351	2.92	0.004
Width*Length	9	0.27872	0.03097	3.85	0.000
Depth*Length	9	0.82851	0.09206	11.44	0.000
Width*Depth*Length	27	0.46134	0.01709	2.12	0.003
Error	127	1.02221	0.00805		
Total	191	7.45248			

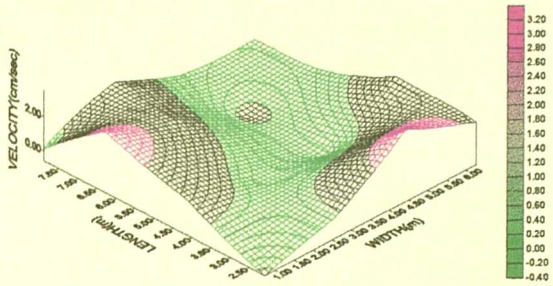

Figure B1.1 - Velocity Vx(run 1) at depth D4

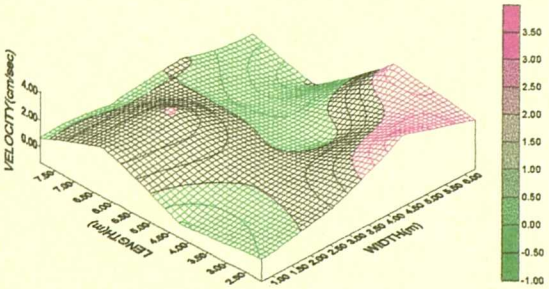

Figure B1.5 - Velocity Vx(run 2) at depth D4

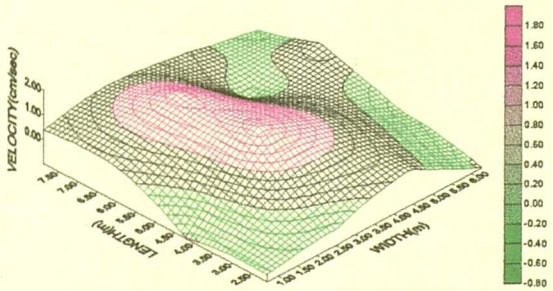

Figure B1.2 - Velocity Vx(run 1) at depth D3

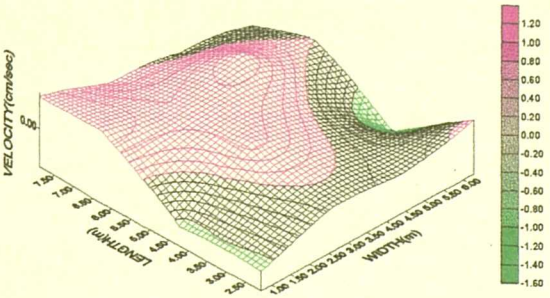

Figure B1.6 - Velocity Vx(run 2) at depth D3

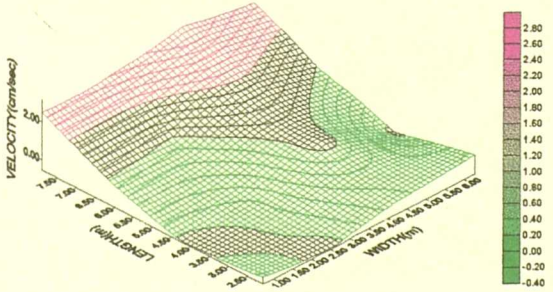

Figure B1.3 - Velocity Vx(run 1) at depth D2

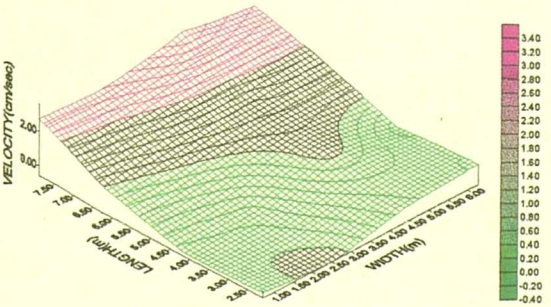

Figure B1.7 - Velocity Vx(run 2) at depth D2

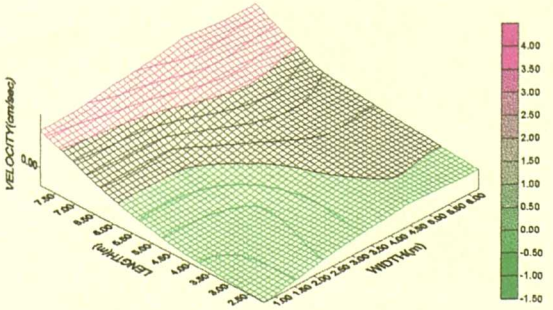

Figure B1.4 - Velocity Vx(run 1) at depth D1

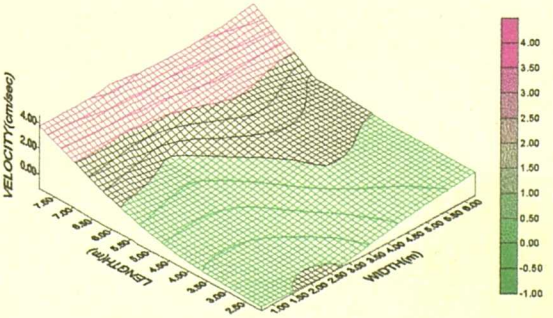

Figure B1.8 - Velocity Vx(run 2) at Depth D1

Note: Velocity scale is not the same for each diagram

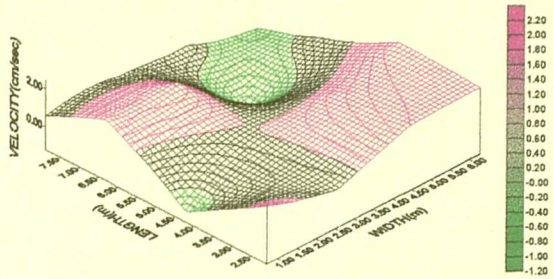

Figure B1.9 - Velocity Vx(run 3) at depth D4

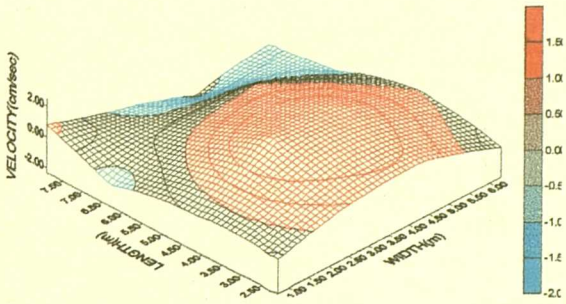

Figure B1.13 - Velocity Vy(run 1) at depth D4

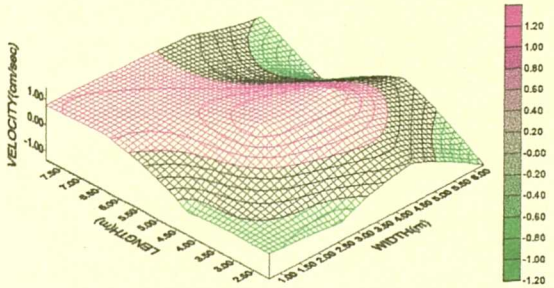

Figure B1.10 - Velocity Vx(run 3) at depth D3

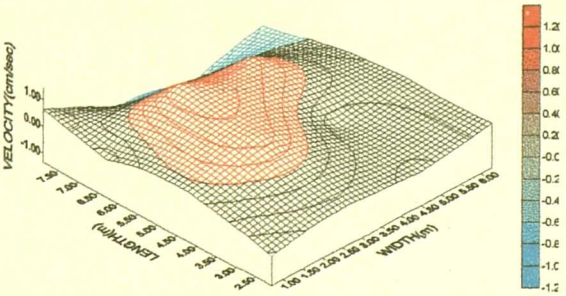

Figure B1.14 - Velocity Vy(run 1) at depth D3

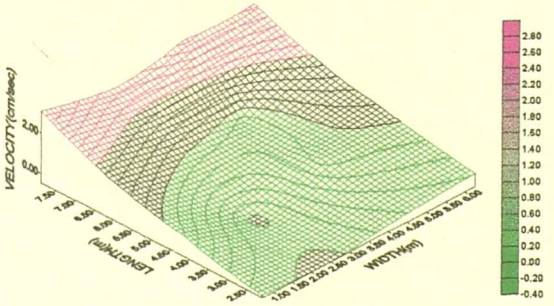

Figure B1.11 - Velocity Vx(run 3) at depth D2

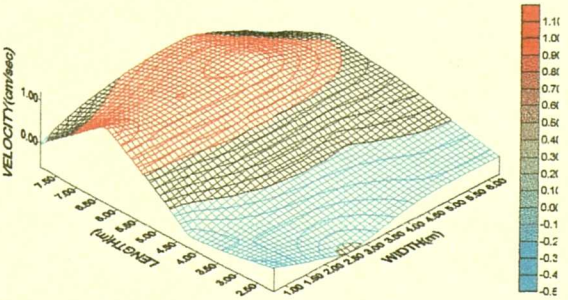

Figure B1.15 - Velocity Vy(run 1) at depth D2

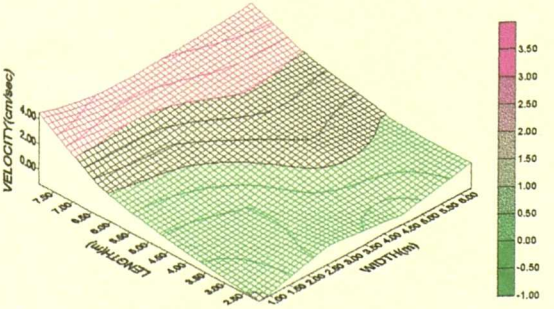

Figure B1.12 - Velocity Vx(run 3) at depth D1

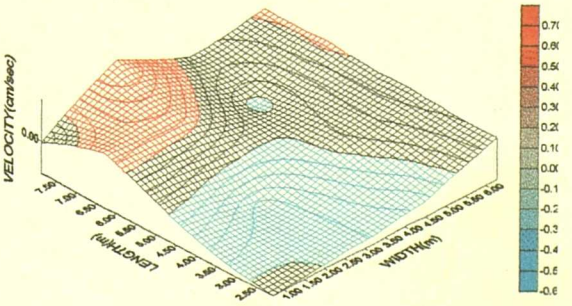

Figure B1.16 - Velocity Vy(run 1) at depth D1

Note: Velocity scale is not the same for each diagram

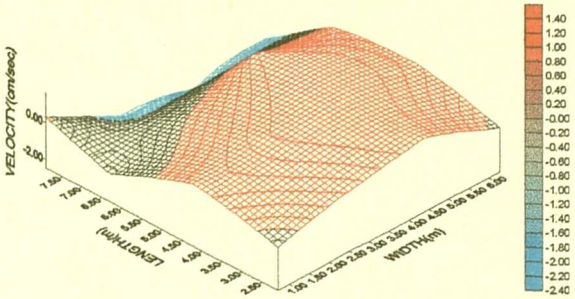

Figure B1.17 - Velocity Vy(run 2) at depth D4

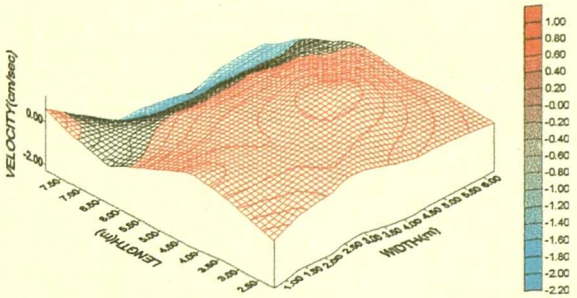

Figure B1.21 - Velocity Vy(run 3) at depth D4

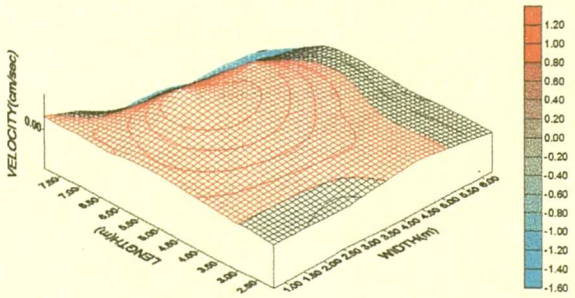

Figure B1.18 - Velocity Vy(run 2) at depth D3

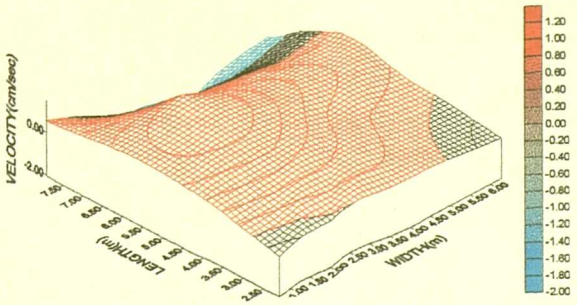

Figure B1.22 - Velocity Vy(run 3) at depth D3

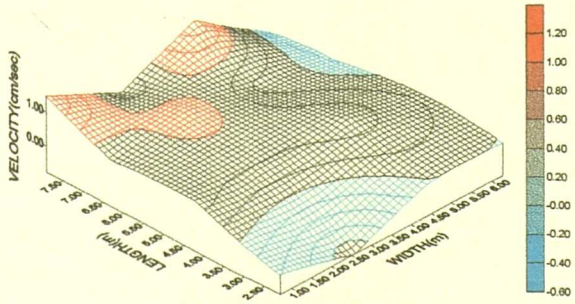

Figure B1.19 - Velocity Vy(run 2) at depth D2

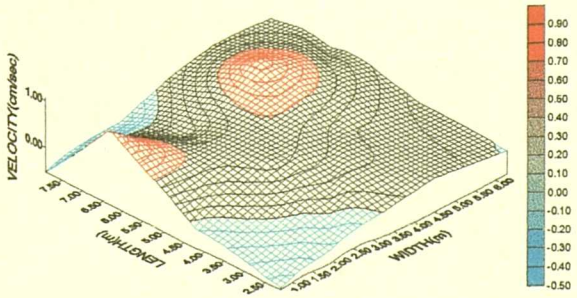

Figure B1.23 - Velocity Vy(run 3) at depth D2

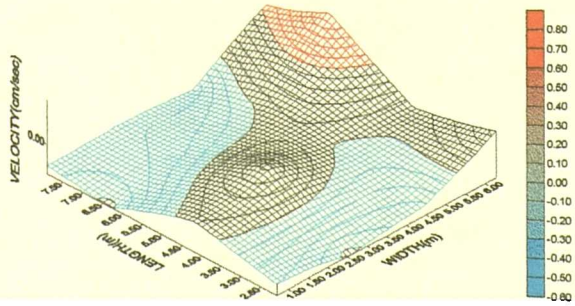

Figure B1.20 - Velocity Vy(run 2) at depth D1

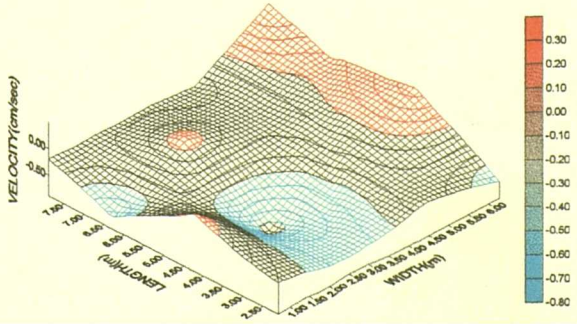

Figure B1.24 - Velocity Vy(run 3) at depth D1

Note: Velocity scale is not the same for each diagram

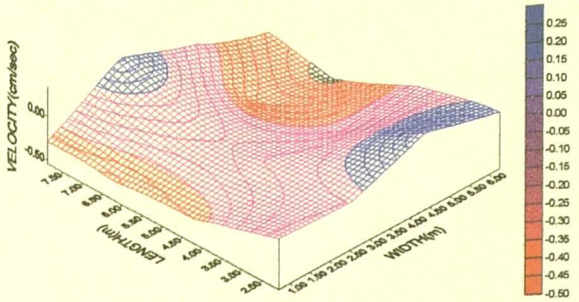

Figure B1.25 - Velocity Vz(run 1) at depth D4

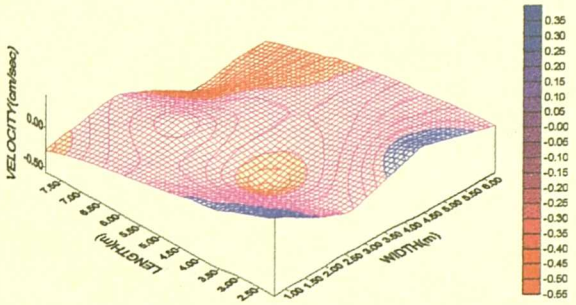

Figure B1.29 - Velocity Vz(run 2) at depth D4

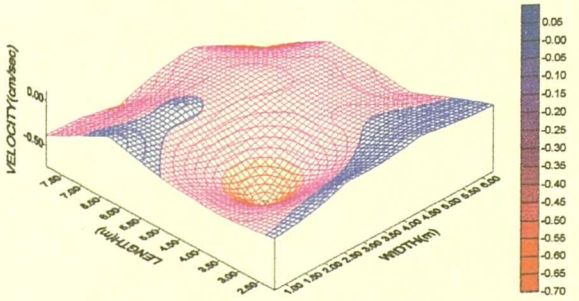

Figure B1.26 - Velocity Vz(run 1) at depth D3

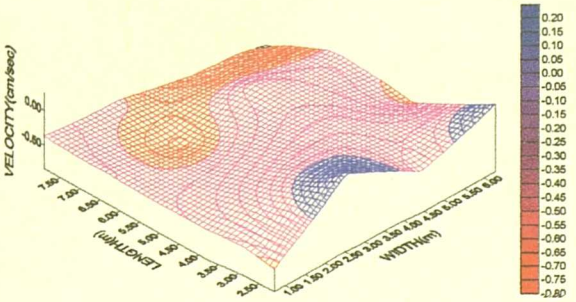

Figure B1.30 - Velocity Vz(run 2) at depth D3

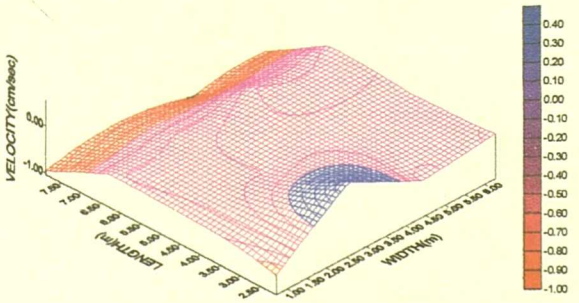

Figure B1.27 - Velocity Vz(run 1) at depth D2

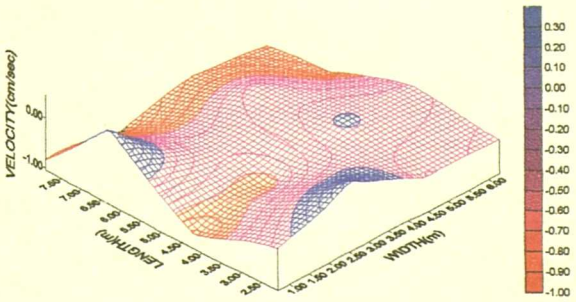

Figure B1.31 - Velocity Vz(run 2) at depth D2

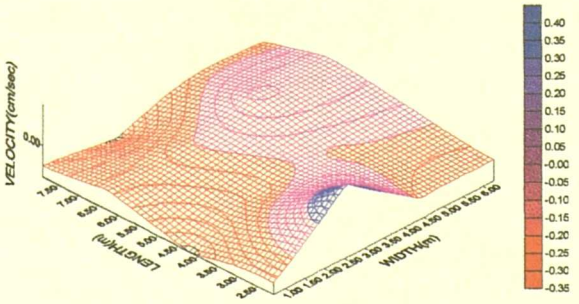

Figure B1.28 - Velocity Vz(run 1) at depth D1

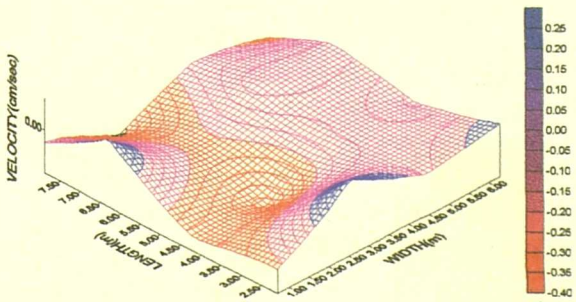

Figure B1.32 - Velocity Vz(run 2) at depth D1

Note: Velocity scale is not the same for each diagram

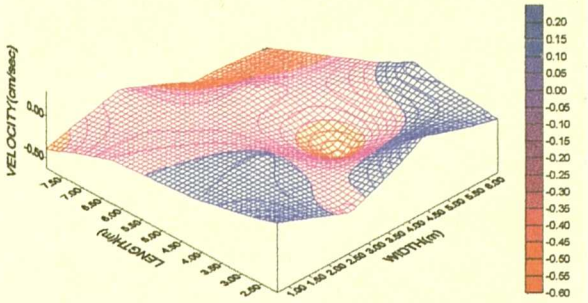

Figure B1.33 - Velocity Vz(run 3) at depth D4

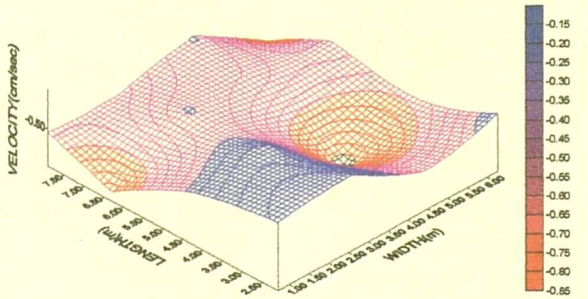

Figure B1.34 - Velocity Vz(run 3) at depth D3

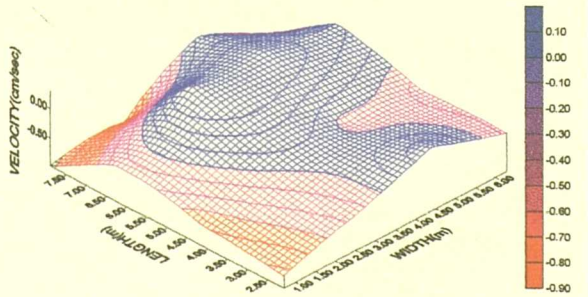

Figure B1.35 - Velocity Vz(run 3) at depth D2

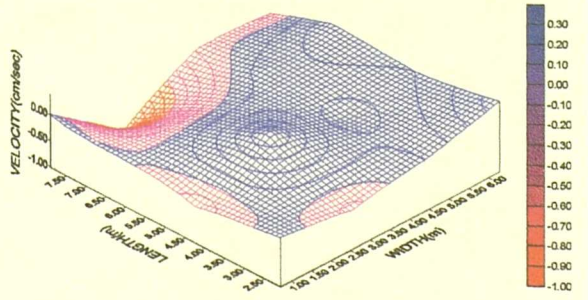

Figure B1.36 - Velocity Vz(run 3) at depth D1

Note: Velocity scale is not the same for each diagram

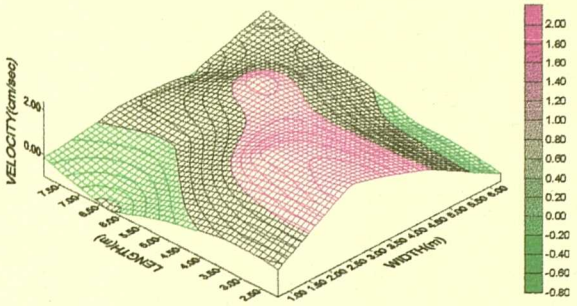

Figure B2.1 - Velocity Vx(run 1) at depth D4

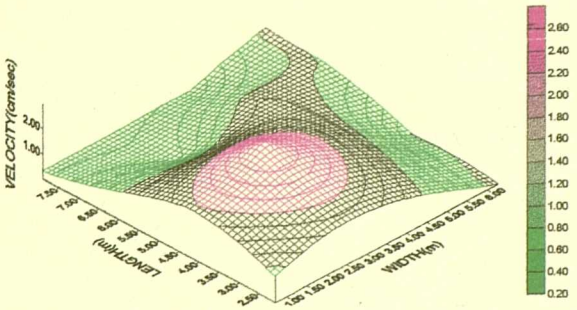

Figure B2.5 - Velocity Vx(run 2) at depth D4

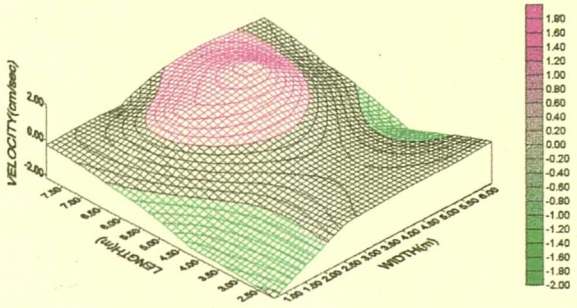

Figure B2.2 - Velocity Vx(run 1) at depth D3

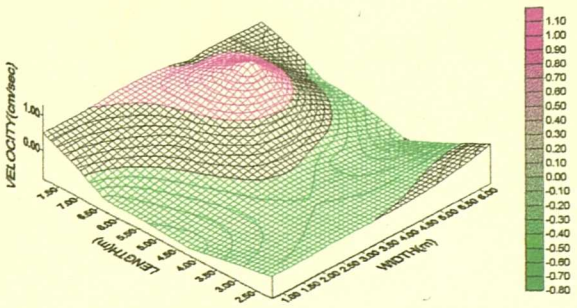

Figure B2.6 - Velocity Vx(run 2) at depth D3

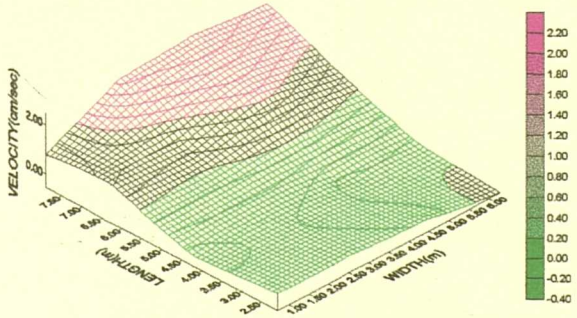

Figure B2.3 - Velocity Vx(run 1) at depth D2

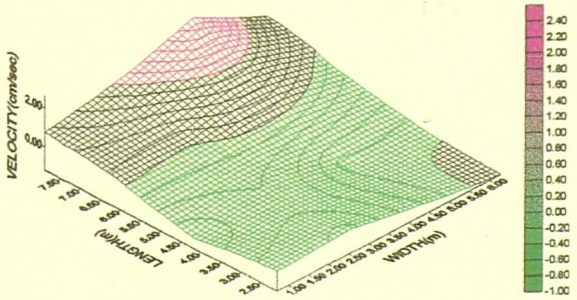

Figure B2.7 - Velocity Vx(run 2) at depth D2

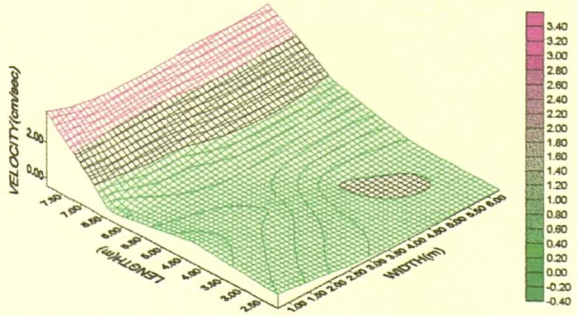

Figure B2.4 - Velocity Vx(run 1) at depth D1

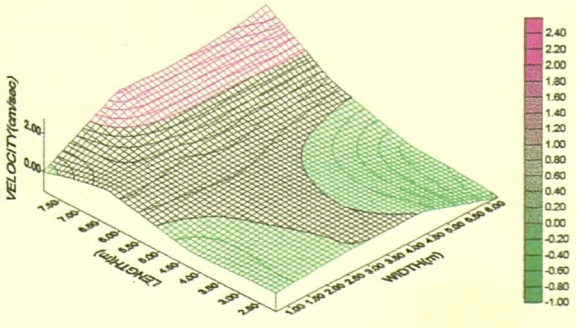

Figure B2.8 - Velocity Vx(run 2) at depth D1

Note: Velocity scale is not the same for each diagram

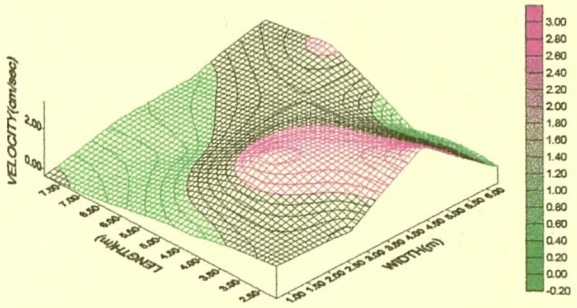

Figure B2.9 - Velocity Vx(run 3) at depth D4

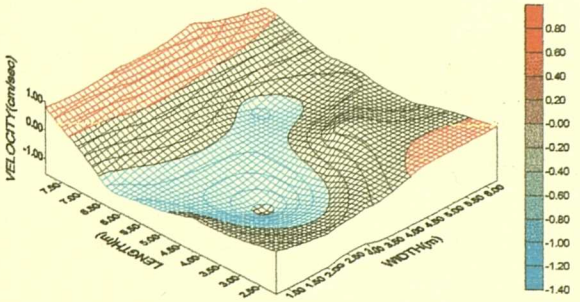

Figure B2.13 - Velocity Vy(run 1) at depth D4

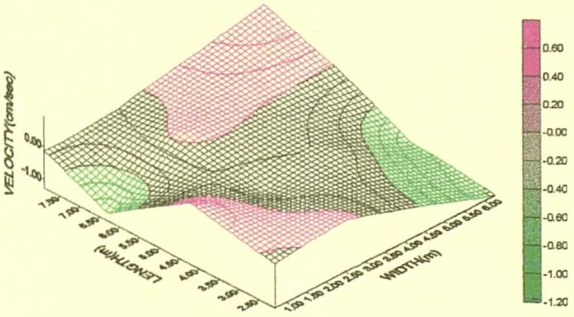

Figure B2.10 - Velocity Vx(run 3) at depth D3

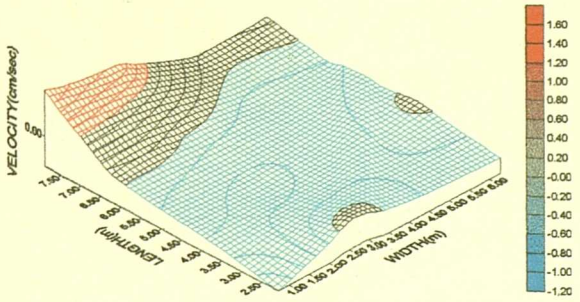

Figure B2.14 - Velocity Vy(run 1) at depth D3

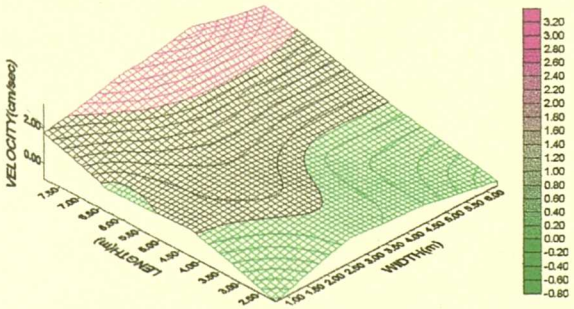

Figure B2.11 - Velocity Vx(run 3) at depth D2

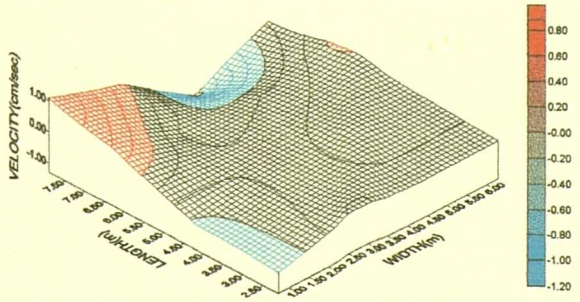

Figure B2.15 - Velocity Vy(run 1) at depth D2

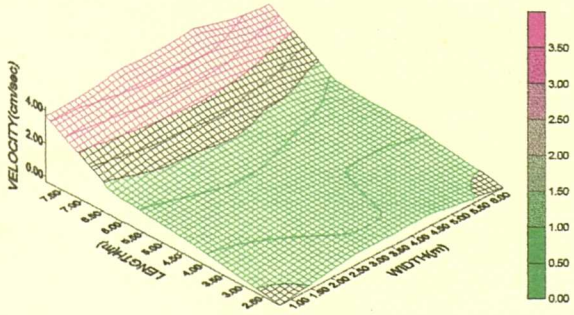

Figure B2.12 - Velocity Vx(run 3) at depth D1

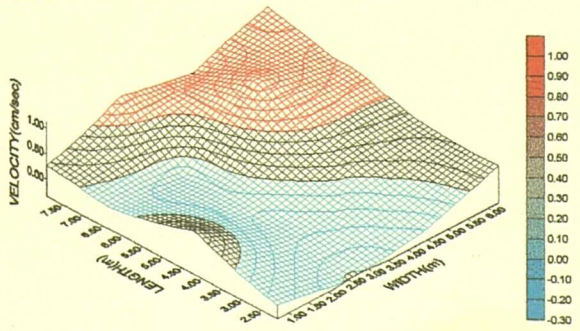

Figure B2.16 - Velocity Vy(run 1) at depth D1

Note: Velocity scale is not the same for each diagram

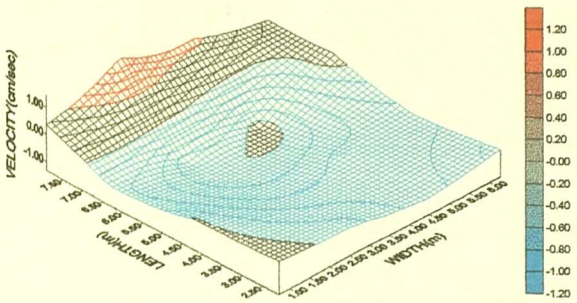

Figure B2.17 - Velocity Vy(run 2) at depth D4

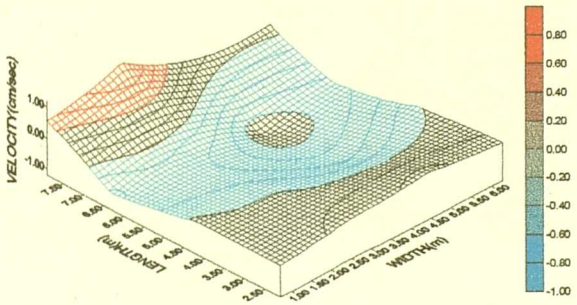

Figure B2.18 - Velocity Vy(run 2) at depth D3

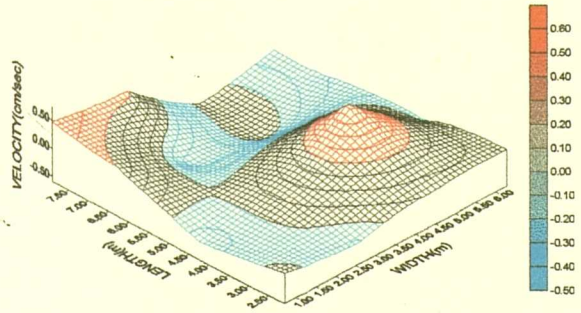

Figure B2.19 - Velocity Vy(run 2) at depth D2

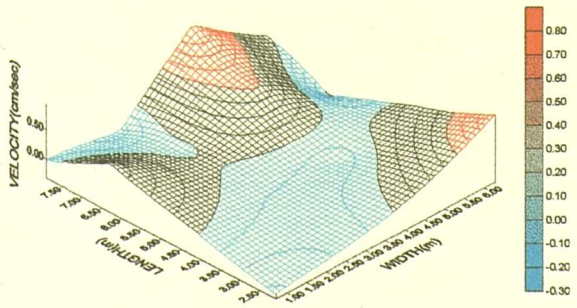

Figure B2.20 - Velocity Vy(run 2) at depth D1

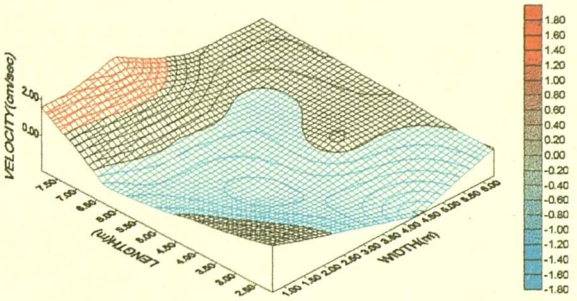

Figure B2.21 - Velocity Vy(run 3) at depth D4

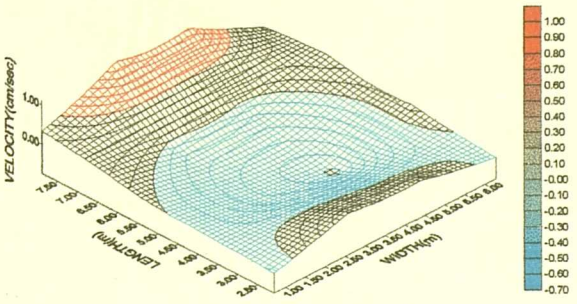

Figure B2.22 - Velocity Vy(run 3) at depth D3

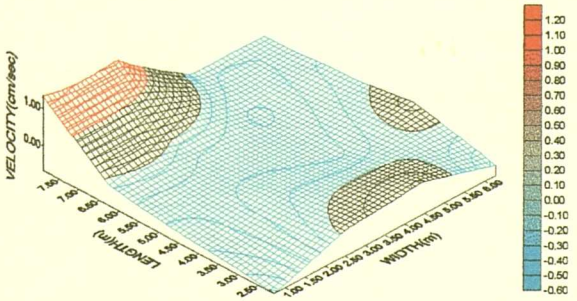

Figure B2.23 - Velocity Vy(run 3) at depth D2

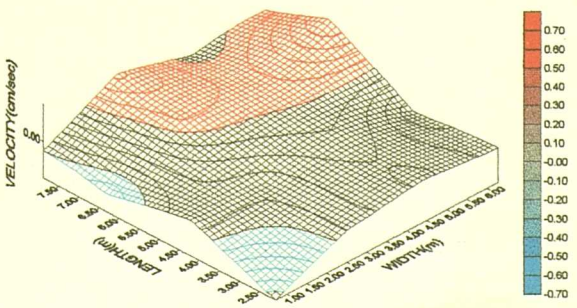

Figure B2.24 - Velocity Vy(run 3) at depth D1

Note: Velocity scale is not the same for each diagram

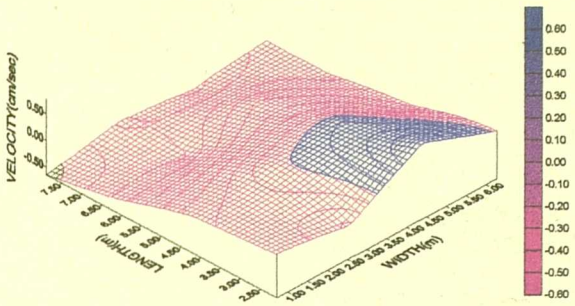

Figure B2.25 - Velocity Vz(run 1) at depth D4

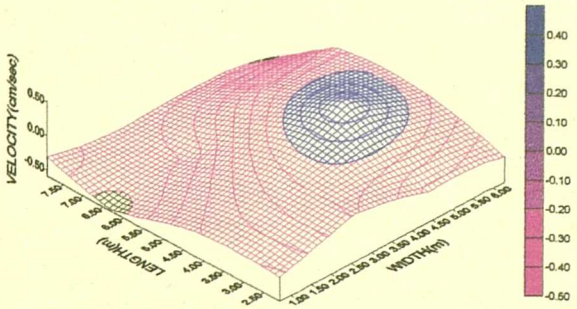

Figure B2.29 - Velocity Vz(run 2) at depth D4

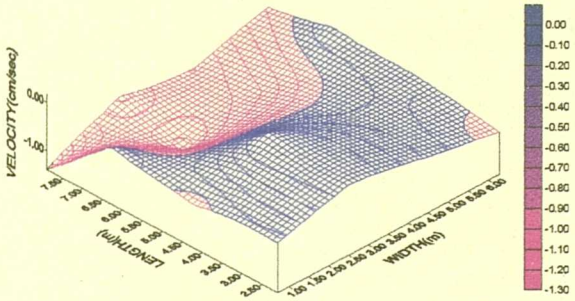

Figure B2.26 - Velocity Vz(run 1) at depth D3

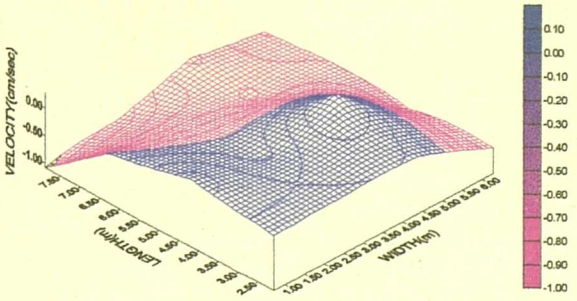

Figure B2.30 - Velocity Vz(run 2) at depth D3

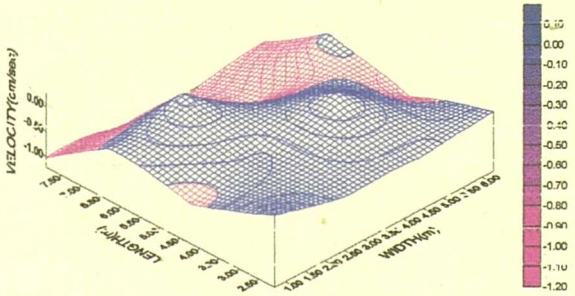

Figure B2.27 - Velocity Vz(run 1) at depth D2

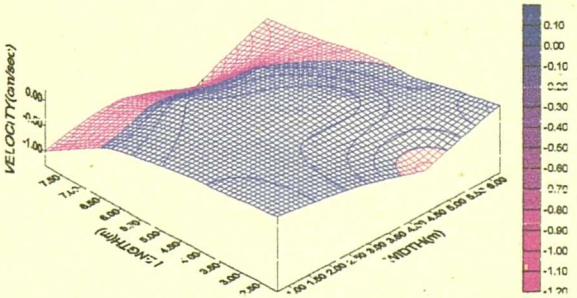

Figure B2.31 - Velocity Vz(run 2) at depth D2

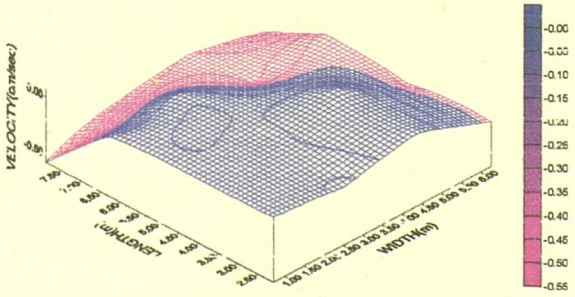

Figure B2.28 - Velocity Vz(run 1) at depth D1

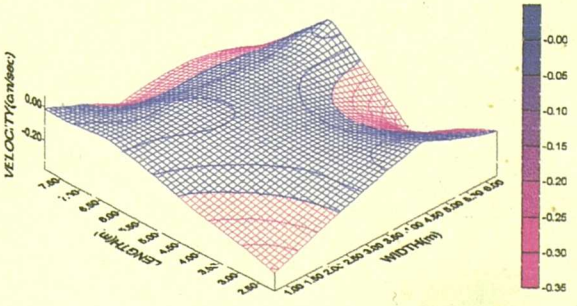

Figure B2.32 - Velocity Vz(run 2) at depth D1

Note: Velocity scale is not the same for each diagram

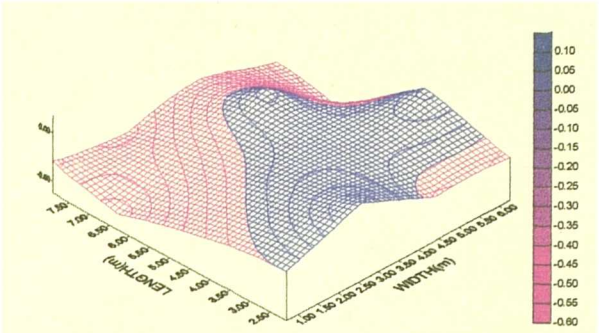

Figure B2.33 - Velocity Vz(run 3) at depth D4

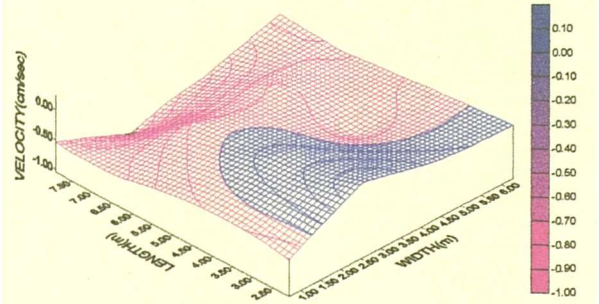

Figure B2.34 - Velocity Vz(run 3) at depth D3

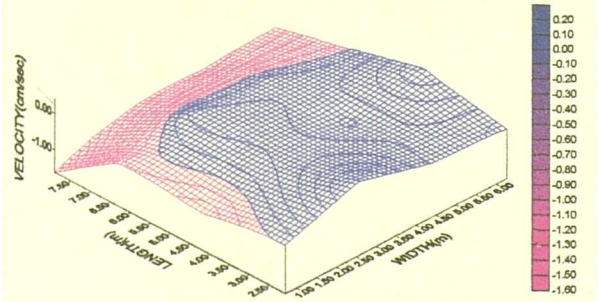

Figure B2.35 - Velocity Vz(run 3) at depth D2

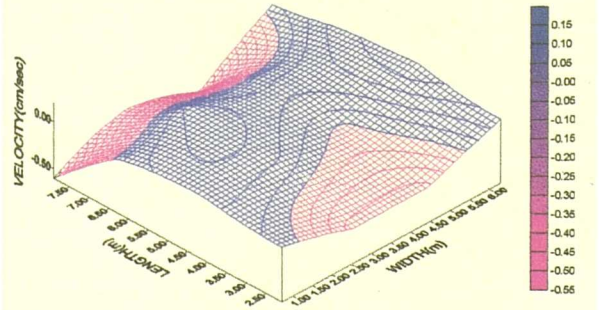

Figure B2.36 - Velocity Vz(run 3) at depth D1

Note: Velocity scale is not the same for each diagram

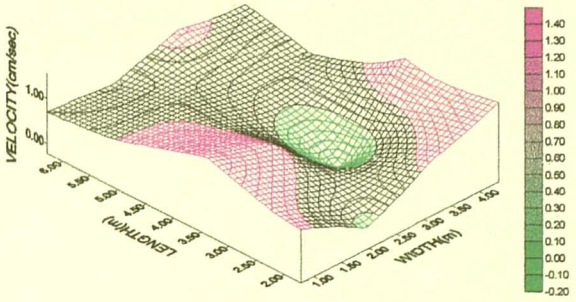

Figure B3.1-Velocity Vx(run 1) at depth D4

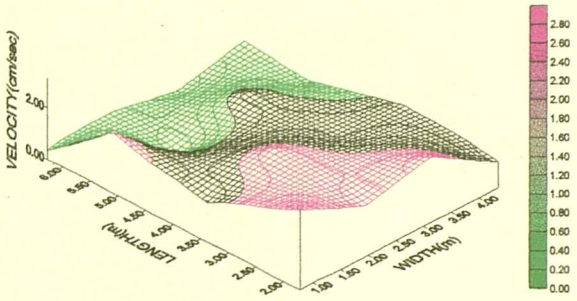

Figure B3.5 - Velocity Vx(run 2) at depth D4

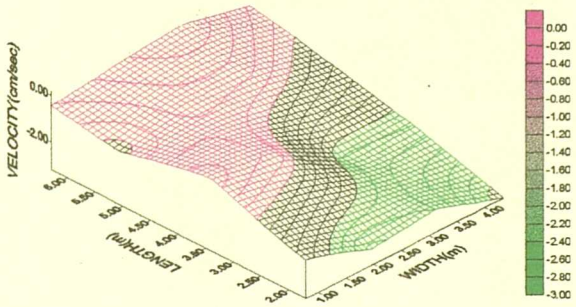

Figure B3.2 - Velocity Vx(run 1) at depth D3

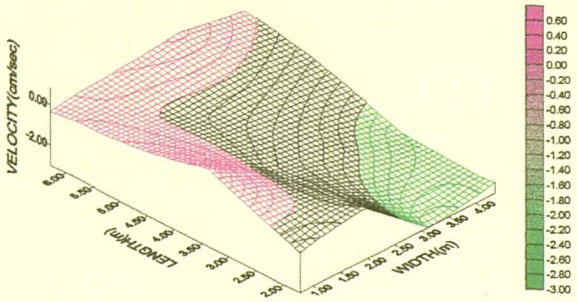

Figure B3.6 - Velocity Vx(run 2) at depth D3

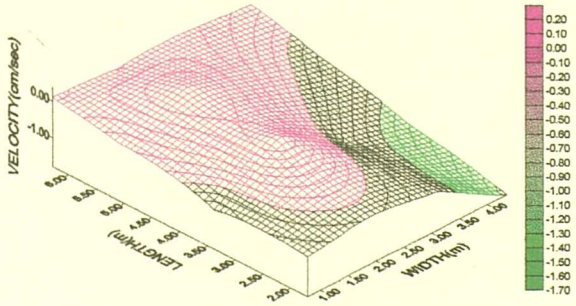

Figure B3.3 - Velocity Vx(run 1) at depth D2

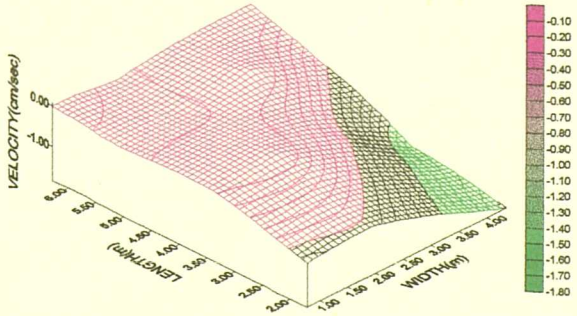

Figure B3.7 - Velocity Vx(run 2) at depth D2

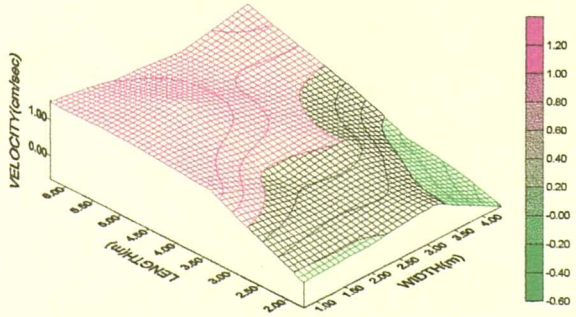

Figure B3.4 - Velocity Vx(run 1) at depth D1

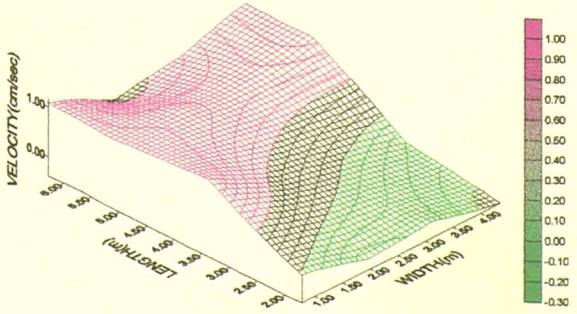

Figure B3.8 - Velocity Vx(run 2) at depth D1

Note: Velocity scale is not the same for each diagram

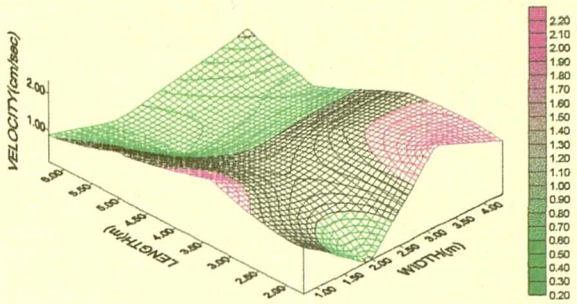

Figure B3.9 - Velocity Vx(run 3) at depth D4

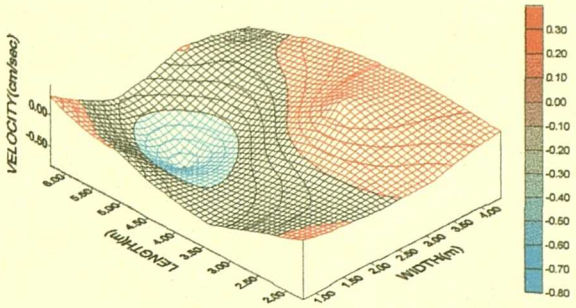

Figure B3.13 - Velocity Vy(run 1) at depth D4

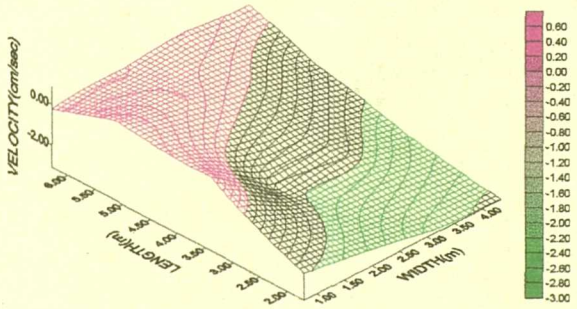

Figure B3.10 - Velocity Vx(run 3) at depth D3

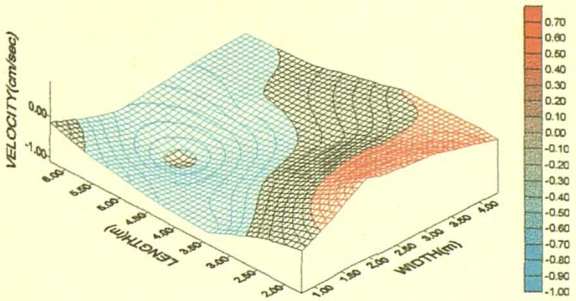

Figure B3.14 - Velocity Vy(run 1) at depth D3

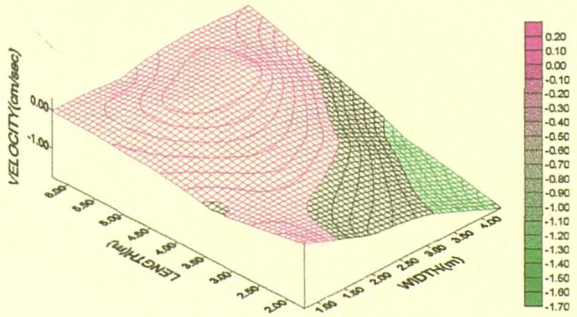

Figure B3.11 - Velocity Vx(run 3) at depth D2

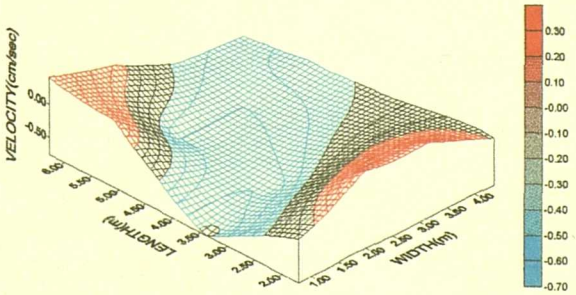

Figure B3.15 - Velocity Vy(run 1) at depth D2

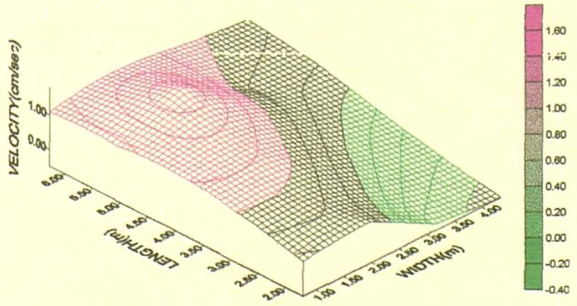

Figure B3.12 - Velocity Vx(run 3) at depth D1

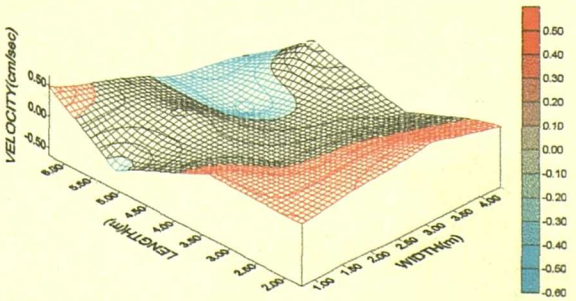

Figure B3.16 - Velocity Vy(run 1) at depth D1

Note: Velocity scale is not the same for each diagram

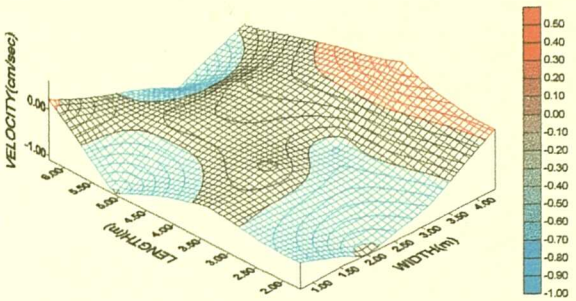

Figure B3.17 - Velocity Vy(run 2) at depth D4

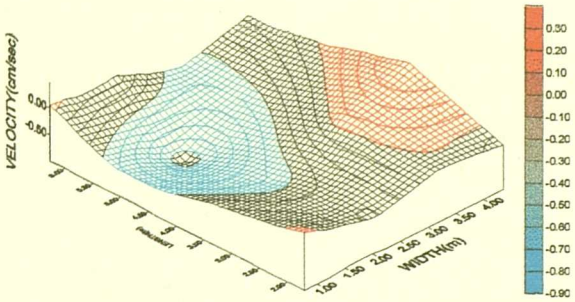

Figure B3.21 - Velocity Vy(run 3) at depth D4

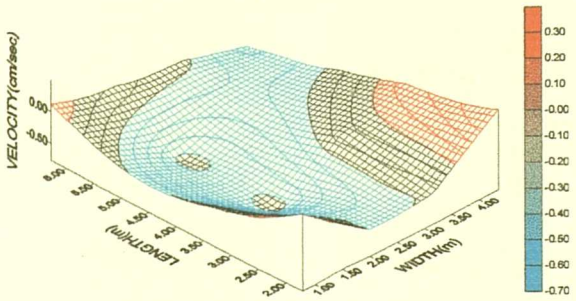

Figure B3.18 - Velocity Vy(run 2) at depth D3

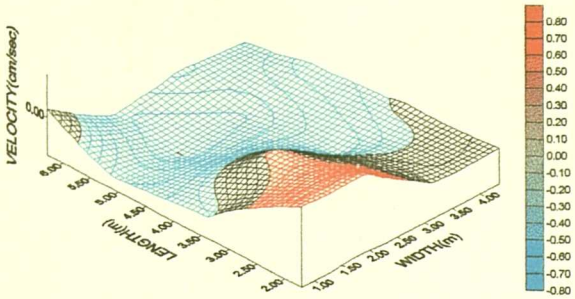

Figure B3.22 - Velocity Vy(run 3) at depth D3

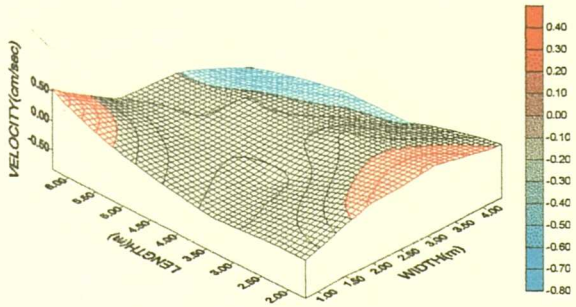

Figure B3.19 - Velocity Vy(run 2) at depth D2

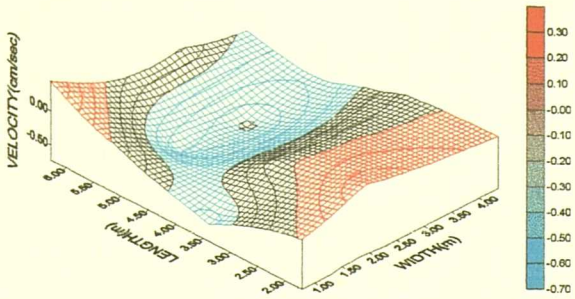

Figure B3.23 - Velocity Vy(run 3) at depth D2

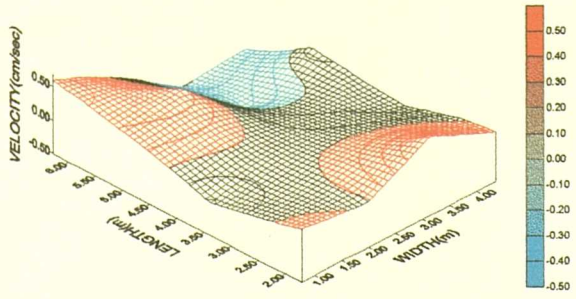

Figure B3.20 - Velocity Vy(run 2) at depth D1

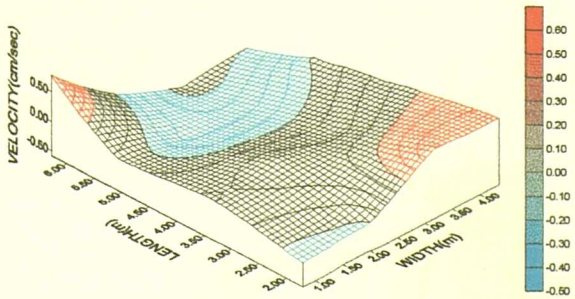

Figure B3.24 - Velocity Vy(run 3) at depth D1

Note: Velocity scale is not the same for each diagram

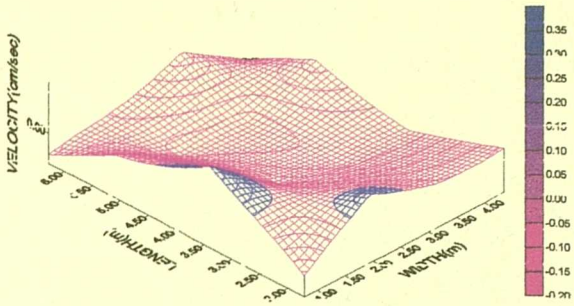

Figure B3.25 - Velocity Vz(run 1) at depth D4

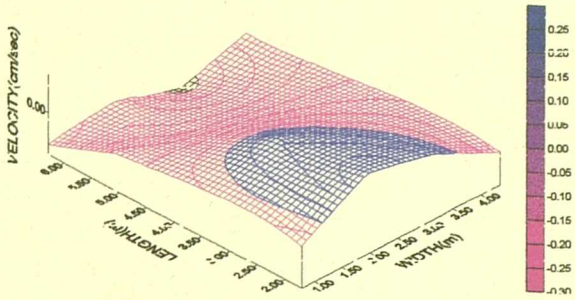

Figure B3.29- Velocity Vz(run 2) at depth D4

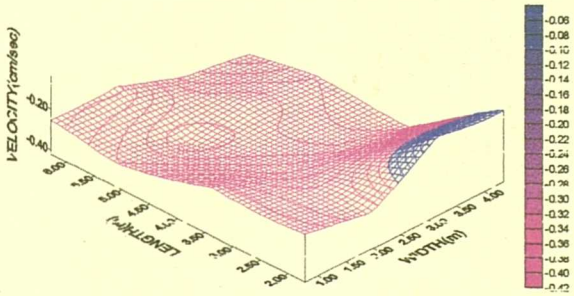

Figure B3.26 - Velocity Vz(run 1) at depth D3

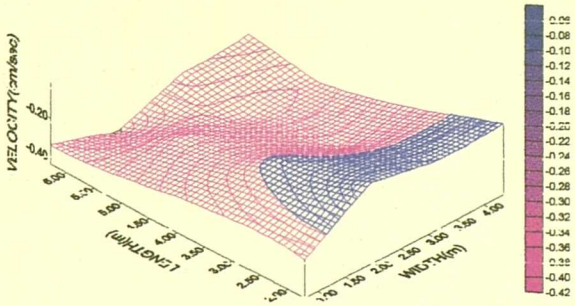

Figure B3.30 - Velocity Vz(run 2) at depth D3

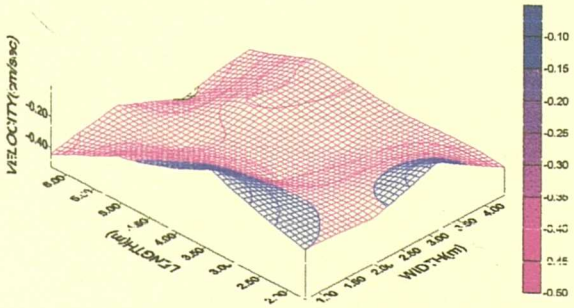

Figure B3.27 - Velocity Vz(run 1) at depth D2

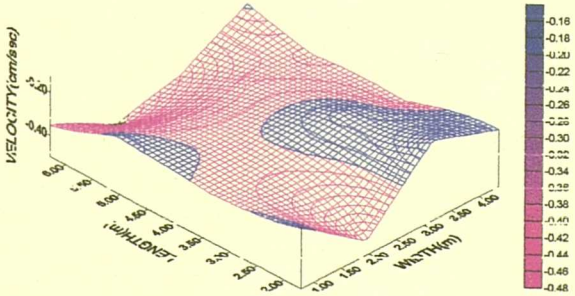

Figure B3.31 - Velocity Vz(run 2) at depth D2

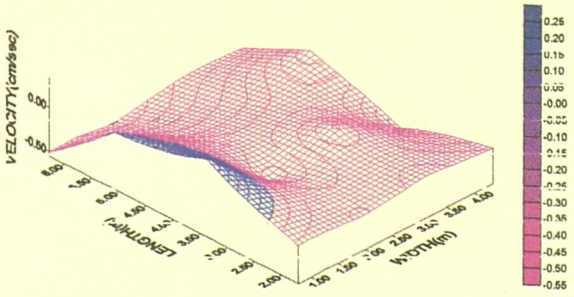

Figure B3.28 - Velocity Vz(run 1) at depth D1

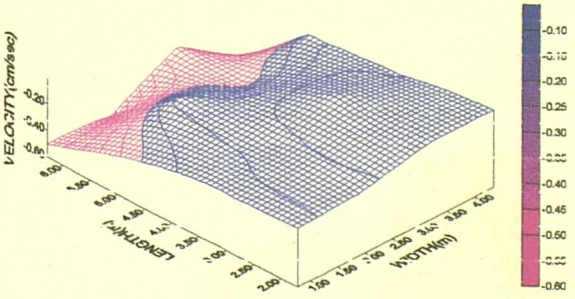

Figure B3.32 - Velocity Vz(run 2) at depth D1

Note: Velocity scale is not the same for each diagram

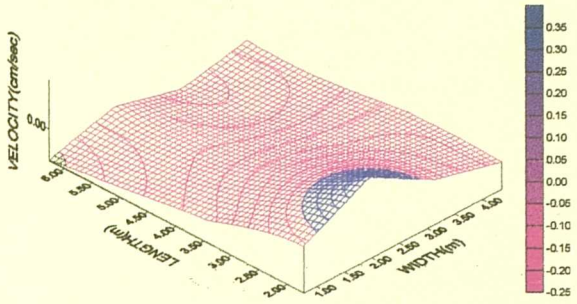

Figure B3.33 - Velocity Vz(run 3) at depth D4

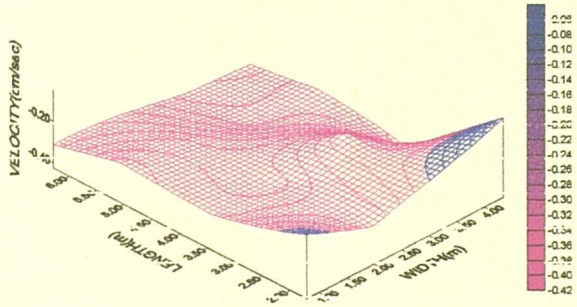

Figure B3.34 - Velocity Vz(run 3) at depth D3

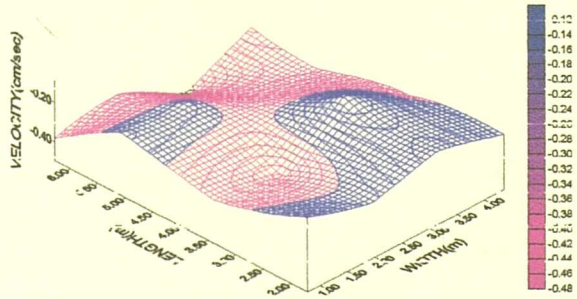

Figure B3.35 - Velocity Vz(run 3) at depth D2

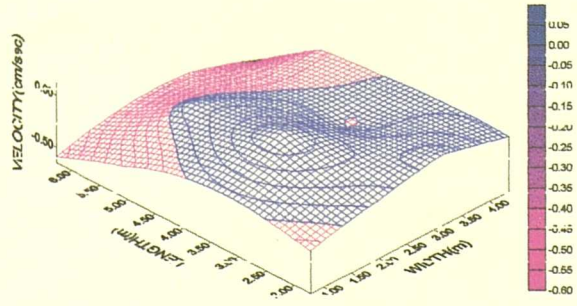

Figure B3.36 - Velocity Vz(run 3) at depth D1

Note: Velocity scale is not the same for each diagram

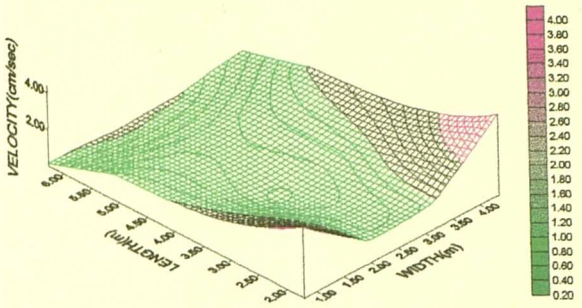

Figure B4.1 - Velocity Vx(run 1) at depth D4

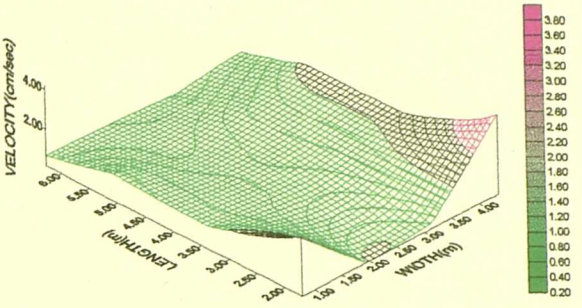

Figure B4.5 - Velocity Vx(run 2) at depth D4

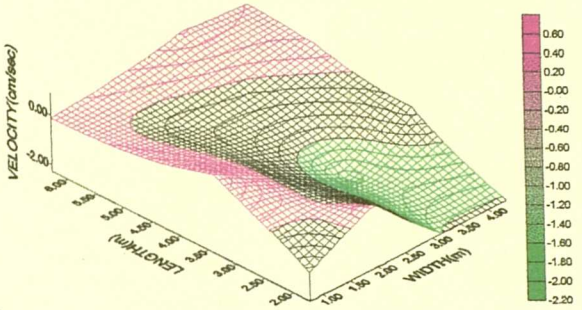

Figure B4.2 - Velocity Vx(run 1) at depth D3

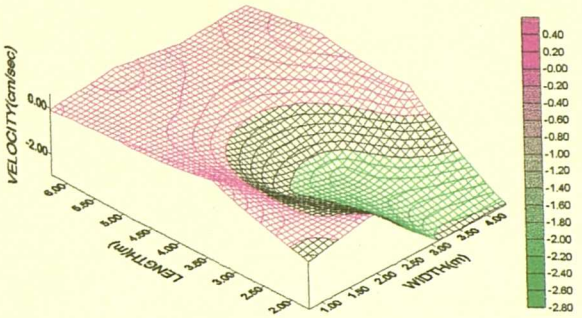

Figure B4.6 - Velocity Vx(run 2) at depth D3

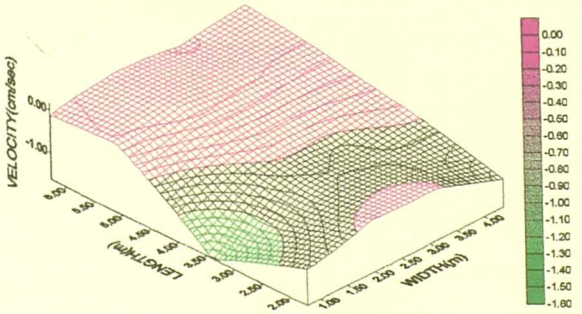

Figure B4.3 - Velocity Vx(run 1) at depth D2

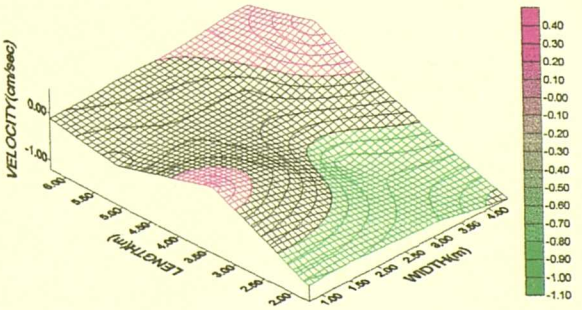

Figure B4.7 - Velocity Vx(run 2) at depth D2

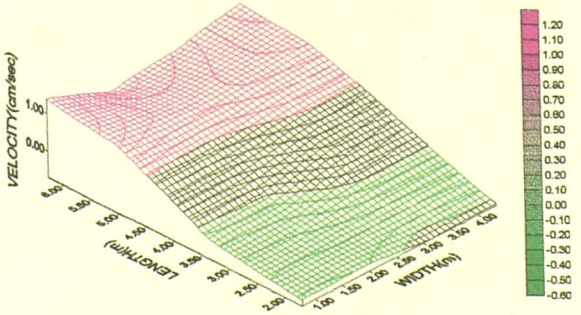

Figure B4.4 - Velocity Vx(run 1) at depth D1

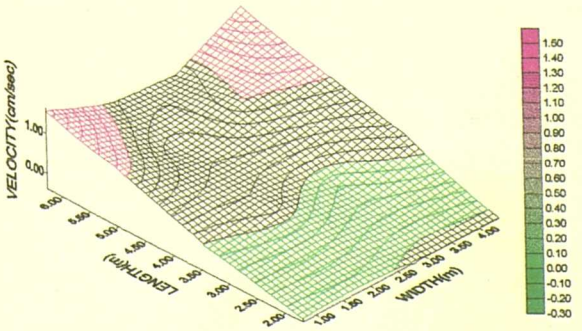

Figure B4.8 - Velocity Vx(run 2) at depth D1

Note: Velocity scale is not the same for each diagram

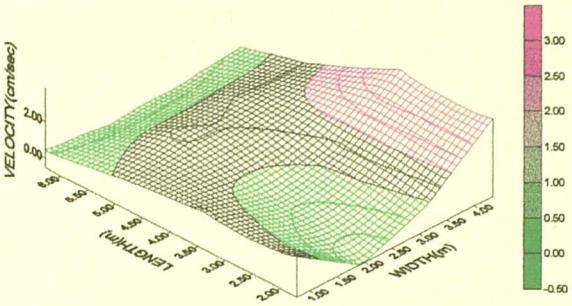

Figure B4.9 - Velocity Vx(run 3) at depth D4

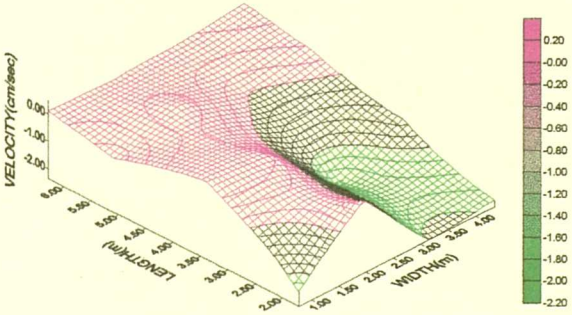

Figure B4.10 - Velocity Vx(run 3) at depth D3

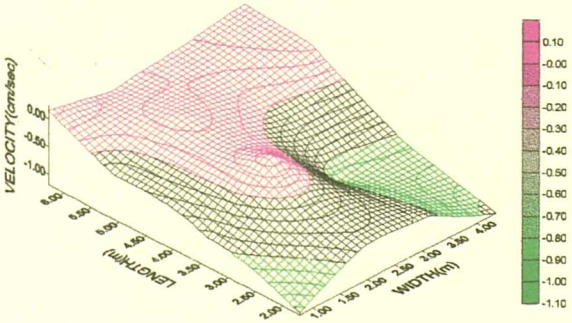

Figure B4.11 - Velocity Vx(run 3) at depth D2

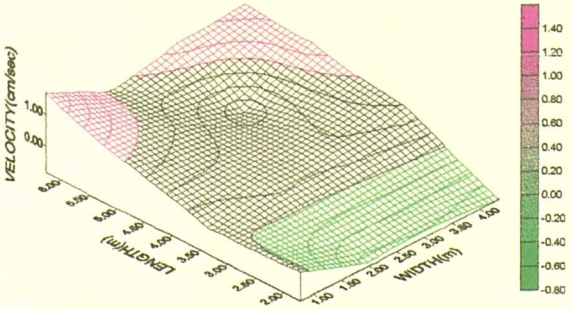

Figure B4.12 - Velocity Vx(run 3) at depth D1

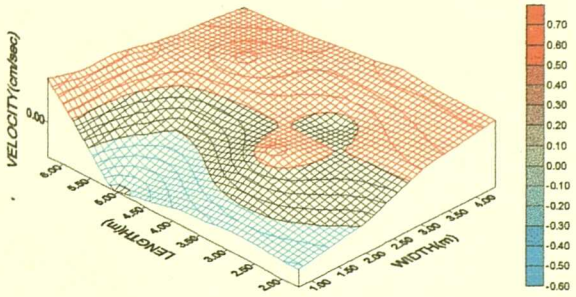

Figure B4.13 - Velocity Vy(run 1) at depth D4

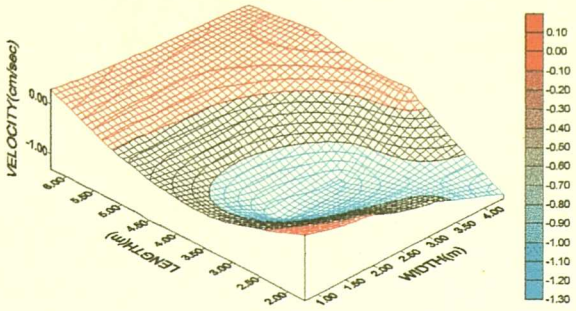

Figure B4.14 - Velocity Vy(run 1) at depth D3

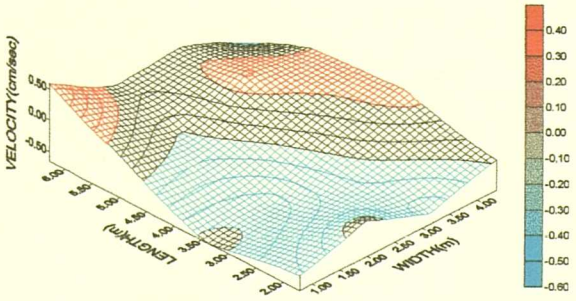

Figure B4.15 - Velocity Vy(run 1) at depth D2

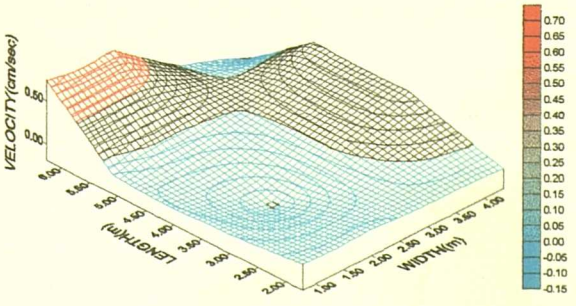

Figure B4.16 - Velocity Vy(run 1) at depth D1

Note: Velocity scale is not the same for each diagram

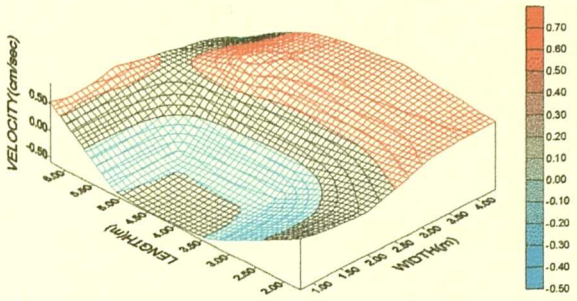

Figure B4.17 - Velocity Vy(run 2) at depth D4

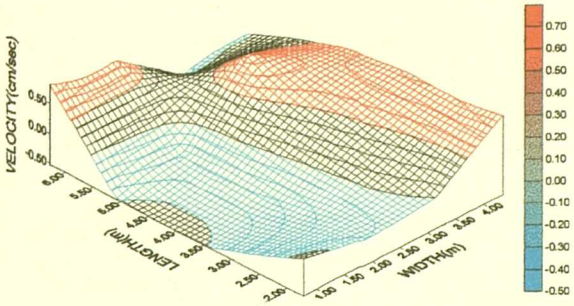

Figure B4.21 - Velocity Vy(run 3) at depth D4

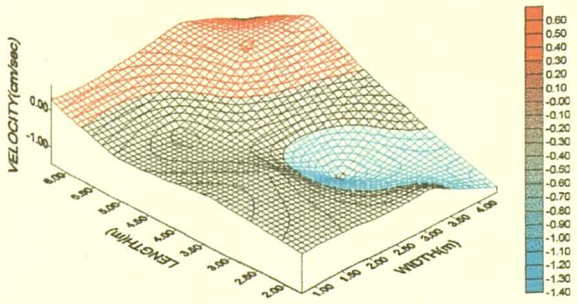

Figure B4.18 - Velocity Vy(run 2) at depth D3

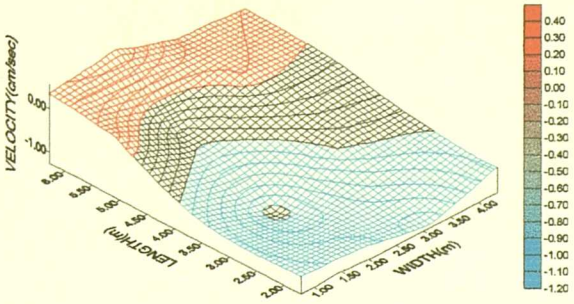

Figure B4.22 - Velocity Vy(run 3) at depth D3

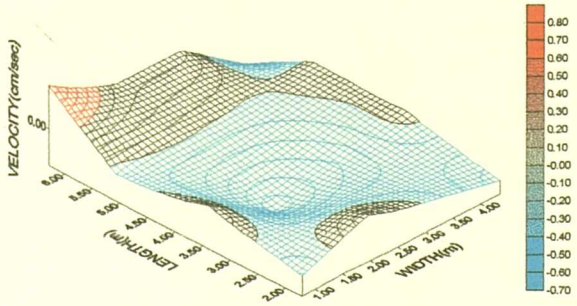

Figure B4.19 - Velocity Vy(run 2) at depth D2

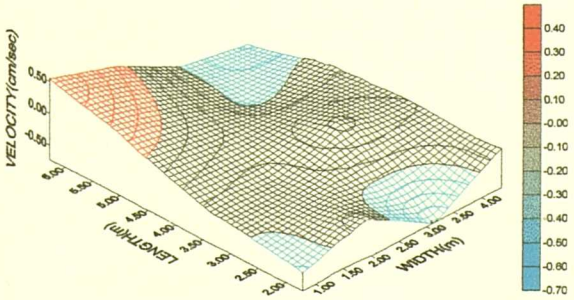

Figure B4.23 - Velocity Vy(run 3) at depth D2

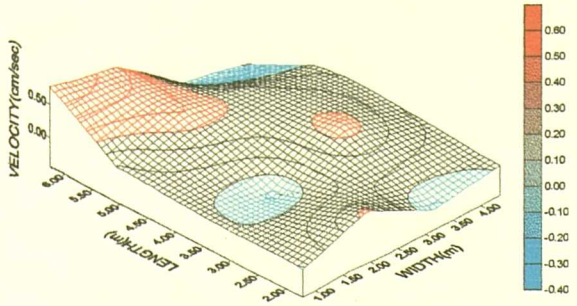

Figure B4.20 - Velocity Vy(run 2) at depth D1

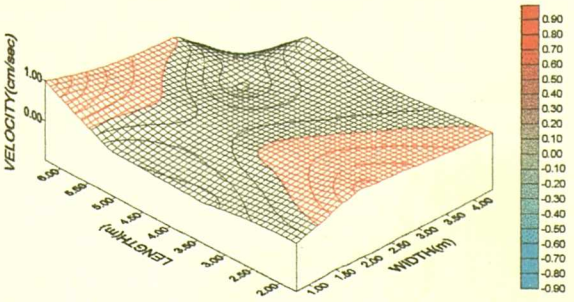

Figure B4.24 - Velocity Vy(run 3) at depth D1

Note: Velocity scale is not the same for each diagram

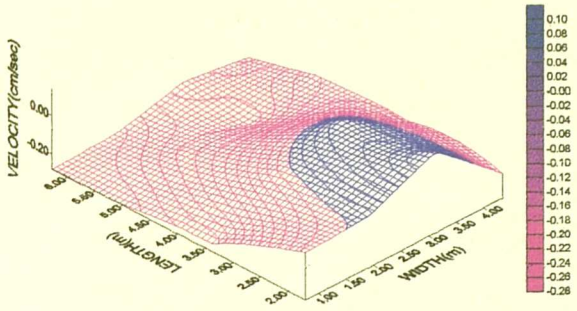

Figure B4.25 - Velocity Vz(run 1) at depth D4

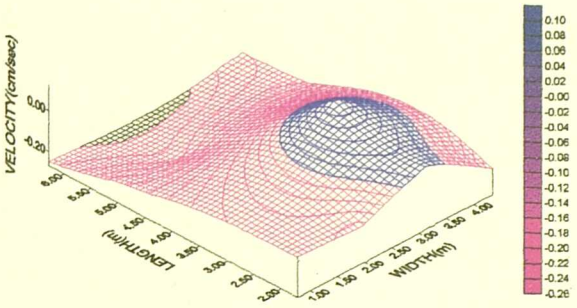

Figure B4.29 - Velocity Vz(run 2) at depth D4

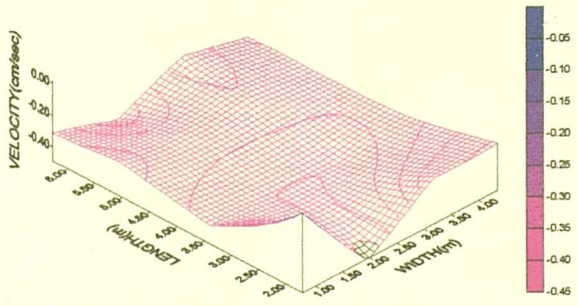

Figure B4.26 - Velocity Vz(run 1) at depth D3

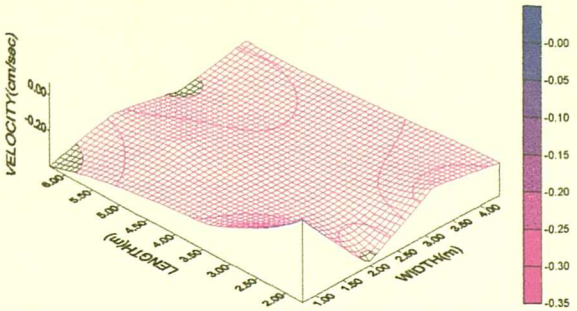

Figure B4.30 - Velocity Vz(run 2) at depth D3

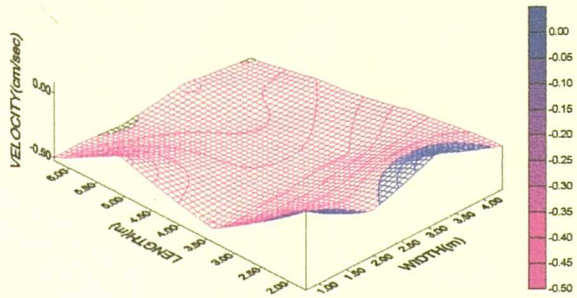

Figure B4.27 - Velocity Vz(run 1) at depth D2

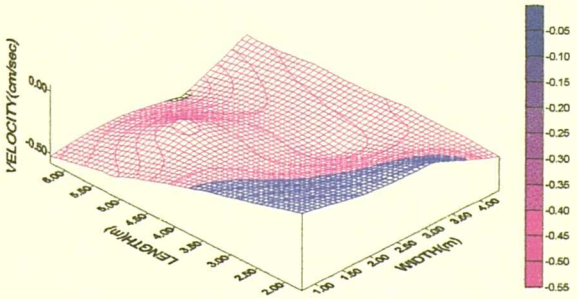

Figure B4.31 - Velocity Vz(run 2) at depth D2

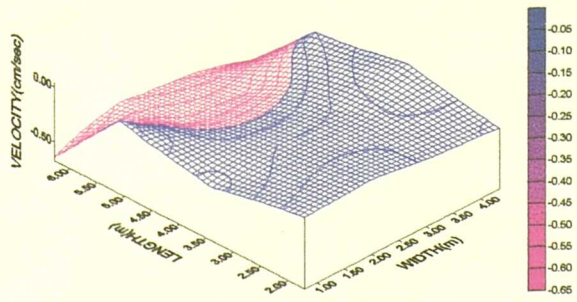

Figure B4.28 - Velocity Vz(run 1) at depth D1

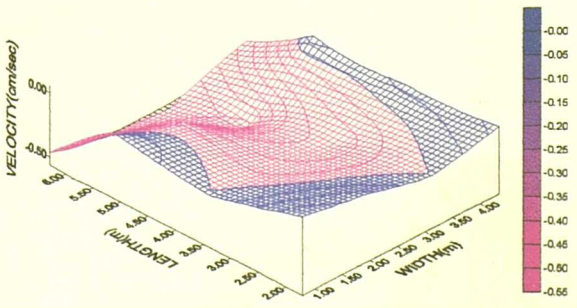

Figure B4.32 - Velocity Vz(run 2) at depth D1

Note: Velocity scale is not the same for each diagram

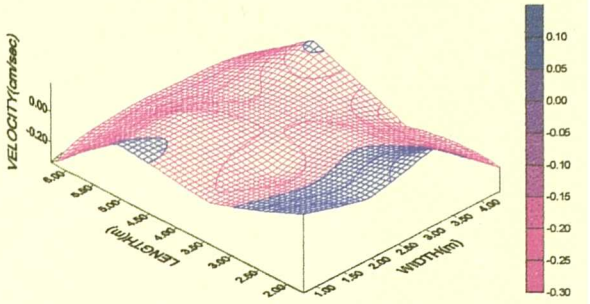

Figure B4.33 - Velocity Vz(run 3) at depth D4

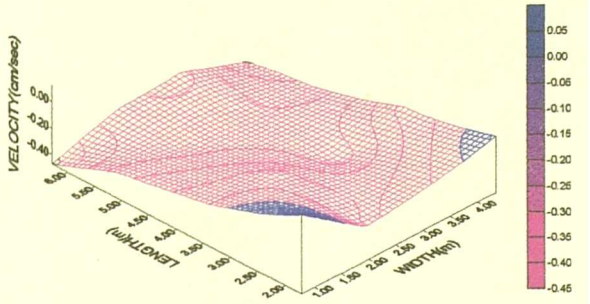

Figure B4.34 - Velocity Vz(run 3) at depth D3

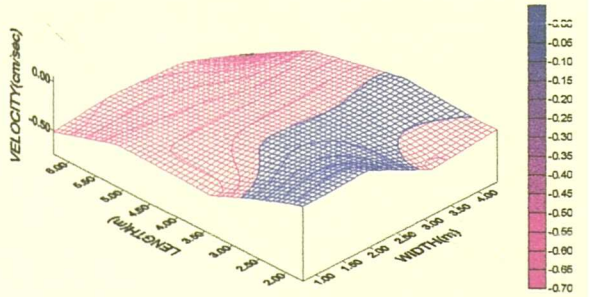

Figure B4.35 - Velocity Vz(run 3) at depth D2

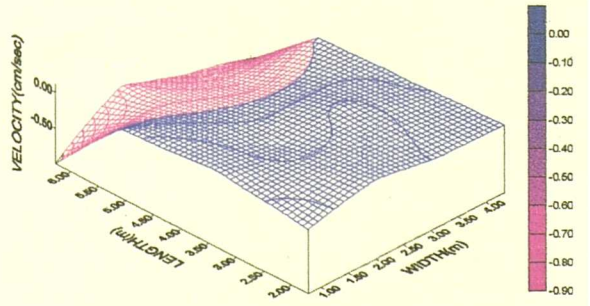

Figure B4.36 - Velocity Vz(run 3) at depth D1

Note: Velocity scale is not the same for each diagram

Table C1.1 - Analysis of variance for velocities in x-direction(run 1,2 & 3) using multifactor balanced designs (Tank A3, Frankley WTW)

Source	DF	SS	MS	F	P
Width	3	14.8351	4.9450	11.59	0.000
Depth	3	30.4302	10.1434	23.77	0.000
Length	3	54.6521	18.2174	42.69	0.000
Width*Depth	9	2.0466	0.2274	0.53	0.848
Width*Length	9	12.1903	1.3545	3.17	0.002
Depth*Length	9	61.2139	6.8015	15.94	0.000
Width*Depth*Length	27	18.5612	0.6875	1.61	0.042
Error	128	54.6166	0.4267		
Total	191	248.5461			

Note: * is for interaction

Table C1.2 - Analysis of variance for velocities in x-direction(run 1,2 & 3) using multifactor balanced designs (Tank C7, Trimpley WTW)

Source	DF	SS	MS	F	P
Width	3	9.3473	3.1158	21.85	0.000
Depth	3	101.8784	33.9595	238.14	0.000
Length	3	15.3661	5.1220	35.92	0.000
Width*Depth	9	20.9559	2.3284	16.33	0.000
Width*Length	9	3.2435	0.3604	2.53	0.011
Depth*Length	9	48.6216	5.4024	37.88	0.000
Width*Depth*Length	27	30.9588	1.1466	8.04	0.000
Error	128	18.2530	0.1426		
Total	191	248.6246			

Note: * is for interaction

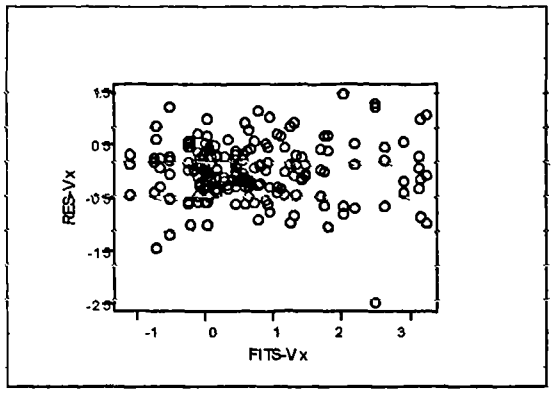

Figure C1.1 - Plot of residuals versus fitted values from the analysis of variance for velocities in x-direction (Tank A3, Frankley)

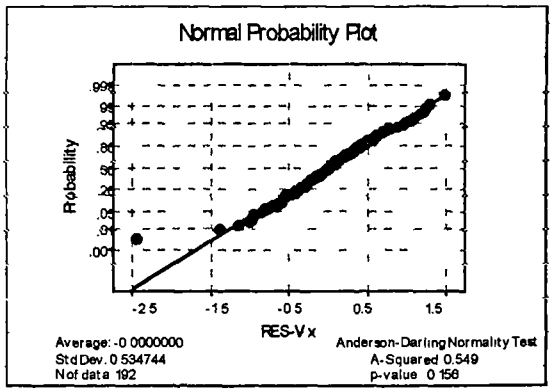

Figure C1.2 - Normal probability plot of residuals from the analysis of variance for velocities in x-direction Tank A3, Frankley)

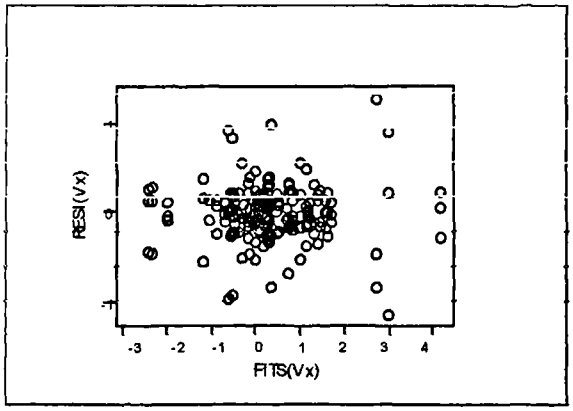

Figure C1.3 - Plot of residuals versus fitted values from the analysis of variance for velocities in x-direction (Tank C7, Trimpley)

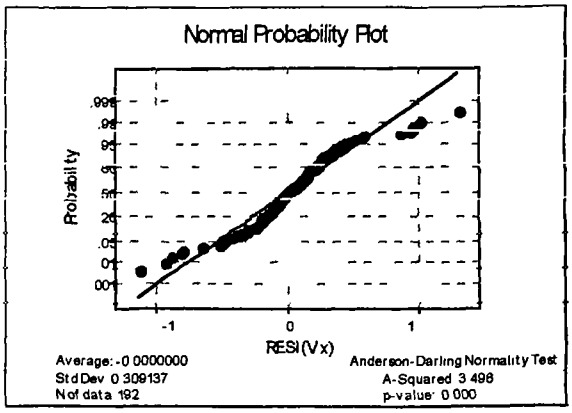

Figure C1.4 - Normal probability plot of residuals from the analysis of variance for velocities in x-direction (Tank C7, Trimpley)

Table C1.3 - Analysis of Covariance for Vx (Tank A3, Frankley)

Source	DF	ADJ. SS	MS	F	P
Covariates	1	3.6043	3.6043	9.28	0.003
Width	3	17.4492	5.8164	14.97	0.000
Depth	3	33.7177	11.2392	28.93	0.000
Length	3	51.4815	17.1605	44.16	0.000
Width*Depth	9	2.2111	0.2457	0.63	0.768
Width*Length	9	12.9697	6.9993	18.01	0.000
Depth*Length	9	62.9935	6.9993	18.01	0.000
Width*Depth*Length	27	16.4179	0.6081	1.56	0.052
Error	127	49.3467	0.3886		
Total	191	248.6640			

Note: * is for interaction

Table C1.4 - Analysis of Covariance for Vx (Tank C7, Trimpley)

Source	DF	ADJ. SS	MS	F	P
Covariates	1	0.0091	0.0091	0.06	0.802
Width	3	9.3537	3.1179	21.70	0.000
Depth	3	101.8875	33.9625	236.42	0.000
Length	3	14.8565	4.9522	34.47	0.000
Width*Depth	9	20.9599	2.3289	16.21	0.000
Width*Length	9	3.0053	0.3339	2.32	0.019
Depth*Length	9	48.6069	5.4008	37.60	0.000
Width*Depth*Length	27	30.8971	1.1443	7.97	0.000
Error	127	18.2439	0.1437		
Total	191	248.6246			

Note: * is for interaction

Table C1.5 - Analysis of variance for velocities in z-direction(run 1,2 & 3) using multifactor balanced designs (Tank A3, Frankley)

Source	DF	SS	MS	F	P
Width	3	0.18217	0.06072	0.96	0.414
Depth	3	2.50115	0.83372	13.17	0.000
Length	3	8.90787	2.96929	46.90	0.000
Width*Depth	9	0.78527	0.08725	1.38	0.205
Width*Length	9	0.64891	0.07210	1.14	0.340
Depth*Length	9	3.08185	0.34243	5.41	0.000
Width*Depth*Length	27	1.49904	0.05552	0.88	0.642
Error	128	8.10347	0.06331		
Total	191	25.70972			

Note: * is for interaction

Table C1.6 - Analysis of variance for velocities in z-direction(run 1,2 & 3) using multifactor balanced designs (Tank C7, Trimpley)

Source	DF	SS	MS	F	P
Width	3	0.061385	0.020462	2.07	0.107
Depth	3	0.990994	0.330331	33.45	0.000
Length	3	3.286790	1.095597	110.96	0.000
Width*Depth	9	0.202352	0.022484	2.28	0.021
Width*Length	9	0.346073	0.038453	3.89	0.000
Depth*Length	9	0.833481	0.092609	9.38	0.000
Width*Depth*Length	27	0.467540	0.017316	1.75	0.020
Error	128	1.263867	0.009874		
Total	191	7.452481			

Note: * is for interaction

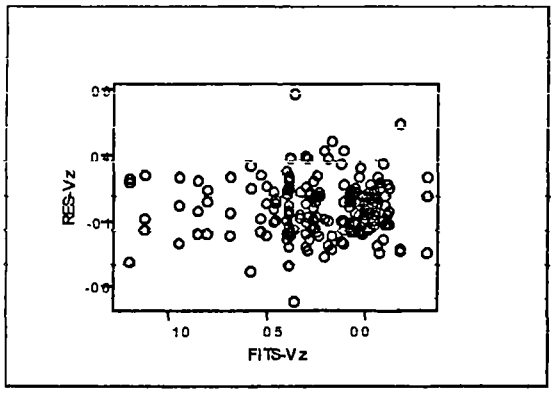

Figure C1.5 - Plot of residuals versus fitted values from the analysis of variance for velocities in z-direction (Tank A3, Frankley)

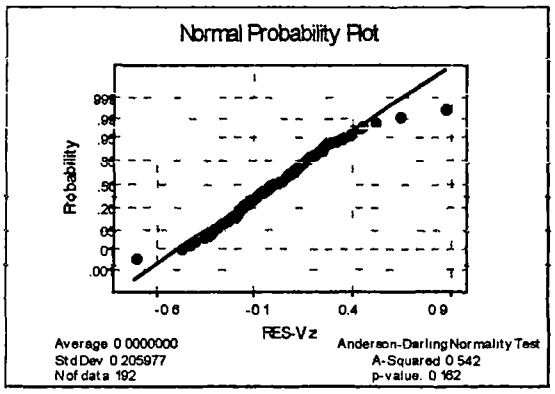

Figure C1.6 - Normal probability plot of residuals from the analysis of variance for velocities in z-direction (Tank A3, Frankley)

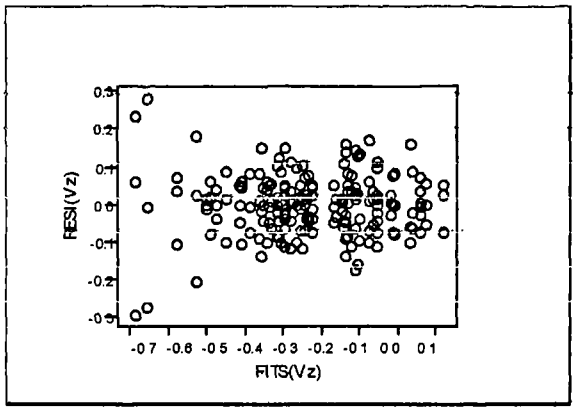

Figure C1.7 - Plot of residuals versus fitted values from the analysis of variance for velocities in z-direction (Tank C7, Trimpley)

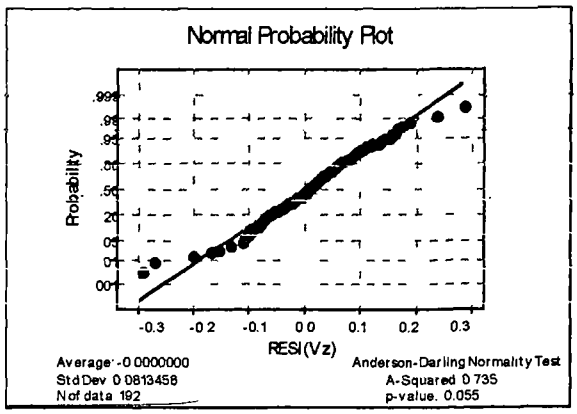

Figure C1.8 - Normal probability plot of residuals from the analysis of variance for velocities in z-direction (Tank C7, Trimpley)

Table C1.7 - Analysis of Covariance for Vz (Tank A3, Frankley)

Source	DF	ADJ. SS	MS	F	P
Covariate(discharge)	1	0.00672	0.00672	0.12	0.724
Width	3	0.36977	0.12326	2.29	0.081
Depth	3	3.09192	1.03064	19.15	0.000
Length	3	10.28514	3.42838	63.70	0.000
Width*Depth	9	0.51924	0.05769	1.07	0.388
Width*Length	9	0.66775	0.07419	1.38	0.204
Depth*Length	9	2.76413	0.30713	5.71	0.000
Width*Depth*Length	27	1.54876	0.05736	1.07	0.390
Error	127	6.83501	0.05382		
Total	191	26.09574			

Note: * is for interaction

Table C1.8 - Analysis of Covariance for Vz(Tank C7,Trimpley WTW)

Source	DF	ADJ. SS	MS	F	P
Covariate(discharge)	1	0.24166	0.24166	30.02	0.000
Width	3	0.04785	0.01595	1.98	0.120
Depth	3	0.98564	0.32855	40.82	0.000
Length	3	2.73531	0.91177	113.28	0.000
Width*Depth	9	0.21156	0.02351	2.92	0.004
Width*Length	9	0.27872	0.03097	3.85	0.000
Depth*Length	9	0.82851	0.09206	11.44	0.000
Width*Depth*Length	27	0.46134	0.01709	2.12	0.003
Error	127	1.02221	0.00805		
Total	191	7.45248			

Table D1.1 - ANOVA on flow rate between different runs (Tank A3, Frankley)

Source	DF	SS	MS	F	P
Runs	2	103.31	51.66	30.70	0.000
Error	189	318.02	1.68		
Total	191	421.33			

Table D1.2 - ANOVA on flow rate between different runs (Tank C2, Frankley)

Source	DF	SS	MS	F	P
Runs	2	331.21	165.61	160.60	0.000
Error	189	194.89	1.03		
Total	191	526.11			

Table D1.3 - ANOVA on flow rate between different runs (Tank C1, Trimpley)

Source	DF	SS	MS	F	P
Runs	2	98.227	49.113	227.68	0.000
Error	189	40.769	0.216		
Total	191	138.996			

Table D1.4 - ANOVA on flow rate between different runs (Tank C7, Trimpley)

Source	DF	SS	MS	F	P
Runs	2	173.691	86.845	444.30	0.000
Error	189	36.943	0.195		
Total	191	210.634			

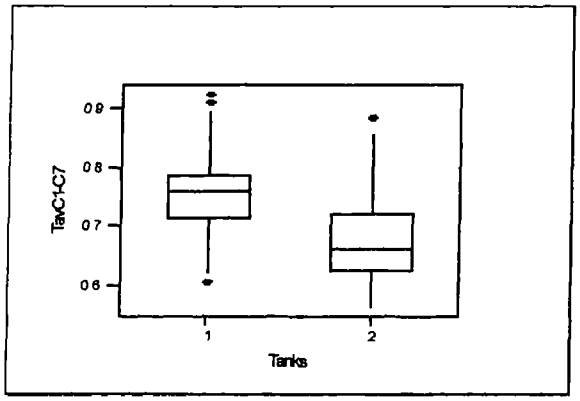

Figure D1.1 - Boxplots of turbidity between Tanks C1 and C7 (Trimpley WTW)
Note: Tank 1=Tank C1 Tank 2=Tank C7 and y-axis=discharge in million litres per day

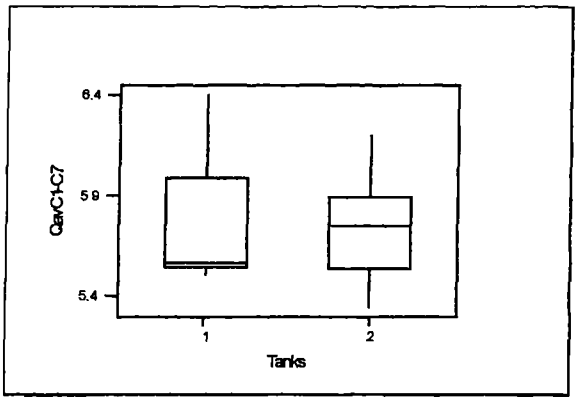

Figure D1.2 - Boxplots of discharge between Tanks C1 and C7(Trimpley WTW)
Note: Tank 1=Tank C1, Tank 2=Tank C7 and y-axis=discharge in million litres per day.

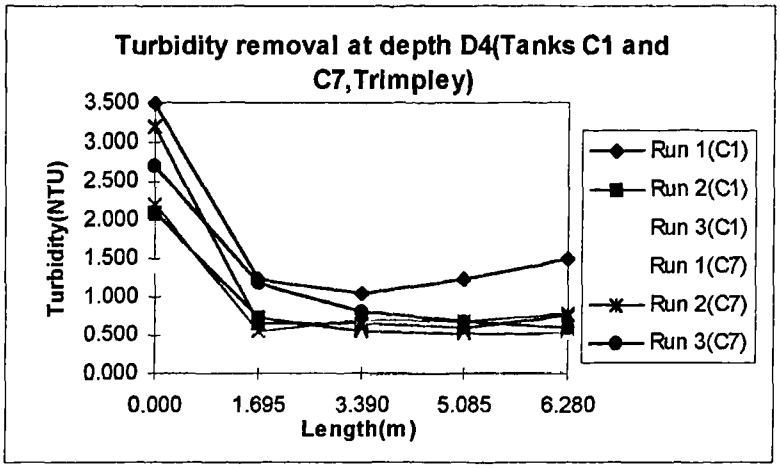

Figure D1.3-Turbidity removal along the length of the tank at depth D4, Trimpley WTW

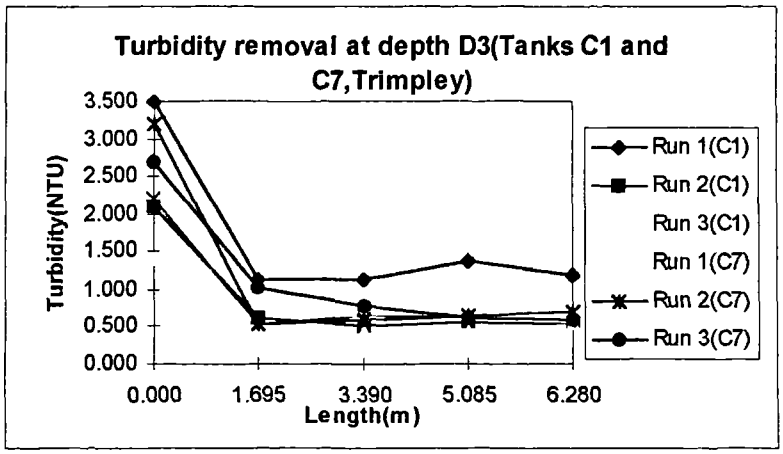

Figure D1.4-Turbidity removal along the length of the tank at depth D3, Trimpley WTW

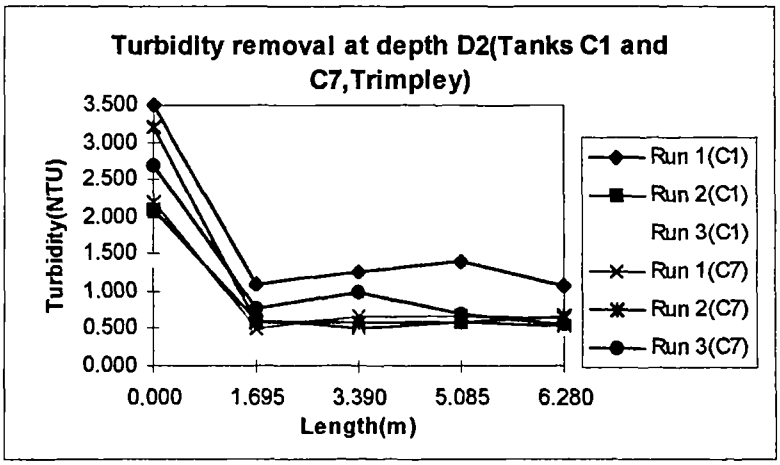

Figure D1.5-Turbidity removal along the length of the tank at depth D2, Trimpley WTW

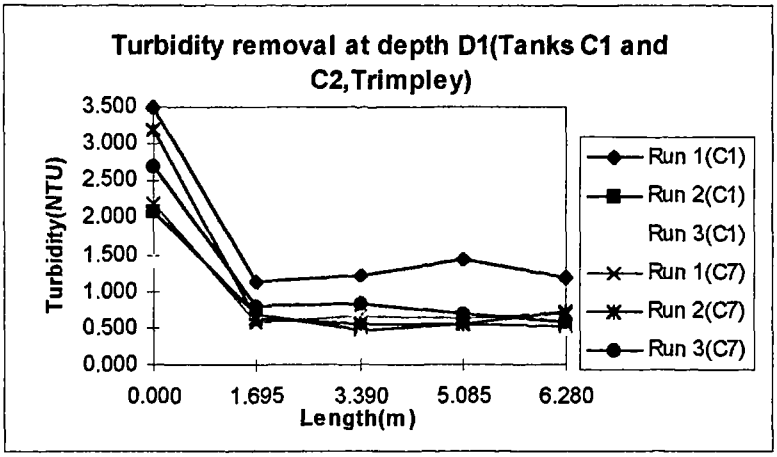

Figure D1.6-Turbidity removal along the length of the tank at depth D1, Trimpley WTW

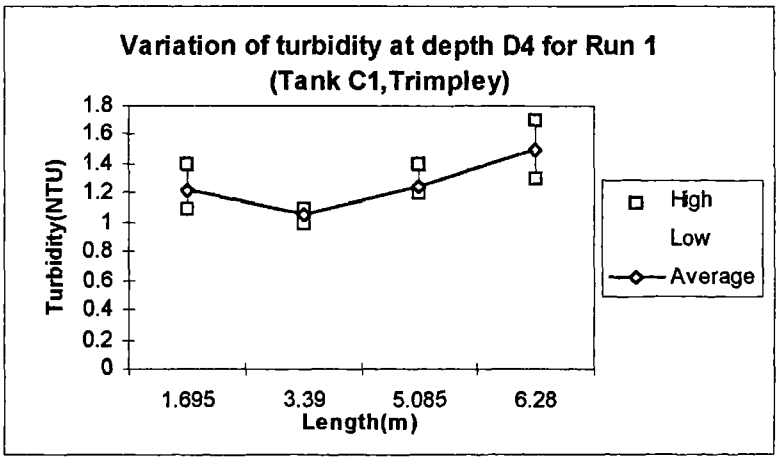

Figure D1.7 - Turbidity variation at depth D4, Trimpley WTW

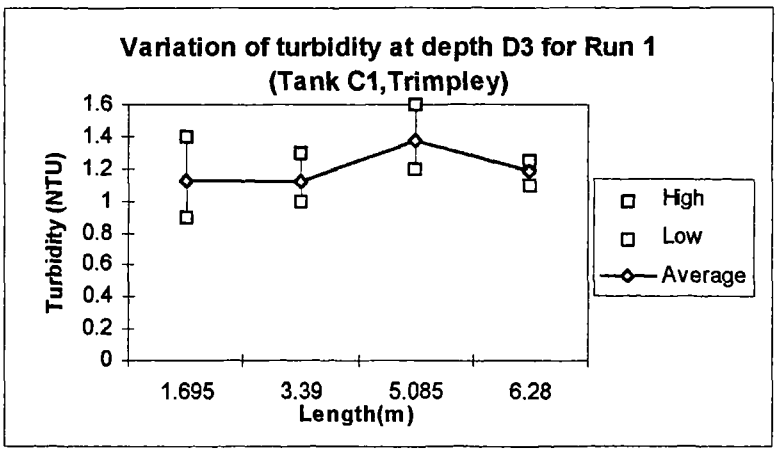

Figure D1.8 - Turbidity variation at depth D3, Trimpley WTW

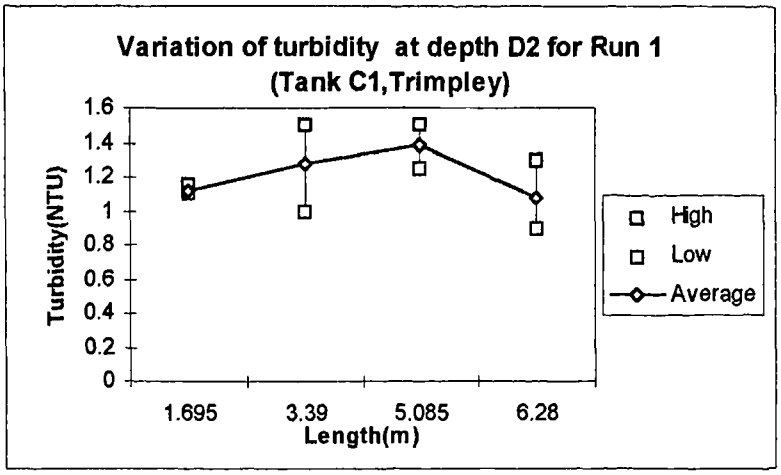

Figure D1.9 - Turbidity variation at depth D2, Trimpley WTW

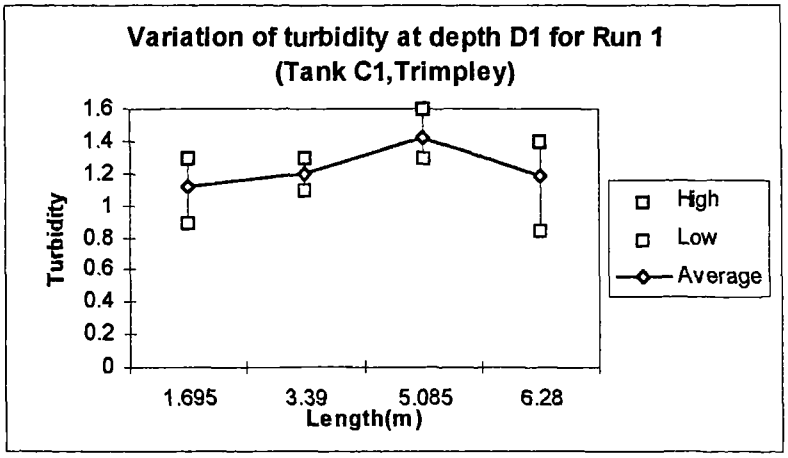

Figure D1.10 - Turbidity variation at depth D1, Trimpley WTW

Table D1.5 - ANOVA between runs and depths for Tank C2 (Frankley WTW)

Source	DF	SS	MS	F	P
Run	2	1.24414	0.62207	20.71	0.000
Depth	3	0.11151	0.03717	1.24	0.308
Error	42	1.26138	0.03003		
Total	47	2.61703			

Table D1.6 - ANOVA between runs and depths for Tank C1 (Trimpley WTW)

Source	DF	SS	MS	F	P
Run	2	5.4399	2.7199	328.72	0.000
Depth	3	0.0092	0.0031	0.37	0.773
Error	42	0.3475	0.0083		
Total	47	5.7966			

Table D1.7 - ANOVA between runs and depths for Tank C7 (Trimpley WTW)

Source	DF	SS	MS	F	P
Run	2	0.17007	0.08503	6.60	0.003
Depth	3	0.03266	0.01089	0.84	0.477
Error	42	0.54108	0.01288		
Total	47	0.74380			

Table D1.8 - Significant test for turbidity between half length and three-quarter length from the baffle (Tank A3, Frankley)

Source	DF	SS	MS	F	P
Length	1	0.35648	0.35648	30.32	0.000
Run	2	0.47521	0.23760	20.21	0.000
Error	20	0.23516	0.01176		
Total	23	1.06685			

Table D1.9 - Significant test for turbidity between half length and three-quarter length from the baffle (Tank C2, Frankley)

Source	DF	SS	MS	F	P
Length	1	0.09065	0.09065	4.57	0.000
Run	2	0.72859	0.36430	18.36	0.000
Error	20	0.39677	0.01984		
Total	23	1.21602			

Table D1.10 - Significant test for turbidity between half length and three-quarter length from the baffle (Tank C1, Trimpley)

Source	DF	SS	MS	F	P
Length	1	0.0394	0.0394	8.20	0.010
Run	2	3.2022	1.6011	332.81	0.000
Error	20	0.0962	0.0048		
Total	23	3.3379			

Table D1.11 - Significant test for turbidity between half length and three-quarter length from the baffle (Tank C7, Trimpley)

Source	DF	SS	MS	F	P
Length	1	0.020126	0.020126	4.87	0.039
Run	2	0.105470	0.052735	12.76	0.000
Error	20	0.082632	0.004132		
Total	23	0.208228			

Table D1.12 - Significant test for turbidity between one-quarter length and half length from the baffle (Tank A3, Frankley)

Source	DF	SS	MS	F	P
Length	1	0.06253	0.06253	6.37	0.020
Run	2	0.74266	0.37133	37.80	0.000
Error	20	0.19646	0.00982		
Total	23	1.00164			

Table D1.13 - Significant test for turbidity between one-quarter length and half length from the baffle (Tank C2, Frankley)

Source	DF	SS	MS	F	P
Length	1	0.00940	0.00940	0.76	0.395
Run	2	0.21937	0.10969	8.83	0.002
Error	20	0.24849	0.01242		
Total	23	0.47727			

Table D1.14 - Significant test for turbidity between one-quarter length and half length from the baffle (Tank C1, Trimpley)

Source	DF	SS	MS	F	P
Length	1	0.0049	0.0049	0.63	0.436
Run	2	3.3299	1.6650	214.40	0.000
Error	20	0.1553	0.0078		
Total	23	3.4901			

Table D1.15 - Significant test for turbidity between one-quarter length and half length from the baffle (Tank C7, Trimpley)

Source	DF	SS	MS	F	P
Length	1	0.002763	0.002763	0.87	0.361
Run	2	0.010132	0.005066	1.60	0.227
Error	20	0.063349	0.003167		
Total	23	0.076243			

Table D1.16 - Average turbidity at various positions in the tanks at Frankley WTW

Position	POINTS (length in metre)	Run 1 Tank A3 (NTU)	Run 2 Tank A3 (NTU)	Run 3 TankA3 (NTU)	Run 1 Tank C2 (NTU)	Run 2 Tank C2 (NTU)	Run 3 Tank C2 (NTU)
Inlet	0.000	1.9	4.5	2.1	5.1	1.6	2.3
D/D1	2.100	1.225	1.45	1.775	1.575	1.275	1.225
C/D1	4.200	1.5	1.575	1.9	1.85	1.225	1.275
B/D1	6.300	1.05	1.55	1.575	1.45	1.3	1.475
A/D1	7.900	1.35	1.675	1.825	1.475	1.1	1.275
D/D2	2.100	1.65	1.95	1.475	1.875	1.2	1.35
C/D2	4.200	1.7	1.5	1.625	1.925	1.425	1.225
B/D2	6.300	1.15	1.4	1.525	1.5	1.15	1.325
A/D2	7.900	1.125	1.65	1.475	1.375	1.25	1.15
D/D3	2.100	1.45	1.725	1.875	1.65	1.45	1.2
C/D3	4.200	1.425	1.575	1.75	1.7	1.125	1.475
B/D3	6.300	1.175	1.4	1.625	1.75	1.25	1.125
A/D3	7.900	1.275	1.475	1.55	1.425	1.225	1.35
D/D4	2.100	1.725	2	2.3	2.2	1.6	1.6
C/D4	4.200	1.575	1.55	1.775	1.775	1.3	1.425
B/D4	6.300	1.1	1.325	1.65	1.325	1.325	1.275
A/D4	7.900	1.275	1.475	1.6	1.425	1.325	1.4

Note: Position indicates point from the baffle and the depth, for example A/D4 indicates it is 7.9m from the baffle and at depth D4(refer to Figure 4.5 in Chapter 4).

Table D1.17 - Average turbidity at various positions in the tanks at Trimpley WTW

Position	POINTS (length in metre)	Run 1 Tank C1 (NTU)	Run 2 Tank C1 (NTU)	Run 3 Tank C1 (NTU)	Run 1 Tank C7 (NTU)	Run 2 Tank C7 (NTU)	Run 3 Tank C7 (NTU)
Inlet	0.000	3.500	2.100	1.400	2.2	3.2	2.7
D/D1	1.695	1.125	0.698	0.455	0.565	0.635	0.7925
C/D1	3.390	1.200	0.465	0.433	0.655	0.56	0.8175
B/D1	5.085	1.425	0.538	0.448	0.64	0.5575	0.7
A/D1	6.280	1.185	0.535	0.478	0.68	0.7125	0.5875
D/D2	1.695	1.1125	0.6275	0.4425	0.5225	0.595	0.78
C/D2	3.390	1.275	0.505	0.445	0.665	0.6025	0.99
B/D2	5.085	1.3875	0.5875	0.44	0.6775	0.6025	0.6925
A/D2	6.280	1.075	0.53	0.4925	0.655	0.6775	0.5675
D/D3	1.695	1.125	0.625	0.4825	0.5475	0.545	1.0225
C/D3	3.390	1.125	0.51	0.4375	0.6425	0.585	0.7875
B/D3	5.085	1.375	0.5775	0.4375	0.655	0.6525	0.63
A/D3	6.280	1.1875	0.5425	0.525	0.705	0.7125	0.605
D/D4	1.695	1.225	0.73	0.51	0.565	0.665	1.175
C/D4	3.390	1.05	0.55	0.48	0.7025	0.665	0.8125
B/D4	5.085	1.25	0.535	0.4475	0.6775	0.6125	0.6925
A/D4	6.280	1.5	0.535	0.52	0.7875	0.7575	0.6